Investigating PAMP-triggered immunity in the *Arabidopsis thaliana/Hyaloperonospora arabidopsidis* interaction

E. Fantozzi

A thesis submitted in partial fulfilment of the University's requirements for the Degree of Doctor of Philosophy

2016

University of Worcester

DECLARATION OF AUTHORS RIGHTS

I declare that the thesis embodies the results of my own research or advanced studies and that it has been composed by myself. Where appropriate, I have made reference to the work of others.

Abstract

Every year around 10-16% of all crops worldwide are lost due to plant pathogens. In addition, climate change and post-harvest losses pose a serious threat to food security. These factors represent a serious problem for the goal of increasing food production by 50% by 2050 in order to feed the growing population worldwide. In this light, plant pathology represents an important tool to reduce the losses due to plant pathogens.

Different approaches can be adopted to render plants more resistant to pathogens, including breeding programmes to select plants carrying resistance genes (used in the past but still very useful) and studies on molecular plant-microbe interactions, in particular on pathogen effectors and pathogen-associated molecular patterns (PAMPs) and their receptors. The outcomes on PAMPs studies can be used both to directly elicit a defence reaction in the plants using a newly discovered molecule (by priming the plant before an actual pathogen attack) or to create GM plants containing receptors able to recognise a particular PAMP. Therefore, the study on PAMPs and their related receptors in plants embodies an active field of plant pathology.

In this study, we wanted to shed light on PAMP-triggered immunity (PTI) using the model pathosystem composed by the model plant *Arabidopsis thaliana* and one of its natural pathogens, the obligate biotrophic oomycete *Hyaloperonospora arabidopsidis* (*Hpa*). Specifically, we wanted to discover whether a) *Hpa* contains new PAMP molecules, which would trigger defence responses, b) *Arabidopsis* has the relevant receptors and c) there are genes that are involved in the PAMP-triggered immune response of *Arabidopsis*.

To do so, we directly looked for *Hpa* PAMPs by studying *Hpa* asexual spore extracts and their ability to cause reactive oxygen species (ROS) accumulation and callose deposition (which are two distinctive signs of PTI) in *Arabidopsis*. In addition, we investigated cellulose-binding elicitor lectin (CBEL) proteins in *Hpa*, because the orthologue protein in *Phytophthora parasitica* var. *nicotianae*, was found to act as a PAMP in both *Arabidopsis* and *Nicotiana benthamiana*. As for the *Arabidopsis*

receptors involved in PAMP recognition, the important co-receptor BRI1-associated kinase 1 (BAK1) and the adaptor SOBIR1 were studied to understand their involvement in the recognition of any PAMP molecules derived from *Hpa*. Finally, *Arabidopsis* genes involved in the *Arabidopsis*/*Hpa* interaction were studied as well.

Our data showed that *Hpa* contains molecules able to elicit ROS production and callose deposition and at least one of them is of proteinaceous nature. They are recognised by receptors that associate to BAK1 to transmit the signal, while on the other hand SOBIR1 seems not to be involved. Furthermore, the two *Hpa* CBEL proteins were found to contain the same domain recognized as PAMP in CBEL from *Ppn*. They also induce a slight callose accumulation in *Arabidopsis* plant overexpressing them and leaf discolouration when transiently expressed in *N. benthamiana*. Finally, seven *Arabidopsis* genes were found to play a role in *Arabidopsis* defence against *Hpa*.

The data obtained from this work could lay the foundations of future research, where the PAMP molecules could be identified using proteomics and used to isolate the receptors. In the future, the outcomes may be translated into practical resources to protect crops belonging to Brassicaceae (relatives of *Arabidopsis*) from devastating diseases caused by oomycetes.

Acknowledgements

Finally, here I am. This PhD has been an emotional roller-coaster and an invaluable experience, that shaped me as a scientist and as a person. I will always be grateful for this opportunity and for the wonderful people I met along the way.

Firstly I would like to thank my supervisory team. A huge thank you goes to my Director of Study, Prof Mahmut Tör, for always believing in my abilities and supporting me throughout the project. Thank you for giving me the freedom to shape my own research, although always being there with precious advices and guidance. A big thank you also to my internal and external supervisors, Dr Mike Wheeler and Prof Cyril Zipfel. I always felt your support and encouragement. I am really grateful for the help you have given me.

I also want to thank the previous and current members of the Tör Lab: Dr Alison Woods-Tör, Gülin and Osman, together with Ryan, Lisa, Tom and Hannah. It has been a pleasure working with all of you. I will not forget all the moments we shared, the fun we had and the support I got from you.

I cannot thank enough all the colleagues at the National Pollen and Aerobiology Research Unit (NPARU) and all the people at the Institute of Science and Environment (ISE) at the University of Worcester. Thank you very much for all the help you have given me, for the chats (both scientific and not!) and the support.

Finally, the biggest thank you to my parents, Antonio and Maria and to my other half Michele. It goes without saying that your love and precious support helped me achieve this huge step in my life!

...and as I already said once...thanks to me, because I made it!

Elena

Table of Contents

Published paper

List of Figures

xiv

List of Tables

Frequently Used Abbreviations

aa	Amino acid
APS	Ammonium Persulfate
At	*Arabidopsis thaliana*
ATR	*Arabidopsis thaliana* recognized
avr	avirulence gene
bar	Metric unit of pressure
BAR	Basta® resistance gene
bp	Base pair
ºC	Degree Celsius
Ca^{2+}	Calcium ion
CBD	Cellulose-binding domain
CBEL	Cellulose-binding elicitor lectin
CBM1	Carbohydrate-binding module 1
CDS	Coding sequence
cm	Centimetre
CO$_2$	Carbon dioxide
Col-0	Columbia (accession)
C-terminal	Carboxy-terminal
Cys	Cysteine
DNA	Deoxyribonucleic Acid
EDTA	Ethylenediaminetetraacetic acid
ETI	Effector-triggered immunity
ETS	Effector-triggered susceptibility
F$_2$	Second filial generation
FHB	Fusarium Head Blight
flg22	Flagellin (22 amino acids-recognized epitope)
Gen	Gentamicin
GP34	Glycoprotein 34 (later renamed CBEL)

h	Hour
H$^+$	Hydrogen ion
H$_2$O$_2$	Hydrogen Peroxide
HCl	Hydrogen Chloride
Hpa	*Hyaloperonospora arabidopsidis*
HRP	Horseradish Peroxidase
IPTG	Isopropyl β-D-1-thiogalactopyranoside
K$^+$	Potassium ion
K$_2$HPO$_4$	Dipotassium Phosphate
kb	Kilobase
kDa	Kilo Dalton
KOH	Potassium Hydroxide
kV	Kilovolt
LB	Luria-Bertani medium
LRR	Leucine-rich repeat
M	Molar
mA	Milliampere
MAPK	Mitogen-activated protein kinase
mg	Milligram
MgCl$_2$	Magnesium chloride
min	Minute
ml	Millilitre
mm	Millimetre
mM	Millimolar
MS	Murashige and Skoog
N-terminal	Amino terminal
NaCl	Sodium Chloride
NaOH	Sodium Hydroxide
NASC	The European Arabidopsis Stock Centre
ng	Nanogram
nm	Nanometre
OD	Optical density

PAMP	Pathogen-associated molecular pattern
PBS	Phosphate Saline Buffer
PCR	Polymerase Chain Reaction
PM	Protein Marker
Ppn	*Phytophthora parasitica* var. *nicotianae*
Pro	Proline
PRR	Pattern-recognition receptor
PTI	PAMP-triggered immunity
***R*-gene**	resistance gene
Rif	Rifampicin
RLK	Receptor-like kinase
RLP	Receptor-like protein
RNA	Ribonucleic Acid
ROS	Reactive Oxygen Species
rpm	Revolutions per minute
RPP	Recognition of *Peronospora parasitica*
RT	Room temperature
RT-PCR	Reverse Transcription Polymerase Chain Reaction
sdH$_2$O	Sterile distilled water
SDS	Sodium Dodecyl Sulfate
SDS-PAGE	Sodium Dodecyl Sulfate Polyacrylamide Gel Electrophoresis
s	Second
TBS	Tris-Buffered Saline
TBS-T	Tris-Buffered Saline - Tween 20
T-DNA	Transfer DNA
Thr	Threonine
v/v	Volume/volume
w/v	Weight/volume
µg	Microgram
µl	Microlitre
µm	Micrometre

Chapter 1

General Introduction

1.1 Plant diseases and their impact on food security

The definition of food security evolved during the years. However, the accepted and more recent version defines food security as "a situation that exists when all people, at all times, have physical, social and economic access to sufficient, safe and nutritious food that meets their dietary needs and food preferences for an active and healthy life" (FAO, 2003). Considering the continuously increasing population worldwide, it has been estimated that the food production, to be able to adequately (as per definition) feed everyone, must increase of the 50% by 2050 (Chakraborty & Newton, 2011). There are many problems to face before being able to reach the fixed target: first of all the increase in urbanisation and the consequent reduction in lands devoted to crops; water scarcity, but most importantly the changing climate and pests and pathogens threatening crops (Chakraborty & Newton, 2011; Flood, 2010; Qi & Fitt, 2014; Strange & Scott, 2005).

1.1.1 Role of plant science to achieve food security

Science and technology will have a great impact in achieving the goal of feeding an ever-growing world population. As mentioned by Beddington (2010) we may probably need a new greener revolution. It is, in fact, clear that the focus of the question are plants. They are a fundamental source of food for both humans and animals (which eventually will be used for human consumption). The point is that, as mentioned above, crops must produce more yield (to achieve the fixed goal of 2050), even though the lands dedicated to agriculture are contracting and will probably reduce even more (due

to the rise of sea level and drought advance) as well as is diminishing the water available for agricultural practises. In addition, the central problem of climate change has to be considered. The rise in temperatures (on the long-term) but also the advent of more extreme weather conditions (on the short-term) will threaten crops and plants worldwide. It has been estimated that the global temperatures will increase of about 4 °C by 2080, while the atmospheric CO_2 concentration may double (FAO, 2011; Beddington, 2010). These two factors (temperature and CO_2) may lead to different consequences. Indeed, on the one hand, the rise of CO_2 concentration may have the so-called "fertilization" effect, leading to an increase in productivity and therefore crop yield (Chakraborty & Newton, 2011). On the other hand, though, an increase in global temperatures will lead to a detrimental effect due to reduction in water availability and a direct effect on the life of plants (Chakraborty & Newton, 2011; FAO, 2011). In the light of what have been said, we may be led to think that the CO_2 concentration rise might mitigate the unfavourable effects of a rise in temperature on crops. However, it is difficult to predict, since it is also possible that by the time the CO_2 reaches the levels needed for the beneficial effects, the rise in the temperatures has already affected the plant life (FAO, 2011). Moreover, it has to be considered that the effects of the temperatures on plants may be different in various parts of the globe. In fact, it is possible that in temperate and northern regions the rise in temperature may help to extend the growing season, while in already dry regions (e.g. Sub-Saharan Africa) it may lead to hotter and drier climates, leading to loss in cultivable lands and crops (FAO, 2011; Beddington, 2010). Finally, the everlasting problem of plant pests and pathogens needs also to be taken into consideration (see Section 1.1.2).

Therefore, in light of what has been said, science and technology, and plant science in specific, must quickly act in order to limit the damages to future crops and agriculture through both crop improvement and crop protection (Beddington, 2010).

In terms of crop improvement, it will be important to breed new crop varieties able to resist the upcoming unfavourable conditions depicted above. For instance, through breeding programmes or new techniques, such as marker-assisted selection, it will be fundamental to introduce into staple crops, traits to render them resistant to drought or salt or heat stress. In addition to these features, another important aspect of crop

improvement will be the production more nutritious crops, containing elements like vitamins and minerals especially important for developing countries (Beddington, 2010).

Strange and Scott (2005) made a list of 14 staple crops fundamental for human consumption worldwide and they included: barley, cassava, lentil, maize, millet, pearl millet, potato, rice, rye, sorghum, soybean, sweet potato, wheat and yam. Unfortunately, all of them suffer from diseases caused by a myriad of pests and pathogens, ranging from viruses, bacteria, oomycetes and fungi, to nematodes and parasitic plants (Strange & Scott, 2005). That being said, it is clear that plant scientists worldwide will be challenged not only in terms of crop improvements but also in terms of crop protection. In the past, crop protection has been based on the use of chemical pesticides, which are still valuable today (Beddington, 2010). However, new measures must be taken to improve the defences against plant diseases. One line of research may focus on stimulating plants' own defences (Beddington, 2010) through the study of pathogen-associated molecular patterns (PAMPs) or effector molecules (see Section 1.3 for a more in depth explanation on plant's immune system) and their related receptors (Boyd et al., 2013). By doing so, it may be possible to achieve a long-term and durable resistance to the disease, due to the highly conserved nature of the PAMP molecules. Jointly, the search for durable plant resistance may focus also on the plant side, by the study and identification of quantitative trait loci (QTL) to aim for durable and wide-spectrum resistance (Boyd et al., 2013). Finally, genetically modified organisms (GMOs) may help in the fight against pathogens. Indeed, they enable the transfer of a specific resistance gene or set of genes from a plant that has no agricultural or economic importance to a crop species that already shows valuable features. By doing that, it will be possible to avoid the wait of the conventional breeding programmes and in addition, it could be helpful to limit the use of pesticides for a more sustainable agriculture (Boyd et al., 2013; Bruce, 2012).

1.1.2 Plant pests and pathogens threaten plant health and food security

Every year, crop losses due to plant pests and pathogens are around 10-16% of the global production (Chakraborty & Newton, 2011). Therefore it is of fundamental

importance to gain more insights into the relationships between plants and their pathogens (Boyd et al., 2013). More importantly, in the light of the changing climate, plant pests and pathogens have to be included into studies and projections, since it is still unclear which will be the consequences of climate change on plant pathogens and therefore on plants and crops (Pautasso et al., 2012). Although the staple importance of the topic for food security, too many studies do not consider the influence of climate change on plant pathogens (Qi & Fitt, 2014; Chakraborty & Newtons, 2011; Flood, 2010); this may be due to the difficulty of including into a forecast model such complex topics as climate change and its influence on pathogens and crop yields (Gregory et al., 2009).

1.1.2.1 Plant-pathogen interactions and the importance of climate change

When thinking about plant pests and pathogens, both the short-term and the long-term effects of the changing climate should be considered (Gregory et al., 2009).

Short-term effects of climate change are related to extreme weather events that may happen over a short period of time, such as floods, drought, heat waves and storms (Gregory et al., 2009). These events may have the ability to enhance the spread of pathogenic microorganisms, such as water-borne ones due to flooding and wind-borne pathogens in relation to storms. In addition, in conditions caused by high temperatures such as drought and heat waves, plants might be affected and therefore they might become more prone to disease (Pautasso et al., 2012). Considering the long-term effects of climate change, on the other hand, such as the rise in global temperatures and in the atmospheric concentration of CO_2, it is still unclear which will be the effects on plant-pathogen interactions. However, it can be predicted that these important changes will have great effects on the populations of pathogens, in relation to their dispersal, reproduction and survival (Qi & Fitt, 2014), making, in certain cases, their effects on crops and plants even worse (Flood, 2010 Pautasso et al., 2012). In this scenario, the response of the plant to the pathogen has to be included as well. Indeed, it has been noted that plant's resistance may be affected under high temperature or high CO_2 concentration (Gregory et al., 2009; Huang et al., 2006). For instance, it has been observed that some resistance genes, inducing resistance to phoma stem canker in

winter oilseed rape, demonstrated reduced effectiveness at higher temperatures (Huang et al., 2006).

Few examples demonstrate how plant-pathogen interactions might be influenced in the future by the changing climate: in their article, Qi and Fitt (2014) explain that the projections for England forecast winters characterized by higher temperature and increase in rainfall, followed by hotter and dryer summers. In this scenario, plants will increase their growing period but as a consequence, also pest and pathogens might do the same. This is the case of the cyst nematode of sugar beet *Heterodera schachtii*, which is expected to double the number of generations per cropping season by 2080, from 3 at the current weather conditions to 6. It is however difficult to forecast such interaction, although the authors showed results on the incidence of powdery mildew on sugar beat in England using a weather-based disease forecasting model. The model showed that the incidence of powdery mildew is expected to increase; a sensible result considering that powdery mildew is favoured by warm and dry weather (Qi & Fitt, 2014). Moreover, Chakraborty & Newton (2011) presented an interesting case study on Fusarium Head Blight (FHB) of wheat. FHB can be caused by a number of *Fusarium* and *Microdochium* species and is favoured by warm and wet weather. These fungi produce mycotoxins, which contaminate wheat and result detrimental for the wheat chain production because toxic for humans and animals. In addition, FHB causes blighting of the wheat heads, resulting in yield and quality loss. Lately, the rise in temperatures has favoured the species *F. graminearum* (which is more toxigenic) over the previously most diffuse species *F. culmorum* (less toxigenic than *F. graminearum*) and *M. nivale* (which is non-toxigenic) in the Netherlands, England, Wales and northern Germany. In addition, considering also the rise of CO_2 concentration level, it should be expected a further increase of FHB events. Indeed, higher CO_2 levels will favour the production of FBH inoculum and therefore the infection rate between growing seasons will increase (Chakraborty & Newton, 2011).

That being said, it will therefore be of fundamental importance to higher the surveillance over plant diseases, in order to be able to set up effective and rapid measures of containment, taking into consideration the risk of pesticides inactivity due to the extreme weather events. Furthermore, it will be essential to avoid the spread of

alien species (which may be favoured by the new climate conditions) in new areas using tools such as crop monitoring, surveillance and quarantine. Moreover, it will be of great importance to maintain the diversity in germplasm collections, since they represent the source of resistance genes for breeding programmes. Finally, as already mentioned, increase the research on the effect of climate changes on plant-pathogen interactions, with a special attention for increase in CO_2, since it will favour plant growth (and therefore a denser canopy), with chances of increasing foliar disease outbreaks (Qi & Fitt, 2014).

1.1.3 Economically important plant pathogens: a brief overview

Many are the categories of pathogenic organisms that continuously threaten plants, crops and ornamentals. Mainly bacteria, viruses, nematodes, fungi and oomycetes (please see Section 1.2) (Mansfield et al., 2012; Scholthof et al., 2011; Jones et al., 2013; Dean et al., 2012; Kamoun et al., 2015).

Bacteria

Plant pathogenic bacteria are diverse and belong to both Gram-positive and Gram-negative classifications. They can enter and infect plants via several entries, such as natural openings on the leaf surface (e.g. stomata), or through wounds or stems and roots (Vidaver & Lambrecht, 2004). They can cause economically important diseases on trees, ornamentals and crops; among them a special mention can be certainly done for *Xanthomonas* spp., which cause serious diseases among a large varieties of crops. In particular, *Xanthomonas oryzae* pv *oryzae* (Figure 1.1a) is recognized as one of the most destructive pathogens of rice (Mansfield et al., 2012). As well as *Xanthomonas axonopodis* pv *manihotis*, causing bacterial blight of cassava, one of the staple food in Africa, similarly to rice in Asia (Mansfield et al., 2012; Strange & Scott, 2005). In addition, *Ralstonia solanacearum* (Figure 1.1b) can be mention. This pathogen is able to cause disease on a wide variety of hosts (crops including potato, tomato, eggplant, banana, just to mention few of them and some ornamentals) worldwide, having a particular incidence in developing countries (Mansfield et al., 2012). Finally, although many more should be cited, *Erwinia amylovora* (Figure 1.1c) and *Xylella fastidiosa* (Figure 1.1d) must be included in this description, because of their role in affecting food safety worldwide through the diseases they cause on fruit plants (and ornamentals, in

the case of *Erwinia amylovora*) and crops (and tree, in the case of *Xylella fastidiosa*) (Mansfield et al., 2012).

Figure 1.1 Symptoms of bacterial diseases on crops and fruit plants. a: symptoms caused by *Xanthomonas oryzae* pv *oryzae* on an infected rice leaf. The arrow shows a drop of yellow exudate produced by the infection. **b**: *Ralstonia solanacearum* on a tomato fruit and branch. The arrows show the spot caused by the bacteria on the tomato fruit and the symptoms on the branch. **c**: *Erwinia amylovora* causing fire blight (white arrow) on an apple fruit. **d**: *Xylella fastidiosa* affecting an orange tree. Yellow discolourations and brown spots (indicated by the white arrows) are visible on the leaves on the infected tree. (**a**: adapted from Mansfield et al., 2012; **b**: picture adapted from Gerald Holmes, California Polytechnic State University at San Luis Obispo, Bugwood.org; **c**: adapted from Clemson University - USDA Cooperative Extension Slide Series, Bugwood.org; **d**: adapted from Alexander Purcell, University of California, Bugwood.org).

Viruses

Viruses are obligate parasites, that due to their reduced genome have evolved a lifestyle highly reliant on the host, for genome replication and viral particle assembly. They are able to spread internally, moving along the plant phloem (Dawson et al., 2013) and they spread from plant to plant often via vectors including insects such as aphids, flies, or thrips. In addition, they can move long distances through movement of infected plants or infected plant material (Dawson et al., 2013; Scholthof et al., 2011). Among the several plant pathogenic viruses, there are many requiring a special mention, due to the severity and economic importance of the diseases they cause.

Tomato spotted wilt virus (Figure 1.2a) causes great economic losses worldwide, due to the wide range of crops it is able to infect (more than 800 plant species), including potato, pepper, lettuce and peanut (Scholthof et al., 2011). In addition, another important plant virus is the *African cassava mosaic virus*. The symptoms (Figure 1.2b) can vary, but in the worst cases it could also result in the total loss of the plant, and as previously mentioned, cassava is one of the staple foods in developing countries. In the

same category of viruses infecting cassava, the *Cassava brown streak virus* can also be mentioned as an emerging pests in Africa (Scholthof et al., 2011; Strange and Scott, 2005). *Citrus tristeza virus* is another devastating virus (Scholthof et al., 2011), affecting plants belonging to the *Citrus* spp., causing different levels of symptoms: decline, the most severe one, characterized by the death of the plant; stem pitting (Figure 1.2c), distinguished by an anomalous growth of the phloem and seedling yellows, characterized by chlorosis of the plant (Moreno et al., 2007; Dawson et al., 2013). Finally, *Tomato yellow leaf curl virus* needs a special mention, due to the wide spreading of the devastating disease it causes, resulting, in many cases, in the complete loss of the plant (Scholthof et al., 2011).

Figure 1.2 Symptoms of viral diseases on crops and plants. a: the symptoms of the *Tomato spotted wilt virus* infection are shown: the white arrows indicate the characteristic spots visible on tomato fruits. **b**: a leaf of Cassava showing symptoms of infection by the *African cassava mosaic virus*. **c**: a grapefruit trunk showing "stem pitting" symptoms caused by *Citrus tristeza virus*. (**a**: picture adapted from William M. Brown Jr., Bugwood.org; **b**: picture adapted from Scholthof et al., 2011; **c**: picture adapted from L. Navarro, Instituto Valenciano de Investigaciones Agrarias, Bugwood.com).

Nematodes

Plant pathogenic nematodes are small, soil-borne worms (Jones et al., 2013). More than 4100 species are known to parasitize plants (Decraemer & Hunt, 2006). They represent a constant threat to food security, because of the number of species and the wide spread. They are a particular menace in developing countries, attacking staple crops and often showing non-specific symptoms, therefore not being easily recognized. Nematodes can have three different lifestyles: ectoparasitic, in which they do not enter the plant interior, but use their feeding structures (protrusible stylets or mouth spears) to feed from plant

roots; endoparasitic, where they enter the plant and migrate through the tissues and finally semi-endoparasitic, characterized by both features. The biotrophs, cyst and root-knot nematodes (Figure 1.3a and Figure 1.3b, respectively), represent the most important categories from an economical point of view. In particular, the potato cyst nematode (Figure 1.3a), originally from South America, and now widely spread globally, is among the most damaging species. Root-knot nematodes are obligate biotrophs and forms galls on the roots of their hosts; they show a wide host range and cause symptoms including wilting, stunted growth and leaf discolouration. *Meloidogyne incognita* (Figure 1.3b) is among one of the most important species. Following cyst and root-knot nematodes, *Pratylenchus* spp. have the ability to parasitize various crops, such as cereals, legumes, sugarcane, coffee and banana just to mention few of them. Figure 1.3c shows the consequences of an infection by a *Pratylenchus* spp.: the wheat seedlings appear stunted. Finally, although many more should be cited, *Radophilus similis* (Figure 1.3d) parasitizes pepper plants, *Citrus* spp. and banana. It is especially destructive in tropical environments, such as South America, Africa, Asia, the Pacific and the Caribbean (Jones et al., 2013).

Figure 1.3 Infections by plant pathogenic nematodes. a: Potato cyst nematodes causing yellow cysts on potato roots. **b**: *Meloidogyne incognita* (root-knot nematode). Gall formations are present on the roots on the infested tomato plant (right), whereas on the left is shown a healthy tomato root system. **c**: *Pratylenchus* spp. causing stunted growth of wheat plants. Patches of affected plants are visible among non-affected ones. **d**: *Radophulus similis* infestation of a *Citrus* root cortex. (**a**: Bonsak Hammeraas, NIBIO - The Norwegian Institute of Bioeconomy Research, Bugwood.org; **b**: Gerald Holmes, California Polytechnic State University at San Luis Obispo, Bugwood.org; **c**: image adapted from Jones et al., 2013; **d**: J.H. O'Bannon, Bugwood.org).

Fungi

Plant pathogenic fungi are eukaryotic organisms, which cause about 70% of all plant diseases, accounting more than 15000 species (Carris et al., 2012; Gonzáles-Fernándes et al., 2010). They show different nutrition modes and therefore they can be divided in:

biotrophs, relying on living plants to acquire nutrients; necrotrophs, which kill the infected plant in order to feed and finally fungi that show and intermediate lifestyle between the previous two, called hemibiotrophs (Talbot, 2010; Gonzáles-Fernándes et al., 2010). One of the most devastating plant pathogenic fungi is *Magnaporthe oryzae*, causing rice blast (Figure 1.4a). Because it parasitizes one of the major sources of carbohydrates in developing countries, this fungus represents a real threat for food security (Dean et al., 2012; Wilson & Talbot, 2009). Another example of plant pathogenic fungi, which have a great economic impact, is represented by fungi belonging to the genus *Fusarium* (Figure 1.4b). In particular, *Fusarium graminearum* infects several cereal crops, while *Fusarium oxysporum* has a wider host-range, including tomato, cotton and banana, just to mention but a few (Dean et al., 2012). In addition, *Botrytis cinerea* (Figure 1.4c), the grey mold has to be mentioned. Because it can infect more than 200 plant species, showing therefore a broad-host range, it poses risks to many economically important crops and fruit plants, not only during their growing period but also in the post-harvest (Dean et al., 2012). Last but not least, another important threat for cereal production worldwide comes from the fungi belonging to the genus *Puccinia* (Figure 1.4d). They cause rust disease on wheat and pose a big threat to food security, especially following the emergence of a new race of *Puccinia graminis* f. sp. *tricici* (causal agent of black stem rust), called Ug99, which is spreading from Africa to the Middle East and to South Asia (Dean et al., 2012; Flood, 2010).

Figure 1.4 Fungal infections on cereals, fruits and potato. a: *Magnaporthe oryzae* causing rice blast disease on a rice leaf. The symptoms are characterized by spots displaying internal necrotic lesions surrounded by a chlorotic area. **b**: *Fusarium oxysporum* causing root rot and wilt on sweet potato. **c**: *Botrytis cinerea* infecting raspberries. The characteristic appearance of the "grey mold" is visible. **d**: *Puccinia striiformis* f. sp. *tritici* on a wheat leaf causing stem rust. (**a**: picture adapted from Wilson & Talbot, 2009; **b**: Charles Averre, North Carolina State University, Bugwood.org; **c**: picture adapted from Dean et al., 2012; **d**: picture adapted from Dean et al., 2012).

1.2 Oomycetes as plant pathogens

Oomycetes are eukaryotic microorganisms belonging to the Kingdom Chromista (Stramenipila), together with diatoms and brown algae (Thines & Kamoun, 2010), though for many years they have been erroneously classified in the Kingdom of Fungi, due to striking similarities in their dispersion and propagation habits and in the infectious structures (hyphae) developed during the infection of the host plant, but also in the reaction and defences used by the plant towards these two classes of pathogens (Hardham, 2007; Thines and Kamoun, 2010; Kamoun, 2003). They seem to have evolved around 300-350 million years ago (Kamoun et al., 2015) and are distributed in almost every environment on Earth, both terrestrial and aquatic (Thines & Kamoun, 2010). Most of them are pathogens (although some species are known to be saprophytic) able to parasitize various eukaryotic organisms such as insects, fish, animals or other microorganisms (Kamoun, 2003). However, the majority of known oomycetes (more than 60 % of the species) are destructive plant pathogens (Thines & Kamoun, 2010), able to cause great economic losses by infecting important crop plants but also ornamental plants and natural environments (Kamoun, 2003; Hardham, 2007). One of the first evidence of oomycete parasitism in plants came from the Carboniferous period (in UK). The oomycete, most probably related to the *Pythiales* is known as *Combresomyces williamsonii* and it was found to be associated to the extinct seed fern *Lyginopteris oldhamia* (Strullu-Derrien et al., 2011). Having said that, it is generally believed that plant parasitism in oomycetes has independently evolved three times in the two main oomycete lineages: the Saprolegniales (e.g. *Aphanomyces euteiches*) and the Peronosporalean (including *Phytophthora* spp., *Pythium* spp., *Albugo* spp. and downy mildews) (Thines and Kamoun, 2010).

1.2.1 Major classes of pathogenic oomycetes

As mentioned above, plant pathogenic oomycetes can be roughly divided into two classes: the Saprolegniales and the Peronosporalean (Thines and Kamoun, 2010). In regard to the first ones, although at least one species (*Aphanomyces euteiches*) is known to cause disease on crop plants (i.e. legumes; Thines & Kamoun, 2010) they are mostly known to be parasites of fish, crustaceans, mosquito larvae and midge eggs (Hulvey et al., 2007). For this reason and for the aim of the project, the attention will be directed on

the members belonging to the second category; due also to their important role in plant-pathogen interactions both economically and scientifically as recently highlighted in a thorough review by Kamoun and colleagues (2015).

The second class is composed by two orders: the Pythiales and the Peronosporales. The order Pythiales contains facultative plant parasites and is further divided into two families: the Pythiogetonaceae (about which little is known) and the most known family of the Pythiaceae, containing two important plant pathogenic genus, *Phytophthora* and *Pythium*. The Peronosporales on the other hand, contains obligate parasites of plants and includes the families known as Albuginales or white rusts (genus *Albugo*) and Peronosporaceae or downy mildews (Riethmüller et al., 2002).

Genus *Phytophthora*

This genus is one of the most studied by plant pathologists (Kamoun et al., 2015) and contains more than 60 species known to cause devastating diseases on economically and socially important crop plants, such as potatoes, tomatoes, soybean or peppers, just to mention only but a few. In addition, they also infect ornamental plants and trees therefore causing damages to natural ecosystems and plant nurseries (Kamoun, 2003).

The most known oomycete belonging to the *Phytophthora* genus is, without doubt, *P. infestans*. This oomycete is the causal agent of the disease known as potato late blight affecting potato plants (Figure 1.5a and Figure 1.5b) and in the 1840s caused the historically infamous Irish Potato Famine (Flood, 2010; Kamoun et al., 2003), which led to over a million of deaths and a huge emigration flux. Affecting the third staple food in the world (potato), *P. infestans* remains one of the main risks globally to food security (Kamoun et al., 2015). Another important *Phytophthora* oomycete is *P. capsici*. It has a fairly wide host range, affecting plants belonging to the Solanaceae such as tomato and pepper, as well as legumes and some cucurbits (Kamoun et al., 2015). This oomycete, as well as *P. infestans* (Flood, 2010) is favoured by wet and warm conditions. It can spread quite quickly, transitioning from an initial biotrophic stage to a necrotrophic one with the appearance of heavy sporulation of infected tissues (Figure 1.5b) leading to an infection which is difficult if not impossible to control once in the field (Kamoun et al., 2015). *P. parasitica*, also known as *P. nicotianae*, is another member of the genus *Phytophthora* showing quite a wide host range. It is mainly known

for causing black shank on tobacco, but it is also able to infect *Citrus* plants, causing root rot and gummosis. In addition, it infects also more than 250 species of both herbaceous and perennial, causing crown and root rot and severe foliar and fruit diseases (Figure 1.5c) (Kamoun et al., 2015). This oomycete is also believed to gain even more importance globally in the near future due to the changing climate and increase in global temperatures. In fact, its host range is similar to that of other oomycetes, but being favoured by warmer temperature, it is believed that it will overcome other competitors in areas where normally it is not the predominant species (Kamoun et al., 2015; Erwin & Ribeiro, 1996).

Figure 1.5 Devastating effects of members belonging to the genus *Phytophthora* on crops and trees.
a: *Phytophthora infestans* late blight symptoms on potato tuber (left) and leaf (right). Typical necrotic lesions are shown both in the tuber and on the leaf **b**: *Phytophthora capsici* infecting tomato fruits. The heavy sporulation is clearly visible and appears as a white mat of sporangiophores. **c**: *Phytophthora parasitica* infecting a Brinjal fruit. The infection is characterized by heavy and rapid sporulation. **d**: *Phytophthora sojae* causing root and stem rot on soybean. **e**: *Phytophthora cinnamomi* affecting pine trees in a nursery. Dead tree (brown/red) are evident among the still alive and healthy ones (bright green). **f**: *Phytophthora ramorum* affecting a tanoak tree (left) and an oak tree (detail, right). (**a**: pictures adapted from Scott Bauer, USDA Agricultural Research Service, Bugwood.org (potato tuber, left) and Howard F. Schwartz, Colorado State University, Bugwood.org (potato leaf, right); **b**: adapted from Kamoun et al., 2015; **c**: adapted from Kamoun et al., 2015; **d**: adapted from Daren Mueller, Iowa State University, Bugwood.org; **e**: adapted from L. Barnard, Florida Department of Agriculture and Consumer Services, Bugwood.org; **e**: pictures adapted from Joseph O'Brien, USDA Forest Service, Bugwood.org (tanoak tree, left) and Bruce Moltzan, USDA Forest Service, Bugwood.com (oak tree detail, right)).

In addition to the aforementioned species, *P. sojae*, *P. cinnamomi* and *P. ramorum* deserve a mention. Indeed, although *P. sojae* has a quite narrow host range, mainly infecting soybean plants, causing root and stem rot (Figure 1.5d) (Kamoun et al., 2015),

it is a threat for food security, being soybean one of the global staple food (Strange and Scott, 2005). Therefore, despite being so species-specific it represents one of the most important causes of economic losses for soybean growers (Kamoun et al., 2015). Finally, *P. cinnamomi* (Figure 1.5e) and *P. ramorum* cause detrimental diseases in a range of plant communities, including forests and nurseries infecting both hardwood trees and ornamental plants worldwide. In particular, *P. ramorum* is known to cause sudden oak death (Figure 1.5f), sudden larch death and *raromum* blight on a wide host range (actually, among the genus *Phytophthora*, it has the widest host range) (Kamoun et al., 2015).

Genus *Pythium*

The oomycetes belonging to the genus *Pythium* are ubiquitous soil-borne pathogens: they can be found both in fields, ponds, and streams, since they are favoured by wet and moist conditions (Kamoun et al., 2015; Buyten & Höfte, 2013). Their lifestyle ranges from opportunistic (growing on soils and plant debris) to highly virulent, infecting a wide range of plants (more than 300), including corn, soybean, wheat, rice, sugar beet, barley, sorghum and turf grass (Kamoun et al., 2015; Buyten & Höfte, 2013; Wei et al., 2011). They prefer warm and humid weather, with temperatures ranging from 28°C during the day to 21°C during the night. The disease caused by *Pythium* spp. is known as *Pythium* blight, characterized by damping off and root rot, but it is also known as cottony leaks, due to the cotton candy-like appearance of the white and fluffy aerial mycelium (Figure 1.6a) that appears on infected tissues or fruits (Kamoun et al., 2015; Allen et al., 2004).

Two species are principally known to cause the blight (although it is believed that at least 15 *Pythium* species are able to cause this disease: *P. ultimum* and *P. aphanidermatum* (Allen et al., 2004). The symptoms appear as patches in the grass (Figure 1.6c (left)), however the leaves usually do not show any characteristic or particular symptoms, although they may sometimes appear slimy. For this reason, the disease management may be difficult and they often cause extensive damages to golf grasses and athletic fields or lawns (Allen et al., 2004; Kamoun et al., 2015). As mentioned above, the recurrent symptomatology is characterized by fruit rot (Figure

1.6b) and the appearance of an extended white mycelium, resembling cotton candy (therefore the definition of cottony leaks; Figure 1.6a) (Allen et al., 2004).
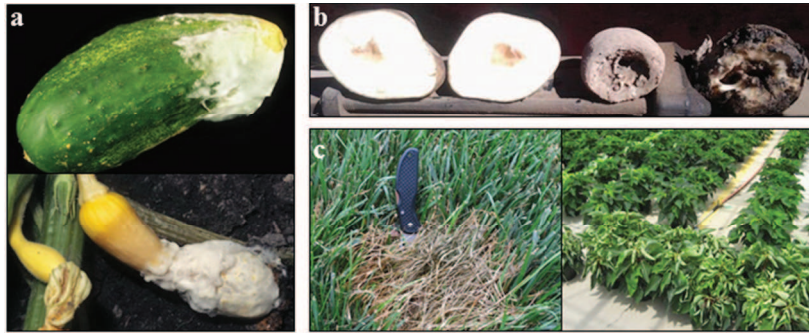
Figure 1.6 Symptoms of *Pythium* spp. infection on crops, turf grass and plants. a: *Pythium* spp. causing "cottony leaks" on cucumber (upper picture) and yellow summer squash (bottom). The white mycelium conferring to appearance of cotton candy on the infecting vegetables is evident. **b**: *P. ultimum* on potato tubers. The hollow core is a result of the infection. **c**: infection of turf grass (left) and poinsettia plants (right) caused by *P. aphanidermatum*. The symptoms of *Pythium* blight are evident as a patch of dead grass (left) caused by the rotting of the roots; the symptoms on poinsettia plants are characterized by severe wilting and leaves upturning (left). (**a**: pictures adapted from Gerald Homes, California Polytechnic State University at San Luis Obispo, Bugwood.org; **b**: picture adapted from Ben Phillis, Michigan State University, Bugwood.org; **c**: pictures adapted from Lee Miller, University of Missouri, Bugwood.org (turf grass) and Emma Lookabaugh, Bugwood.org (poinsettia)).

White rusts and downy mildews

The last category of plant pathogenic oomycetes includes obligate parasites of plants (Riethmüller et al., 2002).

The genus *Albugo* contains more than 50 species and it is known to cause disease on more than 400 plants worldwide: for instance *A. candida* infecting mustard plants (Figure 1.7a), *A. tragopogonis* affecting sunflowers (Figure 1.7b) or *A. occidentalis* causing disease on spinach (Figure 1.7c). They infect plants belonging to various important families of crop plants and ornamentals, including Brassicaceae, Crucifereae, Solanaceae, Asteraceae, Fabaceae, Cichoraceae, Orchidaceae and many more. The disease they cause is known as white rust, white blister or white blister rust and also stagheads (due to the abnormal growth of the infected plants inflorescence). The disease is favoured by cool temperatures, in the range of 12 °C-15 °C, and high relative humidity (more than 70%). The infected plant shows symptoms characteristic of the infection on all aerial parts. The initial stages of the disease development are

characterized by the formation of tiny (1-2 mm in diameter), white pustules (Figure 1.7a) or blisters. They preferentially develop on leaves or cotyledons. As the disease progresses, usually more than one pustule converge to form a bigger one (Figure 1.7b, leaf on the right) and the symptoms may become visible also on the upper side of the leaf as discoloration (Figure 1.7b, leaf on the left). The pustules on the lower side of the leaf might assume a creamy appearance and usually they are white or creamy-white in colour (Figure 1.7c, right). Finally, white sporangia are released by the rupture of mature pustules (Figure 1.7c, left) (Saharan et al., 2014).

Figure 1.7 Symptoms of *Albugo* spp. on crop plants. a: *A. candida* on a mustard (Brassicaceae) leaf. Typical white rust pustules are evident on the underside of the affected leaf. **b**: *A. tragopogonis* on sunflower leaves. White rust symptoms are present both on the upper side (left) and underside (right) of the leaf. **c**: *A. occidentalis* infecting spinach leaves. White rust pustules appear on the underside of the leaves (left); a close up of an affected lower leaf side (right). The pustules appear raised and of a white-creamy colour. (**a**: picture adapted from Gerald Homes, California Polytechnic State University at San Luis Obispo, Bugwood.org; **b**: picture adapted from Howard F. Schwartz, Colorado State University, Bugwood.org; **c**: pictures adapted from Paul Bachi, University of Kentucky Research and Education Center, Bugwood.org).

There are more than 700 species of downy mildews pathogens. They are obligate parasites of several important crop plants, including grape, maize, sorghum, lettuce and cucurbits (Kamoun et al., 2015; Lucas et al., 1995). They belong to the family Peronosporaceae and they include different genus, such as *Peronospora* (Figure 1.8c), *Bremia* (Figure 1.8a), *Plasmopara* (Figure 1.8b), and *Hyaloperonospora* to mention few of them. Being obligate parasites, they usually show a narrow host range, although being able of causing important problems on the crops they infect. The downy mildew infections are mostly air-borne. The newly produced spores are often released from the tree-shaped structures called sporangiophores (Figure 1.8b, pictures on the right) emerging mostly from the lower leaf surface, thanks to the wind or water droplets. Once they land on a leaf, following the penetration, they start a new infection cycle.

Infectious hyphae will develop intracellularly inside of the infected leaf, with the production of feeding structures called haustoria and will terminate with the emergence from the lower side of the leaf (usually taking advantage of natural openings such as stomata) of sporangiophores carrying the new generation of spores. They usually characterize the downy mildew infection thanks to the white and fluffy appearance of these structures (Figure 1.8). They can also survive during the winter in the soil or in plant debris thanks to the formation of sexual oospores (Kamoun et al., 2015).
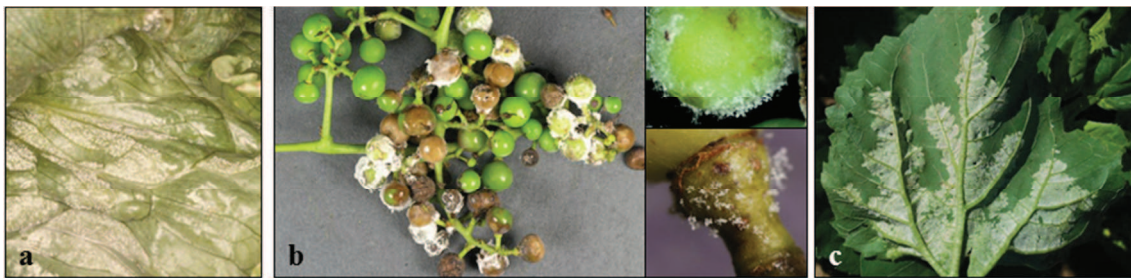
Figure 1.8 Downy mildew symptoms on lettuce, grapevine and sunflower. a: *Bremia lactucae* infecting lettuce. The typical downy mildew infection symptoms are present: white and fluffy sporangiophores carrying the next generation of spores. **b**: *Plasmopara viticola* affecting a grapevine (left picture). Detail of the infection on the fruit (upper picture on the right) and on the petiole (bottom picture on the right). In the two close ups the tree-shaped sporangiophores can be distinguished. **c**: *Peronospora halstedii* on a sunflower leaf. Again the white fluffy mat of sporangiophores on the affected leaf is evident. (**a**: picture adapted from Gerald Homes, California Polytechnic State University at San Luis Obispo, Bugwood.org; **b**: pictures adapted from Bruce Watt, University of Maine, Bugwood.org; **c**: picture adapted from Howard F. Schwartz, Colorado State University, Bugwood.org).

A well-known and studied downy mildew, not affecting economic important crop plants, but instead able to infect the scientifically important model plant *Arabidopsis thaliana* is *Hyaloperonospora arabidopsidis*. It has therefore acquired importance in the field of oomycete-plant interactions, constituting with *Arabidopsis* a good model pathosystem to study the interactions between a plant and an obligate biotroph.

1.3 *Hyaloperonospora arabidopsidis,* the obligate pathogen of *Arabidopsis thaliana*

Hyaloperonospora arabidopsidis (hereafter *Hpa*) is an obligate biotrophic oomycete pathogen, causing downy mildew on the model plant *Arabidopsis thaliana* (Slusarenko

& Schlaich, 2003; Coates & Beynon, 2010; Holub, 2008). It has been formerly known as *Hyaloperonospora parasitica*; nomenclature introduced by Constantinescu & Fatehi (2002) following molecular phylogenetic analysis that separated the genus *Hyaloperonospora* from the genus *Peronospora* (it was indeed previously known as *Peronospora parasitica*) (Constantinescu & Fatehi, 2002; Thines & Choi, 2016).

Due to the natural co-evolution history of the model plant and its pathogen across Europe and mainly in the UK, it has been possible to obtain a vast and complete germplasm collection for both *Arabidopsis* and *Hpa*. A terminology to name the different *Hpa* isolates was therefore introduced and was based on the location where the isolate was found and on the relative *Arabidopsis* accession on which the isolate is able to proliferate. For instance, the isolate Emoy was named after the location East Malling, (Kent, UK; with the first two letters referring to the initials of the location) and the Oystese accession (the last two letters instead refer to the *Arabidopsis* susceptible accession) (Coates and Beynon, 2010; Holub, 2008).

1.3.1 Life cycle of *Hpa*

As previously mentioned, *Hpa* is an obligate biotroph; therefore it relies entirely on the plant for the completion of its life cycle. In order to be able to grow and reproduce, the plant tissues must be healthy and living (Coates and Beynon, 2010).

The asexual life cycle starts with a conidium (spore) reaching the surface of a leaf (Figures 1.9c-d). Following its attachment, the spore develops a germ tube and an appressorium. The latter is a penetration structure, which tries to breach the space between two epidermal cells in order to penetrate the leaf surface thanks to the development of a penetration peg developing into an invading hypha (Figure 1.9d). In many cases, one or two feeding structures, called haustoria, will originate from the hypha. The haustorium is basically a feeding formation, produced by the pathogen to uptake nutrients from the plant cell. It does not penetrate the cell, however it invaginates the plasma membrane after the degradation of the cell wall by degrading enzymes. However the damage to the plant is kept to the minimum. In the extra-haustorial matrix, formed between the plant cell plasma membrane and the haustorial membrane, and separated by the apoplastic space by a neckband (Figure 1.10b), trafficking between the

pathogen and the plant cell takes place: absorption of nutrients from the plant by the pathogen and the input of effector molecules into the plant cell to rearrange host metabolism and cellular organization.
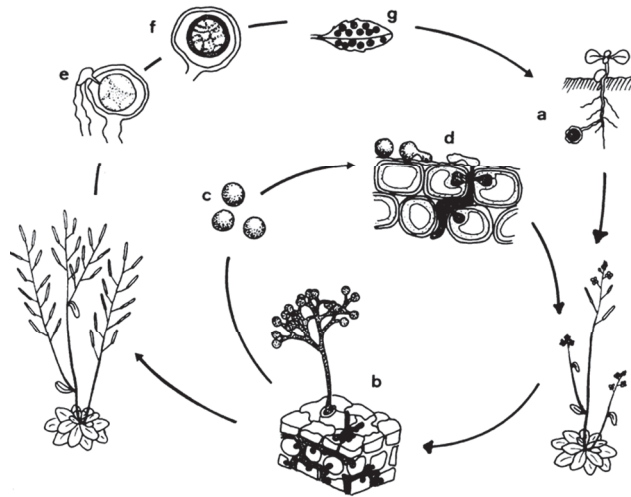
Figure 1.9 Complete *Hpa* life cycle. In spring a new infection is initiated by an oospore germinating into the soil (a). The oospore will infect the plant from the roots. A mycelium will grow inside of the plant, until conidiophores will emerge from the leaf displaying asexual conidiospores (b) that will be afterwards dispersed (c). When the conidiospores reach a leaf, they will germinate and develop into a new organism (d). Sexual oospores are formed inside of the leaf, when an oosphere, contained inside the oogonia, is fertilized a fertilization tube growing from the antheridium (e). The fertilized oosphere will finally develop into an oospore (f) that will survive the winter into the leaf debris on the soil (g) to initiate a new infection cycle the following spring (a) (Slusarenko and Schlaich, 2003).
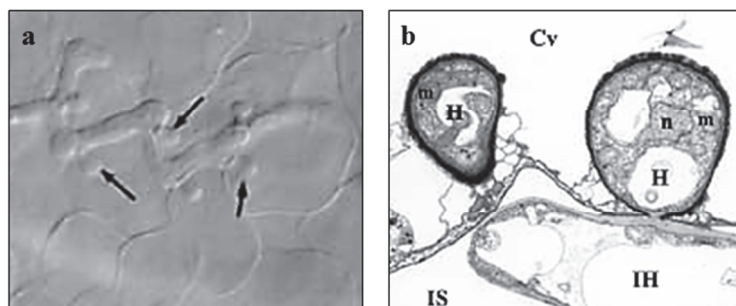
Figure 1.10 *Hpa* feeding structures (haustoria). a, image captured with the light microscope showing an intracellular growing hyphae with several haustoria outgrown inside of neighbouring cells during a compatible interaction. **b**, transmission electron microscopy (TEM) showing an intercellular hyphae (IH) in the intercellular space (IS) with the related haustorium (H). In the haustorium are visible also a nucleus (n) and a mitochondrion (m). It is possible to appreciate the neckband formed at the interface hyphae/haustorium and the lobate structure, typical of *Hpa* haustoria (Costantinescu and Fatehi, 2002). The cellular vacuole (Cv) and a second (smaller) haustorium are showed as well (images adapted from Soylu and Soylu, 2003).

In compatible interactions, the hypha will develop further into the leaf, into a branched structure with multiple haustoria (Figure 1.10a), to finally emerge outside of the leaf with a tree-shaped structure, called sporangium (Figure 1.11a) that carries the newly formed asexual spores (conidia). The conidia will later be dispersed to start a new infection cycle and propagate the pathogen once again.
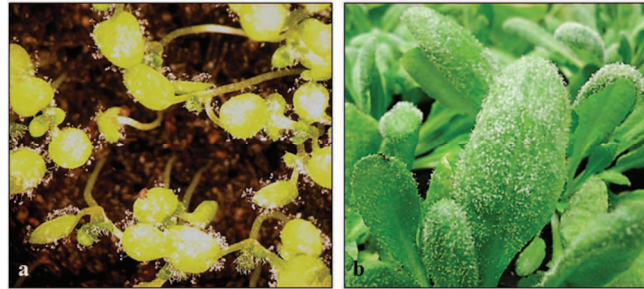
Figure 1.11 *Hpa*-infected *Arabidopsis* plants. The picture shows two different examples of *Hpa* infections on *Arabidopsis*. **a**, 2-week-old Ws-*eds1* susceptible plants infected with *Hpa*-Cala2. Due to the plants young stage, it is possible to appreciate the tree-shaped structures (conidiophores) carrying the new generation of spores. **b**, six-week-old Ws-*eds1* plants infected with *Hpa*-Emoy2. In this occasion the infection resembles a mat, almost completely covering older *Arabidopsis* leaves.

At the same time, sexual spores (oospores) will be also formed inside of the leaf (Figure 1.9g). *Hpa* is, indeed, homothallic; therefore the hyphae inside of the leaf will develop into both male and female reproductive structures (antheridium and oogonium, respectively; Figures 1.9e-f) to produce oospores that will survive during the winter into the leaf debris on the soil to start a new infective cycle the following spring (Figure 1.9a) (Coates and Beynon, 2010; Slusarenko and Schlaich, 2003).

1.3.2 Research on *Arabidopsis* and *Hpa*: a model pathosystem

Arabidopsis has been used in plant research for more than 30 years. It has initially been established as a model organism for genetic studies because of the ease in manipulation, due to the short generation time, the small size and also the abundance of seed production and self–pollination. The first to start experimental research on *Arabidopsis* was Friedrich Laibach, who, for the first time in 1907, described the exact number of *Arabidopsis* chromosomes. However *Arabidopsis* research have seen some major drawbacks, until it was rediscovered during the end of 1970s, when it was established as a plant model for research in molecular genetics. From that moment on, a big

community of scientists in *Arabidopsis* research started to rise, with availability of funds and manipulation tools development (Koornneef & Meinke, 2010). However, despite being a model organism, in the 1980s it was still not implicated in studies of plant-pathogen interactions, because of the lack of an appropriate pathogen to be coupled with. Two main methods were used to search for a pathogenic organism useful to build, together with *Arabidopsis*, a model pathosystem. An indirect method used to look for pathogens infecting plants relative to *Arabidopsis* followed by inoculation of *Arabidopsis* with these pathogens in order to see whether they were able to infect *Arabidopsis* as well. On the other hand, in a more direct way, scientists were looking for naturally infected *Arabidopsis* plants. The first to find and report *Arabidopsis* plants infected with *Hpa* was Paul Williams in a field trip to Europe, although the first accurate description of the pathosystem formed by *Arabidopsis* and *Hpa* came from Koch and Slusarenko in 1990 (Slusarenko & Schlaich, 2003). It was indeed in 1990s that the pathosystem was established as a genetic model to study plant-pathogen interactions regarding both plant's defence mechanisms against pathogens and host metabolic manipulation by the pathogen (Coates & Beynon, 2010).

1.3.2.1 *Arabidopsis/Hpa* interaction

Section 1.3.1 depicted what is known as a "compatible" interaction between the plant and the oomycete for the aim of the section to describe a complete *Hpa* life cycle (Figure 1.9). However, the interaction between the two organisms is much more complex and it gives rise to several levels of host-pathogen compatibility, in terms of ability of the pathogen to colonize the plant and finally complete its life cycle.

Mainly two methods can be used to measure the interaction between a plant and a pathogen: one is based on scoring disease severity (in terms of host damage and induction of immune responses), while the second one considers pathogen transmissibility (in terms of the ability of the pathogen to complete its life cycle with spores production) (Krasileva et al., 2011). An example of the first method is the scoring system developed by Eric Holub, where *Hpa*-infected *Arabidopsis* cotyledons are valued in terms of their immune response (cell death) triggered towards *Hpa* infection (Figure 1.12) (Holub, 2008; Krasileva et al., 2011).
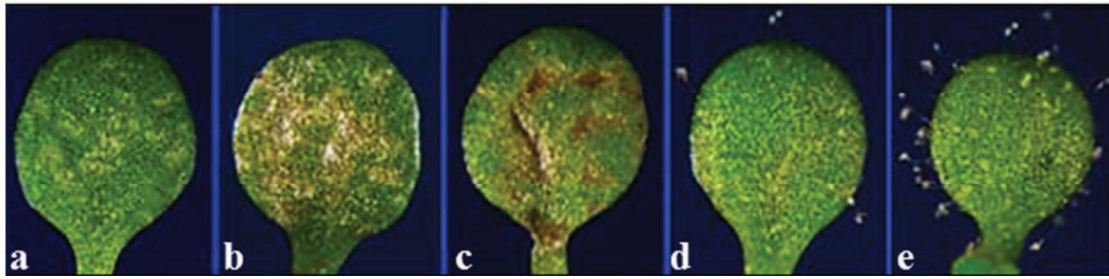
Figure 1.12 Variation in compatibility levels between *Arabidopsis thaliana* and *Hpa*. The 5 pictures show, from **a** to **e**, the phenotypic variation in the outcome of the *Arabidopsis*/*Hpa* interaction. In detail: **a**, complete incompatibility between the organisms. There is no colonisation of the host nor sporulation. The cotyledon is characterised by "flecking" necrosis, with small yellow spots (flecks) visible at the attempted penetration site. **b**, incompatibility. No sporulation and very low colonisation. The phenotype is intermediate between "flecking" (**a**) and "pitting" (**c**). **c**, incompatibility. No visible sporulation and low host colonisation. This phenotype is called "pitting" due to the "pits" caused by healthy and colonised cells that developed hypersensitive response (HR) resulting in tissue collapse (pit). **d**, semi-compatibility. Host colonisation and low to medium sporulation. The phenotype is known as "trailing". In this case the host HR (characterized by dying cells) is some steps behind the growing hyphae, therefore resulting in a "trail". **e**, compatible interaction. High host colonisation, high degree of sporulation. No signs on the leaf of plant defence and HR (Adapted from Holub, 2008; Coates and Beynon, 2010).
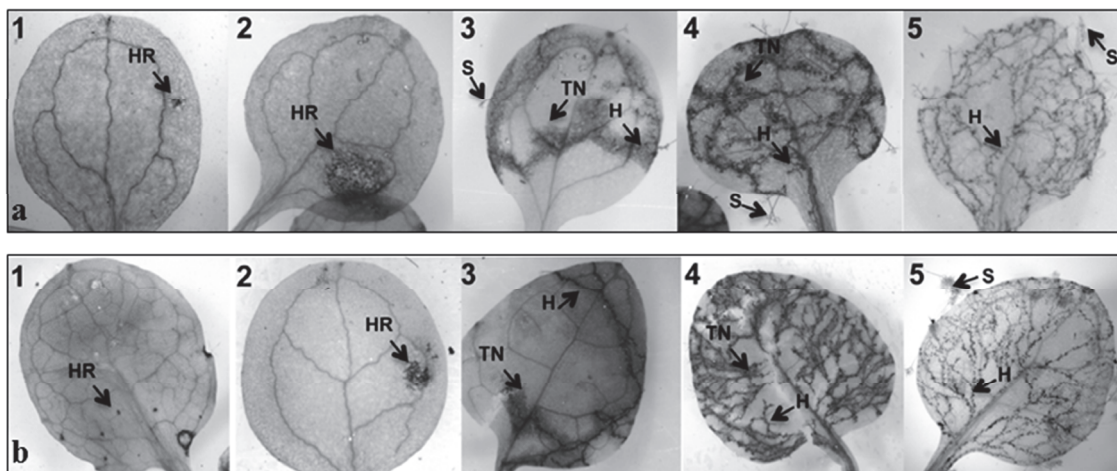
Figure 1.13 *Arabidopsis*/*Hpa* interaction on cotyledons and true leaves. a: *Arabidopsis* cotyledons; **b**: *Arabidopsis* true leaves. The interaction between *Arabidopsis* and *Hpa* is assessed in terms of increasing compatibility (from Type 1, fully resistant to Type 5, fully susceptible), both in cotyledons (**a**) and true leaves (**b**). Both the extent of plant cell death and of pathogen growth have been considered. Plant cell death could be either radial/circular (Type 2) or trailing, following hyphae extension (Type 3-4). In terms of pathogen growth: Type 1 and Type 2 have completely arrested pathogen growth and no sporulation is observed, while Type 3 supports limited pathogen growth. On Type 4, extensive pathogen growth is observed (this Type is commonly known as "trailing necrosis", see Figure 1.11) together with sporulation. finally, no cell death and full pathogen sporulation are observed on Type 5 (adapted from Krasileva et al., 2011; **HR**: hypersensitive response, **H**: hyphal growth, **TN**: trailing necrosis, **S**: sporangiophores).

An example of the second method, instead, comes from the scoring system developed by Nemri and colleagues (2010), where the results of the infection with *Hpa* of *Arabidopsis* true leaves are scored as susceptible, resistant, or intermediated in relation to the presence of pathogen's spores (Nemri et al., 2010; Krasileva et al., 2011).

A third scoring system has been developed by Krasileva and colleagues (2011) in which they considered both cotyledons and true leaves (in order to consider also the developmental control on the interaction). For the analysis they mainly considered both the two previous conditions (production of pathogen's asexual spores and degree of plant cell death), but also the amount of pathogen growth. In this case they developed a five-stages scoring system (Figure 1.13) and they mainly registered incomplete host resistance and an important contribution of the plant developmental stage (Krasileva et al., 2011).

1.3.2.2 Molecular players of compatibility and incompatibility: *RPP* and *ATR* genes

The reason behind different levels of compatibility is the recognition and interaction of so-called <u>r</u>ecognition of <u>P</u>eronospora <u>p</u>arasitica (*RPP*) genes from *Arabidopsis* and <u>A</u>rabidopsis <u>t</u>haliana <u>r</u>ecognised (*ATR*) genes from *Hpa* (Holub et al., 1994; Holub, 2008; Coates and Beynon, 2010). The natural genetic variation found throughout different *Arabidopsis* accessions and *Hpa* isolates is responsible for the presence or absence of *RPP* genes and their related *ATR* genes, respectively (Holub et al., 1994). Therefore, an *Hpa* isolate able to grow and proliferate on a particular *Arabidopsis* accession, might not be able to do the same on a different accession because of the presence in the second one of an *RPP* gene able to recognise the particular *ATR* gene present in that specific *Hpa* isolate (Holub et al., 1994).

To date, four *ATR* genes have been cloned from *Hpa* (Solovyeva et al., 2015): *ATR1* (Rehmany et al., 2005), *ATR13* (Rentel et al., 2008), *ATR5* (Bailey et al., 2011), and only recently *ATR39* (Goritschnig et al., 2012). They represent effector molecules (for a detailed explanation please see Section 1.4.2) produced by the oomycete *Hpa* to manipulate *Arabidopsis* immune machinery and successfully colonize the host plant (Solovyeva et al., 2015). For instance, it has been demonstrated that ATR13 is able to

suppress immune reactions in plants (please see Section 1.4.1), such as callose deposition and ROS production (Sohn et al., 2007). Although their clear role in promoting *Hpa* virulence, in cases where they are recognized by the related receptors in *Arabidopsis* they acquire an avirulence function and they are referred to as avirulence (avr) factors (Solovyeva et al., 2015). For instance, Rentel and colleagues (2008) demonstrated that the recognition of ATR13 by the *Arabidopsis* receptor RPP13Nd (where Nd stands for the *Arabidopsis* accession Niederzen) triggers immune reactions that confer protection against infections of bacteria, oomycetes and viruses (Rentel et al., 2008).

Studies on these avirulence genes and on their cognate *Arabidopsis* receptors revealed a high level of allelic variation reflecting the close co-evolution history of the plant and its biotrophic pathogen. As an example, the couple composed by the *avr* gene *ATR1* and its related receptor *RPP1* can be mentioned. In the *Arabidopsis* accession Wassileskija (Ws-0) there are three allelic forms of the *RPP1* gene, known as *RPP1*-WsA, *RPP1*-WsB and *RPP1*-WsC (Botella et al., 1998), while in the Niederzen (Nd) accession, only one allelic form, known as *RPP1*Nd, is found. The four different allelic forms specify resistance to different *Hpa* isolates (Sohn et al., 2007). Indeed, it has been found that different allelic forms of the *avr* gene *ATR1*^{NdWsB} (previously cloned by Rehmany and colleagues, 2005) are recognized by different allelic forms of the *RPP1* gene. In detail, the *Hpa*-Emoy2 allele of *ATR1* is recognized by both *RPP1*Nd and *RPP1*-WsB, while the allele from *Hpa*-Maks9 is only recognized by *RPP1*-WsB (Rehmany et al., 2005). This example explains what previously mentioned about the ability of certain *Arabidopsis* accession of recognizing specific *Hpa* isolates (and not others) and therefore form an incompatible interaction (Holub et al., 1994). This concept has also been confirmed by structural studies on the ATR1 protein. It has been demonstrated that ATR1 is a modular protein that shows high level of polymorphism in the protein surfaces, specifically in the carboxy-terminal (C-terminal) domain. This variability represents what has been previously said: only specific allelic forms of the related RPP1 receptor protein will be able to recognize different versions of the ATR1 C-terminal domain. This is mainly due to high polymorphism occurring in the leucine-rich repeat (LRR) domain, which is the one supporting the recognition function (Chou et al., 2011).

As aforementioned, overall the C-terminal residues of oomycete effectors show high variability (Rehmany et al., 2005; Chou et al., 2011), while they are characterized by an N-terminal domain which is quite conserved, being composed of a signal peptide for export outside of the cell, followed by a conserved "RXLR" motif (Rehamny et al., 2005). The motif (RXLR-X$_{5-21}$-ddEER) has been found to be conserved also in other oomycete genomes (e.g. in the *Avr1b* from *P. sojae* and in *Avr3a* from *P. infestans*) for translocation into the host cell cytoplasm (Rehmany et al., 2005; Sohn et al., 2007). However, after molecular characterization, an exception has been discovered: ATR5 does not carry the canonical RXLR motif, although still possessing the ddEER motif in the translocation locus (Bailey et al. 2011).

1.4 How plants react to the invading pathogens: the plant immune system

As seen in the previous Sections, plants are constantly challenged by several pathogens trying to enter the plant interior to find shelter and access the nutrients to grow and reproduce.

Nevertheless, although plant pathogens are able to cause devastating losses to crops, trees and ornamentals (see Sections 1.1.2 and 1.2.1), the disease is far from being the norm (Ingle et al., 2006). Indeed, plants are protected by strong pre-formed defences, such as a wax and cuticle layer, thick epidermal cells protected by a rigid and hard-to-penetrate cell wall and a range of antimicrobial molecules (Ingle et al., 2006; Herman & Williams, 2012; Guest & Brown, 1997). In addition, plants have evolved a very sophisticated immune system which, in most of the cases, confers them protection by detecting and fighting back the pathogens. It has been described by Jones and Dangl (2006) and it can be schematically depicted as a three-step process (Jones & Dangl, 2006; Herman & Williams, 2012). At first, the plant recognizes well-conserved molecules, important for the fitness of the pathogen, known as pathogen-associated molecular patterns (PAMPs), establishing an immune reaction termed PAMP-triggered immunity (PTI). Secondly, the plant immune reaction might be stopped by the delivery of highly variable pathogenic molecules, named effectors, which are able to target the

PTI machinery, in a condition known as effector-triggered susceptibility (ETS). Thirdly, the plant immune system might once again be elicited (culminating in a potent immune reaction) by the recognition of the effector molecules, in case the plant has the related receptors. This final condition is known as effector-triggered immunity (ETI) (Jones & Dangl, 2006).

1.4.1 Plant-microbe interactions: PTI

As briefly introduced above, PTI results from the recognition of PAMP molecules derived from pathogens by pattern recognition receptors (PRRs) situated across the plant cell membrane. It would probably be more correct to refer to these molecules as MAMPs (microbe-associated molecular patterns) rather than PAMPs, since they are present in microbes whether they are pathogenic or not (therefore the definition MTI rather than PTI; Boller & Felix, 2009); nevertheless, the term PAMPs will be used throughout since pathogens are the focus of this project.

1.4.1.1 PAMP molecules

Important features that are characteristics of PAMPs are: their conservation among a whole class of microbes, their absence in the host and their importance for the fitness of the microorganism (Boller & Felix, 2009). Together with damage-associated molecular patterns (DAMPs, which are danger signals released from the host during a pathogenic attack or a wound), they are generally referred to as general elicitors (Henry et al., 2012).

PAMPs can have various natures: proteinaceous (such as bacterial flagellin or elongation factor-Tu), oligosaccharide (such as fungal chitin) or lipophilic (such as the ergosterol in oomycetes) (Boller & Felix, 2009). One of the first-studied and best-known PAMP examples is flagellin, the building block of the bacterial flagellum (Felix et al., 1999). In detail, a 22 amino acid-long peptide (flg22) at the N-terminal of the protein is recognised by the *Arabidopsis* RLK FLS2 as an eliciting molecule and therefore acts as a PAMP (Gómez-Gómez & Boller, 2000). Flg22 includes all the aforementioned PAMP features: it is widely conserved among motile eubacteria (Felix et al., 1999), it has not been found in plants and it is very important for the motility of these bacteria, especially during host invasion through stomata, and therefore for their

virulence (Penn & Luke, 1992; Melotto et al., 2006). Because they are so important for the survival of the microbe, PAMPs are usually under a strong negative selection, thus they do not easily evolve or change. However, it has been studied that flg22 may undergo positive selection as an adapted strategy to evade recognition. In some rare cases, indeed, bacteria are able to mutate residues within the epitope of the protein flagellin (Monaghan and Zipfel, 2012; Zipfel, 2009).

In regards to oomycetes, only few PAMP molecules have been identified so far (Table 1.1). They are mostly derived from oomycete belonging either to *Phytophthora* spp. or to *Pythium*. Only one PAMP has been found in *Hpa* to date (nlp24; Oome et al., 2014).

Table 1.1 Oomycete-derived PAMP molecules.

Oomycete	Protein	PAMP epitope	Host	References
P. sojae	Cell wall glycoprotein GP42	Pep-13	Parsley Potato	Nürnberger et al., 1994 Brunner et al., 2002
Phytophthora spp. *Pythium* spp.	Elicitins INF1	NA	*Nicotiana* spp. Brassicaceae Tomato	Kamoun et al., 1997 Vidhyasekaran, 2013 Kawamura et al., 2008
P. parasitica var. *nicotianae*	Cellulose-binding elicitor lectin (CBEL*)	Cellulose-binding domain (CBD)	Tobacco *Arabidopsis*	Séjalon-Delmas et al., 1997 Villalba Mateos 1997 Gaulin et al., 2006
Phytophthora spp. *Pythium* spp. *Hpa*	NEP1-like protein**	nlp24 (*Hpa*)	*Arabidopsis*	Vidhyasekaran, 2013 Oome et al., 2014 Cabral et al., 2012
P. sojae	Cell wall glucans	Hepta-β-glucoside	Soybean Fabaceae	Cheong & Hahn, 1991 Robinson & Bostock, 2015
P. sojae	Glycosil hydrolase family12 (GH12) XEG1	NA	Soybean Solanaceae	Ma et al., 2015

The table shows PAMPs derived from oomycete pathogens. The oomycete, the protein containing the PAMP, the PAMP epitope, the host in which they are recognized are indicated. The related literature is shown as well.
*For more information on: CBEL, see Section 4.1
**For more information on: NEP1-like (*Hpa*), see Section 3.1.1

They are mostly of proteinaceous nature, found either in the cell wall such as the cell wall glycoprotein GP42 (Brunner et al., 2002) or the cellulose-binding elicitor lectin (CBEL) (Gaulin et al., 2006) or secreted outside of the oomycete as for the small (10 kDa) elicitin proteins (Kamoun et al., 1997) or the glycosil hydrolase (Ma et al., 2015) and the NEP1-like proteins (Vidhyasekaran , 2013). Finally, the cell wall glucans (Cheong & Hahn, 1991), are part of the oomycete cell wall, together with cellulose and other carbohydrates and molecules depending on their lineage (Mélida et al., 2012).

1.4.1.2 PAMP-triggered immunity

On the cellular membrane of every cell in a plant there are pattern recognition receptors (PRRs), able to recognize invading microorganisms, thanks to the conserved patterns that are characteristics of each class of microbes. They are mainly divided into two classes: receptor-like kinases and receptor-like proteins. Both are characterised by a transmembrane domain and by an extracellular domain for the actual binding of the PAMP (or the DAMP, in case of wound or cell wall disruption due to the invading microorganism). The difference in between the two classes is the presence (in RLKs) or absence (in RLPs) of an internal kinase domain, able to transmit the danger signal. In many instances, PRRs may be accompanied by additional receptors, which can act as a co-receptor or as an adaptor, in order to transmit and amplify the signal (please see Sections 3.1.3 and 3.1.3.1 for a more in depth explanation) (Tör et al., 2009). Following the recognition of the PAMP molecule by PRRs many changes are initiated inside of the plant cell. They can be divided in: early (seconds to minutes), intermediate (minutes to hours) and late (hours to days) responses, depending on their time of activation after the recognition (Zipfel & Robatzek, 2010). One of the first consequences of PAMP recognition is the initiation of ion fluxes across the plasma membrane: in particular H^+ and Ca^{2+} will be imported inside of the cell from the apoplast, while K^+ will be exported outside, creating a depolarisation of the membrane and an alkalinisation of the extracellular space (Boller & Felix, 2009; Zipfel & Robatzek, 2010). Another early response is the oxidative burst (Boller & Felix, 2009), characterised by a fast and important production of reactive oxygen species (ROS), both by NADPH oxidases (Zipfel & Robatzek, 2010) and type III membrane peroxidases (O'Brien et al., 2012; Daudi et al., 2012). ROS are believed to act both as messengers and as antimicrobial

molecules, rendering the cellular environment inhospitable for the invading pathogen. In addition, they can also strengthen the cell wall thanks to cross-links they can induce in its components (Boller & Felix, 2009). Among the intermediate responses, there is the activation of mitogen-activated protein kinases (MAPKs). This will start a phosphorylation cascade, which will eventually lead to the activation of WRKY-type transcription factors and therefore to transcriptional reprogramming (Zipfel & Robatzek, 2010). Defence-related genes will be translated and in particular, RLKs have been reported to be overexpressed in a positive feedback mechanism. In addition, the stress hormone ethylene will be produced and the stomata will be closed. Finally, among the late responses, there is the production of salicylic acid and of the polysaccharide callose, a β-1,3-glucan polymer, which will strengthen the cell wall in the sites of attempted penetration in order to stop the advance of the pathogen (Boller & Felix, 2009; Ellinger & Voigt, 2014). All these cellular changes are known as basal immunity or PTI (Boller & Felix, 2009) and most of the time they are enough to stop the advance of non-pathogenic microbes (Herman & Williams, 2012).

1.4.2 Plant-microbe interactions: ETS and ETI

In some cases though, adapted pathogens are able to overcome the first set of defences triggered after the recognition of PAMP molecules, thanks to very specific and highly variable secreted molecules, called effectors.

1.4.2.1 Effector-triggered susceptibility

Effectors can remain into the apoplast or they can be delivered into the cytoplasm. Apoplastic effectors usually are used for protection against host defences (Wawra et al., 2012), especially by either preventing PAMP recognition or avoiding activation of the related PRRs (Asai & Shirasu, 2015; Mazzotta & Kemmerling, 2011). In detail, among apoplastic effectors can be mentioned: protease inhibitors or glucanase inhibitors, to protect the pathogens against the damaging effects of plant proteases and glucanases which may degrade proteins and cell wall glucans, damage the pathogen and generate PAMP molecules. In addition, apoplastic effectors can also have hydrolytic roles (i.e. glycosil hydrolases), in order to damage the host cell wall and allow the penetration of the pathogen. Finally, effectors can also act as toxins, which are usually required to

induce necrosis. This is especially true for necrotrophs or hemibiotrophs, which will eventually kill the host cell to uptake the nutrients (Wawra et al., 2012; Stassen & Van den Ackerveken, 2011).

Cytoplasmic effectors, on the other hand, mainly interfere with host immunity by targeting the PTI machinery (e.g. by suppressing callose deposition, ROS production or programmed cell death), affecting the signalling or the expression of defence genes (Asai & Shirazu, 2015; Wawra et al., 2012). When considering in particular oomycete pathogens, two different cytoplasmic effector families have been described: the RXLR-type and the Crinklers. Both families can be defined as modular proteins, in which the N-terminal domain is mostly conserved (or at least presents motifs and domains which are conserved among the studied effectors) and a C-terminal domain which shows a high level of polymorphism (Stassen & Van den Ackerveken, 2011; Schornack et al., 2009). This feature demonstrates that effectors are under strong positive selection (to evade host recognition) and that most probably the C-terminal module is the one conferring the biochemical activity to the effector (Schornack et al., 2009). On the other hand, the N-terminal moiety of the proteins is more conserved and is dedicated to secretion and translocation into the host. In detail, the RxLR effector family presents a N-terminal signal peptide for secretion, followed by a conserved RxLR-motif (Arg-any amino acid-Leu-Arg). In some cases, the dEER (Glu-Glu-Arg) motif follows the RxLR (Stassen & Van den Ackerveken, 2011; Schornack et al., 2009). The translocation process is still not completely understood, although it has been demonstrated that the RxLR and the dEEr motifs are involved in translocation into the host (Whisson et al., 2007). The N-terminal of the Crinkler effectors is characterised by a signal peptide, a LxLFLAK-motif, a conserved DWL-domain and finally a HVLVxxP-motif. In this case, the LxLFLAK-motif has been associated with intracellular localization and therefore translocation. (Stassen & Van den Ackerveken, 2011).

In conclusion, the overall purpose of effectors is to suppress the defence reactions (PTI) and allow the growth and spreading of the infection to finally establish infection (Asai & Shirasu, 2015). These events are collectively known as effector-triggered susceptibility (ETS) (Jones & Dangl, 2006). Nevertheless, in addition to the offensive role, cytoplasmic effectors are also used by filamentous (i.e. fungi and oomycetes) and

bacterial pathogens as a mean to interfere with and control host metabolism. In fact, these effectors are able to change host metabolic pathways in order to redirect, for instance, the transport of sugars from the host to the pathogen (Stassen & Van den Ackerveken, 2011).

1.4.2.2 Effector-triggered immunity

Plants, on the other hand, have evolved resistance genes (*R*-genes) that encode for receptors able to recognize and stop this second wave of attack, establishing effector-triggered immunity (ETI) (Jones & Dangl, 2006).

The receptors are divided into two categories: the ones that reside on the plasma membrane and exposed on the cell surface, which recognize also PAMP molecules (PRRs) and the cytoplasmic ones, belonging to the nucleotide-binding leucine-rich repeat protein family (NLRs). The latter are characterized by a central nucleotide-binding domain (NB) and by a C-terminal leucine-rich domain (LRR), with variable number of repeats depending on the receptor, and with high frequency of polymorphism, conferring therefore different binding specificity. In addition, at the N-terminal, these receptors are distinguished by the presence of either one of two different domains: a coiled-coil (CC) domain or a Toll/Interleukin1 receptor domain (TIR) (Bonardi & Dangl, 2012). The NLR receptors are able to detect the presence of the delivered effectors, both directly or indirectly. In fact, they can directly bind to the related effector (direct recognition) or they can recognize and bind to the target of the effector (indirect recognition; guard model). The receptor in this case will recognize the effector-modified state of the target rather than the effector itself. Similarly, the plant may also have evolved a molecule able to imitate the real effector target (decoy model) (Muthamilarasan & Prasad, 2013; Hoorn & Kamoun, 2008). For instance, there are two NLRs guarding a plant protein called RIN4, which is the target of several bacterial effectors. These effectors are able to induce changes in the protein, either by phosphorylation or protein degradation. The two guards, RPM1 and RPS2, detect those changes in RIN4 conformation and therefore establish ETI (Muthamilarasan & Prasad, 2013).

Following the direct or indirect recognition of effector molecules by the products of the related *R*-genes, ETI is established. To some extent, the immune reaction established during ETI is similar to the one established during PTI, with some overlapping pathways. For instance, MAPK cascade will be initiated with the consequent activation of WRKY transcription factors and the production and activation of PR genes. Similarly, salicylic and jasmonic acid, together with ethylene, will be produced. The cell wall will strengthen and lignify and antimicrobial compound will be generated. However, the main difference between PTI and ETI is the amplitude of the reaction: indeed during ETI we assist to the development of the hypersensitive reaction (HR, absent during PTI), characterized by programmed cell death (PCD) at the site of infection that will restrict pathogen growth (Muthamilarasan & Prasad, 2013).

What has just been described are the highlights of how plants and their pathogens are co-evolving in a continuous (and probably never ending) arms race for survival (Dodds and Rathjen, 2010).

1.5 Aims of the Project

In light of a continuously growing population worldwide and the need to feed 9 billion people by 2050, plant-pathogen interactions is a pivotal theme of scientific research. In particular, the study of PAMP molecules, to be used as triggers of plant immunity (Henry et al., 2012) or their related receptors, to be transferred into different plant families to create resistance, is of particular interest. *Arabidopsis* and one of its natural pathogen, the oomycete *Hpa* represent a pathosystem to study plant-oomycete interactions. The knowledge acquired with this model could be transferred to valuable crop plants (especially to plants belonging to, but not restricted to Brassicaceae) in order to make them resistant to the devastating diseases that oomycetes are able to cause.

This PhD research project aimed at shedding light on PAMP molecules deriving from *Hpa* and on their related receptors and recognition pathways in *Arabidopsis*.

Specifically, we aimed to:

➢ Determine whether *Hpa* contains any PAMP molecules, understand their nature and finally their recognition in *Arabidopsis*

➢ Investigate whether the cellulose-binding elicitor lectin (CBEL) molecules from *Hpa* are recognised in *Arabidopsis* as PAMP molecules (similarly to CBEL from *P. parasitica* var. *nicotianae*; Gaulin et al., 2006)

➢ Discover genes involved in the establishment of PAMP-triggered immunity (PTI) in *Arabidopsis-Hpa* interactions

The following chapters present the materials and methods employed during the study and the obtained and discussed results.

Chapter 2

Materials and Methods

2.1 Materials

2.1.1 Chemicals, enzymes and kits

All the chemicals were purchased, unless otherwise stated, from Invitrogen™ (Life Technologies, Paisley, UK), Melford (Ipswich, UK), Merck Chemicals (Merck KGaA, Darmstadt, Germany), Sigma-Aldrich® (Gillingham, UK) and VWR Chemicals (VWR International Ltd, Lutterworth, UK).

The enzymes were obtained from Bioline (London, UK), Invitrogen™ and Sigma-Aldrich®.

The kits for molecular biology were purchased from Bioline and Qiagen (GmbH, Germany).

2.1.2 Plant material

Several ecotypes of *Arabidopsis thaliana* (*At*) were used and these were as follows: Col-0, RMX-A02, Ws-0 (N6891), Wu-0 (N6897), Edi-0 (N6688), Po-0 (N6839), Bur-0 (N6643), Zu-0 (N6902), Ler-0 (NW20), Can-0 (N6660), Sf-2 (N6857), Ct-1 (N6674) and Hi-0 (N6736).

Arabidopsis thaliana mutant plants were used as well: Col-*rpp4*, Col-*bak1-5 bkk1-1* (Roux et al. 2011), Col-*bak1*-5, Col-*bkk1-1* and Wassilewskija-*eds1.1* (Ws-*eds1*; Parker et al. 1996) were available as lab stocks. Col-*sobir1* seeds were kindly provided by Prof T. Nürnberger (University of Tübingen, ZMBP Center for Plant Molecular Biology

Plant Biochemistry, Tübingen, Germany). Col-*pen1*, Col-*pen2*, Col-*pen3*, Col-*pen1 pen2*, Col-*pen2 pen3*, Col-*pen1 pen3* and Col-*pen1 pen2 pen3* were gently donated by Dr M. X. Andersson (University of Gothenburg, Department of Biological and Environmental Sciences, Göteborg, Sweden).

T-DNA mutant lines (see Section 5.2.2 and Appendix for a complete list of the genes ID, NASC and Salk Id and primers) were purchased from The Nottingham *Arabidopsis* Stock Centre (NASC, http://arabidopsis.info/).

Nicotiana benthamiana, *Nicotiana tabacum*, *Cucumis sativum* (cucumber), *Solanum lycopersicum* (tomato), *Ocimum basilicum* (basil) and *Petroselinum crispum* (parsley) were available as lab stocks.

The plants were grown in a growth room at 20 ºC and with 14 h light and 10 h dark regime (Lumilux Cool White L36W/840, Osram, Munich, Germany).

2.1.3 Pathogen isolates

The pathogen that has been extensively used throughout this study is the biotrophic oomycete pathogen *Hyaloperonospora arabidopsidis* (*Hpa*) (Holub et al. 1994). The main focus was on the well-known and sequenced isolate *Hpa*-Emoy2.

Other isolates of the pathogen used during the study were *Hpa*-Cala2, *Hpa*-Noks1 and *Hpa*-Maks9.

2.1.4 Bacterial strains

- *Escherichia coli* (*E. coli*) ElectroSHOX Competent Cells (Bioline) to subclone and propagate the plasmids.
- *Agrobacterium tumefaciens* strain GV3101 (available as lab stock) to stably or transiently transform plants with the desired gene (Sections 2.2.1.9 and 2.2.1.10).
- Chemically competent *E. coli* BL21 (DE3) pLysE (Bioline) for protein expression in bacteria (Section 2.2.2.8).
- Chemically competent DB3.1™ *E. coli* (Bioline), to propagate empty Gateway® vectors.

2.1.5 Plasmid vectors

During the project different vectors have been used. The majority uses the Gateway® Cloning Technology (Invitrogen™, UK; Earley et al., 2006):

- pDONR™/Zeo used as entry vector (Figure 2.1)

- pEarlyGate100 used for protein expression in planta (pEG100; Figure 2.2)

- pEarlyGate103 used for fusion protein (GFP-6xHis) expression in planta (pEG103; Figure 2.2)

- pDest™17 used for fusion protein (6xHis) expression in bacteria (Figure 2.3)

- pGR106::CBEL (Cellulose-Binding Elicitor Lectin) from *Phytophthora parasitica var. nicotianae* (*Ppn*) was kindly donated by Dr E. Gaulin (Université de Toulouse, Laboratoire de Recherche en Sciences Végétales, Toulouse, France) and used to amplify the gene to be used as a positive control in the experiments.
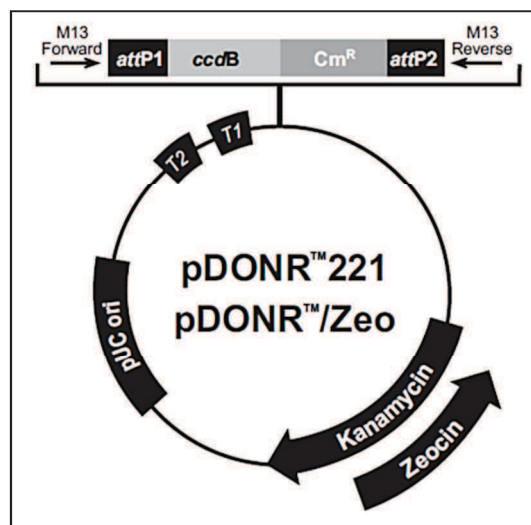
Figure 2.1 pDONR™/Zeo vector map. In the vector backbone are present the pUC origin of replication (pUC ori), the gene conferring resistance to the antibiotic Zeocin™ and the T1 and T2 transcription terminators, to avoid unwanted expression of the cloned gene. In between the two recombination sites for the Gateway® Cloning (attP1 and attP2) there are the *ccdB* killer gene, for the negative selection of the plasmid and the chloramphenicol resistance (Cm^R) gene. Right outside the two recombination sites, there are the M13 forward and reverse priming sites, to allow an easy sequencing of the cloned gene (Invitrogen™, UK).
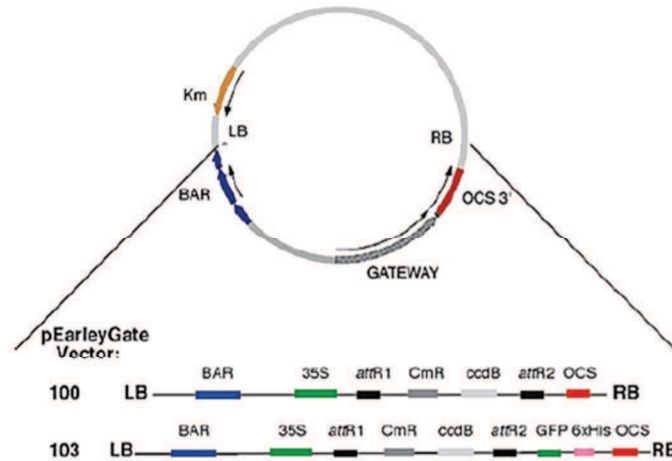
Figure 2.2 pEarleyGate 100 and 103 vectors organisation. In the picture is shown the organisation of the two pEarleyGate vectors used: pEG100 and pEG103. In the plasmid backbone they both carry a Kanamycin resistance (Km). The vectors are binary vectors and they both have left (LB) and right (RB) borders for *Agrobacterium*-mediated T-DNA transfer. From the LB: BASTA herbicide resistance gene (*BAR*) for transgenic plants selection, cauliflower mosaic virus promoter (35S), attR1 site (Gateway recombination), chloramphenicol resistance gene (CmR), *ccdB* killer gene, attR2 site (Gateway recombination) and the 3' octopine synthase gene (OCS). In pEG103 are present the sequences for the green fluorescent protein (GFP) and for a tag of 6 histidines (6xHis) (image adaptation from Earley et al., 2006).
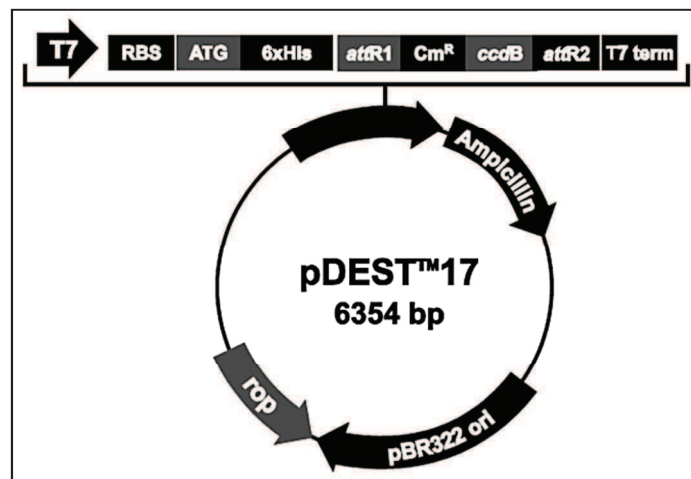
Figure 2.3 pDest™17 vector map. In the vector backbone there are an ampicillin resistance gene, the pBR322 and the rop orf for the low copy replication and maintenance of the plasmid in *E. coli*. There is also a bacteriophage T7 promoter, followed by a ribosome-binding site (RBS), an ATG initiation site and a sequence for the 6xHis tag at the N-terminal of the protein. Following the sequence for the tag, there are the two recombination sites (AttR1 and AttR2) for the insertion of the gene of interest using the Gateway® technology. In between them there are a chloramphenicol resistance (Cm^R) gene and the killer gene *ccdB*. Finally there is the bacteriophage T7 transcription termination region (Invitrogen™, UK).

2.2 Methods

2.2.1 Molecular Biology

2.2.1.1 DNA extraction

To isolate DNA, both from plant tissues and *Hpa* (*Hpa*-infected Ws-*eds1* plants were used), the DNeasy® Plant Kit (Qiagen) was employed. All the procedures were carried out according to the manufacturer's instructions.

2.2.1.2 Polymerase chain reaction (PCR)

To amplify the genes of interest, the Elongase® Enzyme Mix (Life Technologies™) was used. The reaction (1 µl DNA, 2.5 µl dNTP 10 mM, 0.5µl each primer, 1µl buffer A, 4µl buffer B, 1 µl Elongase® Enzyme Mix, 14.5 µl PCR grade water) was set up following the manufacturer's instruction. The three-step cycling was adopted and the annealing temperature was adjusted accordingly to the primer pair used. The amplification reaction was checked by loading 5µl of the products on 1% agarose (UltraPure™ Agarose, Invitrogen™) gel in 1X TAE buffer (Omega Bio-Tech Inc, Norcross, GA, USA) added of 1:10000 GelRed™ stain (Biotium Inc., Hayward, CA, USA). To load the samples 1X DNA Loading Buffer Blue (Bioline) was added to each sample. The gel was then visualized using BioSpectrum® - MultiSpectral Imaging System (UVP, Upland, CA, USA), set on fluorescent light (EtBr) and the related VisionWorks LS Software.

2.2.1.3 PCR to exchange the signal peptide

To replace the *Hpa*-801903 (CBEL03) and *Hpa*-801904 (CBEL04) signal peptide with the one belonging to the *Arabidopsis thaliana* Pathogenesis-related protein 1 (PR1) (see the Appendix for the DNA sequences), the sequences were amplified using the enzyme Elongase® Mix (Section 2.2.1.2), according to the manufacturer's instructions (three-step PCR procedure).
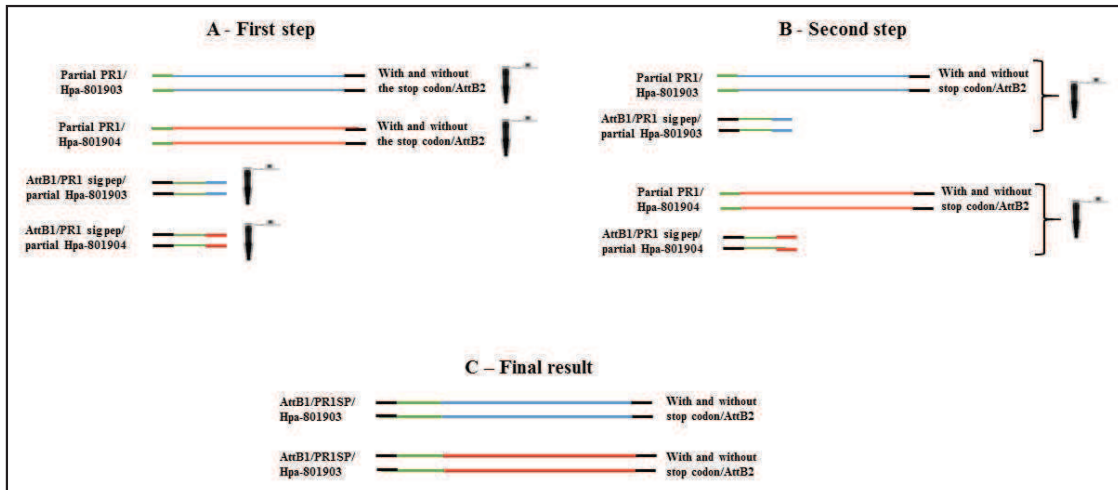
Figure 2.4 PCR procedure to replace the *Hpa*-801903 and *Hpa*-801904 endogenous signal peptides with PR1 signal peptide. To exchange the signal peptide belonging to the proteins CBEL03 (blue lines) and CBEL04 (red lines) with the one belonging to the PR1 protein (green lines), a two-step procedure was used. In the first step (A), the three sequences were amplified using selecting primers to obtain: the two CBEL proteins with the signal peptide replaced by the final portion of PR1 signal peptide and an AttB2 sequence at the end, while the PR1 signal peptide was amplified to carry in one case the initial portion of the protein CBEL03 and in the second case with the initial portion of the protein CBEL04. In both cases, the AttB1 sequence is at the beginning of the amplicons. In the second step (B), the two corresponding amplicons (CBEL03 and PR1 with partial CBL03/CBEL04 and PR1 with partial CBEL04) were mixed together in an PCR reaction in order to finally ligate them and obtain (C) the final outcomes: the two CBEL sequences (*Hpa*-801903 and *Hpa*801904) with the endogenous signal peptide substituted by the PR1 signal peptide, with AttB1 and AttB2 sequences at the beginning and at the end for the following Gateway® cloning procedure.

To obtain the final result, the first PCR reaction (Figure 2.4, A) was performed using tailored primers (see the Appendix). After the PCR reaction was completed, the mixture was loaded on a 1% agarose gel to check the size of the amplicons and if correct, the bands were excised and the products cleaned using the MinElute® Gel Extraction Kit (Qiagen) following the manufacturer's instructions. In the second step, a new PCR was set up using the Elongase® Enzyme Mix. In this case, the 1 μl DNA of the mix was composed, as shown in Figure 2.4 (B), by the PR1 signal peptide amplicon (0.5 μl) and the corresponding CBEL amplicon (0.5 μl). Once again, a three-step cycling was adopted but with different settings than the previously used: 94 ºC for 4 min / 94 ºC for 30 sec, 5 cycle of touch down from 65 ºC to 60 ºC, 68 ºC for 1 min / 94 ºC for 30 sec, 60 ºC for 30 sec, 68 ºC for 1 min for 30 cycles. Once again the PCR products were fully loaded on 1% agarose gel and afterwards selected according to the correct size. The bands were excised and cleaned using the Minelute® Gel Extraction Kit. The final and

cleaned products were then cloned into the appropriate final vectors (pEG100: amplicons with the stop codon, pEG101: amplicons without the stop codon) using the Gateway® Cloning Technology (Section 2.2.1.5).

2.2.1.4 PCR to screen T-DNA mutant lines for homozygosis

To identify the homozygous plants between the seeds purchased from NASC, the REDExtract-N-Amp™ Plant PCR Kit (Sigma-Aldrich®) was used. In brief, 5-10 plants were grown for each T-DNA mutant line. A core leaf was cut off using the lid of a 1.5 ml centrifuge tube and the extraction/reaction was carried out following the manufacturer's protocol. The results were visualized on a 2% agarose gel (see Section 2.2.1.2) and analysed according to the instructions available online on the NASC website.

2.2.1.5 Gene cloning using Gateway® technology

Plasmids for both bacterial protein expression (pDest™17 vector) and in planta expression (pEarlyGate100, pEarlyGate101 and pEarlyGate103) were employed. The Gateway® pDONR™/Zeo vector was used as donor vector. The enzymes used for the two-steps-reaction cloning were the Gateway® BP Clonase® Enzyme Mix and the Gateway® LR Clonase® Enzyme Mix. The procedures were carried out following the manufacturer's protocol.

Briefly, to clone the gene of interest into the expression vector, a two-step-cloning was carried out. Firstly, ~100 ng of AttB-PCR product (containing the AttB1 and the AttB2 sequences, see the Appendix) were mixed with 1 µl pDONR™/Zeo vector and a variable quantity of EB buffer (pH 8.0) to bring the mixture up to 8 µl total. 2 µl of BP Clonase® were added to the previous mixture. The reaction was incubated at 25 ºC for an hour and terminated by adding 1 µl of 2 µg/µl Proteinase K solution and incubating it at 37 ºC for 10 min.

The cloned vector was then transformed into ElectroSHOX *E. coli* (Section 2.2.1.6) and after the selection on a selective media, a colony was picked and the plasmid extracted (Section 2.2.1.8) for the second step of the Gateway® cloning procedure. To complete the cloning, 1 µl of the pDONR™/Zeo vector containing the gene of interest was mixed with 1 µl of the final destination vector (depending on the purpose, Section 2.1.5) and 2

µl of the Gateway® LR Clonase® enzyme. The mixture was incubated at 25 ºC for an hour and terminated by adding 1 µl of 2 µg/µl Proteinase K solution and incubating it at 37 ºC for 10 min. Afterwards the vector was cloned in ElectroSHOX *E. coli* and selected as described in Section 2.2.1.6.

After the final plasmid extraction (Section 2.2.1.8) the plasmid was cloned into the final bacterial host (depending on the purpose) according to the procedure in Section 2.2.1.6.

2.2.1.6 Bacterial transformation

Depending on the purpose, different competent bacterial cells and transformation methods were used.

To amplify the product of a gene cloning procedure, the plasmid of interest was transformed via electroporation into ElectroSHOX Competent Cells (Bioline). Briefly, 20 µl of *E. coli* electro-competent cells were mixed with 1 µl of the plasmid carrying the gene of interest and kept on ice for 1 min. The mix was then transferred to a cold electroporation cuvette (1 mm Gap, VWR International Ltd.) and immediately electroporated using a Bio-Rad MicroPulser™ (Bio-Rad Laboratories, Inc. – Hercules, USA) set on Ec1 (settings for *E. coli*, 0.1 cm cuvette, 2.5 kV, 1 pulse). The cells were successively recovered in 250 µl of SOC medium (2% (w/v) Tryptone, 0.5% (w/v) yeast extract, 10 mM NaCl, 2.5 mM KCl, 10 mM $MgCl_2$, 20 mM Glucose; the first four ingredients were added to water and autoclaved for 15 min at 121 ºC and afterwards the remaining two sterile ingredients were added to complete the formulation) and incubated at 37 ºC, in agitation at 200 rpm for an hour. Finally, they were plated on a selective LB agar plate and incubated at 37 ºC overnight.

To transform plants (stably or transiently) with the desired gene, electrocompetent *A. tumefaciens* strain GV3101 was selected. In brief, 50 µl of electrocompetent Agro cells were mixed by stirring with 2 µl of plasmid and left on ice for 1 min. They were then transferred to a cold cuvette (VWR) and they were transformed using the same above protocol. They were recovered and incubated for an hour in 250 µ of SOC at 28 ºC in agitation at 250 rpm, and afterwards they were plated on a selective LB agar plate and incubated overnight at 28 ºC.

With the aim of expressing proteins, *E. coli* BL21 (DE) Competent Cells (Bioline) were used. The bacteria were chemically transformed using the following procedure: 20 µl of bacteria were mixed, by stirring, with 1 µl of plasmid and incubated for 30 min on ice. Subsequently they were transferred in a 42 ºC water-bath for 30-45 sec and immediately transferred back on ice for 2 min. They were recovered by incubation at 37 ºC for an hour in 125 µl SOC media and then plated on a selective LB agar plate and incubated overnight at 37 ºC.

To propagate an empty Gateway® vector, DB3.1™ *E. coli* (Bioline) resistant to the CcdB were used. They were transformed via electroporation following the same procedure used to transform ElectroSHOX *E. coli.* They were previously made electrocompetent (see Section 2.2.4.1).

2.2.1.7 Colony PCR

To confirm the bacterial transformation with the cloned vector, colony PCR was performed using Biomix™ (Bioline) as enzyme.

A master mix was prepared using 10 µl Biomix™, 1 µl forward primer, 1µl reverse primer and 8 µl of ultrapure water for each colony to be screened. Each individual colony was picked with a sterile tip and dissolved into the PCR solution. The PCR reaction was carried out with the following three-step cycling conditions: 94 ºC for 5 min / 94 ºC for 30 sec, 10 cycles of touchdown with temperature selected according to the primers used , 72 ºC for 1 min per 1 kb / 94 ºC for 30 sec, 57 ºC for 30 sec, 72 ºC for 1 min for 25 cycles. The PCR products were finally loaded on a 1% agarose gel (see Section 2.2.1.2) to verify the presence of the band corresponding to the cloned gene of interest.

2.2.1.8 Plasmid extraction

All the plasmid extractions were performed using the QIAprep® Miniprep Kit (Qiagen) following the manufacturer's instructions.

2.2.1.9 Transient transformation of *N. benthamiana*

To transiently transform *N. benthamiana* with the gene of interest, cultures of *A. tumefaciens* (strain GV3101) were grown overnight at 28 ºC at 250 rpm.

In detail, *A. tumefaciens* harbouring the vector pEG100 or pEG103 transformed with the desired gene and, as a control, empty Agro and Agro transformed with the empty vector were grown overnight in 10 ml selective LB broth. Successively, the bacteria were pelleted at 3050 g at RT for 5 min. The medium was discarded and the bacterial pellet was resuspended into 10 ml of autoclaved 10 mM $MgCl_2$. The OD_{600} was measured and the bacteria were diluted to reach the same concentration (OD_{600}= 0.5 or 0.25) adding 10 mM $MgCl_2$ where necessary. Using a 1 ml needleless syringe the bacteria were pressure injected into fully expanded *N. benthamiana* leaves. $MgCl_2$ was pressure injected as a control. The plants were transferred in a growth room with a photoperiod of 14 h light/10 h dark at 20 ºC for maximum a week and were checked daily for altered phenotype that may be caused by the expression of the investigated protein.

2.2.1.10 Stable transformation of *A. thaliana*

To stably transform *Arabidopsis thaliana* with the gene of interest, Col-0 plants were grown in large pots (2-4 per pot) until new flowering bolts were visible. *Agrobacteria* carrying the desired gene were grown overnight in 10 ml selective LB broth at 28 ºC in agitation at 250 rpm. The 10 ml culture was then transferred into 250 ml of fresh selective LB broth and grown overnight at 28 ºC in agitation at 250 rpm. Subsequently they were pelleted and resuspended in 250 ml 5% sucrose and 50 µl of Silwet L-77 (Momentive™, Stanlow, UK). The plants were then dipped into the solution for 30-60 sec (floral dipping) and incubated overnight on the bench. They were finally transferred to a growth room at 20 ºC with a photoperiod of 14 h and 10 h dark until the seeds collection.

2.2.1.11 Selection of the transformants

To select the transformed seeds after the floral dipping procedure, BASTA® non-selective herbicide (glufosinate-ammonium, Bayern, Hawthorn East, Australia) was used.

A 0.1% BASTA® solution was used to evenly wet the soil (Levington Seed and modular plus sand compost, Everris Ltd., Ipswich, UK). The seeds were then uniformly distributed all over, covered and left to stratify for a week at 4 ºC in the dark. They were then transferred to a growth room with a long day light cycle (14 h light/10 h dark) and

successively the surviving plants (bright green and distinctly bigger than the rest) were transferred to new soil, clear from the herbicide and let growing until the seed stage. After the seed collection, the procedure was repeated once again, until the F_2 population.

To further select the homozygous seeds of the F_2 population, ~15 seeds for each line were sown again on BASTA-treated soil (using the same procedure seen above). After two weeks the surviving plants (bright green) were counted against the dead ones (pale green). The lines where all the plants survived the BASTA selection (thus stopped segregating) where considered homozygous and used for the following experiments.

2.2.2 Biochemical

2.2.2.1 Protein extractions

Different methods have been used to extract proteins (in the form of a crude extract) from, healthy and *Hpa* infected *At* tissues, and from *Hpa* spores.

Cold water method

To extract proteins from plant tissues, a modified protocol from Roux et al. 2011 was used. Healthy or *Hpa*-Emoy2 infected 2-week-old *Ws-eds1* plants were harvested and ground in liquid nitrogen. Five ml of cold sterile distilled water (sdH$_2$O) were added to the frozen powder and mixed thoroughly by vortexing. The solution was, subsequently, filtered using Miracloth filter paper (Calbiochem®, Merck KGaA, Darmstadt, Germany) in order to eliminate all the plant debris. The aqueous part was then centrifuged for 15 min at 425 g, the supernatant was discarded and the pellet resuspended in 3 ml of sdH$_2$O. The extract was further heated at 95 ºC for 10 min and finally stored at -20 ºC for further use.

PBS (phosphate buffer saline) extraction

A second method to obtain protein extracts was taken from Gabor et al. (1993) and modified as follows: 2-week-old *Hpa* (Emoy2) infected or healthy *Ws-eds1* plants were ground to a powder in liquid nitrogen using pestle and mortar. The frozen powder was then transferred to a micro centrifuge tube and then, 2 ml of cold and sterile 1× PBS was added, and mixed vigorously by vortexing. The mixture was centrifuged at 8500 g

for 5 min to remove insoluble components and the supernatant was collected and used as crude extract.

Autoclave

This extraction method was taken and modified from Thuerig et al. (2006). It was used to extract proteins both from *Hpa* spores and healthy or *Hpa*-infected *At* tissues.

Frozen *Hpa* spores were defrosted on ice and subsequently resuspended in 1 ml sdH$_2$O. The suspension was transferred to a glass beaker and 9 ml of sdH$_2$O were added. The prepared spores were successively autoclaved at 126 ºC for about 15 min at a pressure of 1.5 bar. The autoclaved spores were then stirred and the mixture was aliquoted to micro centrifuge tubes and centrifuged at 18500 g for 5 min at RT to remove all the debris. The supernatant was collected without disturbing the pellet and stored at -20 ºC until further use.

The same procedure was applied to plant tissues except for the sample preparation: 2-week-old cotyledons, healthy or *Hpa* (isolate Emoy2, 7 dpi) infected, were harvested and frozen in liquid nitrogen. They were either ground or directly put in a beaker containing 10 ml sdH$_2$O. They were then autoclaved following the same identical steps as above.

Extraction buffer

This method of extraction was applied both to *Hpa* spores and *At* tissues with some differences, depending on the nature of the sample. The method is based on the use of an extraction buffer (20 mM Tris-HCl pH 8.0, 1 mM EDTA, 100 mM NaCl, 0.125% Triton X-100) applied to the ground sample in order to extract proteins from the tissues.

With the aim of getting proteins from *Hpa* spores, a modified protocol from Prigneau et al. (2000) was used. Frozen spores were thawed on ice; 6 ml of cold and filtered-sterilized (0.20 μm Minisart® - Sartorius Stedim Biotech filter) extraction buffer were added along with 800 mg of glass beads, acid-washed 425-600 μm (Sigma-Aldrich®). The mixture was agitated on a vortex, at maximum speed for a total of 5-10 min (with intervals of 30 sec vortexing and 30 sec on ice to cool down the sample). After the extraction procedure, the suspension was centrifuged at 3200 g at 4 ºC for 5 min, in

order to collect the supernatant. The same procedure was repeated two more times and subsequently the extracted fractions were pooled together and filtered from any debris and sterilised using a 0.20 μm filter. The extract was frozen in liquid nitrogen and stored at - 20 ºC for further purpose.

A similar procedure was applied to plant tissues with some differences on the sample preparation. The cotyledons from infected and non-infected 2 week-old seedlings were harvested (one week after the infection in the case of *Hpa* infected tissues) and immediately frozen in liquid nitrogen. They were then ground to a powder using pestle and mortar in liquid nitrogen. The fine frozen powder was then transferred to a Falcon tube and immediately 6 ml ice-cold sterile extraction buffer were added, and the extract was vortexed vigorously at a maximum speed. Afterwards, the solution was kept on ice for at least 40 min and vortexed from time to time, in order to keep the solution as suspension. The mixture was then centrifuged at 3200 g at 4 ºC for 10 min to pellet cellular debris. The supernatant was collected without disturbing the pellet and the extraction procedure was repeated for a second time by the addition of 6 ml of extraction buffer. After the second extraction the extracts were combined, filter-sterilized using a 0.20 μm filter, frozen in liquid nitrogen and stored at - 20 ºC for future use.

2.2.2.2 Protein quantification

The protein quantification was carried out using the Bradford Assay (Bio-Rad Laboratories) and Bovine Serum Albumin (BSA) as the standard, according to the manufacturer's instructions.

Alternatively, the proteins were quantified using the NanoDrop 2000c Uv-Vis Spectrophotometer (Thermo Fisher Scientific), using the tool Protein280 on the pedestal mode.

2.2.2.3 Protein fractionation

To fractionate the extracts obtained from *Hpa* spores and healthy and *Hpa* infected *At* tissues, 1 ml manual HiTrap Q HP (GE Healthcare Life Sciences, Buckinghamshire, UK) strong anion exchange columns were used.

The samples were prepared by desalting using a PD 10 Desalting column (GE Healthcare) following manufacturer's instructions and filter-sterilizing using a 0.20 μm filter afterwards. For the fractionation procedure the buffer of choice (start buffer) was 20 mM Tris-HCl, pH 8.0, whereas the elution buffers were prepared adding increasing quantities of NaCl (0.1M, 0.15M, 0.2M, 0.25M, 03M, 0.35M, 0.4M, 0.45M, 0.5M, 0.55M) to the start buffer. The regeneration buffer (suggested by the manufacturer to completely clean the column after use) was produced by adding NaCl to the start buffer to a concentration of 1M. The column was prepared for use following the purification protocol while the sample was applied and eluted following the elution with stepwise ionic strength gradient protocol, both supplied by the manufacturer.

To recover a good yield of proteins, the 4 ml fractions where precipitated overnight with 4 volumes of cold acetone at - 20 ºC. Subsequently the samples were centrifuged at 3200 g at 4 ºC for 15 min. The acetone was discarded and the pellet was air-dried and finally resuspended in an adequate amount of extraction buffer.

2.2.2.4 Reactive oxygen species accumulation assay

To determine the production of Reactive Oxygen Species (ROS), a modified assay from Felix *et* al., (1996) was used. Briefly, 6 core leaves, for each treatment, were excised using a 5 mm cork-borer from 4 to 5-week-old *At* plant fully expanded leaves and they were shaken for 30 min in 1 ml 1X Murashige and Skoog (MS) buffer at room temperature. They were subsequently placed in a 96-well plate, one for each well, which was previously filled with 50 μl 1X MS buffer whereas the edges were filled with sdH$_2$O in order to avoid evaporation. The treatments were then added (the amount of protein added was always normalized between the treatments, in order to add the same amount of protein each time), including positive (20 μl 0.2M horseradish peroxidase in sodium phosphate buffer) and negative (sdH$_2$O and sterile extraction buffer) controls. After sealing the plates, they were shaken overnight (14-16 hours) at 500 rpm, keeping the lights on. A developing solution was prepared by adding 10 mg of 5-aminosalycilic acid to 10 ml of heated (70 ºC) sdH$_2$O. After leaving the solution to cool down, the pH was adjust to 6 using 1M NaOH and just before adding it to the wells, 100 μl of 1% H$_2$O$_2$ were added to the solution. The assay was developed by the addition of 100 μl of developing solution to each well. The absorbance at 450 nm was read just after the

addition of the developing solution using a Biotek EL800 Microplate reader (Biotek, Potton, UK).

2.2.2.5 Callose deposition assay

To visualise the formation of callose deposits, a method from Nguyen et al. (2010) was used. In brief, fully expanded 6-8 week-old *At* (Col-0 accession) and *N. benthamiana* leaves were pressure injected using 1 ml needleless syringe (Terumo) with *Hpa* spore extracts, healthy and *Hpa* infected *At* tissue extracts. SdH$_2$O and sterile extraction buffer were used as a negative control, while 100 nM flg22 was used as a positive control. The concentration of the extracts was adjusted at 0.6 mg/ml. Leaf disks were excised after 6, 12 and 24 hours and placed into wells of a 25-well plate. They were destained from chlorophyll by adding 2 ml 95% ethanol in each well. The plate was incubated at 37 ºC and the ethanol replaced at necessity until chlorophyll was completely removed. After the leaf disks were completely cleared from the pigment, they were washed once with 70% ethanol and three times with sdH$_2$O. Following the washing step, they were placed into a new 25-well plate and added of the callose staining solution (1% aniline in 150 mM K$_2$HPO$_4$, pH adjusted to 9.5 with KOH) and incubated for 30 min to 1 hour for *At* and *N. benthamiana*, respectively. Subsequently, the disks were placed on glass microscope slides with 60% glycerol and examined for any fluorescence using a Leica CTR5500 microscope under ultraviolet light.

2.2.2.6 SDS-PAGE gels preparation

Proteins were separated using SDS-PAGE gels (Laemmli, 1970). Resolving gels were at 12.5% acrylamide, while the stacking gels were prepared at 4% acrylamide; the list of ingredients is given in Table 2.1. In brief, the resolving gel mixture was poured between two glasses (with 1 mm spacer). SDS at 0.1% solution was added on top of it to flatten the surface of the polymerizing gel and it was left to set at room temperature, on the bench for about an hour. Afterwards, the 4% acrylamide stacking gel was prepared, the 0.1% SDS solution was removed from the gel and the stacking gel was poured on the top of the resolving gel. The comb was immediately inserted and the gel was once again left to set. The tank (Bio-Rad MiniProtean® Tetra System) was filled with 1X running buffer (25 mM Tris-HCl, 0.192 M Glycine, 0.1% (w/v) SDS) and the gel was allocated

into the support after the removal of the comb. The samples were prepared by adding 5X SDS reducing sample buffer (60 mM Tris-HCl, pH 6.8, 25% (w/v) glycerol, 2% (w/v) SDS, 10% (v/v) 2-mercaptoethanol, 0.1% (w/v) bromophenol blue) and boiling them for 2-3 min. They were briefly centrifuged and the soluble part was loaded on the gels. The gels were run at 25 mA at first and then the run was completed at 50 mA, until the dye was run off the gel. The protein marker (PM) used was HyperPAGE Prestained Protein Marker (Bioline).

Table 2.1 Ingredients used in the preparation of 12.5% acrylamide resolving gel and 4% acrylamide stacking gel.

Ingredients	Resolving	Stacking
Water	1.785 ml	3.05 ml
Buffer	1.875 ml	1.25 ml
20% (v/v) SDS	37.5 µl	50 µl
30% Acrylamide/Bis-Acrylamide (37:5:1)	3.0 ml	650 µl
TEMED	3.7 µl	5 µl
10% (w/v) APS	37.5 µl	25 µl

The buffer used in the preparation of the resolving and stacking gel were 1.5 M Tris pH 8.8 and 1 M Tris pH 6.8, respectively.

2.2.2.7 Gel staining, destaining and visualization

In order to visualise the proteins on the SDS-PAGE gel, the gel was placed into a staining solution (0.1% (w/v) Coomassie Blue R-250, 45% (v/v) methanol, 10% (v/v) acetic acid) from 5 h to overnight in agitation at 25 rpm. When the bands were clearly visible on the gel, it was de-stained by exchanging the staining solution with a de-staining solution (10% (v/v) methanol, 10% (v/v) acetic acid) in agitation at 25 rpm until the gel was completely cleared off from the dye.

The gel was afterwards visualised using the BioSpectrum® - MultiSpectral Imaging System set on white light.

2.2.2.8 Protein expression

To express the oomycetal CBEL proteins from *Ppn* (X97205) and *Hpa* (*Hpa*G801903 and *Hpa*G801904) the *E. coli* strain BL21 (DE) Competent Cells (Bioline) was chemically transformed as described in Section 2.2.1.5 with the expression vector pDest™17 (see Section 2.2.1.4 for the cloning procedure).

For each protein expression the following procedure was followed: one colony was picked from a selective plate and dissolved into 10 ml of selective LB medium. The culture was incubated overnight at 37 ºC in agitation (~160 rpm). 2 ml of the culture were afterwards transferred into 250 ml of fresh LB medium (selective) and agitated at 37 ºC at 160 rpm until they reached OD_{600}= 0.4 - 0.6. 50 ml of non-induced culture were collected and pelleted at 3050 g for 20 min and then frozen at -20 ºC. The remaining 200 ml of culture were induced by the addition of isopropyl β-D-1-thiogalactopyranoside (IPTG, Sigma Aldrich®) to a final concentration of 1 mM. During the induction period the temperature was lowered at 18 ºC while the agitation was kept at 160 rpm.

To establish the expression timing, a sample of 10 ml of culture was collected every hour for a total of 4 h, while the remaining culture was left to induce overnight and the sample was collected the following morning. All samples were pelleted at 3050 g for 20 min and frozen until further use.

2.2.2.9 Recombinant protein recovery

Lysis of the bacterial cells

The frozen bacterial pellet (10 ml culture) was ground in liquid nitrogen with pestle and mortar to a fine powder. The obtained powder was then transferred to a micro centrifuge tube and added of 1 ml Lysis buffer (40 mM Tris-HCl, pH 8.0, 0.5 % Tween-20, 0.5% Triton X-100, 25 mM sucrose, 5 % glycerol) and 1 µl (25 U/µl) of Benzonase® Nuclease (Novagen®, Merck KGaA) and vortexed thoroughly until all the visible DNA was dissolved. The samples were kept in agitation at 1000 rpm for 20 min. The samples were afterwards centrifuged at 20000 g for 20 min. The resulting supernatant was transferred to a new tube and added of 5 % glycerol and stored at -20 ºC for further analysis.

When processing larger samples the amount of Lysis buffer and Benzonase ® Nuclease were increase accordingly.

Inclusion bodies preparation and solubilisation

The pellet resulting from the previous step was further processed in order to clean and then solubilize the possible inclusion bodies.

The pellet was washed with 1 ml of Wash buffer (40 mM Tris-HCl, pH 8.0, 2 % Triton X-100, 2 M Urea) by pipetting and further vortexing. It was centrifuged at 7000 g for 10 min. The supernatant was discarded and the wash step was repeated once more. The pellet was finally resuspended in about 10 volumes of Solubilisation buffer (40 mM Tris-HCl, pH 8.0, 0.5% Triton X-100, 8 M Urea) by thorough pipetting and brief vortexing. The solution was centrifuged at 22000 g for 10 min. The supernatant was collected and stored at -20 ºC for further use.

2.2.2.10 Dot blot assay

To quickly check the presence of the recombinant protein in both the soluble and insoluble (inclusion bodies) fractions at different time points, the extracts obtained with the previously seen methods (Section 2.2.2.9) were screened on a dot blot assay.

The protocol used was the one suggested in the QIA*express*® Detection and Assay Handbook (Protocol 5 - Preparation of dot blots and Protocol 8 - Immunodetection with Anti-His Antibodies or Anti-His HRP Conjugates, Chromogenic Method), with minor changes. Briefly the protein concentrations were normalized towards the lowest concentration and afterwards they were "dotted" (2 µl each) on a dry nitrocellulose membrane (0.45 µm - Bio-Rad Laboratories, Inc.). The membrane was left to air dry at RT for at least one hour and afterwards it was washed for three times (for 10 min each) with Tris-Buffered Saline (TBS) buffer (50 mM Tris-HCl, pH 8.0, 150 mM NaCl) in slow rotation. The membrane was then blocked for one hour in Blocking buffer (0.5 % (w/v) Blocking reagent, 1 X Blocking Reagent Buffer, 0.1 % (v/v) Tween 20 - the reagents were provided within the Penta·His™ HRP Conjugate kit - Qiagen). The Blocking buffer was then washed off with two wash steps (10 min each) in TBS-Tween 20 (TBS-T) buffer (TBS, 1 % Tween 20), followed by one wash step in TBS for 10 min. The membrane was then incubated for one hour at room temperature with Anti·His

HRP Conjugate Solution (Blocking buffer, 1:2000 Anti·His antibody coupled with horseradish peroxidase (HRP)). Afterwards three wash steps (10 min each) in TBS-T removed the non-bound antibody. The assay was developed with the application directly on the membrane (without rotation), of the chromogenic HRP substrate 3,3',5,5'-Tetramethylbenzidine (TMB) Liquid Substrate System for Membrane (Sigma-Aldrich®) for 5 - 15 min. The assay was stopped by washing the membrane twice with water.

2.2.2.11 Western Blot

To confirm the presence of the protein of interest in the bacterial extract (see Section 2.2.2.9 - Inclusion bodies), a Western Blot was performed.

Briefly, a 12.5% polyacrylamide gel (see Table 2.1 for the ingredients) was prepared and run as in Section 2.2.2.6. The gel was then equilibrated in pre-chilled (4 ºC) Transfer Buffer (25 mM Trizma Base, 1992 mM Glycine, 20 % Methanol, pH 8.3) for approximately 5 min, along with the nitrocellulose membrane, two filter papers and two fibre pads. The "sandwich" was then assembled in the following order: fibre pad, filter paper, gel, membrane, filter paper and fibre pad. A glass rod was rolled over the sandwich to eliminate any air bubbles and finally the cassette was sealed and placed into the apparatus chamber (Bio-Rad Mini Trans-Blot® Electrophoretic Transfer Cell) for the blotting. A frozen cooling block was inserted into the tank as well and the tank was then filled with cold Transfer Buffer. To help maintaining a low temperature, the tank was placed over a stirrer (200 rpm) and the buffer was continuously agitated throughout the blotting procedure. The Rapid Protocol from the Instruction Manual of the tank (Bio-Rad) was followed: 100 V (constant), 250-350 mA for 1 h. After the completed transfer, the immuno-detection was carried out as in Section 2.2.2.10.

2.2.2.12 Nitrocellulose membrane staining

To reversibly stain the total proteins blotted onto the nitrocellulose membrane, the Ponceau S stain (Sigma-Aldrich®) was used. The protein bands appear red on a clear background.

Briefly, a working solution containing 0.1% Ponceau S (w/v) in 5% acetic acid was made up. Around 50 ml of the solution were used to stain the membrane for 5 min. The

stain was afterwards discarded and the membrane was washed twice in distilled water to remove the excess stain. To destain the membrane, it was immersed in a 0.1 M NaOH solution for 1 min or until clear and afterwards thoroughly washed in distilled water. The immunodetection was then carried out as described in Section 2.2.2.10.

2.2.2.13 Recombinant protein purification

To purify the recombinant proteins expressed in *E. coli* BL21, the Ni-NTA Spin Columns or the Ni-NTA Agarose (Qiagen) were used. The resin is nickel-charged and allows the binding of His-tagged proteins.

Ni-NTA Spin Columns

The protein purification was carried out according to the manufacturer's instructions with minimal variations. Briefly, since the proteins were purified from the inclusion bodies using the Solubilisation buffer (Section 2.2.2.9), this buffer was used throughout the procedure as follows: in the first step of column equilibration instead of the suggested Denaturing lysis/Binding buffer; as a Wash buffer, added of 10 mM imidazole in substitution of the Denaturing Wash buffer suggested and finally as an Elution buffer, when added of 100 mM imidazole as an alternative to the Denaturing Elution buffer. The rest of the procedure was followed as suggested by the manual and a flow through (FT) fraction, together with two Wash and two Elution fractions were collected.

Ni-NTA Agarose

The resin was thoroughly resuspended (the resin is provided as a 50% slurry). Afterwards 500 µl (bead volume: 250 µl) were transferred to a new microcentrifuge tube and centrifuged at 3400 g for 1 min. The supernatant (storage buffer) was removed and discarded. The resin was equilibrated by mixing it with 1 ml of inclusion bodies solubilisation buffer (Section 2.2.2.9). The resin was once again centrifuged at 3400 g and the buffer was removed and discarded. The equilibrated resin was finally added to the inclusion bodies resuspension and incubated at RT on a shaker for 1 hour. After the binding step, the resin and the inclusion bodies suspension were centrifuged at 3400 g for 2 min. The supernatant was discarded and the resin was washed twice with 1ml of Wash buffer (Solubilisation buffer and 20 mM Imidazole), to remove the unspecific

bound proteins. To elute the His-tagged proteins from the resin, 500 µl of Elution buffer (Solubilisation buffer and 100 mM Imidazole) were thoroughly mixed with the resin by pipetting up and down multiple times and mixed for 30 min at room temperature. To obtain the eluate without any contamination from the resin, the mix was added to a Ni-NTA Spin Column (Qiagen) and centrifuged at 1500 g for 5 min. The eluate was stored at -20 ºC until further use.

2.2.2.14 Protein electro-elution

To further purify the recombinant proteins, the electro-elution technique was used.

The Ni-NTA Agarose purified proteins (~ 0.400 µg/µl) were loaded (15 µl in each well) on a SDS-PAGE gel (12.5%). The gel was run (Section 2.2.2.6) until the loading dye left the gel and afterwards it was removed from the glasses (Figure 2.5, A). The protein marker lane and one lane corresponding to the desired protein were cut off from the gel and stained with Coomassie Blue R-250 (Figure 2.5, B) using a fast protocol to reduce the staining and destaining time (by warming up in the microwave the staining and destaining solution for 20 sec at 100 W), to be used as a reference. The remaining gel was maintained in 1X Running Buffer. When the band corresponding to the protein of interest and the possible contaminants were visible on the gel, the gel portion was moved into running buffer to reacquire the original dimension (the methanol contained in both the staining and destaining solutions shrinks the gel). Once the two portions of the cut gel were of the same size they were put together and the gel fraction presumably containing the protein of interest was cut off from the un-stained gel using the stained portion as a position reference (Figure 2.5, C). The excised gel was further reduced to pieces and placed into the prepared Model 422 Electro-Eluter (Bio-Rad) assembled as suggested into the User's Manual. The membrane caps had a MWCO of 12000-15000 Dalton. The elution was carried out at 10 mA/glass tube used for a total of four hours. After the elution procedure, the membrane caps were carefully removed and washed, by pipetting up and down few times, using the elution buffer contained, in order to resuspend and remove the eluted proteins. The buffer was finally transferred to a new microcentrifuge tube and the solution containing the protein of interest was stored at -20 ºC until further use.
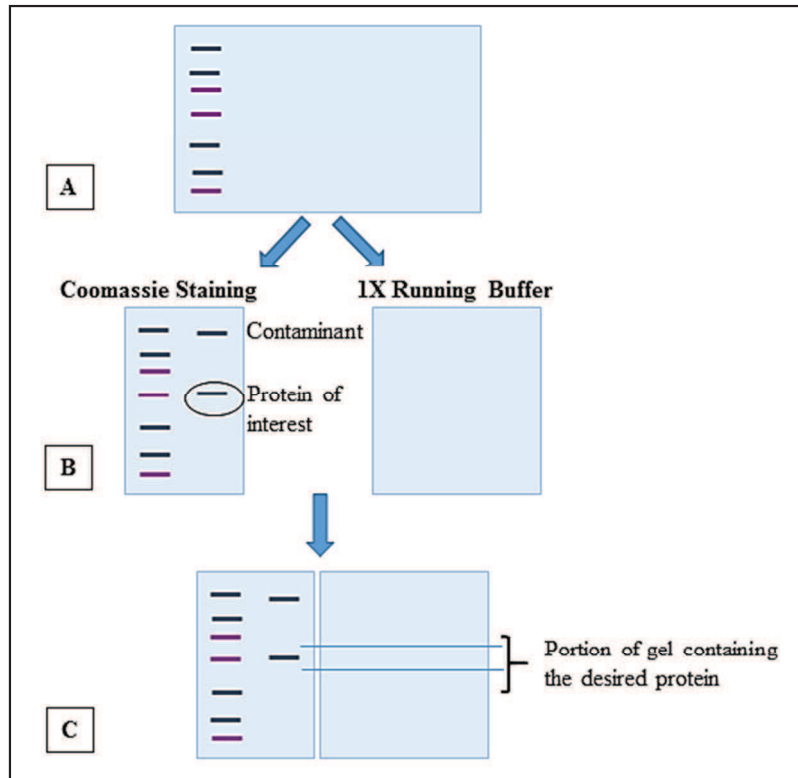
Figure 2.5 Electro-elution sample preparation procedure. To prepare the samples for the electro-elution procedure, the protein of interest was loaded on a SDS-PAGE gel (**a**). Subsequently, the gel was cut and the portion containing the protein marker and one lane of the protein of interest were stained in Coomassie Blue stain (**b**). Once the portion has been destained and the protein of interest appeared on the gel, the two portions of the gel were brought together so that it was possible to cut off the fraction containing the protein of interest (**c**).

2.2.2.15 Protein concentration

Following the electro-elution procedure, the recovered proteins were concentrated using the Pierce™ Concentrator, PES 10K MWCO, 0.5 ml (Thermo Scientific).

The samples were processed following the manufacturer's instructions. Briefly, the concentrator column was equilibrated by the addition of 500 µl of Elution buffer (used in the electro-elution procedure) and centrifuged for 2 min at 15000 g. The flow through was discarded and the column reservoir was emptied as well. Afterwards, 500 µl of the sample were added to the column and centrifuged at 15000 g for 5 min. The flow through was discarded and this step was repeated one more time (being the electro-eluted volume ~1 ml). The volume left into the column reservoir was about 75 µl and it was used to wash the membrane in order to release all the concentrated proteins. The

recovered proteins were transferred to a new microcentrifuge tube. The membrane was washed once again with an additional 25 µl of buffer. This second fraction was added to the previous one and stored at -20 ºC until further use.

2.2.2.16 Proteinase K treatment

The *Hpa* spore crude extracts were treated with Proteinase K (the enzyme was provided as part of the kit for the Gateway® cloning technology) in order to eliminate the proteins contained.

Briefly, 100 µl of the extract were added 0.5 µl of Proteinase K. The mixture was quickly vortexed to evenly distribute the enzyme and afterwards incubated at 50 ºC for 3 to 4 hours. The enzymatic reaction was stopped by 10 min incubation of the mixture at 95 ºC. 100 µl of extraction buffer, to be used as a control, were added of the same amount of Proteinase K and treated in the same way. The extracts and the control were then stored at -20 ºC until further use.

2.2.3 Plant pathology

2.2.3.1 Pathogen maintenance and infections

To maintain the infection, the pathogen was weekly sprayed on healthy one-week-old susceptible Ws-*eds1* plants. Briefly, the spores were collected from the previously infected seedlings by cutting the cotyledons covered in sporangiophores and putting them into a tube containing 20 ml of cold sdH$_2$O. The tube was subsequently shaken or vortexed in order for the spores to be released and afterwards the water containing the spores was filtered using Miracloth (Calbiochem®) to eliminate all the plant and soil debris. One-week-old Ws-*eds1* seedlings were then spray-inoculated with the previously collected spores and the transparent lid was sealed with electrical tape to maintain humidity inside of the tray. The tray was then incubated for a week at 16 ºC with a photoperiod of 12 h light/12 h dark.

2.2.3.2 *Hpa*-Emoy2 spore growth and collection

In order to grow and collect enough spores for the purposes of the study, Ws-*eds1* plants were grown until they were four-week-old. They were successively spray-inoculated with a suspension of *Hpa*-Emoy2 spores. The lids were then sealed over the trays to

maintain humidity inside and favour the growth of the spores. Since the plants were older than usual, the sporulation process took around 10 days. To collect the spores, leaves were collected in sterile cabinet and put into cold sdH$_2$O. The leaves were then washed thoroughly but gently to release the spores. The spore suspension was filtered using Miracloth (Calbiochem®) filter paper to eliminate all the leaves and soil. The spore suspension was finally repeatedly centrifuged to collect the spores. They were then stored at -80 ºC until further use.

As an alternative, a new "dry" method was adopted. The spores were grown following the same procedure seen above. The spores were then collected using a Cyclon Surface Sampler (Burkard Manufacturing Co. Limited, Hertfordshire, United Kingdom) connected to a pump, to collect the spores formed on a leaf (Figure 2.6). The spores were collected inside of a 1.5 ml tube placed at the bottom of the instrument. Afterwards, sterile cold water was used to wash the spores left inside of the instrument. They were added to the previously collected inside of the 1.5 ml tube and altogether washed with water and filtrated through a 70 µm Falcon™ Cell Strainer (Fisher Scientific, Waltham, Massachusetts, United States) to eliminate any debris. They were finally centrifuged at g for 5 min. The water was discarded and the spores were stored at -80 ºC for further use.

2.2.3.3 Counting sporangiophores

Different *A. thaliana* accessions or mutants (depending on the purpose of the experiment) were sown in 40 modules pot, three replicates each in a random way and grown for a week in a growth room at 20 ºC with a photoperiod of 14 h/10 h dark. Afterwards, one-week-old plants were spray-inoculated with *Hpa* conidiospores (different isolates were used for different purposes: Emoy2 and Cala2) suspended in cold sdH$_2$O at a concentration of 5×10^4 spores ml^{-1}. The infected plants were kept in sealed plastic containers in order to maintain the humidity in an incubator at 16 ºC with a photoperiod of 10 h light/14 h dark. One week after the infection the cotyledons were screened under a Wild Heerbrugg M3Z Stereozoom microscope (Gais, Switzerland, combined to a Schott KL 1500 electronic light source (Mainz, Germany)) to count the number of sporangiophores. 15 plants were chosen randomly and counted for each pot; two leaves per cotyledon was considered. The average number (and standard deviation)

was calculated for each accession or mutant and the plants were classified based on their tendency to develop the infection.

2.2.3.4 Spore counting (*Hpa*-Noks1 and *Hpa*-Maks9)

Col-0 plants are highly susceptible to the infection with the *Hpa* isolate Noks1. In order to count the sporulation on T-DNA line plants with Col-0 background and to assess any change in sporulation due to the knock-out of the gene of interest or to an over-expression, a different technique from the sporangiophores counting was adopted. In brief, the growth of the plants and the infection were carried out as stated in the previous paragraph. One week after the infection, the spores were counted. Fifteen plants were collected from each pot (3 pots for each mutant line) and placed into a 1.5 ml centrifuge tube containing 250 µl of sdH$_2$O. The tube was briefly vortexed and immediately 10 µl of water (containing the released spores) were loaded on a haemocytometer (LO-Labor Optik Ltd., Lancing, UK). The number of spores was counted placing the slide on a microscope stage (ML6520 PCM Asbestos Microscope, Meiji Techno UK Ltd., Axbridge, UK) under a 10× magnification lens. The four squares at the angles were considered and the average number of spores was calculated.

2.2.4 Microbiology

2.2.4.1 Electrocompetent *Agrobacteria* and *E. coli* DB3.1 preparation

A. tumefaciens (strain GV3101) were plated on a selective LB agar plate (Rif and Gen) and grown for 1-2 days (until colonies were visible) at 28 ºC, while *E. coli* DB3.1 were grown over night at 37 ºC on LB agar plate. The same procedure was carried out for both Agrobacteria and *E.* coli.

A colony was picked and placed in 20 ml LB broth (added of the required antibiotics where necessary) and grown overnight at 28 ºC/37 ºC at 250 rpm. 10 ml of the culture were then poured into a 100 ml of fresh LB broth (selective media) for about 4 h at 28 ºC/37 ºC (until the OD$_{600}$ value 0.7). The culture was then split into two cold 50 ml tubes and incubated for 20 min on ice. Subsequently the tubes were centrifuged for 15 min at 3050 g at 4 ºC; the media was discarded and the bacterial pellet was gently resuspended in cold sdH$_2$O. The water was then removed after centrifugation, for 15

min at 3050 g and 4 ºC. The washing step was repeated four more times, substituting sdH$_2$O with 10% cold and sterile glycerol in order to remove the salts. After the last centrifuge step, the glycerol was poured off and the two bacterial pellets were resuspended in 5 ml 10% glycerol and combined. They were further centrifuged for 10 min at 1700 g and 4º C, and following the discard of the supernatant they were resuspended in 1 ml 10% cold and sterile glycerol, aliquoted in 1.5 ml centrifuge tubes (50 µl each), frozen in liquid nitrogen and stored at - 80º C.

2.2.4.2 Bacterial glycerol stock preparation

In order to maintain and store a transformed strain of bacteria with the chosen gene, glycerol stocks were prepared.

One single colony picked from the selective LB agar plate, was grown overnight into 5 ml of LB broth added of the necessary antibiotics, at 250 rpm and 28 ºC or 37 ºC for *A. tumefaciens* or *E. coli*, respectively. The culture was then aliquoted into 1.5 ml centrifuge tube, 750 µl each and mixed with an equal amount of 50% sterile glycerol. The tube were subsequently frozen in liquid nitrogen and stored at - 80º C for further use.

2.2.5 Bioinformatics, statistics and image analysis

2.2.5.1 Primer design and sequence analysis

The bioinformatic work was mostly carried out using the software Geneious® version 6.1.2 (BioMatters Ltd., Auckland, New Zealand). The program was used to design primers, compare sequences, analyse sequencing results, prepare pictures by adding annotations and domains on the sequences and to design new sequences (*Hpa*-801903 and *Hpa*-801904 with a new signal peptide, see Section 2.2.1.3).

During the project, on-line resources were used as well. To perform sequence searches and comparisons, the genetic sequence database GenBank® was consulted, together with the Basic Local Alignment Search Tool, BLAST®. To look for the presence of signal peptides in the sequences of interest, the SignalP 4.1 Server software was used, along with WoLF PSORT Prediction, while the SMART tool was used for domain

prediction. Finally, to acquire more information on the *Hyaloperonospora arabidopsidis* 801903 and 801904 sequences, the website Ensembl Protist was used.

2.2.5.2 Statistical analysis and graphs design

To analyse the data and prepare graphs, the software Microsoft Excel 2010 (Microsoft, Redmond, Washington, United States) was used. In detail, the software was used to plot the data obtained from the experiments and mainly to calculate the average and standard deviation. The results were then used to produce histograms, to visually compare the outcomes.

To perform more advanced statistical analysis, Minitab 17 Statistical Software (Minitab Inc., State College, Pennsylvania, United States) was used. In brief, it was used to analyse the data, looking for any outsider to be excluded from the analysis, to perform T-Student tests and one-way ANOVA, to analyse the differences in the means of data sets, using the Tukey post-hoc test.

2.2.5.3 Image analysis

The image analysis was performed using the image processing program ImageJ (http://imagej.nih.gov/ij/).

The program was used to count the number of callose deposits in *N. benthamiana* leaves and the number of *Arabidopsis* rosette leaves in over-expressing plants.

Chapter 3

Hpa-derived PAMPs and their receptors in *Arabidopsis*

Abstract

The *Arabidopsis*/*Hpa* pathosystem has been extensively used in many studies and many effector molecules have been discovered and studied. On the other hand, less is known about PAMP molecules deriving from it; to date only one PAMP molecule originating from *Hpa*, the necrosis and ethylene-inducing peptide 1 (Nep-1)-like protein (NLP), has been discovered.

To identify new PAMPs in *Hpa* and their related receptors in *Arabidopsis*, crude extracts were obtained from *Hpa* spores and from *Hpa*-infected *Arabidopsis* leaves. The initial extracts were able to trigger ROS production and callose deposition (signs of PAMP-triggered immunity), however, they were found to be contaminated by *Arabidopsis*-derived molecules. For this reason, the *Hpa*-infected *Arabidopsis* extracts were no longer included in the study.

Instead, after few adjustments in the spore collection method, it was found that the *Hpa* spore extracts contained at least one active molecule of proteinaceous nature and that the active molecules were perceived by *Arabidopsis* thanks to the contribution of the co-receptor BAK1. Furthermore, the perception of the active molecules, contained in the spore extracts, varied among different *Arabidopsis* wt accessions and that most probably the perception is Brassicaceae specific, if not *A. thaliana* specific.

3.1 Introduction

3.1.1 What do we know about PAMPs in *Hyaloperonospora arabidopsidis*?

The oomycete *Hpa* has been extensively used in plant-pathogen research since 1990s. However, most of the studies have been done in the field of effector molecules (from *Hpa*) and the related *R*-genes in *Arabidopsis* and less is known about PAMPs (Coates & Beynon, 2010).

To date, only one molecule has been identified as a PAMP in *Hpa*: the necrosis and ethylene-inducing peptide 1 (Nep-1)-like protein (NLP). In detail, a small peptide fragment of 24 amino acids (nlp24) derived from the protein *Ha*NLP3 is able to trigger ethylene production and induction of immunity in *Arabidopsis* plants (Oome et al., 2014). In the *Hpa* genome, 10 NLP-encoding genes were firstly identified (Baxter et al., 2010). However, in a more detailed study, Cabral and colleagues (2012) discovered 4 more genes encoding NLPs, together with at least 15 pseudogenes and fragmented sequences. They observed that, although NLPs are an important family of secreted proteins found in several plant pathogens such as bacteria and fungi, in the genomes of oomycetes, the number of NLP genes is much more expanded (Cabral et al., 2012). This is visible in particular in *Phytophthora* spp. and downy mildews, suggesting an important function of these proteins in the fitness of the microorganisms (Oome et al., 2014).

Despite the NLP family is known to be cytotoxic, being able to cause tissue necrosis in dicotyledonous plants through plasma membrane permeabilisation, the *Hpa*-derived proteins did not cause necrosis (therefore considered non-cytotoxic) when expressed in tobacco or *Arabidopsis* (Cabral et al., 2012). In addition, the level of expression of these genes seems to increase at the beginning of the colonisation process, differently from hemibiotrophic oomycetes, such as *P. sojae* or *P. infestans*, in which the genes are mostly expressed during the transition from the biotrophic to the necrotrophic stage (Cabral et al., 2012). This feature is in accordance with what suggested by Oome and colleagues (2014), about the ability of nlp24 to trigger immune reactions through direct

recognition, rather than through the breakage of the membrane (and possible release of danger signals) as in the cytotoxic counterparts.

3.1.2 How to identify new PAMP molecules

After the recognition of the non-self, many processes are initiated inside the cells in the premises of the infection site. These changes could be used as a tool to investigate the immune response and two of them have been chosen to detect the presence of molecules able to trigger plant immunity (PTI): the production of reactive oxygen species (ROS) and the deposition of the polysaccharide callose.

One of the first events happening inside the plant cell after the recognition of the pathogen is a rapid Ca^{2+} and H^+ influx and K^+ efflux. This ion movement leads to the production of superoxide (O^{2-}), hydrogen peroxide (H_2O_2) and nitric oxide (NO) mainly, collectively known as reactive oxygen species or ROS. These molecules are the first detectable event during plant immunity and they serve multiple purposes. They can, indeed, act directly as antimicrobial agents or indirectly, inside or outside the cell, alone or in conjunction with other important signalling molecules, such as salicylic acid (Torres et al., 2006; Daudi et al., 2012; O'Brien et al., 2012). Many ROS sources exist, both in the protoplast and the apoplast. With regard to the first one, mitochondria, chloroplasts and peroxisomes can be mentioned, but they are mainly involved in the production of ROS after abiotic stress. Important sources of ROS, involved in biotic stress, are the cell membrane NADPH oxidases or NADH-dependent superoxide synthases, which generate the superoxide anion. Other important ROS producers are the apoplastic peroxidases, amine oxidases and the oxalate synthases generating H_2O_2, which may also be produced by the action of superoxide dismutases, which is able to convert O^{2-} into hydrogen peroxide (Bolwell et al., 2001). Nevertheless, it has been shown in different studies that NADPH oxidases and class III cell wall peroxidases represent the main sources of ROS following pathogen recognition, even though with different roles. It has been argued that the apoplastic burst upon pathogen-associated molecular pattern (PAMP) recognition may be due to the apoplastic peroxidases, whereas NADPH oxidases may have a major role in the effector-triggered hypersensitive response (HR). Normal development of PTI responses, for instance the

production of callose and the transcription of defense-associated genes, requires the production of H_2O_2 by peroxidases (Daudi et al., 2012).

A second event, following pathogen recognition, which can be used to study PTI and in particular to look for new elicitor molecules, is the production and deposition of callose. It can be stained with the dye aniline blue, which will bind specifically to the callose deposits and it can be visualized using a fluorescence microscope (see Section 2.2.2.5, Figure 3.1) (Luna et al., 2011; Ellinger and Voigt, 2014).
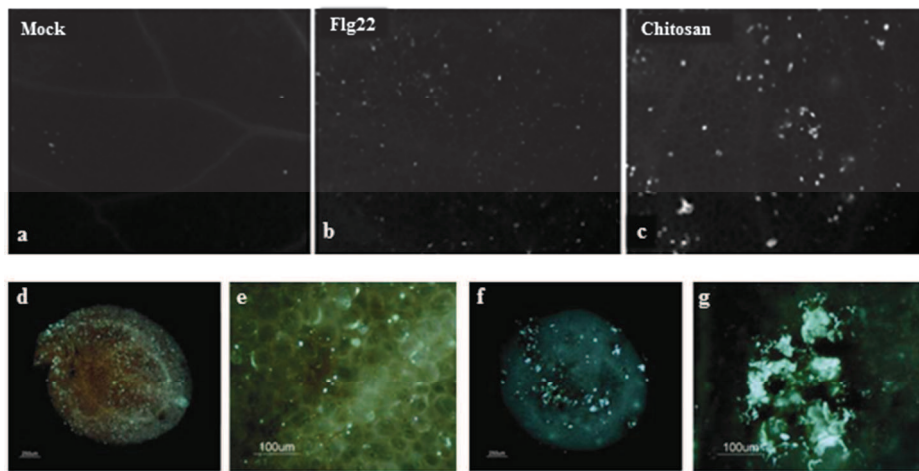
Figure 3.1 Callose deposits stained with aniline blue. a, **b** and **c:** callose deposits triggered by mock treatment, 1 µM flg22 and 0.01% chitosan, respectively, on *Arabidopsis thaliana* (Col-0) seedlings. They are visible as white spots and the differences in terms of shape and size are visible between the flg22 and chitosan treatments. It is possible to notice the difference between the treatments with known PAMP molecules (flg22 and chitosan) and the mock treatment. The pictures were taken after aniline blue staining under UV epifluorescence. **d** and **e:** a cotyledon and a detail, respectively, after treatment with 1 µM flg22. **f** and **g**: the cotyledon and its detail following 0.01% chitosan treatment. Also in this case, the pictures were taken by exposing the samples to UV after the treatment with the dye aniline blue (Pictures adapted from Luna et al., 2011).

Callose is a β-(1,3)-glucan polymer, found in cell wall appositions (papillae) which are deposited between the plasma membrane and the cell wall at sites of attempted pathogen penetration. The papillae can be regarded as physical barriers built by the plant upon pathogen attack in order to prevent or slow down the spreading of the invading microorganism; in the attempt of avoiding more sacrificial responses such as hypersensitive response (HR) or cell death and to allow the time to longer responses that require gene expression. Callose is not only the component of papillae, but also it acts as a matrix, in which many other defensive components are allocated, such as ROS,

peroxidases, lignin, phenolic conjugates and phenolic compounds, other cell wall polymers and proteins. It is interesting that although callose-containing papillae have been studied for over a century, a role for callose in these structures has not yet been clarified (Ellinger and Voigt, 2014; Underwood, 2012; Voigt, 2014).

It has, indeed, many roles outside immunity, during pollen production and development or during cytokinesis, just to mention some of them. With regard to resistance towards invading microbes, what is known is that the recognition of conserved pathogen molecules during PTI triggers its deposition. However it is not yet clear whether its role would be a defensive one or its production would be just a consequence of the immune reaction (Ellinger and Voigt, 2014). From this point of view, two possible functions have been hypothesized: since, as stated above, the papillae contain other defensive compounds, which could be toxic even for the plant, callose may act as a barrier to avoid their diffusion and it may also limit the spread of pathogen-derived molecules. Indeed, in the case of pathogens that produce haustoria as feeding structures, it has been shown that many formations, such as haustorial encasements, haustorial collar and neckbands or papillae are produce around the haustoria in order to delimit their action (Underwood, 2012). However, even though its role in immunity is not completely clarified it is undeniable that it represents a useful tool to study PTI and the molecules able to trigger it (Luna et al., 2011; Ellinger and Voigt, 2014).

3.1.3 Pattern-recognition receptors (PRRs): how PAMPs are detected

In order to sense danger, plants display a set of transmembrane receptors, known as pattern recognition receptors or PRRs and they are classified as receptor-like kinases (RLKs) or receptor-like proteins (RLPs) (Greeff et al., 2012; Monaghan and Zipfel, 2012). In *Arabidopsis*, the RLK family is known to have more than 600 members and they can be categorized in 44 families based on their N-terminus domain (Greeff et al., 2012). On the other hand, at least 57 RLPs have been identified in *Arabidopsis*. They are not only involved in immunity but they are also implicated in development, such as the RLP TMM (Too Many Mouths) and the RLP CLV2 (Clavata2) (Wang et al., 2008).

The best-studied plant PRRs are the RLKs FLS2 (Flagellin Sensing 2, from *Arabidopsis*), EFR (the receptor for the Elongation Factor-Tu, from *Arabidopsis*) and

XA21 (the receptor conferring resistance to *Xanthomonas oryzae* pv. *oryzae* in rice), which recognize the epitope flg22, elf18/26 and Ax21, respectively. They are characterized by having leucine-rich repeats domain in their N-terminus and therefore they bind to molecules of proteinaceous nature (peptides). A second important category of PRRs is distinguished by the presence of a carbohydrate-binding module, which is the Lys-M domain, at their N-terminus. Comprised in this category, the RLP CEBiP (required for chitin recognition in rice) and the RLK CERK1 (a chitin-binding protein in *At*) can be given as an example (Monaghan and Zipfel, 2012).

The intracellular kinase domain of numerous RLKs is a serine/threonine kinase. Usually these kinases display a conserved aspartate residue (D) in the catalytic loop required for activity, mostly associated with an arginine residue (R), therefore they are called RD kinases. However the majority of known RLKs involved in defense against microbes lack the arginine residue, so they don't belong to the category of the RD-kinases. For this reason they are usually found to be associated with other kinases in order to modulate their activity (Greeff et al., 2012).

3.1.3.1 Need a help? *BAK1* and *SOBIR1*

As previously introduced, in some cases RLKs and RLPs need to interact with another receptor carrying the kinase domain to transfer the signal inside of the cell and activate the defense machinery (Liebrand et al., 2013).

Two receptor-like kinases have been found to play a major part in this signalling/helping process: the LRR-RLK SUPPRESSOR OF BIR-1 (*SOBIR1* or also called *EVERSHED*, *EVR*) and the LRR-RLK BRI1-associated kinase1 (*BAK1*) (Liebrand et al., 2013; Chinchilla et al., 2009). These two LRR-receptor-like kinases act as an adaptor and a co-receptor, respectively. Indeed, some of the RLPs tend to associate with *SOBIR1* or *SOBIR1*-like kinases even in the absence of an extracellular ligand, forming an RLK-like complex, ready to sense any external stimuli that may arrive (Figure 3.2a). In contrast, *BAK1* tends to combine with another RLK upon ligand binding (Figure 3.2b). In the case of the LRR-RLK FLS2, which senses and binds to flg22, *BAK1* associates with it after flg22 binds to the receptor. It is able to bind to flg22 through its LRR extracellular domain, resulting in a co-receptor, rather than an adaptor.

After they bind to the related receptor, they will be able to activate the cytoplasmic signalling pathway (Figure 3.2b) via their kinase domain (Gust and Felix, 2014).

Apart from their role in plant immunity, both are known for their involvement in other important processes. BAK1 belongs to the SERK (somatic embryogenesis receptor kinase) family, which is involved in the sensing of brassinosteroids, through the association with the LRR-RLK brassinosteroid insensitive-1 (BRI1). BAK1 is also important in other *Arabidopsis (At)* developmental processes, such as root development and photo morphogenesis, but also plays a role in containing cell death. SOBIR1, on the other hand, has a part in stress signalling processes, including high light, auxins and salt concentration (Liebrand, 2013; Chinchilla et al., 2009).
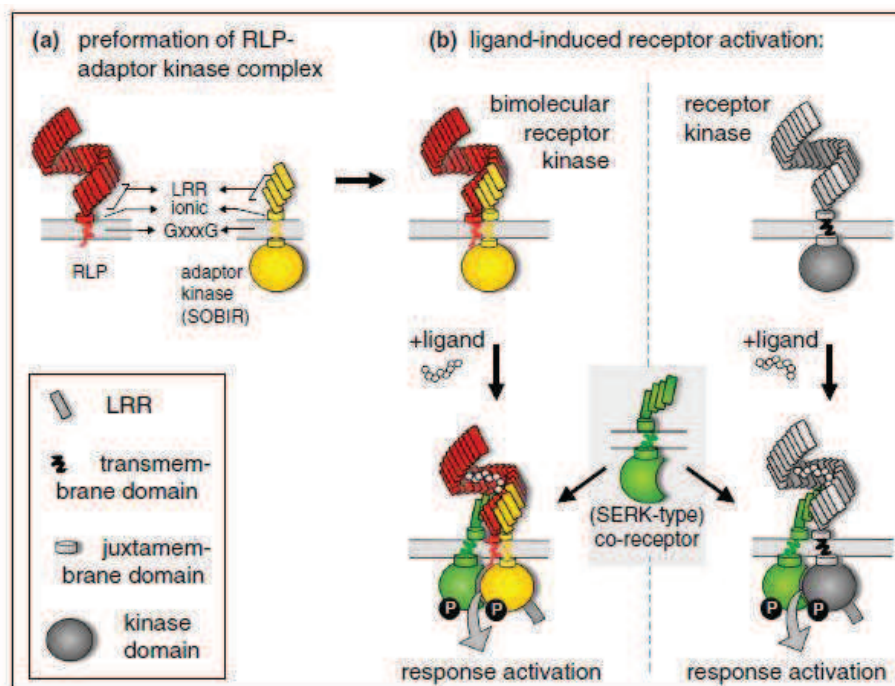
Figure 3.2 Formation of RLP and RLK complexes at the plasma membrane. RLP-adaptor kinase complex is pre-formed even in the absence of a ligand (**a**), whereas the RLK/co-receptor complex is formed upon ligand perception and binding (**b**) (Gust and Felix, 2014).

3.1.4 Aims of the study on *Hpa* spore extracts

As previously mentioned, the *Arabidopsis*/*Hpa* pathosystem has been extensively used to study the field of plant-pathogen interactions. Most of the works regarded the study

of effector molecules, but less is known about PAMPs; to date, indeed, only one PAMP molecule has been discovered in *Hpa*. Therefore, to fill the gap in the research, the aims and objectives of this project were as follows:

- ➢ Determine whether *Hpa* spores contain molecules able to activate PAMP-triggered immunity
- ➢ Investigate the nature of these molecules
- ➢ Identify possible receptors involved in the recognition of the active *Hpa* PAMP molecules

3.2 Results

3.2.1 Optimisation of a method to obtain extracts from *Hpa*-Emoy2 spores and *Hpa*-Emoy2 infected *Arabidopsis* tissues

In order to identify PAMP molecules deriving from *Hpa*, extractions (Section 2.2.2.1) from both spores and *Arabidopsis* infected tissues were carried out. Healthy *Arabidopsis* tissues were processed in the same way and used as a control for the background given by the plant. To establish the most suitable method, several protocols were tried. To assess the validity of each method, the obtained extracts were tested using a Reactive Oxygen Species accumulation assay (from now on referred to as ROS assay – Section 2.2.2.4), being ROS accumulation one of the main signs of PAMPs perception.

The first method tried was a modified protocol from Roux et al. (2011), and based on extraction using cold sterile water on frozen plant tissues, followed by vigorous vortexing in order to break the plant cells and release the internal content. After centrifugation of the extracts no pellet was visible. The resuspension was tried with cold sterile water and the activity was assessed in a ROS assay; however, no considerable reaction was found. The second protocol followed was adapted from Gabor et al. (1993). In this case the tissues were ground in liquid nitrogen using pestle and mortar and then phosphate buffer saline (PBS) was added. The buffer was tested in a ROS along with the extracts. The PBS was quite reactive (data not shown), and therefore considered not suitable for the purpose of the study. The third method consisted in autoclaving the healthy and infected tissues and the spores for 15 min at 126 ºC and 1.5

bar of pressure. Although the reactivity was comparable to the positive control flg22 (the epitope of the protein flagellin), while the reactivity of water used to immerse the tissues was low, therefore overall it could be considered to be a good method, once visualized on an SDS-PAGE gel the protein bands appeared as a smear and not as a typical banding pattern (Figure 3.3a). This was most probably due to a degradation of the proteins caused by the autoclave cycle. For this reason this methodology was not preferred. The last extraction protocol tried and adopted for all the extractions carried on during this project is based on the use of an extraction buffer (Section 2.2.2.1 for the method), which is able to bring the proteins into solution after the tissues have been broken. With regard to *Hpa* spores, they were broken using a pestle and mortar and sand and lastly by adding the extraction buffer. Even though the procedure seemed to work at first, the rupture of the spores was not effective enough. Thus they were finally opened by vortexing them in extraction buffer and glass beads. Both the spore extracts and the *At* tissues extracts obtained with this process displayed a proper banding pattern on a gel (Figure 3.3b), with no signs of degradation.
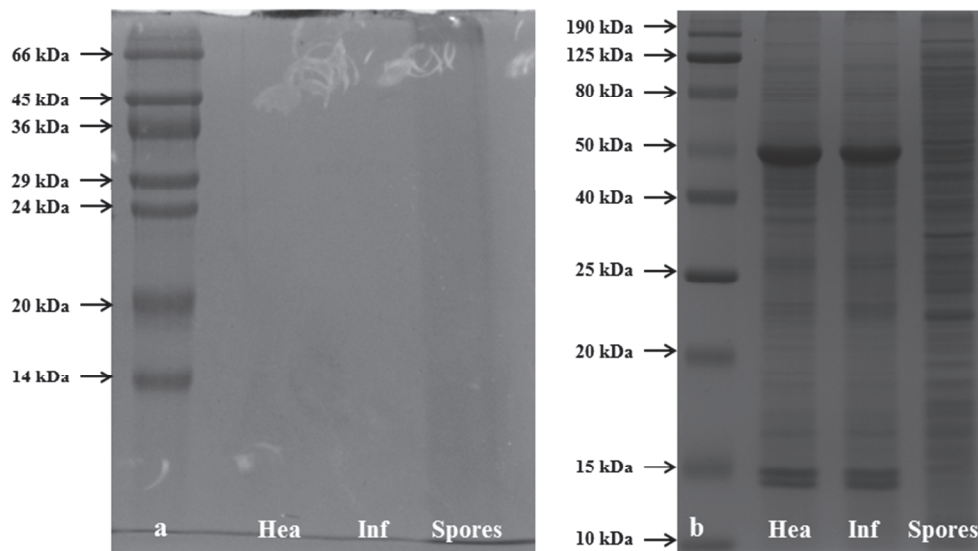
Figure 3.3 Comparison of autoclave and extraction buffer as extraction methods. a: healthy *Arabidopsis* tissues (Hea), *Hpa*-infected *Arabidopsis* tissues (Inf) and *Hpa*-Emoy2 spores (Spores) extracts obtained by autoclaving. It is visible, especially in the lane corresponding to the spores extracts, how the bands are not defined, but appear as a smear. **b**: healthy *Arabidopsis* tissues (Hea), *Hpa*-infected *Arabidopsis* tissues (Inf) and *Hpa*-Emoy2 spores (Spores) extracts obtained using the extraction buffer method. In this case, the distinct banding pattern with no signs of protein degradation was observed. In both gels, 5 μg total protein were loaded. In both gels, the first lane corresponds to the protein marker: picture **a**, Molecular weight marker kit for molecular weight range 14,000 – 70,000 (Sigma-Aldrich); picture **b**: HyperPAGE Prestained Protein Marker (Bioline), used from this point on in every gel showed.

The extracts were also reactive during the used ROS assay. For all these reasons, this method was selected as the preferred method for protein extractions from *Hpa* spores and healthy and *Hpa*-infected *At* tissues.

The banding pattern (Figure 3.3b) of the healthy and infected extracts resulted very similar, almost identical. This may be due to the high representation of the plant tissues in the extract: for example there are three bands (one at ~56 kDa and two at ~14 kDa), which may correspond to the Rubisco subunits. Since *Hpa* is an obligate biotroph (Coates & Beynon, 2010) it was impossible to avoid processing the plant tissues together with the microorganism. On the other hand, even though some bands seemed to be shared in between the three extracts, the band pattern of the *Hpa*-spore extracts looked very different, with several bands distributed throughout the length of the gel.

3.2.2 Testing the extracts for PAMP-triggered immunity

To determine whether *Hpa* contains PAMP molecules, the extracts obtained from the spores and the infected *Arabidopsis* leaves were tested on their ability to trigger ROS production and callose deposition (Section 2.2.2.5), which are between the different events generated by PAMP molecules recognition during PAMP-triggered immunity (PTI) (Muthamilarasan & Prasad, 2013). The healthy *Arabidopsis* leaves extracts were used as well in the assay as a control, to monitor the background reaction given by the damaging of the leaves during the production of the extracts (DAMPs release).

3.2.2.1 The *Hpa*-spore extracts trigger ROS production

To test whether the molecules contained in the extract were able to cause production of ROS, a modified protocol from Felix et al. (1996) was used. It is an indirect method that detects the activity of the extracellular peroxidases responsible for the ROS production after the interaction between the plant and the pathogen, rather than directly measuring the quantity of ROS produced. The presence and reactivity of the peroxidases are displayed as a colour change of the substrate of the assay, 5-aminosalycilic acid, which is converted by the peroxidases from an almost colourless solution, to an orange-brown one. The reaction is measured using a spectrophotometer set at 450 nm. During the assay, pure horseradish peroxidase and flg22 (the reactive epitope of the protein flagellin, Felix et al., 1999) were used as positive controls, whereas sdH2O (used to

resuspend flg22) and extraction buffer (which is the base of the spore extract) were employed as negative controls. Although it would be more correct to refer to the results obtained as a measure of the amount of peroxidases activity after the recognition of any PAMP molecules, for the sake of readability, they will hereafter referred to as ROS produced.
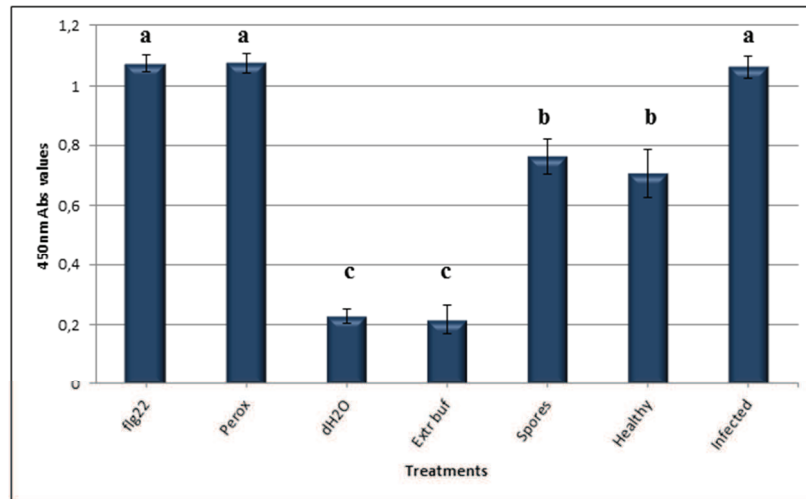
Figure 3.4 ROS assay on Col-0 plants testing the three obtained extracts. The picture shows the results obtained from Col-0 leaf disks treated with: flagellin (flg22, positive control), sterile distilled water (dH2O, background control for flg22), extraction buffer (Extr buf, background control for the extracts), and *Hpa* spore extracts (Spores), healthy *Arabidopsis* leaf extracts (Hea) and *Hpa*-infected *Arabidopsis* leaf extracts (Inf). Pure peroxidase (Perox) was used as a positive control, since the technical nature of the ROS assay. Both water and the buffer triggered low reactivity, while flg22 caused a high reaction, comparable to the one obtained with the pure peroxidase. The three extracts resulted quite active in comparison to the positive controls, with the infected extracts triggering the greatest reaction between the three. Statistical analysis: ANOVA One-Way, Tuckey post-test. Different letters represent statistical differences in between the results.

Figure 3.4 shows the results obtained in a ROS assay after the application of various treatments to Col-0 leaf disks (see Section 2.2.2.4 for the procedure). The background controls (water and extraction buffer) generated a low amount of ROS, which could be considered as the amount of ROS produced by the handling and cutting of the leaf disk. The positive control, the very well-known PAMP flg22 (Felix et al., 1999), caused a reaction that is comparable to the one produced by pure peroxidase. Compared to the positive controls, the reactions obtained with the three extracts are quite important, even though it has to be kept in mind that the background reaction obtained with the healthy extracts has to be subtracted from the one obtained with the infected extracts. From this

point of view, the remaining activity is not so different from the one obtained with the extraction buffer itself.

3.2.2.2 The *Hpa*-spore extracts trigger callose deposition

In a second attempt to understand the nature of the molecules contained in the extracts, the latter were pressure injected into fully expanded *Nicotiana benthamiana* leaves, to check whether they contained molecules able to cause callose production and deposition. Flg22 (positive control), sterile distilled water and extraction buffer (background controls) were included as well.
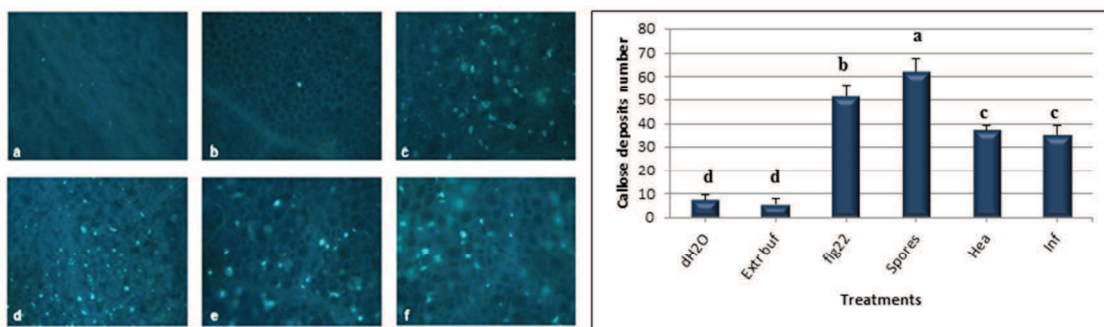
Figure 3.5 Callose deposition assay on *Nicotiana benthamiana* leaves. The three extracts (*Hpa*-Emoy2 spores, healthy and *Hpa*-infected *Arabidopsis* tissues) have been tested on their ability to trigger callose deposition. The callose deposits were displayed as white spots after the leaves were pressure injected and stained with the dye aniline blue. The images were taken with a fluorescence microscope under ultraviolet light. **a**: sterile distilled water, **b**: extraction buffer, **c**: flg22, **d**: spore extracts, **e**: healthy tissues extracts, **f**: *Hpa*-infected tissues extracts. On the right, the graph displays the count of callose deposits, showing the statistical analysis as well (ANOVA One-Way, Tuckey post-test: different letters indicate statistically different values).

As shown in Figure 3.5 (pictures a-f on the left), it is noticeable that both the background controls (water, a and extraction buffer, b) did not trigger a great reaction (less than 10 callose deposits per area considered), while in the case of the injection of flg22 (c) or the extracts (d, e and f) it is evident a much greater reaction represented by a high number of deposits. The real differences are however displayed in the graph (Figure 3.5 on the right): even though quite similar if observed from the pictures, the number of callose deposits appears to be statistically different between the three extracts and the positive control. Briefly, the *Hpa*-spore extracts seem to cause more callose deposition than flg22, while a reduced amount of deposits were produced after the injection of the healthy and *Hpa*-infected *Arabidopsis* extracts. In detail, the two

extracts do not show any statistical difference in the number of callose deposits triggered. Therefore, as previously mentioned regarding the ROS assay results, extracts obtained from the infected leaves do not seem to cause any striking reaction. Once again, most probably the reactivity of any possible PAMP molecule contained might be obscured by the plant tissues contamination.

3.2.3 Fractionation of the extracts

In order to simplify the mixture of molecules contained in the extracts and therefore to try to identify the active ones, the extracts were fractionated using a strong anion exchange chromatographic column (Section 2.2.2.3).

The fractions were obtained by eluting the proteins from the column using increasing concentrations of NaCl: 0.1M, 0.15M, 0.2M, 0.25M, 0.3M, 0.35M, 0.4M, 0.5M and 0.55M. The fraction of proteins that did not bind to the column in the used conditions was collected as well (flow through, FT). All the fractions were afterwards visualized on an SDS-PAGE gel (Figure 3.6 – fractions from *Hpa*-spore extracts, Figure 3.7 – fractions from *Hpa*-infected *Arabidopsis* tissue extracts and Figure 3.8 – fractions from healthy *Arabidopsis* tissue extracts) and the gel was stained with Coomassie Brilliant Blue.
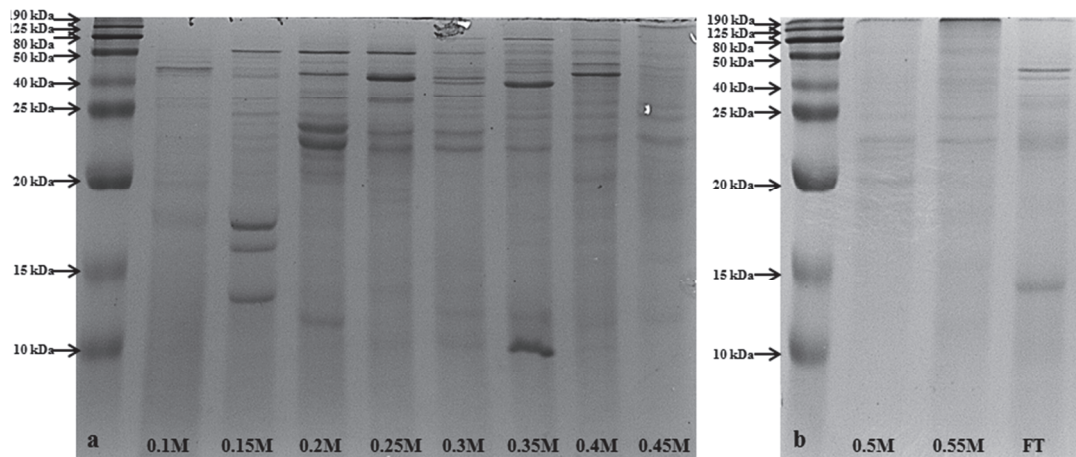
Figure 3.6 Fractionation of the *Hpa*-spore extracts. a: fractions obtained using step-wise elution, from 0.1M NaCl to 0.45M NaCl. In the first lane the protein marker was loaded; the molecular weights are indicated. **b**: the remaining eluted fractions (0.5M NaCl and 0.55M NaCl) are visualized. The last lane corresponds to the portion of proteins that did not bind to the column during the application of the sample: FT (flow through). Both gels were stained with Coomassie Brilliant Blue.
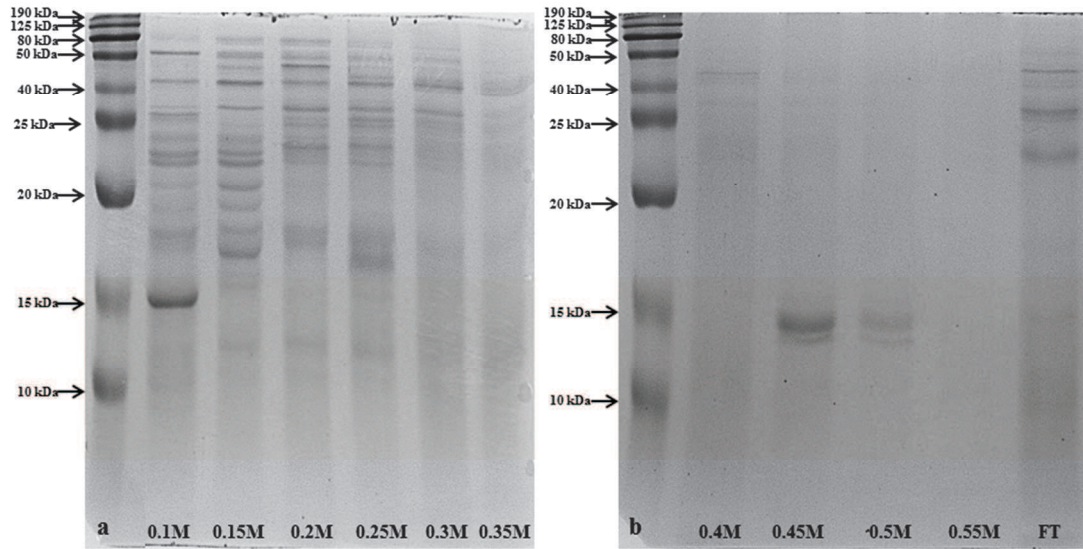
Figure 3.7 Fractionation of the *Hpa*-infected *Arabidopsis* extracts. a: the first lane corresponds to the protein marker (the molecular weights are indicated). The fractions from 0.1M NaCl to 0.35M NaCl are loaded. **b**: the last four fractions, eluted with 0.4M, 0.45M, 0.5M and 0.55M NaCl are visualized. The last lane corresponds to the flow through fraction that did not bind to the column. The first lane was loaded with the protein molecular marker. Both gels were stained with Coomassie Brilliant Blue.
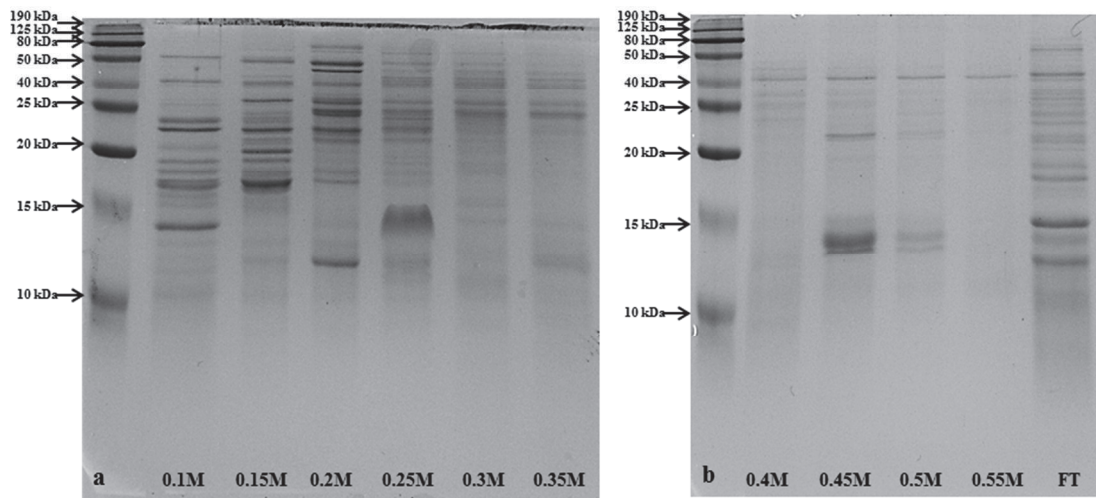
Figure 3.8 Fractionation of healthy *Arabidopsis* extracts. Picture a: the first lane corresponds to the protein marker (the molecular weights are indicated). The fractions from 0.1M NaCl to 0.35M NaCl are loaded. Picture **b**: the last four fractions, eluted with 0.4M, 0.45M, 0.5M and 0.55M NaCl are visualized. The last lane corresponds to the flow through fraction that did not bind to the column. The first lane shows the molecular marker bands (the molecular weights are indicated). Both gels were stained with Coomassie Brilliant Blue.

It is visible that the fractions obtained from the *Hpa*-spore extracts show a different band pattern in respect to the fractions obtained from the *Hpa*-infected *Arabidopsis*

tissue extracts and the healthy *Arabidopsis* tissue extracts. While, on the other hand, it is noticeable that the band pattern of the two *Arabidopsis* extracts (*Hpa*-infected and healthy) are very similar, with various bands in common. This may be due, once again, to the high representation of the plant tissues in the infected extracts.

3.2.3.1 Testing the fractions in triggering ROS production

To understand whether the fractionation process successfully simplified the complex initial protein mixture and whether it was possible to identify any fraction that triggers defence response, they were tested in a ROS assay using Col-0 plants (from now on the results will be displayed with the value of the extraction buffer subtracted from the results obtained after the application of the extract or the fraction).

From the results obtained (Figure 3.9 – fractions from *Hpa*-spore extracts, Figure 3.10 – fractions from *Hpa*-infected *Arabidopsis* tissue extracts and Figure 3.11 – fractions from healthy *Arabidopsis* tissue extracts) it was noticeable that the only fraction able to trigger a significant reaction in Col-0 plants is the FT fraction.
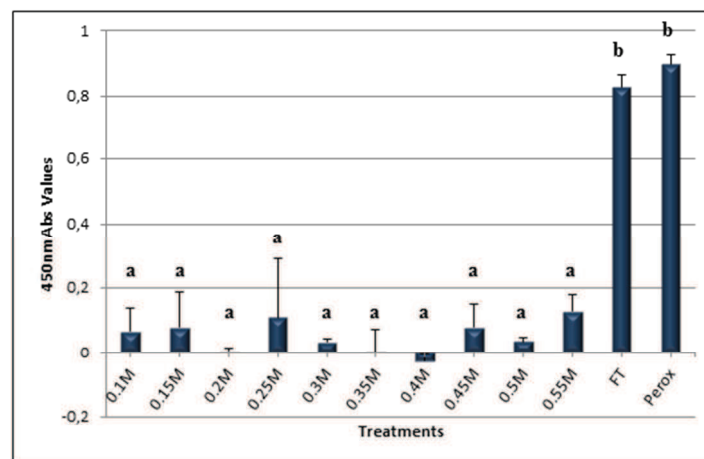
Figure 3.9 ROS assay on Col-0 plant to assess the activity of the *Hpa*-spore fractions. The pure peroxidase enzyme (Perox) was used as a positive control. Among all fractions, only the one corresponding to the flow through (FT) has a significant activity if compared with the one of the positive control. Statistical analysis: ANOVA One-Way (Tuckey Post-test). Different letters indicate significantly different results.
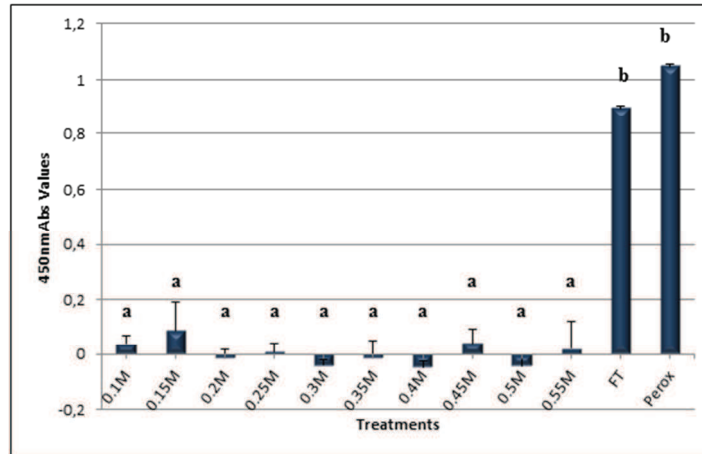
Figure 3.10 ROS assay on Col-0 plant to assess the activity of the *Hpa*-infected *Arabidopsis* tissues fractions. The pure peroxidase enzyme (Perox) was used as a positive control. Among all fractions, only the one corresponding to the flow through (FT) has a significant activity if compared with the one of the positive control. Statistical analysis: ANOVA One-Way (Tuckey Post-test). Different letters indicate significantly different results.
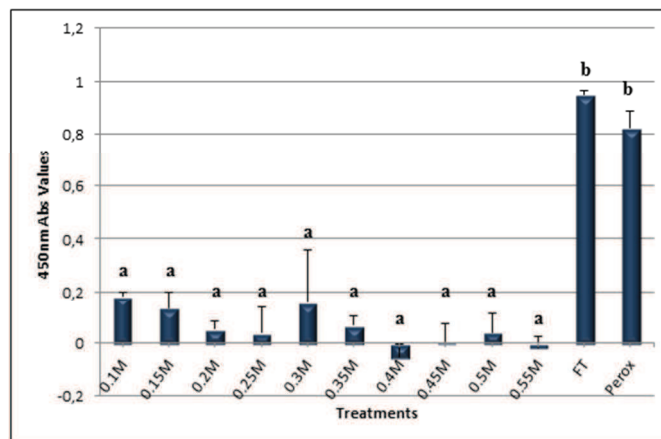
Figure 3.11 ROS assay on Col-0 plant to assess the activity of the healthy *Arabidopsis* tissues fractions. The pure peroxidase enzyme (Perox) was used as a positive control. Among all fractions, only the one corresponding to the flow through (FT) has a significant activity if compared with the one of the positive control. Statistical analysis: ANOVA One-Way (Tuckey Post-test). Different letters indicate significantly different results.

For every ROS assay performed the FT fraction reached a value comparable to the one obtained using the pure peroxidase enzyme. All other fractions triggered a negligible if not null reaction in the plants. Most probably the active molecules did not bind to the column and passed through, since no detectable activity is left in the eluted fractions. Both the fractionations and the ROS assays were repeated several times with similar

results. However, because of the similarity of the reactions caused by the healthy and *Hpa*-infected extracts (Figure 3.4 and Figure 3.5) or by their fractions (Figure 3.10 and Figure 3.11) and because of the similarity of their banding pattern (Figure 3.7 and Figure 3.8), the *Hpa*-infected *Arabidopsis* tissue extracts were no longer used in the search for PAMP molecules originating from *Hpa*.

3.2.3.2 Study of the *Hpa*-spores flow through fraction

Since it was confirmed several times that the FT was the only active fraction, the fractionation method was simplified. In detail, after the application of the *Hpa*-spore extract to the column and the collection of the flow through (the fraction of interest), the remaining proteins were eluted from the column using 0.55M NaCl buffer, in order to collect them altogether in only one sample (afterwards renamed eluate). As a confirmation of the new methodology, the FT and the eluate fractions were visualized on a SDS-PAGE (Figure 3.12a) gel and tested in a ROS assay (Figure 3.12b) on Col-0 plants (both the gel and the ROS assay were repeated with different spore extracts with similar results).

The gel in Figure 3.12a shows the results of the new fractionation process, in which after the collection of the FT, the remaining proteins are eluted by the addition of the 0.55M NaCl buffer. The different banding patterns between the FT and the Eluate fractions are shown. In particular, there are few bands (indicated by the blue arrows) that seem to belong exclusively to the FT. However, there are still some bands (indicated by the blue box) that seem to be shared by both fractions.

The two fractions were tested in a ROS assay to confirm that the main activity resides in the FT fraction. As shown by the graph in Figure 3.12b, the FT triggers a reaction that is comparable to the one obtained adding the pure peroxidase enzyme. In addition, even though there is some activity left in the eluate fraction, it is not comparable to the one given by the FT, considering that in the eluate case all the remaining proteins are combined in only one fraction.
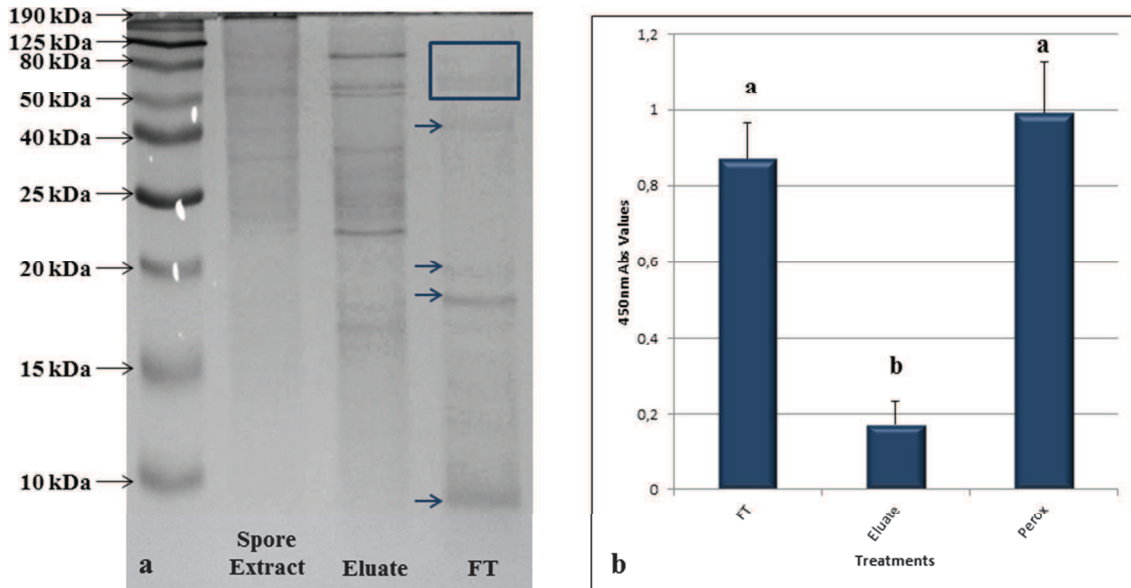
Figure 3.12 Visualisation and testing of the *Hpa*-spore FT and eluate fractions. a: visualisation of the *Hpa*-spore extract (Spore Extract), the eluate fraction (Eluate) obtained using 0.55M NaCl and the flow through (FT) fraction. The first lane on the left was loaded with the protein marker: the band sizes are highlighted. The bands were visualised using Coomassie Brilliant Blue. The blue arrows indicate bands that belong exclusively to the FT, while the blue box shows band belonging to both the FT and eluate fractions. **b**: the activity of the FT and of the 0.55M eluate were tested in a ROS assay using Col-0 plants. Once again it is confirmed that the active molecules are contained in the FT. Pure peroxidase was used a positive control. Statistical analysis: ANOVA One-Way (Tuckey post-test); different letters indicate significantly different results.

3.2.3.3 Elucidating the immune response triggered by the active molecules contained in the FT

The FT (together with the eluate fraction) was tested on some available Columbia mutant plants: Col-*rpp4*, Col-*sobir1* and Col-*bak1-5 bkk1-1*.

The plants used in the ROS assay were *At* Col-0, while the *Hpa* isolate used for protein extractions is *Hpa*-Emoy2. Thus, within the chosen plant-pathogen pair, the recognition is mediated by the *ATR4-RPP4* gene pair resulting in an almost incompatible interaction and very low sporulation (Holub et al., 1994). Therefore, Col-*rpp4* mutant plants were included to determine whether the cause of the reactivity of the FT fraction would have been a consequence of the presence and recognition of the effector *ATR4*. As shown in Figure 3.13, the ROS production is not impaired at all if compared with Col-0 wt plants (Figure 3.12b). This may indicate that in the FT, molecules other than *ATR4* may be present that are able to trigger an immune reaction. And once again the activity is

almost completely retained by the FT (comparable with the positive control peroxidase), with a minimal activity left in the eluate fraction.

On the other hand Col-*sobir1* and Col-*bak1-5 bkk1-1* mutants were first screened because of their important role as an adaptor kinase and a co-receptor for RLPs and RLKs (see Section 3.1.3.1). Understanding their involvement in the recognition of the molecules contained in the FT fraction may help to elucidate the recognition mechanism used by the plant towards the pathogen.
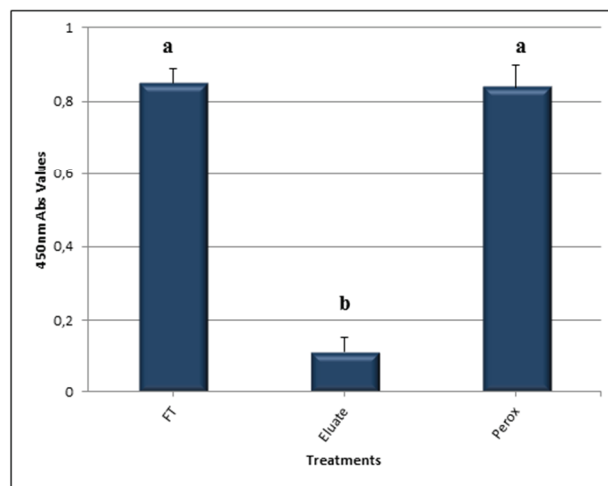
Figure 3.13 ROS assay using *Hpa*-spore FT and eluate fractions on Col-*rpp4* mutant plants. Pure peroxidase has been used as a positive control and a reference for the reactivity of the fractions tested. The recognition of the molecules in the FT (in terms of ROS production) is not impaired in the *rpp4* mutant. As previously seen in Figure 3.12b, the eluate fraction does not seem to contain molecules able to trigger an immune reaction. Statistical analysis: ANOVA One-Way, Tuckey post-test. Different letters represent statistically different values.

Figure 3.14a shows the results of a ROS assay testing the FT and eluate fractions on two different mutants of the receptor *SOBIR1*. As shown by the graph, there is no actual reduction in ROS production due to the mutation of the receptor. Actually the ROS production obtained after the application of the FT is comparable to the amount of ROS obtained using the pure peroxidase (positive control). When compared to the previous results obtained on wt Col-0 plants (Figure 3.12, b), the overall pattern of ROS production for the FT and the eluate is very similar. These results may be an indication that the receptor is not involved in the recognition and the signalling of the active molecules contained in the FT.
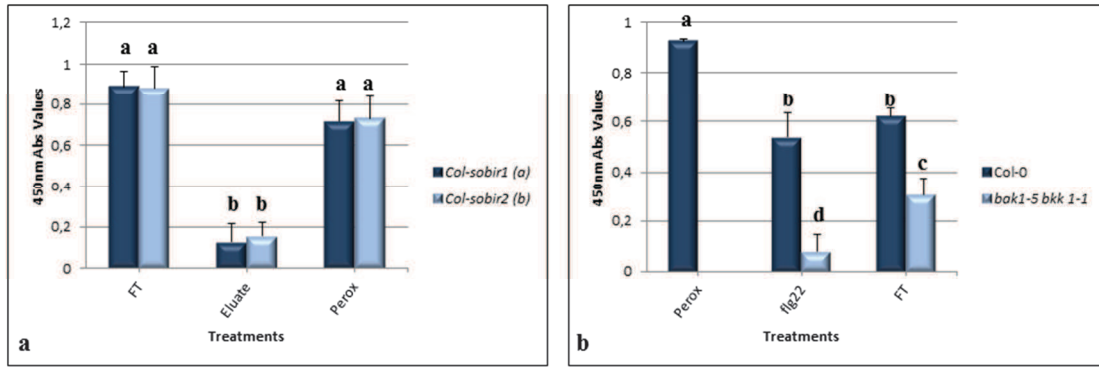
Figure 3.14 ROS assay on Col-*sobir1* and Col-*bak1-5 bkk1-1* mutant plants using *Hpa*-spore FT and eluate. a: ROS assay using the FT and eluate fractions on two *sobir1* mutants. The recognition of the active molecules in the FT and therefore the ROS production are not impaired in the mutant plants. The eluate, once again, triggers a negligible ROS production. **b**: comparison of the ROS production following the application of the FT on Columbia wt and on Col-*bak1-5 bkk1-1* plants. There is a significant reduction in recognition of the active molecules contained in the FT in Col-*bak1-5 bkk1-1* plants when compared with Col-0 wt. flg22 had been used as a standard for the loss of reactivity in Col-*bak1-5 bkk1-1* mutant plants (Roux et al., 2011). Statistical analysis: ANOVA One-Way, Tuckey post-test. Different letters represent statistically different values.

In the ROS assay using Col-*bak1-5 bkk1-1* mutants, wt Col-0 plants have been used as a control. As shown in Figure 3.14b, there is a significant difference in the reaction obtained using the FT on Col-0 and Col-*bak1-5 bkk1-1* plants. In detail, in the plants where the two receptors are mutated there is a reduction in recognition and in ROS production. This may be due to an involvement of the receptors in the signalling of one or more active molecules contained in the FT fraction. In the same experiment, flg22 has been used as a reference for the reduced reactivity of the mutants in respect to Col-0. It is known indeed that the flg22 receptor (*FLS2*) binds to *BAK1* in a flg22-dependent manner and helps in the signalling of the PAMP molecule and it has been shown that in plants impaired in the *BAK1* receptor there is a reduced ROS production (Chinchilla et al., 2007).

3.2.4 Changes in the methodology, changes in the results

Although the promising results obtained so far, due to the spore collection method (spores have been collected from sporulating material by producing a spore suspension), there was still a possibility of contamination of the spore extracts with *Arabidopsis*-derived molecules. Therefore the possibility arose that the obtained activity may have been due to the presence of *Arabidopsis* DAMPs rather than PAMP molecules found in the *Hpa* extracts.

Some of the bands in the active FT of the spore extracts (Figure 3.6b) may be shared with the FT fractions of the healthy *Arabidopsis* extracts (Figure 3.8b). If this was the case, the very similar results obtained in the ROS assays using the fractions, where in all the three cases, only the FTs were reactive (Figure 3.9, Figure 3.10 and Figure 3.11), may be a confirmation of the hypothesis. To test this hypothesis, a mock spore collection using healthy *Arabidopsis* leaves was performed. Afterwards, the obtained pellet, was processed in the same way as if it was spores and the extract obtained was tested in a ROS assay. The "mock extract" was very reactive when confronted with the *Hpa*-spore extract (data not shown).

For all these reasons, the method to collect *Hpa* spores from infected *Arabidopsis* tissues was changed (Section 2.2.3.2). In detail, it was modified from a "wet" method (washing off the spores from the leaves in sterile distilled water) to a "dry" method (using a surface sampler). With this new procedure the spores appeared much cleaner than with the previously used method. Afterwards, the newly collected spores were extracted and fractionated obtaining the FT and eluate fractions. They were tested in a ROS assay on Col-0 plants (Figure 3.15a). The results were different from the previously obtained when using the FT and the eluate (Figure 3.12b). In this case the eluate fraction, that had a negligible activity in the previous ROS assay, was significantly more active than the FT. The FT still triggered a reaction in the plant, almost as important as the one of the positive control flg22, however reduced than the previous one (Figure 3.12b).

In this case, the eluate fraction was able to trigger a reaction compared to the one triggered by flg22 and therefore it was decided to re-fractionate it. Thus, it was passed again through the chromatographic column and a new FT fraction and 0.1M NaCl, 0.2M NaCl, 0.3M NaCl, 0.4M NaCl, 0.5M NaCl and 0.55M NaCl fractions were collected. To understand the contribution of each fraction to the activity of the eluate, each fraction was tested in a ROS assay using Col-0 plants. Figure 3.15b shows the results acquired using the fractions obtained from two different *Hpa*-spore extracts. It is noticeable how different fractions contain molecules able to trigger ROS production, while previously, every fraction other than the FT had a negligible reactivity when used in a ROS assay (Figure 3.9).
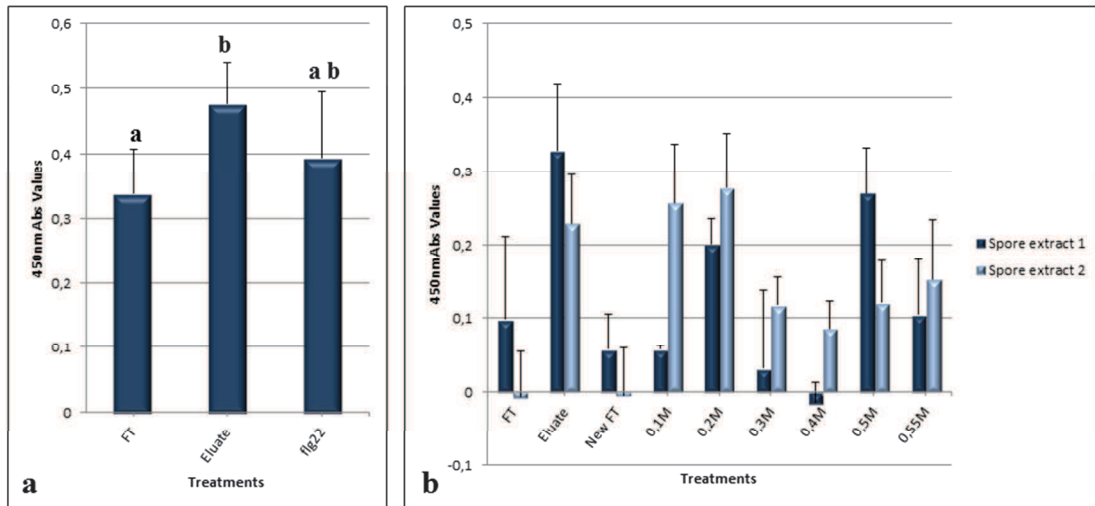
Figure 3.15 ROS assay using the fractions deriving from the newly obtained *Hpa*-spore extracts. a: ROS assay showing the reaction triggered by challenging Col-0 plants with the new FT and the eluate fractions. flg22 has been used as positive control. The eluate triggers a significantly higher reaction than the FT. **b**: ROS assay showing the contribution of the different fractions (new FT, 0.1M NaCl, 0.2M NaCl, 0.3M NaCl, 0.4M NaCl, 0.5M NaCl and 0.55M NaCl) obtained after the eluate fraction was re-fractionated. Statistical analysis: ANOVA One-Way, Tuckey post-test. Different letters indicate statistically different values.

In addition, as shown by the results in Figure 3.15b, but also in other repeated experiments (data not shown), there is not a regular pattern of active and inactive fractions. For example, fraction 0.1M in one extract is as reactive as the eluate fraction, while in the second extract has an almost insignificant activity (Figure 3.15b).

Because it was no longer clear which fractions contained the active molecules, it was decided that it was not worth pursuing the fractionation pathway, also due to practical difficulties in obtaining a considerable amount of spores and thus of the extracts. Therefore, the following experiments addressed at identifying the nature of the active molecules (PAMPs) and the signalling pathways involved, were carried out by using the crude *Hpa*-spore extracts.

3.2.5 Characterizing the active molecules

To gain more information about the active molecules contained in the extracts obtained from *Hpa*-Emoy2 spores, the following experiments were performed: a) treatment of the extracts with Proteinase K to understand if the molecules are of proteinaceous nature; b) ROS assay testing different *bak1* and *bkk1* mutants to shed light on the nature of the signalling; c) ROS assay on various *Arabidopsis* wild type accession to comprehend the

genetic nature of the recognition of the molecules and d) testing on different plant families to investigate the specificity of the recognition.

3.2.5.1 At least one active molecule contained in the spore extract is of proteinaceous nature

Three different *Hpa*-spore extracts have been treated with Proteinase K to destroy and eliminate all the proteins contained. After the treatment, they were loaded on a gel to check if the treatment successfully eliminated the proteins contained and afterwards tested in a ROS assay on Col-0 plants to see if there was any change in ROS production due to the treatment.

Figure 3.16 shows the banding patterns of three individual *Hpa*-spore extracts (a) and what is left after the treatment with proteinase K (b). In detail, it is visible how it is possible to obtain constant extractions after the change in the spore collection. The three distinct band patterns (Spore 1, 2 and 3) look very similar. However, the number of bands looks reduced if compared with the extract (Figure 3.3b) obtained after collecting the spores with the previous method (some bands may have been of plant origin).
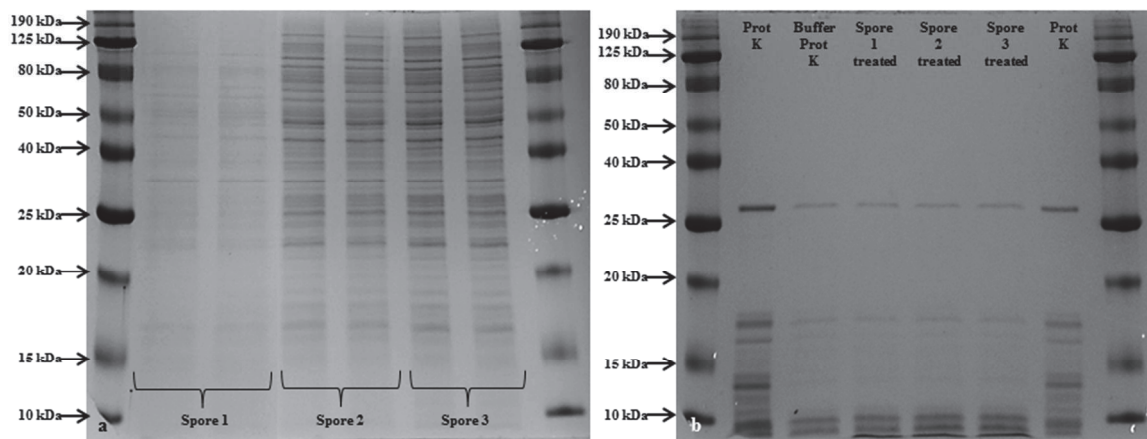
Figure 3.16 Untreated and Proteinase K-treated *Hpa* spore extracts. a: SDS-PAGE gel showing three different *Hpa*-spore extracts obtained after the new collection method. The banding pattern results slightly less complex when confronted with the one (Figure 3.3b) of the extracts obtained after the "wet" collection method. **b**: SDS-PAGE gel showing the same *Hpa*-spore extracts after the treatment with Proteinase K. From the second lane on the left: pure proteinase K (Prot K), extraction buffer containing Proteinase K (Buffer Prot K), the three spore extracts treated with Proteinase K (Spore 1 treated, Spore 2 treated and Spore 3 treated) and finally pure Proteinase K (Prot K). The bands were visualised with Coomassie Brilliant Blue.

As mentioned above, the spore extracts were treated with the enzyme Proteinase K (Section 2.2.2.16) in order to eliminate the protein content. In the gel (Figure 3.16b) the pure enzyme (Prot K), the extraction buffer containing the same amount of Proteinase K used to treat the spore extracts were loaded. In this way, it was possible to observe the Proteinase K banding pattern (first and last lane after and before the protein marker) but most importantly, the Proteinase K banding pattern after the treatment (Buffer Prot K), to be able to compare it with the one of the treated samples. The extraction buffer added with Proteinase K was, indeed, processed in the same way as the samples: 3 – 4 hours at 50 ºC (optimal temperature for Proteinase K) and afterwards at 95 ºC for 10 min to stop the reaction. By doing so, it was possible to establish that all the previously visible protein bands of the extracts (Figure 3.16a) disappeared after the treatment and that the remaining visible bands on the gel (Figure 3.16b) corresponded to what was left of the Proteinase K.

Afterwards, the treated extracts were used in a ROS assay (Figure 3.17). The buffer and buffer treated values were subtracted from the obtained results.
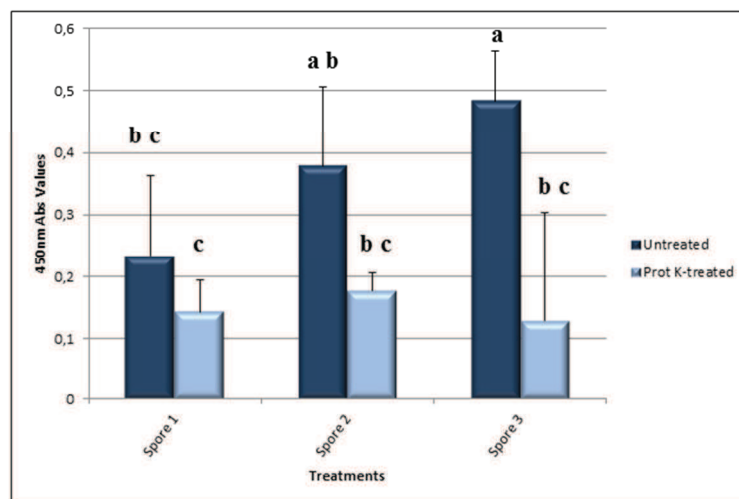
Figure 3.17 ROS assay on Col-0 plants using the Proteinase K-treated *Hpa*-spore extracts. The untreated and Proteinase K-treated spore extracts were tested in their ability to trigger ROS production on Col-0 plants. There is a statistical difference only between the third untreated and Prot K spore samples. However, a diminished activity could be noticed in all three samples. Statistical analysis: ANOVA One-Way (Tuckey post-test). The couples were further analysed with a 2-Sample T-test, $p < 0.05$.

Although in just one case there is a statistically significant difference between the amount of ROS triggered by the untreated and by the Proteinase K-treated extract, a diminished reactivity can be noticed in the remaining two samples. In particular, the results obtained with the sample Spore 2 were also analysed in a 2-Sample T-test, obtaining a p=0.054, that it just above the 0.05 value acceptable for a statistical difference. The ROS was repeated in other two occasions with similar results (data not shown). These outcomes definitely led to the conclusion that at least one of the active molecules contained in the *Hpa*-spore extract is of proteinaceous nature.

3.2.5.2 *Arabidopsis* receptors involved in the recognition and the signalling of the *Hpa*-spores active molecules

Since it was previously demonstrated that the receptor BAK1 is involved in the recognition of some of the molecules contained in the *Hpa*-spore extract (Figure 3.14b), it was of interest to determine whether it still recognizes the molecules contained in the newly obtained spore extract.

Therefore, the extracts were tested in a ROS assay on both Col-0 wt and Col-*bak1-5 bkk1-1* double mutants plants (Figure 3.18a). The values of the extraction buffer and water were subtracted from the obtained results.
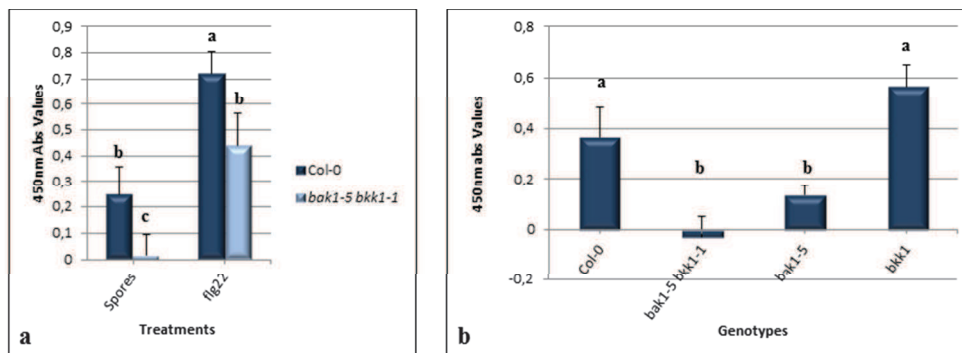
Figure 3.18 ROS production assay on wild-type Col-0, *bak1* and *bkk1* mutant plants. a: comparison of reactivity of the new *Hpa*-spore extracts on Col-0 and Col-*bak1-5 bkk1-1* plants. The application of the extracts on the mutated plants triggers a negligible production of ROS. **b**: ROS assay on Col-0, double mutant plants (Col-*bak1-5 bkk1-1*) and single mutants (Col-*bak1-5* and Col-*bkk1-1*). Once again, it is confirmed an almost null production of ROS by the double mutant, while a significant reduction of ROS is found in the *BAK1* allele. Statistical analysis: ANOVA One-Way, Tuckey Post-test. Different letters represent statistically different values.

As shown in Figure 3.18a, although the general ROS production triggered in Col-0 plants is fairly reduced in the new extracts, there is still a significant reduction in ROS production in Col-*bak1-5 bkk1-1* plants.

In order to reveal the involvement of the single genes *BAK1* and *BKK1*, the assay was repeated (Figure 3.18b), testing the spore extract on single mutant plants: Col-*bak1-5* and Col-*bkk1*. Col-0 plants and Col-*bak1-5 bkk1-1* were included as well in the assay, to have a better comparison with the obtained results (and as a further confirmation of the previous results). In this second assay it appears evident that plants mutated in the receptor *BAK1* show a significant reduction in ROS production when compared with the wt (Col-0). On the contrary, the single mutant *BKK1* shows a normal ROS production, in line with the control Col-0.

3.2.5.3 Different *A. thaliana* accessions have different perception of the *Hpa* active molecules

The *Hpa*-spore extract was used in a ROS assay to test whether different *Arabidopsis* accessions show a different perception of the active molecules. Therefore, eight different *Arabidopsis* genotypes (Ler-0, Bur-0, No-0, Ws-0, Edi-0, Hi-0, Po-0 and Ct-1) were screened, along with Col-0 (as the positive control) widely used throughout this study. The value of the extraction buffer was subtracted from the results obtained after the application of the extract.
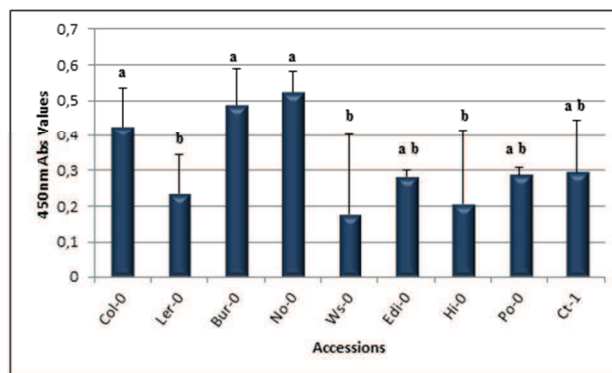
Figure 3.19 ROS assay on various *Arabidopsis* wt accessions reveals different perception of the *Hpa* active molecules. Eight different wt accessions were challenged in a ROS assay with the *Hpa*-spore extract. Three of them, Ler-0, Ws-0 and Hi-0, showed a significantly reduced reaction towards the extract. Statistical analysis: ANOVA One-Way, Tuckey post-test. Different letters indicate significantly different values.

The results displayed in Figure 3.19 show how differently the active molecules are perceived by different *Arabidopsis* accessions. Among the eight screened accessions only two of them (Bur-0 and No-0) reacted to the extract in a way that is comparable to Col-0, (extensively used throughout the study) while, three of them (Ler-0, Ws-0 and Hi-0) showed a significantly lowered reactivity towards the extract. These results show how the genotypic differences in between plants belonging to the same species affect the perception of (and therefore the resistance towards) a pathogen molecule.

3.2.5.4 The reactivity towards the extract may be Brassicaceae-specific

To obtain a more complete view on the perception of the active molecules contained in the *Hpa*-spore extract, a ROS assay was performed on five plants belonging to four different families. In detail, cucumber (*Cucumis sativum*) belonging to Cucurbitaceae, tomato (*Solanum lycopersicum*) and *Nicotiana benthamiana* belonging to Solanaceae, parsley (*Petroselinum crispum*) belonging to Apiaceae and finally basil (*Ocimum basilicum*) belonging to Lamiaceae were screened. As a control, *Arabidopsis* Col-0 was included as well. The value of the extraction buffer was subtracted from the results obtained after the application of the extract.
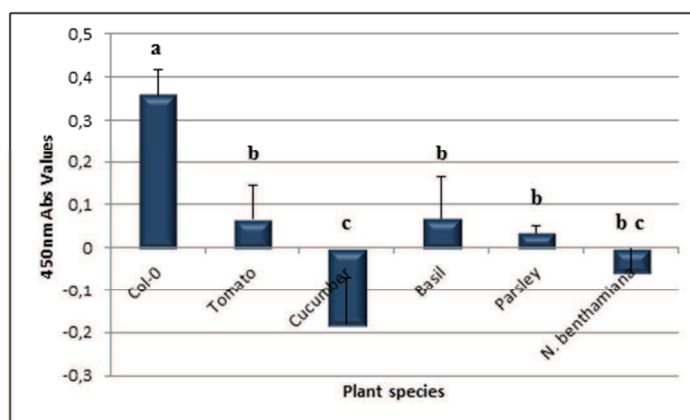
Figure 3.20 ROS assay on four plant families using *Hpa*-spore extract. The spore extract was tested on its capacity to trigger ROS production on five plant species belonging to four different families: Solanaceae (tomato and *N. benthamiana*), Cucurbitaceae (cucumber), Lamiaceae (basil) and Apiaceae (parley). *Arabidopsis* Col-0 (belonging to the Brassicaceae family) was used as a comparison for the obtained reactions. It is evident from the results, that the reactivity towards the active molecules contained in the extracts is found only in *Arabidopsis*, leading to hypothesize a Brassicaceae specificity. Statistical analysis: ANOVA One-Way, Tuckey post-test. Different letters indicate statistically different results.

Figure 3.20 shows how the perception of the reactive molecules contained in the *Hpa*-spore extract might be specific to the Brassicaceae family. In the case of tomato, basil and parsley, a residual activity is found even though it could be considered as a negligible signal, whereas in the case of cucumber and *N. benthamiana*, there is no reactivity at all when compared to the positive control (Col-0). The experiments were repeated twice with similar results.

3.3 Discussion

To increase the knowledge about *Hpa*-derived PAMPs and the related receptors involved in their perception in *Arabidopsis*, crude extracts from *Hpa*-Emoy2 spores and from *Hpa*-infected *Arabidopsis* tissues were obtained.

In a "work-in-progress" approach, the extracts were tested on their ability to trigger ROS production and callose deposition and afterwards fractionated to simplify the complex mixture. Following changes in the methodology, the *Hpa* spore extracts were treated with Proteinase K, tested on different *BAK1* and *BKK1* mutant plants and finally their perception was assessed on various *Arabidopsis* wt accessions and four different plant families.

3.3.1 *Hpa*-spore extracts contain active molecules

To investigate the presence of PAMP molecules in *Hpa*, crude extracts both from *Hpa* spores and from *Hpa*-infected *Arabidopsis* tissues were obtained. This approach was chosen to obtain a more complete set of molecules (both from the spores and from the developed organism). After few trials (see Section 3.2.1), a repeatable and reliable extraction method was established.

Because the aim was to discover new PAMP molecules, the extracts were tested using assays able to highlight signs of PAMP-triggered immunity (PTI), such as ROS production and callose deposition (Muthamilarasan & Prasad, 2013); the events that follow PAMP recognition by the plant are often used in plant pathology to identify PAMP molecules (Lloyd et al., 2014). Figure 3.4 and Figure 3.5 show, respectively, the amount of ROS and callose produced after the application of the extracts to Col-0 and

N. benthamiana plants. Both extracts appeared quite reactive (in terms of ROS production and callose deposition triggered) when compared to the positive controls, flg22 (Felix et al., 1999) and pure horseradish peroxidase. However in the case of *Hpa*-infected *At* tissues, it has to be considered and therefore subtracted the response given by healthy *At* tissues extracts (extracted and tested as well). In fact, since *Hpa* is an obligate biotroph (Slusarenko and Schlaich, 2003), to obtain the extracts from the developed and germinated pathogen, we had to use infected *At* seedlings.

In the attempt to simplify the complex mixture of molecules, the extracts (including the healthy ones) were fractionated using a strong anion chromatography column. In between the techniques used for fractionation, liquid chromatography and in particular ion exchange chromatography, which separates the proteins on the bases of their charge, is especially employed (Martínez-Maqueda et al., 2013). Figures 3.6, 3.7 and 3.8 show the banding patterns of the spore extracts, the infected *Arabidopsis* extracts and of the healthy extracts, respectively. With regard to the fractions, it can be noted that the bands are reasonably different between each other; even though there are few bands shared among two or more fractions. However it is difficult to tell if those are just not well resolved proteins from the fractionation or are different proteins sharing the same molecular weight. Most probably a better gel resolution would be needed, such as bi-dimensional electrophoresis that can separate the proteins on the basis of their molecular weight (as SDS-PAGE does) and their isoelectric point (pI), leading to a gel showing spots corresponding to single protein species (Fey and Larsen, 2001). All fractions were afterwards tested in a ROS assay, challenging Col-0 plants, to understand the distribution of the active molecules after the fractionation procedure. Surprisingly in all three cases (*Hpa* spores, infected and healthy *Arabidopsis*) only the FT fraction retained an activity compared to the positive control (peroxidase).

This result, together with the fact that the FT fractions of the healthy and infected *Arabidopsis* extracts shared many bands and moreover the overall activity of the infected extracts in triggering ROS and callose production (after subtraction of the contribution of the healthy extracts), led to the conclusion that the plant contribution was too high. Therefore the work was carried out only with the *Hpa* spore extracts.

3.3.1.1 Investigating the involvement of *RPP4, SOBIR1* and *BAK1* in the activity and perception of the active molecules

Because only the FT fraction of the *Hpa* spore extract retained the main activity among the 10 fractions obtained, to accelerate the fractionation procedure, after the application of the extract and the collection of the FT, the remaining proteins were collected altogether by eluting them with 0.55M NaCl. The newly obtained fractions (FT and eluate) were tested in a ROS assay to confirm what previously hypothesised and it was confirmed in many occasion that only the FT was mainly active.

To exclude a role for ATR4 in the activation of the plant immunity (ROS production), the FT and the eluate were tested in a ROS assay using Col-*rpp4* mutant plants. Indeed, during an incompatible interaction, the plant recognizes the non-self via a gene-for-gene strategy. Plants and pathogens co-evolved together in a constant arm race to survival (Dodds and Rathjen, 2010). In the studied pathosystem *Arabidopsis*/downy mildew, the bases for compatible and incompatible interactions are given by *R*-genes in the plant and *avirulence* (*avr*) genes in the pathogen. In detail, the genes involved in the recognition of the oomycetes are called *RPP* genes, from Recognition of *Peronospora parasitica* (the former name of *Hpa*), while the *avr* genes are called *ATR*, for *Arabidopsis thaliana* recognized. In the model pathosystem, different accessions of *Arabidopsis* are resistant to the colonization of different isolates of *Hpa* in accordance with the expression and interaction of corresponding *RPP/ATR* gene pairs, as explained by Holub et al. (1994). In this specific case, the spores are from the isolate Emoy2, while the *Arabidopsis* accession mainly in the assay is Col-0, the involved gene pair is *RPP4/ATR4* (Holub et al., 1994). However, as shown in Figure 3.13, there is no difference in between the amount of reaction triggered by the *Hpa* spores FT on Col-0 wt and on Col-*rpp4* mutants. Therefore it was concluded that most probably molecules other than ATR4 are the cause of ROS production. It could be speculated that *ATR4* is not present into the FT. It is, actually, still unclear if *Hpa* spores carry effector molecules in its protein form. There are evidences of the presence of effectors' RNAs, but it is still unknown whether they are translated into active proteins (Fabro et al. 2011).

The FT and eluate fractions were also tested on other mutant plants: Col-*sobir1* and Col-*bak1-5 bkk1-1*. Both of them are relevant receptors: as previously mentioned (see Section 3.1.3.1) they work as "helpers" for RLPs and RLKs, respectively, to transmit the signal. *SOBIR1*, indeed is a receptor kinase which functions as an adaptor for many receptor-like proteins, which otherwise would not be able to transmit the signal because they lack the intracellular kinase domain. *BAK1*, on the other hand, acts as a co-receptor for many RLKs, binding to form heterocomplexes after ligand binding (Liebrand et al., 2013; Gust and Felix, 2014). Consequently, due to their importance in PAMP signalling pathways it was important to determine whether or not *SOBIR1* and *BAK1* are involved in the perception and signalling of the active molecules contained in the FT fraction.

As shown in Figure 3.14a, similarly to the results of Col-*rpp4*, the amount of reactivity triggered by the FT on the mutated (Col-*sobir1*) plants did not change in comparison to the previously challenged Col-0 wt (Figure 3.12b). Because of this result, it was assumed that the adaptor SOBIR1 is not involved in the recognition of the molecules that trigger ROS production in Col-0 plants.

With regard to BAK1, the double mutant Col-*bak1-5 bkk1*-1 was used. In their study, Roux and colleagues (2011) showed that both *BAK1* and *BKK1* are involved in the disease resistance against *Hpa*. Therefore, since they share some common features and belong to the same kinase family and most importantly because they are needed for *Hpa* resistance and they are recruited together, we decided to use the double mutant to avoid the possible residual activity left in *BKK1*, due to functional redundancy (Roux et al., 2011). Because the members of this family have many roles outside of immunity, such as brassinosteroids perception, signalling and cell death control (just to mention some of them) (Liebrand et al., 2013), the double mutant (Col-*bak1-5 bkk1-1*) was selected since it didn't show cell death and growth defects (Schwessinger et al., 2011).

Differently from the previous results (Col-0, Col-*rpp4* and Col-*sobir1*), following the application of the FT on the mutant plants, a reduced accumulation of ROS was recorded in respect to the wt Col-0 (Figure 3.14b). In this experiment, flg22 was used as a reference, because it is known that BAK1 binds to Flagelling-Sensing2 (FLS2 – flg22 receptor) upon flg22 binding, helping in the signal transduction and amplification. It has been demonstrated a decrease in reactivity towards flg22 in plants where the co-receptor

BAK1 has been mutated (Chichilla et al., 2007). The obtained results are therefore in accordance and lead to the assumption of a role for BAK1 in the signalling of the active molecules contained in the *Hpa* spore FT.

3.3.1.2 Changing the methodology led to changes in the results

Despite the previous results, the possibility of plant contamination in the spore extracts (and therefore in the FT) due to the spore collection method was still a possibility. After a control experiment with a mock infection, it was confirmed that the spores were contaminated by plant residues.

For this reason, as explained in Section 3.2.4, the spore collection method was drastically changed from a "wet" method to a "dry" method in an attempt to significantly reduce the amount of contamination derived from the plants. However it has to be kept in mind that due to the nature of the microorganism studied (obligate biotroph), most probably it will be impossible to achieve a complete plant-free extract. Nevertheless, in a repeated mock experiment, the amount of contamination was almost completely eliminated.

The direct consequence of this change in the methodology was a change in the results. As shown in Figure 3.15a, the reactivity of the FT (obtained following the same procedure seen before) triggered a weaker reaction in Col-0 plants in comparison to the previously obtained FT. Surprisingly, the eluate, which previously showed an almost negligible reactivity on Col-0 plants if compared with the FT, in this occasion showed a significant reaction, higher than the FT or flg22. In addition, once the eluate was re-fractioned to highlight the fractions responsible for the activity, it was not possible to find a constant pattern. In fact, as shown in Figure 3.15b, the fractions obtained in two different occasions (but also in other experiments, data not shown), showed different level of reactivity. For instance, the fraction obtained with 0.1M NaCl, in one case was highly reactive, while the same fraction obtained from a different sample showed a weaker reactivity.

One hypothesis could be made: because of the previous high plant contamination, it could have been possible that many active *Hpa* proteins (now found in the different

fractions) passed through the column (therefore found in the FT) either because bound to the contaminants from plants and therefore not available for the binding to the column or because the column was already saturated with plant contaminant and not available to bind *Hpa* proteins.

For these reasons and for the difficulties in obtaining enough spore, extracts and therefore fractions, it was decided to pursuit the study of PTI in the *Arabidopsis*/*Hpa* interaction by studying the un-fractionated *Hpa* spore extracts (collected with the "dry" methodology).

3.3.2 Proteinase K treatment suggests a proteinaceous nature for at least one active molecule

To shed light on the nature of the active molecules present in the *Hpa* spore extracts, they were treated with the enzyme Proteinase K to eliminate the protein fraction.

Proteinase K was chosen among other proteases because of its very strong activity in degrading proteins, both in their native state or denatured. It is also not inhibited by detergents or chelating agents (found in the extraction buffer used – see Section 2.2.2.1) and it is active in a wide pH range (7.5 - 12). The optimum temperature is around 37 °C but it works well also at 50 °C (a temperature that helps in unfolding proteins and expose the cutting points) (Ebeling et al., 1974).

The Proteinase K-treated *Hpa* spore extracts were afterwards loaded on a gel (Figure 3.16) to make sure that the reaction worked and they were finally tested on a ROS assay on Col-0 plants (Figure 3.17). From the two gels in Figure 3.16 (a and b) it is noticeable the striking difference in banding pattern among the spore extract samples before and after Proteinase K treatment. The few bands left on the gels after the treatments correspond to the remaining Proteinase K itself (bands at approximately 29 kDa) or to the products of its autolysis. The banding pattern of the treated samples is indeed identical to the one of the extraction buffer containing the same amount of Proteinase K used in the protein samples. It has been demonstrated that Proteinase K undergoes an autolysis reaction if the incubation time is long enough to enable it (Bajorath et al., 1988). Therefore, it can be concluded that the Proteinase K treatment was able to clear the *Hpa* spore extracts from the proteins they contained.

As mentioned above, the treated *Hpa* spore extracts were tested in a ROS assay on Col-0 plants on their ability to trigger ROS production, to understand whether the triggering activity was lost or not after the elimination of the proteins inside of the samples. The buffer treated with the same amount of Proteinase K was used as a background control to exclude any contribution to the ROS production given by the enzyme itself. Three different *Hpa* spore extracts were used in the experiment. As shown in Figure 3.17, despite the variability in between the three samples of spore extracts, in all three case a reduction in ROS production is visible after the Proteinase K treatment. In sample 2 there is a high difference, while a significant reduction is observed in sample 3. Taken altogether, these results show that the treatment with Proteinase K has an influence in the activity of the spore extracts, leading to the assumption that at least one (if not more) or the active molecules are of proteinaceous nature.

With regard to the left ROS triggering activity in the treated extracts, two hypotheses can be considered: firstly, although all the proteins seemed to be eliminated, it is still possible that not all the small peptides (not visible in the gel used) have been eliminated by the treatment. This could be the case, considering that some of the main studied and well known PAMPs, such as flg22 (Felix et al., 1999) or elf18 (Kunze et al., 2004) are short peptides rather than entire proteins. Secondly, it is known that not all the known PAMPs are of proteinaceous nature; there are indeed, oligosaccharides, lipopolysaccharides, to name but a few (Boller & Felix, 2009). Therefore it is not only possible but it is very likely, that even assuming that the treatment eliminated all the proteinaceous PAMPs, there may still be molecules (with a different nature) able to trigger an immune reaction.

3.3.3 BAK1 is involved in the perception and signalling of the active molecules

The ROS assay on the double mutant Col-*bak1-5 bkk1-1* (Schwessinger et al., 2011; Roux et al., 2011), previously used to test the FT and eluate fractions, was repeated also with the newly obtained extracts (Figure 3.18a) with similar results to the previous experiment (Figure 3.14b).

As previously mentioned (see Section 3.1.3.1), the receptors (BAK1 and BKK1) are not only involved in immune signalling, but also in the signalling of plant hormones called brassinosteroids (BR) (Hee & Li, 2002; Li et al., 2002; Vert, 2008). It is also known that the two receptors are functionally redundant in the brassinosteroids (BR) signalling (He et al., 2007). This is the reason behind the choice of the double mutant.

However, in order to gain more insight in the involvement of the two receptors in the perception and signalling of the active molecules, a ROS assay using Col-*bak1-5* and Col-*bkk1-1* mutant plants was performed (Figure 3.18b). It has been shown that, while there is a statistical reduction in ROS accumulation following the application of the extract on plants mutated in the BAK1 receptor, no statistical difference is shown in plants mutated in BKK1 in respect to Col-0 wt. After these results, it can be speculated that, although they show a redundancy in the BR signalling (see above), this is not completely true in the case of the signalling of the *Hpa* active molecules. Most probably, it could be hypothesised that BAK1 is the receptor mainly involved in the signalling (probably acting as a co-receptor as seen in Section 3.1.3.1; Gust and Felix, 2014). In fact, when BAK1 is mutated and inactivated, the ROS accumulation is significantly reduced (even though not completely eliminated as in the case of the double mutant), while no role for BKK1 as a co-receptor could be hypothesised since no reduced ROS accumulation is shown for BKK1 mutant plants.

3.3.4 The perception of the active molecules differs among *Arabidopsis* accessions and is Brassicaceae specific

The *Hpa* spore extract was finally tested in two ROS assays, involving various *Arabidopsis* wt accessions and plants from four different families respectively, to investigate the perception of the active molecules among *Arabidopsis* and different plants.

As shown in Figure 3.19, among the nine different ecotypes tested (including Col-0 as a reference), only two of them (Bur-0 and No-0) showed ROS accumulation levels similar to the reference Col-0, while the remaining ecotypes showed a decreased ROS production and therefore a decreased sensitivity towards the active molecules contained in the extract. These results may highlight differences in perception due to genotypic

differences in between the different ecotypes. They may have, indeed, inactive or mutated forms of the receptors involved in the perception of the active molecules. Similarly, in the case of the well-known bacterial PAMP flg22 (Felix et al., 1999), it was reported a varied sensitivity among different *Arabidopsis* ecotypes, with a total lack of sensitivity for the ecotype Wassilewskija (Ws-0) due to the mutated receptor for flg22 (Bauer et al., 2001; Vetter et al., 2012). Alternatively, the differences in ROS accumulation in different *Arabidopsis* ecotypes could be attributed to the presence in the *Hpa* spore extract of effector molecules able to address peroxidase enzymes on *Arabidopsis* cell wall. It is known, indeed, that effector molecules target members of the PTI machinery (e.g. peroxidases) (Howden & Huitema, 2012). Therefore, the genetic differences (resulting in different phenotypes of resistance) could be found in the peroxidases pattern or conformation, rather than differences in the receptors.

In addition, it has been shown that the responsiveness to the active *Hpa* molecules is restricted to *Arabidopsis* plants (Figure 3.20). In fact, among the four different plant families tested (Solanaceae, Cucurbitaceae, Lamiaceae and Apiaceae), no one showed appreciable ROS accumulation in comparison to Col-0 plants (representing *Arabidopsis* plants and therefore Brassicaceae). This phenomenon could be easily explained by the high level of interaction established during evolution in between *Arabidopsis* plants and *Hpa*. Indeed, the fact that *Hpa* is an obligate biotroph of *Arabidopsis* (Slusarenko and Schlaich, 2003) could represent the reason why only *Arabidopsis* is able to perceive it. Although a more complete experiment including other members of the Brassicaceae family would be needed, it could be speculated that the perception of the *Hpa* active molecules might be Brassicaceae-specific (being *Arabidopsis* a member of the family). There are indeed other examples, where PAMP molecules are perceived just by the members of the Brassicaceae family (e.g. elongation factor Tu) (Kunze et al., 2004).

Cellulose-Binding Elicitor Lectin (CBEL) proteins from *Hpa*

Abstract

In the *Hpa* genome there are two genes encoding for CBEL or CBEL-like proteins. This fact is important in the light of the discovery that two domains, contained in the CBEL protein from *Phytophthora parasitica* var. *nicotianae*, called cellulose-binding domains (CBDs), are recognised as PAMP molecules in *Arabidopsis* and *N. benthamiana* (Gaulin et al., 2006). In the search for *Hpa*-derived PAMPs, we decided to study the two *Hpa* CBEL proteins to understand whether they contained the CBDs and if they were recognised as PAMPs as well.

A bioinformatic analysis with the three proteins (from *Hpa* and *Ppn*), revealed the presence of a CBD in both *Hpa* proteins. Therefore, both genes have been stably and transiently expressed in *Arabidopsis* and *N. benthamiana*, respectively, and also heterologously expressed in *E. coli*.

Our data indicate that a CBD is present in both *Hpa* proteins and that both proteins are able to cause immune reactions (callose deposition in *Arabidopsis* and leaf discolouration in *N. benthamiana*) in plants, suggesting that they may represent *Hpa*-derived PAMPs.

4.1 Introduction

4.1.1 Where do we start? CBEL from *Phytophthora parasitica* var. *nicotianae*: an orthologous PAMP

The *Phytophthora* Cellulose Binding Elicitor Lectin (CBEL) protein has been extensively studied since the mid-1990s. It was isolated in 1995 as a 34 kDa glycoprotein, (therefore named GP34) from the mycelium of *Phytophthora parasitica* var. *nicotianae* (*Ppn*), the causal agent of black shank in tobacco plants. It was able to elicit defence responses in tobacco (its host plant), activating the lipoxygenase pathway (involved in defence responses) at micromolar concentrations (Séjalon et al., 1995). Localization studies indicated that it is present in the cell wall of the oomycete when grown *in vitro*, and of the zoospores during the formation of a new cell wall (Séjalon-Delmas et al., 1997). Two years later GP34 was renamed CBEL, after experiments revealing its role in cellulose binding and eliciting defence and its behaviour as a lectin (Villalba Mateos et al., 1997). Further studies on *Ppn* strain, in which the expression of the protein was suppressed, demonstrated the role of CBEL in the perception of cellulose (Gaulin et al., 2002). Indeed the transgenic strains were strongly impaired in the attachment to cellulosic and cellophane substrates and in the formation of branching hyphae. However when in contact with roots of the host plant tobacco, they were able to form branched hyphae, showing that most probably their pathogenicity was not compromised (Gaulin et al. 2002). In 2004, a study by Khatib and colleagues about the ability of CBEL to trigger defence responses in *Arabidopsis thaliana* revealed that it was able to elicit the three main signalling pathways dependent on the stress hormones salicylic acid, jasmonic acid and ethylene. In the same article, it was hypothesized that CBEL could act as a PAMP. It was found, indeed, in many *Phytophthora* species (*Ppn* and others), but not in plants. Furthermore, the protein was shown to contain highly conserved domains, called cellulose-binding domains (CBDs) (see Figure 4.1 for CBEL structure). It was also demonstrated to elicit immune reactions in different plant families including, the *Solanaceae* (tobacco) and the *Brassicaceae* (*Arabidopsis*), but also the *Fabaceae* (French bean) and the *Asteraceae* (*Zinnia*). All of the above are known characteristics of PAMP molecules (Khatib et al., 2004, Nürnberger et al., 2004). With the use of synthetic peptides (representing the two CBD domains) and modified

(truncated or mutated) versions of the protein, expressed both in bacteria and *in planta*, it was possible to confirm the previous assumption that CBDs represent novel PAMP molecules. The importance of intact CBD domains for their defence-triggering activity was also shown. Within the same study, it has been also found that the glycan moiety of the protein is not involved in the recognition by the plant. Indeed, the protein CBEL produced *in vitro* in *E. coli* had the same activity as the original CBEL studied by Villalba Mateos and colleagues (1997). Furthermore it was also an interesting discovery that the native CBEL signal peptide was still active in directing the protein towards the extracellular space, when heterologously produced *in planta* (Gaulin et al. 2006).

4.1.2 *Phytophthora* CBEL protein structure

The CBEL-encoding gene was first cloned in 1997 from *Ppn* (Villalba Mateos et al., 1997) and the studies that followed revealed important features about its structure. In *Phytophthora*, only one gene seems to encode for CBEL. The encoded protein is 268 aa-long (with a molecular mass of 26 kDa) and it seems to be synthesized as a pre-protein. It has an 18 aa-long signal peptide, situated at the N-terminal of the mature protein. It is composed of two repeated domains (Figure 4.1), separated by a linker region rich in threonine and proline residues (Figure 4.2).
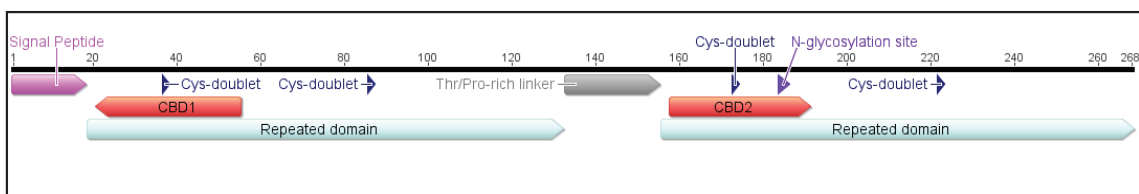
Figure 4.1 Schematic domain structure of CBEL protein from *Phytophthora parasitica* var. *nicotianae*. The main features are highlighted as follows: signal peptide (pink; residues 1-18), repeated domains (light blue; residues 19-132 and residues 156-268), linker region (grey; residues 133-155) and CDB domains (red; residues 21-55 and residues 158-191). In each repeated domain there are two cysteine doublets (Cys-doublet, blue; 1 (37-38), 2 (86-87), 3 (173-174), and 4 (222-223)). The N-glycosylation site (purple; residues 184-186) is also underlined.

The two domains are rich in cysteines, containing 12 residues each (with two Cys doublets/domain). The repeats can be aligned, showing a high percentage of homology (Figure 4.3; Villalba Mateos et al., 1997). Studies on the amino acids and sugar

composition revealed that CBEL is a glycoprotein and that the sugar fraction accounts for around 55%. The main sugar is glucose (representing at least 93%), but it contains also mannose, galactose and glucosamine in minor part. Furthermore, it has been shown to contain also the rare amino acid hydroxyproline, usually found in the cell wall of fungi, green algae, higher plants and animals (Villalba Mateos et al., 1997; Séjalon-Delmas et al., 1997).
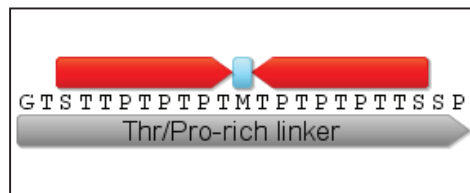
Figure 4.2 Detail of the Threonine/Proline-rich region. The region (23 aa long) that connects the two repeated domains in the sequence of the protein CBEL (*Ppn*) is characterized by being palindromic around the central methionine (light blue).
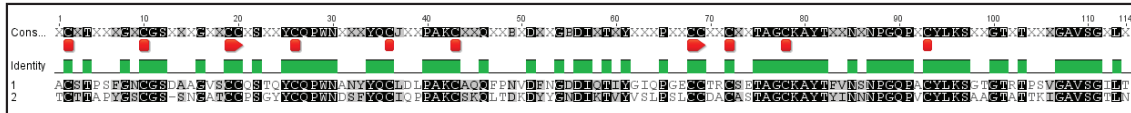
Figure 4.3 Amino acid sequence alignment of the two repeated domains of CBEL from *Ppn*. Out of the 114 aa that compose each domain, 62 are identical (black background letters) between the two domains, representing 54.4 %. The identity between the two is represented by a green bar over the two aligned sequences. The 12 cysteine residues for each repeated domain are also showed, underlined in the consensus (Cons) sequence by the red spot. In each repeat two cysteine doublets (red small arrows) are present.

4.1.3 Cellulose-binding domains (CBDs): novel PAMP molecules

As already mentioned in Section 4.1.1, due to their conserved structure, the two CBDs of the glycoprotein CBEL have been investigated by Gaulin and colleagues (2006) as they represented ideal candidates for new PAMP molecules. During their complete and thorough study, Gaulin and collaborators confirmed what was initially hypothesized; CBEL (*Ppn*) contains two novel oomycete PAMP molecules and these are represented by the two Cellulose-Binding Domains (CBDs) (Gaulin et al., 2006).

CBDs belong to the Family 1 Carbohydrate Binding Modules (CBM_1), which are found mostly in fungi and have not been identified in higher plants yet (Gaulin et al., 2006). Currently, 71 different CBM families have been classified (http://www.cazy.org/Carbohydrate-Binding-Modules.html). CBMs are non-catalytic domains, which are often found in a modular association with catalytic domains within degrading enzymes (i.e. glycoside hydrolases), that are able to degrade insoluble polysaccharides (including cellulose, both crystalline and non-crystalline, chitin, xylan and mannan) (Boraston et al., 2004). In CBEL, however, the domain is associated with a non-catalytic one, the Apple_Factor_XI-like, and generally involved in carbohydrate binding or protein-protein interactions.
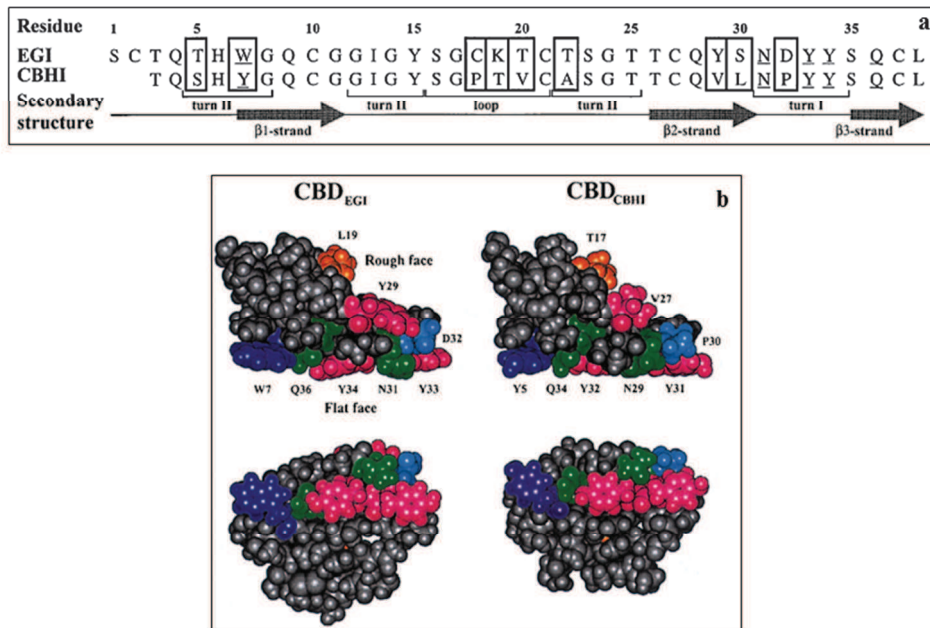
Figure 4.4 Example of a CBD domain structure from *Trichoderma reesei*. a: alignment of amino acid sequences between two CBD domains. They belong to the endoglucanase I (EGI) and the cellobiohydrolase I (CBHI), respectively, both of which are from the cellulolytic filamentous fungus *T. reesei*. It is possible to notice the conserved nature of their structure; only 9 out of 36 amino acids are different (boxed). The underlined residues are exposed on the flat face of the structure. The secondary structure of the domain is shown as well in the lower part of the picture; the domain forms a three-stranded antiparallel β sheet. **b**: the tridimensional structures of the two domains (CBD$_{EGI}$ and CBD$_{CBHI}$). In detail, both the rough face and the flat face are present. The exposed residues are coloured (underlined in picture **a**) (Mattinen et al., 1998).

CBM_1s are composed of around 40 residues; they can be found both at the N- and C-terminal of the protein/enzyme. They fold in a three-stranded antiparallel β-sheet, which

forms a flat surface with usually three aromatic residues involved in the binding of the cellulose (Figure 4.4b). The three residues are separated by 10.4 Angstroms, which enables binding to the glucose units in the cellulose structure. CBM_1 contains also four cysteine residues that are involved in the formation of disulphide bonds (http://prosite.expasy.org/prosite) (Figure 4.4a).

4.1.4 Aims of the study on CBEL proteins

Because of the presence of two genes coding for CBEL proteins in the *Hyaloperonospora arabidopsidis* (*Hpa*) genome, and because of the role as PAMP molecules of the two CBD domains contained in the well-studied CBEL protein in *Ppn*, the main aims of this part of the research project were to:

> ➢ Investigate the two CBEL proteins from *Hpa* using bioinformatics tools
> ➢ Elucidate if the *Hpa* CBEL proteins are recognized as PAMP molecules in *A. thaliana* and *N. benthamiana*.

4.2 Results

4.2.1 Bioinformatic analysis of *Hpa* CBELs proteins

4.2.1.1 Structure comparison with CBEL from *Ppn*

Two genes corresponding to CBEL or CBEL-like proteins were identified in the *Hpa* genome (Baxter et al., 2010). They are located on Scaffold 10 (61,450-61,938 *Hpa*G801903 and 62,305-62,805 *Hpa*G801904) and they seem to have originated from a duplication event; they are indeed paralogs (EnsemblProtists: http://protists.ensembl.org). Their primary structure, compared to the one of CBEL from *Ppn*, is reduced. Both the proteins lack completely the second repeated domain found in CBEL (*Ppn*) after the Thr/Pro-rich linker region (Figure 4.5). Both *Hpa*G801903 and *Hpa*G801904 have a 20 aa-long signal peptide at the N-terminal.

Using the on-line bioinformatic tool SMART (http://smart.embl-heidelberg.de/), it was possible to identify a Pan-like domain in both proteins, however the cellulose-binding

domain was not detected (Figure 4.6a). When the search was extended to the outliers as well, it was possible to identify the CBD in *Hpa*G801904 (Figure 4.6b).
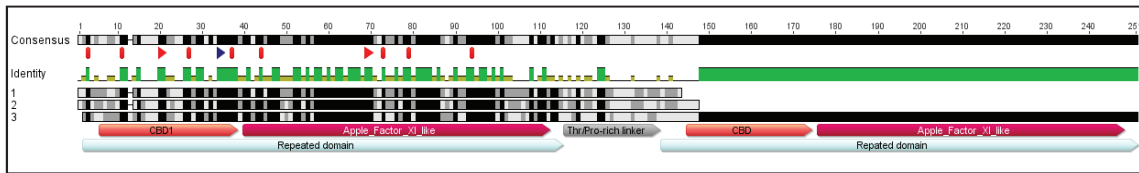
Figure 4.5 Comparison of CBEL proteins from *H. arabidopsidis* and *P. parasitica* var. *nicotianae*. The signal peptides have been removed from the sequences. The consensus obtained from the alignment is given at the top. In the bottom part the annotations referred to the sequence of *Ppn*-CBEL (see Figure 4.1 for the details). The two *Hpa* sequences (1 and 2) align to and cover only the first part of the sequence from *Ppn* (in detail the first repeated domain and the linker region). There is a high percentage of identity (47.9%; showed by the black background or the green line above the three sequences) between the three proteins, especially in the region represented by the Apple_Factor_XI-like and the final part of the CBD. The 12 cysteines (highlighted by the red spots) are conserved in all the sequences as well as the two tyrosines (blue arrow).
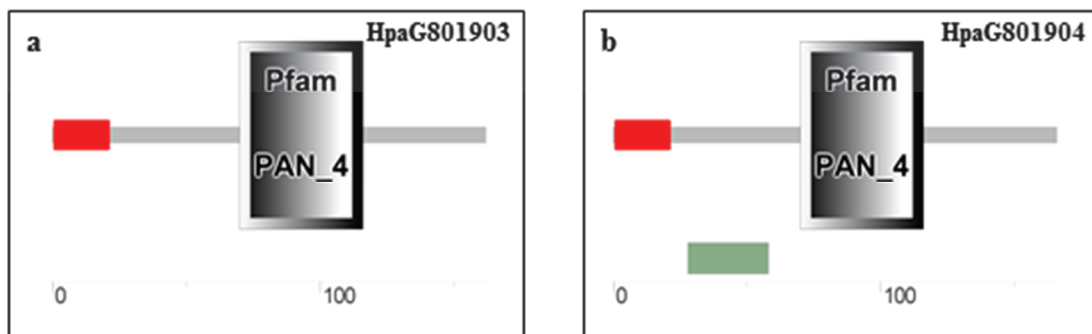
Figure 4.6 Domain comparison between the two *Hpa* CBEL proteins. The figure shows the domains that the online tool SMART found in the sequences of the CBEL proteins (*Hpa*). In both sequences the PAN_4 domain was found (indicated by the grey square); while in *Hpa*G801904 (**b**), the CBD domain, belonging to CBM1, was found only when the search was extended to outliers (green rectangle). The red rectangles represent the signal peptide.

This result is in accordance with what found by Larroque and colleagues (2012) in their study regarding the presence of CBM1-containing proteins in oomycetes and fungi. However, after comparing the two *Hpa* sequences with the two repeated domains found in *Ppn*-CBEL (Figure 4.7b), but primarily with the CBD pattern found in most CBDs found in fungi (Figure 4.7a), it became clear that also the two *Hpa* proteins could

contain the domain. Indeed, as shown in Figure 4.5, there is a high homology between the three sequences and there are many conserved residues. In particular the four cysteines (highlighted in blue in Figure 4.7), supposed to be involved in the formation of two disulphide bonds and fundamental for the backbone structure, are present in both *Hpa* proteins. In particular the pattern of the four cysteine residues, forming two disulphide bonds, seems to be conserved. In addition, it was found that two tyrosine residues (Y_{53} and Y_{54}) are conserved as well in the *Hpa* CBEL proteins. The two aromatic amino acids are found in the first CBD of CBEL *Ppn* (Y_{51} and Y_{52}) as well as in the CBDs of the endoglucanase I (EGI) and the cellobiohydrolase I (CBHI) of *T. reesei* (Figure 4.4a: Y_{33} and Y_{34}, Y_{31} and Y_{32} respectively). These two amino acids are important because they seem to be surface exposed (Figure 4.4b) and involved in the interaction with cellulose.
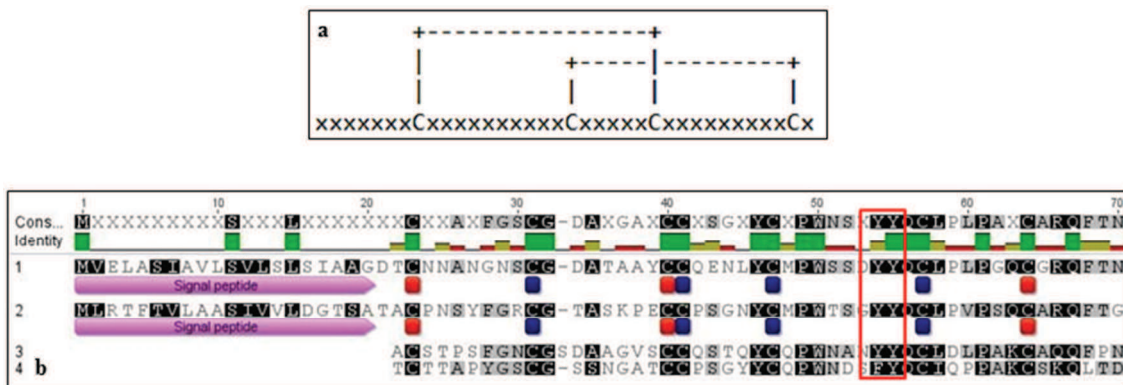
Figure 4.7 Conserved pattern of the fungal CBD domain and its presence in the CBEL proteins structure. a: the pattern formed by the four conserved cysteines in the CBD domain. They form two disulphide bridges, structurally important for the stabilization of the backbone structure and therefore highly conserved (Prosite). **b**: the amino acid sequences of the two CBDs in the CBEL proteins from *Hpa* (1: *Hpa*801903 and 2: *Hpa*801904) and the CBDs from the two portions of CBEL from *Ppn* (3: first repeated domain and 4: second repeated domain). The seven conserved Cys residues are highlighted (red and blue); in blue are the ones involved in the formation of the disulphide bonds. The two conserved tyrosines (Y) are highlighted by the red box.

4.2.1.2 Sequencing of the two *Hpa CBEL* genes from Emoy2 isolate

The *Hpa*801903 (designated *Hpa-CBEL1*) and *Hpa*801904 (designated *Hpa-CBEL2*) genes were amplified from the *Hpa*-Emoy2 genomic DNA (Sections 2.2.1.1 and 2.2.1.2) and afterwards verified by sequencing (see the Appendix for primers used).

In the case of the *Hpa-CBEL2* gene, there was no sequence difference between the cloned and the published gene. Whereas, *Hpa-CBEL1* contained two single nucleotide mutations or single nucleotide polymorphisms (SNPs) in the sequence in respect to the annotated one (Figure 4.8).
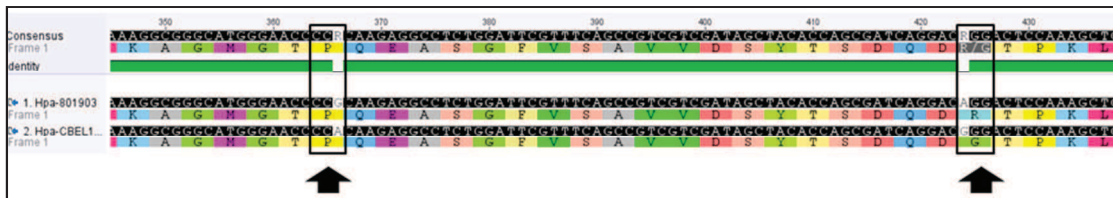
Figure 4.8 Sequence mutations in the sequenced *Hpa-CBEL1* gene. The picture shows two single nucleotide mutations in the sequence of the gene *CBEL1* (*Hpa*-Emoy2) after sequencing (*Hpa-CBEL1*) in respect to the original annotated sequence (*Hpa*-801903). The first mutated nucleotide (G→A) is in position 366 and it results in the same amino acid (P, proline), while the second one in position 424 (A→G) results in the translation of a different amino acid: a glycine (G) instead of an arginine (R).

As highlighted by the first black arrow in Figure 4.8, the first mutation is located in position 366 on the sequence and in detail the nucleotide (nt) is in the third position in the codon. The original nt was a guanine, while in the amplified Emoy2 gene it was an adenine. Because of the degeneration of the genetic code, the resulting amino acid was however proline (P), therefore it resulted in a synonymous mutation. In the second case, the SNP was in position 424 and being at the beginning of the codon, it was more likely to affect the final amino acid product. It resulted indeed in a different amino acid and therefore in a nonsynonymous mutation (missense). The new triplet coded for a glycine, a non-charged amino acid, while the original annotated codon coded for an arginine (a positively charged amino acid). While this second mutation may have had more consequences that the first one, its location was in the very final part of the protein, corresponding to the hinge region in the *Ppn*-CBEL protein (Figure 4.5 – Thr/Pro rich linker, see sequence n.1).

4.2.2 Overexpressing *CBEL* genes in *Arabidopsis thaliana*

With the aim of understanding the nature of the two CBEL proteins encoded by *Hpa*, as mentioned in the above section, the two genes *Hpa-CBEL1* and *Hpa-CBEL2* were amplified from *Hpa*-Emoy2 genomic DNA. As a positive control, *Ppn-CBEL* was

amplified from the vector pGR105, which was kindly donated by Dr Elodie Gaulin (Université de Toulouse, Laboratoire de Recherche en Sciences Végétales, Toulouse, France) and cloned as well.

The three sequences were amplified using the polymerase Elongase® Enzyme Mix (see Section 2.2.1.2) because of its proofreading capacity and cloned in the destination vector pEarlyGate100 (pEG100, belonging to the Gateway® system, see Section 2.2.1.5), for *in planta* protein expression. Although Gaulin and colleagues (2006) demonstrated that CBEL (*Ppn*) signal peptide is sufficient to export the protein into the extracellular space once expressed in tobacco, this was not known for *Hpa* CBEL proteins. Therefore, one modified version of both proteins was produced as well, in which their signal peptide was replaced by the signal peptide of the *Arabidopsis* Pathogenesis-Related 1 (PR-1) protein (see Section 2.2.1.3), known to be exported in the extracellular space (Sudisha et al., 2012). The two additional sequences were cloned in pEG100 vector as well. Once the accuracy of the DNA sequences was confirmed via sequencing, the vectors were transformed into *Agrobacterium tumefaciens* (see Section 2.2.1.6) and Col-0 plants were then transformed by floral dipping (see Section 2.2.1.10).

The transformed plants were selected by the use of the herbicide BASTA® (glufosinate-ammonium, see Section 2.2.1.11), taking advantage of the BASTA® resistance (*BAR*) carried by pEG100 vector. Three homozygous lines were chosen for each construct for the following experiments:

- **Ppn-CBEL**: lines 2A *Ppn*, 4A *Ppn* and 7A *Ppn*
- **Hpa-CBEL1** (*Hpa*801903): lines 1A, 2E and 3A
- **Hpa-CBEL2** (*Hpa*801904): lines 7A, 9A and 11D
- **PR1-*Hpa-CBEL1***: lines 25B, 26C, 28E
- **PR1-*Hpa-CBEL2***: lines 31B, 32B and 35E

For each line, five plants were grown. The DNA was extracted from each plant and a PCR using the same primers used to amplify the genes was performed in order to check that the gene of interest was stably integrated into the *Arabidopsis* genome. The PCR reactions were afterwards run on a gel and the presence of the genes was confirmed for every line produced.

4.2.2.1 Does CBEL overexpression generate ROS production and callose deposition?

In order to shed light on the role of the *Hpa* CBEL proteins as PAMP molecules in *Arabidopsis*, the stably transformed plants were tested using a ROS assay (see Section 2.2.2.4) and a callose deposition assay (see Section 2.2.2.5).

For each construct (pEG100::*Ppn-CBEL*, pEG100::*Hpa-CBEL1,* pEG100::*Hpa-CBEL2*, pEG100::PR1-*Hpa-CBEL1* and pEG100::PR1-*Hpa-CBEL2*), three transformed lines were tested (see above). For each line, four plants were assayed by collecting and testing three leaf disks each.
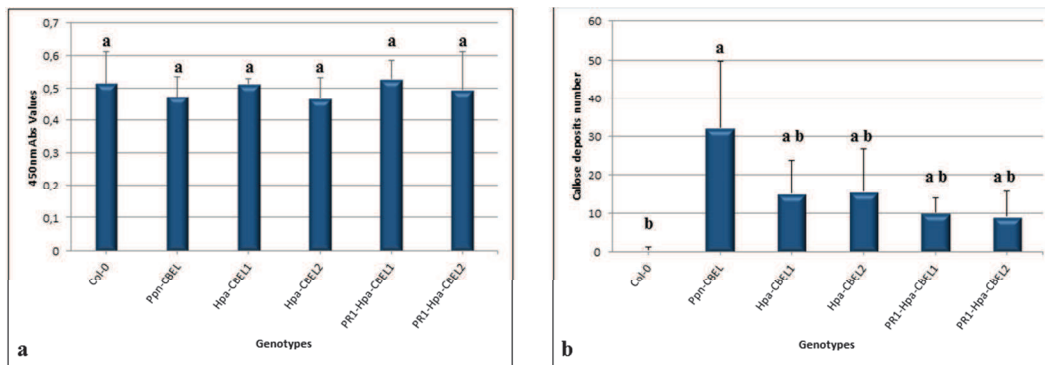
Figure 4.9 ROS production and callose deposition assay on CBEL over-expressing plants. a: ROS production in the transformed plants compared to Col-0 wt. **b**: callose deposits count on stably transformed plants and Col-0. Only the plants transformed with CBEL *Ppn* show a statistically significant increase in the number of callose deposits in respect to wt Col-0 plants. Four plants were tested for each transgenic line and a total of three lines per construct were used. The results deriving from the three different lines were averaged and the average for each construct is shown. Statistical analysis: One-Way ANOVA and Tuckey post-test.

As shown in Figure 4.9a, there is no statistical difference, in ROS production, in between stably transformed plants and Col-0 wild type plants. Whereas it was possible to observe a significant increase in the number of callose deposits produced by the three lines transformed with pEG100::*Ppn-CBEL* in comparison to the non-transformed wild type Col-0 plants (Figure 4.9b). There is a visible increase in the number of callose deposits in the lines transformed with the *Hpa* proteins, although it is not as significant as the number of callose deposits triggered by the *Ppn*-CBEL.

4.2.2.2 Does CBEL overexpression trigger resistance against *Hpa*?

The homozygous lines (see Section 4.2.2) were challenged with two different *Hpa* isolates (Noks1 and Maks9) to understand whether the stable overexpression of the different CBEL proteins would trigger PAMP-triggered immunity and therefore resistance to the *Hpa* infection.

For each construct three different transgenic lines were sown. Each experiment was conducted in duplicate. When the seedlings were one-week-old, they were sprayed with the *Hpa* isolate Noks1 or Maks9 (5×10^4 spores ml^{-1}) and after one week of incubation at 16 ºC, 12h light/12h dark at 100% humidity the spores were counted (see Section 2.2.3.4).

As shown in Figure 4.10, there is no statistical difference in *Hpa*-Noks1 spore production, after the inoculation of Col-0 wild type plants and the stably transformed plants, although a slight reduction in the number of spores counted it is visible in the case of plants transformed with the constructs *Ppn-CBEL*, *Hpa-CBEL1* and PR1-*Hpa-CBEL2*.
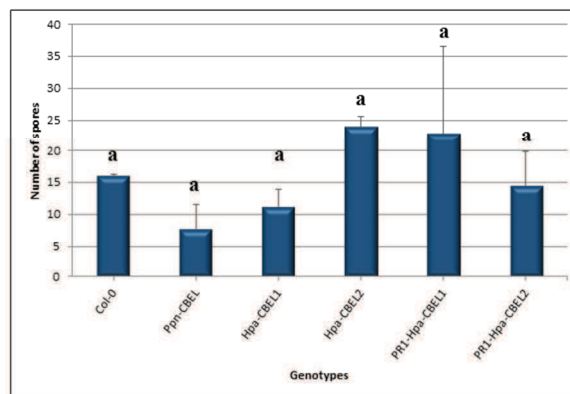
Figure 4.10 Sporulation of *Hpa*-Noks1 on Col-0 plants transformed with *CBEL* genes. Number of spores on CBELs over-expressing lines infected with 5×10^4 spores ml^{-1}. Three transgenic lines were tested for each construct and 15 seedlings were counted for each line. The graph shows the average spore number obtained per construct. Statistical analysis: ANOVA One-Way, Tuckey post-test.

Figure 4.11 shows the results obtained after challenging the transgenic plants with *Hpa*-Maks9. Once again, there is no actual statistical difference in between the number of

spores counted on different transgenic plants; however, few differences can be noticed. There is, indeed, an increase in spore production in the plants transformed with *Hpa-CBEL1*, *Hpa-CBEL2*, PR1-*Hpa-CBEL1* and PR1-*Hpa-CBEL2* when compared with the number of spores produced on Col-0 by *Hpa*-Maks9. There is instead no significant difference in the number of spores produced after the inoculation of the plants producing CBEL *Ppn* when compared with Col-0 wild type.
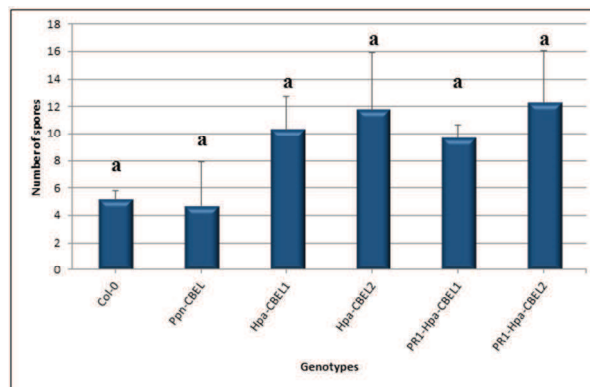
Figure 4.11 Sporulation of *Hpa*-Maks9 on Col-0 plants transformed with *CBEL* genes. Number of spores on CBELs over-expressing lines infected with 5×10^4 spores ml^{-1}. Three lines were tested for each construct and 15 seedlings were counted for each line. The graph shows the average spore number obtained per construct. Statistical analysis: ANOVA One-Way, Tuckey post-test. The experiments were repeated three times with similar results.

4.2.2.3 Phenotypic alterations in *Arabidopsis* plants overexpressing CBEL proteins

The selected homozygous plants were grown altogether (three transgenic lines for each construct and three plants for each line), along with untransformed Col-0 plants as a control, to determine whether the overexpression of CBEL proteins may cause any changes in the phenotype. It was, indeed, expected that if CBEL proteins from *Hpa* were recognized as a PAMP in *Arabidopsis*, it would have triggered the plant immune machinery with consequences visible as a change in the normal development of the plant (Lozano-Durán and Zipfel, 2015), as was shown in the case of flg22 (Gómez-Gómez et al., 1999) and elf18 (Kunze et al., 2004).

All the plants were kept under the same conditions (20 ºC and with 14 h light and 10 h dark regime) to minimise any change or difference due to external conditions rather than the transformation event and the expression of the proteins.

Figure 4.12 Phenotypical analysis on stably transformed Col-0 plants expressing *Ppn*-CBEL, *Hpa*-CBEL1, *Hpa*-CBEL2, PR1-*Hpa*-CBEL1 and PR1-*Hpa*-CBEL2. Column **a**: three transgenic lines transformed with pEG100::*Ppn*-CBEL (4A *Ppn*, 2A *Ppn*, 7A *Ppn*); column **b**: three mutant lines transformed with pEG100::*Hpa*-CBEL1 (1A, 2E, 3A); column **c**: three transgenic lines carrying pEG100::*Hpa*-CBEL2 (7A, 9A, 11D); column **d**: three transgenic lines transformed with pEG100::PR1-*Hpa*-CBEL1 (25B, 26C, 28E); column **e**: three transgenic lines transformed with pEG100::PR1-*Hpa*-CBEL2 (31B, 32B, 35E). For each transgenic line three plants were grown and in every case they were well represented by the plants shown in the picture. Since all the transformants were in Columbia background, col-0 plants (plant in the picture above the others) were grown as a control.

Six weeks after transplant there were no remarkable signs of differential growth or developmental rate (Figure 4.12). To elucidate the growth rate, the leaf number was counted: 14 leaves were developed by Col-0 plants (control) and most of the lines were

at the same developmental stage, with the exception of lines 2A *Ppn* and 4A *Ppn* showing 12 leaves and lines 26C, 28E and 31B counting 16 leaves.

To better understand the impact of CBEL proteins expression on the transformed plants, the pictures taken six weeks after transplant, were analysed using the software ImageJ. The total leaf area, expressed in cm^2 was calculated after cropping the image around the plant shape and converting the obtained image into a binary one. Afterwards, the plant shape was highlighted and the area calculated. The results are shown in Figure 4.13.
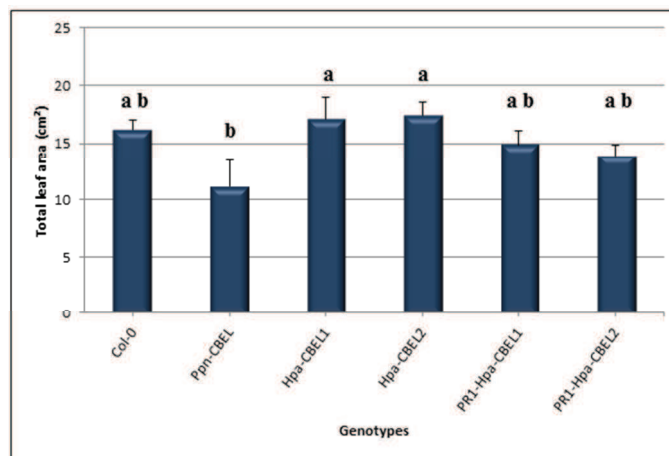
Figure 4.13 Total leaf area in six-week-old stably transformed Col-0 plants. Three plants for each line were considered. Pictures were taken six weeks after transplant in big pots. The pictures were analysed using the image analysis software ImageJ. The total leaf area for each construct was calculated as an average of the three lines considered. Different letters above the histograms indicate a statistical significance (ANOVA One-Way, Tuckey post-test).

As expected there were no significant differences in respect to the untransformed Col-0 plants used as control. The only statistically significant difference was between the plants transformed with CBEL *Ppn* and the two CBEL proteins from *Hpa*.

The plants were observed during the following developmental stages, to check whether the expression of the proteins may interfere with stem appearance time, flower development or seed production. Ten weeks after transplanting, several plants, including Col-0, started to develop the stem. In Figure 4.14 the results of the stem measurements (height in cm) are shown. The results from three different lines (three plants each) for each construct (Section 4.2.2) are averaged. There is no statistical

131

difference in between the different constructs. However, while most of the lines started to develop a stem, no lines transformed with the protein CBEL *Ppn* showed any visible stem development.

After a total of twelve weeks after transplant, the plants were checked one last time to determine if any of them showed a delay in flowering or seeds production. As expected from the previous results, the transgenic plants transformed with *Ppn*-CBEL gene showed a strong delay in flowering and in seeds production. While Col-0 plants were fully grown, showing stems with flowers and seed pods, the *Ppn*-CBEL plants showed a strong delay in development: only few plants were flowering, while many were still at the bolting stage. None of them showed any seed pods development. Overall, the rest of the transformed plants seemed to have reached the same developmental stage as the control Col-0, showing stems with flowers and seed pods in most cases.
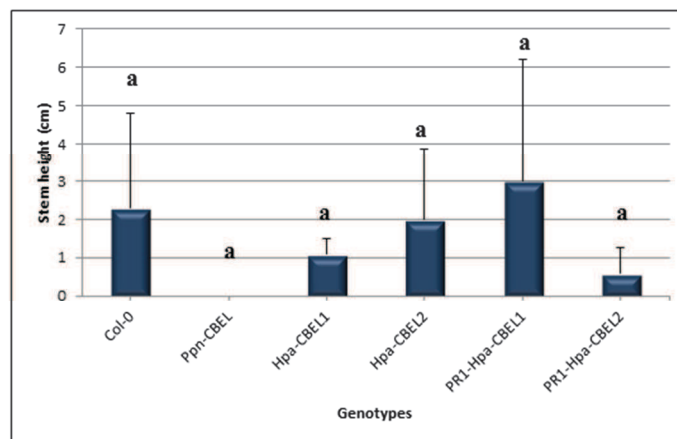
Figure 4.14 Stem height measurements on stably transformed lines. Average measurement of the stem height for each construct. The measures for each line for each construct were averaged. There is no statistical difference in between the different constructs or the Col-0 control plants. Only in the case of the lines transformed with CBEL *Ppn* there is no visible stem development. Statistical analysis: ANOVA One-way, Tuckey post-test.

4.2.3 Transient expression of CBEL proteins from *Ppn* and *Hpa* in *Nicotiana benthamiana*

In order to gain more insights in the role of the *Hpa* CBEL proteins as PAMP molecules, the same constructs (see Section 4.2.2) used to stably transform *Arabidopsis*

plants were used to transiently express CBEL genes in *N. benthamiana* (see Section 2.2.1.9) after *Agrobacterium*-mediated transformation.

CBEL from *Ppn* was used as a positive control, while $MgCl_2$ (used as the buffer for *Agrobacteria* resuspension) represented the negative control. Empty *Agrobacteria* and *Agrobacteria* transformed with the empty pEG100 vector (used to clone the various CBEL constructs) were injected as well, in order to remove any possible background given by the bacteria or the vector themselves. Figure 4.15 shows the pictures of the injected *N. benthamiana* leaves. The experiment was carried out in triplicate.
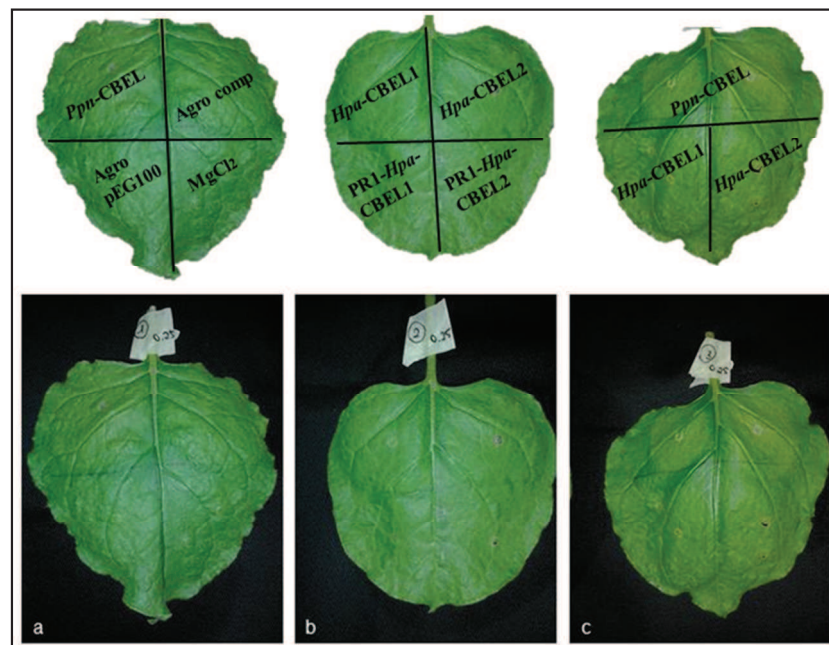
Figure 4.15 Transient expression of CBEL proteins from *Ppn* and *Hpa* in *N.* benthamiana using pEG100 vector. *N. benthamiana* leaves were transiently transformed via *Agrobacterium* injections ($OD_{600}= 0.25$). **a**: positive, negative and background controls, represented respectively by *Agro*/pEG100::*Ppn*-CBEL, $MgCl_2$ and *Agro* competent (comp) and *Agro*/pEG100. It is possible to observe a slight discolouration in correspondence of the injection with *Ppn*-CBEL. **b**: the leaf was injected with *Agrobacterium* carrying *Hpa*-CBEL1, *Hpa*-CBEL2, PR1-*Hpa*-CBEL1and PR1-*Hpa*-CBEL2. In this case no discolouration was visible. **c**: the three different CBEL genes (*Ppn*-CBEL, *Hpa*-CBEL1 and *Hpa*-CBEL2) have been injected altogether. Once again, a slight discolouration is visible in the spot corresponding to the injection of *Agro*/pEG100::*Ppn*-CBEL. The pictures in the upper panel show the injections scheme.

The *Agrobacteria* were injected at an OD_{600} of 0.25 and 0.5. The picture shows the reactions obtained at $OD_{600}= 0.25$. Picture a displays all the controls: $MgCl_2$ (negative),

Agro/pEG100::*Ppn-CBEL* (positive, being a known PAMP molecule, Gaulin et al., 2006) and competent *Agrobacteria* and *Agrobacteria*/pEG100 (background control). It is possible to notice a slight discolouration (yellowing of the leaf, chlorosis) in correspondence of the site of injection with the positive control. In picture b (Figure 4.15), the four different *Hpa* CBEL constructs have been injected: no discolouration appeared in the site of injection for any of them. Finally, in picture c (Figure 4.15), CBEL from *Ppn* and the two original CBEL constructs from *Hpa* were injected. Once again, a discolouration is visible only in correspondence of CBEL from *Ppn*, in the upper side of the leaf. The same results were obtained with the injections at OD_{600}= 0.5 (data not shown). It appears that, in *N. benthamiana*, only CBEL from *Ppn* is able to cause an immune reaction.
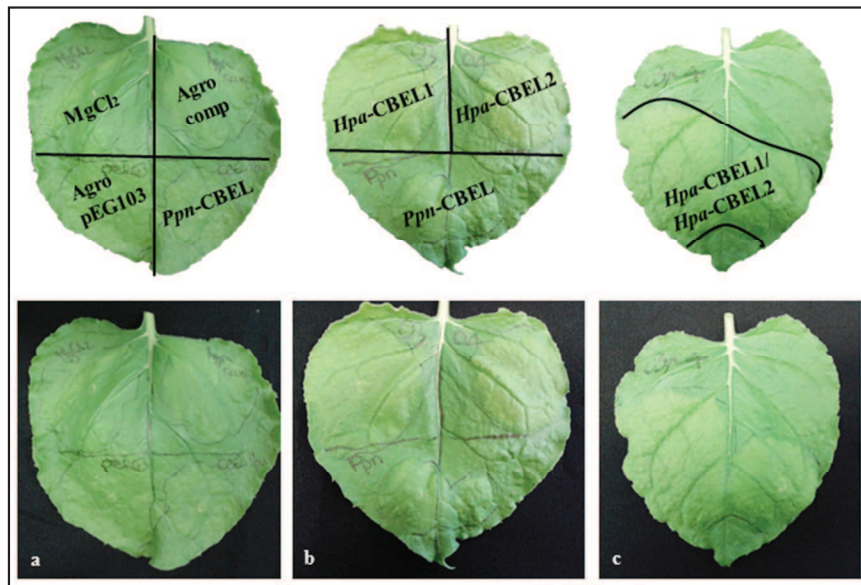
Figure 4.16 Transient expression of CBEL proteins from *Ppn* and *Hpa* in *N. benthamiana* using pEG103 vector. a: negative (MgCl$_2$), positive (*Agro*/pEG103::*Ppn*-CBEL) and background controls (competent *Agrobacteria* and *Agro*/pEG103); **b**: CBEL proteins from *Hpa* (CBEL1 and CBEL2) and CBEL from *Ppn*; **c**: CBEL1 and CBEL2 (*Hpa*) injected together, after mixing *Agro*/pEG103::*Hpa*-CBEL1 and *Agro*/pEG103::*Hpa*-CBEL2 in 1:1 proportions. The pictures in the upper panel show the injections scheme.

In a second similar experiment, CBEL proteins from *Ppn* and from *Hpa* (CBEL1and CBEL2) were cloned into the Gateway® pEG103 expression vector (Section 2.2.1.5). The vector enables the expression of the proteins tagged at their C-terminal with the

green fluorescent protein (GFP) followed by 6x His. Also in this case, the *Agrobacteria* transformed with the different vector combinations (empty pEG103 vector, pEG103::*Ppn-CBEL*, pEG103::*Hpa-CBEL1* and pEG103::*Hpa-CBEL2*) were injected at an OD_{600} of 0.25. In detail, 10 mM $MgCl_2$ was used as a negative control for the experiment (being the buffer for *Agrobacteria* resuspension), *Ppn-CBEL* was used a positive control, while competent *Agrobacteria* and *Agrobacteria* transformed with the empty pEG103 vector were used as a background control.

Differently, in this second experiment, the two CBEL proteins from *Hpa* seemed to provoke a reaction in *N. benthamiana* leaves (Figure 4.16b) after five days after inoculation. The visible discolouration of the leaf is similar to the one in correspondence of the injection site of *Ppn-CBEL* (Figure 4.16b). A similar, if not greater, change in leaf colour was obtained after the injection of *Agrobacteria* transformed with CBEL1 and CBEL2 in a combination of 1:1 (Figure 4.16c). No discolouration (thus, no immune reaction) was observed in the negative and background controls (Figure 4.16a).

4.2.4 Recombinant CBEL proteins expression in *E. coli* BL21

To shed further light on the activity of the CBEL proteins, *Ppn-CBEL* and *Hpa-CBEL2* were heterologously expressed in bacteria (*E. coli* BL21). Both genes were amplified (Section 2.2.1.2) excluding the signal peptide and the stop codon (see the Appendix for primer sequences) and cloned in Gateway® vector pDest™17 (Section 2.2.1.5) for expression in bacteria. The vector was then chemically transformed into *E. coli* BL21 for protein expression.

4.2.4.1 Defining and optimizing protein expression conditions

To establish the optimal expression and extraction conditions, a protocol (see Sections 2.2.2.8 and 2.2.2.9) has been tested using the protein *Hpa*-CBEL2.

The induction conditions were as follows: isopropyl β-D-1-thiogalactopyranoside (IPTG) was applied at 1 mM final concentration and the induction was carried out at 18 ºC in agitation at 160 rpm. To understand the duration of the induction to obtain the highest amount of recombinant protein, 50 ml samples of the media containing the induced bacteria were collected each hour for a total of four hours. A non-induced

sample was collected as well, together with a sample after overnight induction (Section 2.2.2.8).

All time point-collected samples were centrifuged, the supernatant was discarded and the bacteria were stored at -20 ºC. To identify which fraction (soluble or insoluble, i.e. inclusion bodies) contained the expressed proteins, the bacteria (representing all time points), together with empty *E. coli* BL21, were processed following the protocol in Section 2.2.2.9. From all the samples, a soluble and an insoluble fraction were obtained and quickly tested for the presence of the recombinant protein in a dot blot assay (Section 2.2.2.10).
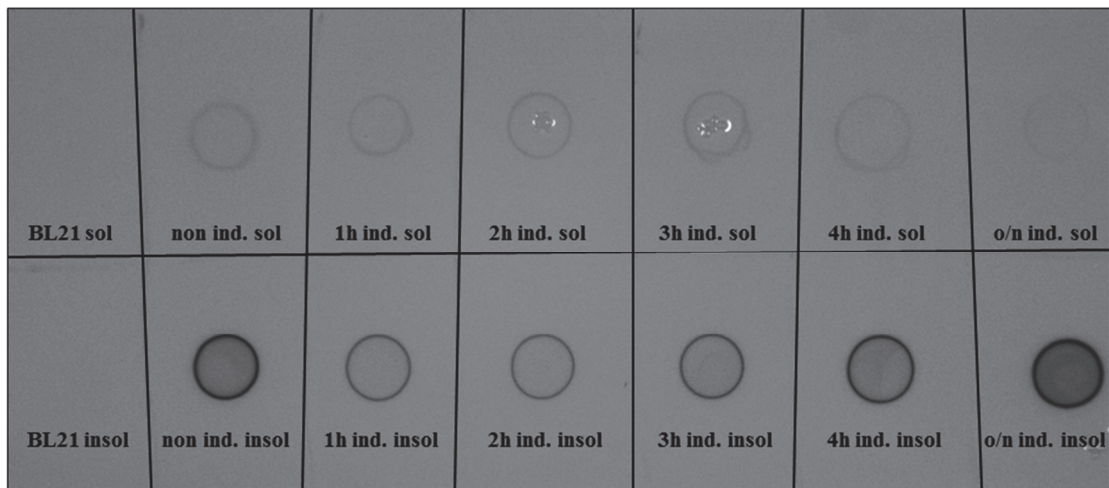
Figure 4.17 Dot blot assay using the soluble and insoluble fractions of *Hpa*-CBEL2 induction time points. BL21 empty bacteria, non-induced BL21/pDest17™::*CBEL2 Hpa* bacteria (non ind.) and five different time points after bacterial induction with 1 mM IPTG. The time collection point were as follows: 1 hour (1h), 2 hours (2h), 3 hours (3h), 4 hours (4h) and overnight (o/n). The recombinant protein was immunodetected using 1:1000 Anti·His antibody coupled with horseradish peroxidase (HRP) (Qiagen) and afterwards visualised with the direct application of the chromogenic HRP substrate 3,3',5,5'-Tetramethylbenzidine (TMB) Liquid Substrate System for Membrane (Sigma-Aldrich®) (see Section 2.2.2.10).

As shown in Figure 4.17, after the application of the chromogenic substrate for the horse radish peroxidase (HRP) enzyme, conjugated to the primary antibody recognizing the His-tag expressed at the C-terminal of the protein, it was possible to detect the presence of the recombinant protein, thanks to a colour production on the membrane. It was clearly visible that there was no colour production in dots corresponding to the soluble fractions, while the presence of the recombinant protein was detected in the

insoluble (inclusion bodies) fractions. No protein was found in the empty *E.coli* BL21, while some protein production was visible in the non-induced bacteria. This event may be due to a leakage in the expression system. An increased protein expression is noticeable in the five time points, starting with a low protein production after one hour of induction (1h ind. insol), culminating with a high production after the overnight induction (o/n ind. insol).

Once established that the inclusion bodies (insoluble fraction) contained the recombinant protein, a further test to confirm the real presence of the protein (molecular size check) was performed. All the insoluble fractions were loaded (15 µg of total protein each) on two 12.5% SDS-PAGE gels (Section 2.2.2.6), one of which was used in a Western Blot (Section 2.2.2.11).

In Figure 4.18a, a visible band appears in correspondence of the estimated molecular weight of *Hpa*-CBEL2 (~16.4 kDa). To confirm that the band corresponds to the expressed protein, one of the two gels was used in a western blot (Figure 4.18b). After the immuno detection and visualization, it appeared clearly that the protein *Hpa*-CBEL2 (tagged with 6xHis at the C-terminal) was expressed at the conditions used and was correctly extracted from the inclusion bodies fraction. Once again it was confirmed that there might have been a leakage in the expression system, since the recombinant protein was also found in the non-induced bacteria. It was also visible an increased accumulation of the protein as the induction proceeded. However, it was estimated that probably the best time point to stop the induction was after 4 hours. There were indeed less contaminants in the inclusion bodies extract after 4 hours of induction, in comparison with the extract obtained after an overnight induction (Figure 4.18a – lanes 4h ind. and o/n ind.). As shown in the western blot, it was also evident that after four hours of induction, the expressed protein was less degraded in respect to the protein obtained after the overnight induction (some immunodetected bands of lower molecular weight are visible in the overnight lane (Figure 4.18b). Overall, four hours of induction seemed to be the best compromise between the protein yield and the quality and feasibility of the extraction.
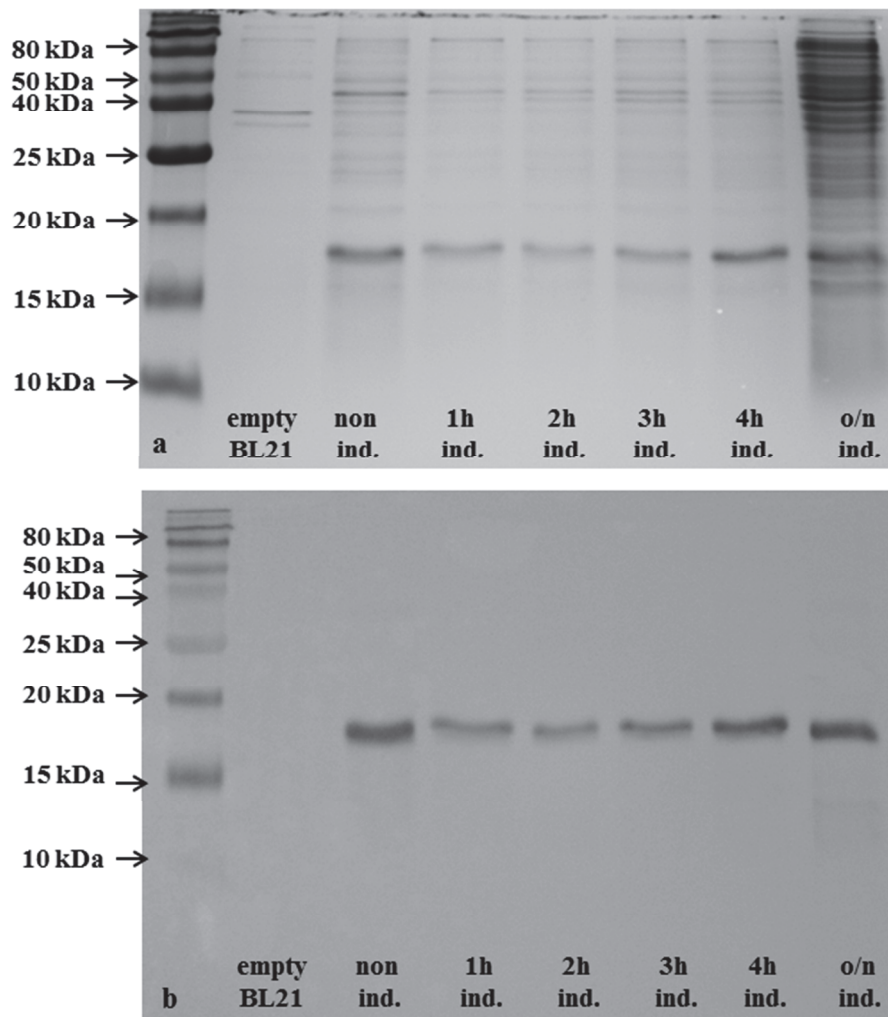
Figure 4.18 Detection of *Hpa*-CBEL2 using Western blot at different induction times. a: SDS-PAGE (12.5%) gel stained with Coomassie Blue (Section 2.2.2.7). From the first lane (left): protein marker (HyperPAGE Prestained Protein Marker, Bioline), empty BL21 bacteria, non-induced (non ind.) bacteria, bacteria collected after 1 hour (1h ind.), 2 hours (2h ind.), 3 hours (3h ind.), 4 hours (4h ind.) induction and overnight (o/n ind.) induction. **b**: Western Blot using a gel loaded in the same order as picture **a**. The visible bands confirm the presence of the *Hpa*-CBEL2 protein (estimated molecular weight ~16.4 kDa).

4.2.4.2 Optimisation of a method to purify His-tagged proteins

The following step towards the production of the CBEL proteins in bacteria was the His-tagged protein purification. Two similar methods were attempted: Ni-NTA spin column and Ni-NTA Agarose (Qiagen – Section 2.2.2.12).

The first method using the Ni-NTA spin columns (Figure 4.19a) was not successful in retaining and purifying the protein of interest. A large amount of protein is visible in the

flow through lane (FT), a sign that the protein did not bind to the column. In addition, multiple bands, corresponding to high molecular weight contaminant are present in the elution fractions (E1, E2): not only the protein was not retained, but the elution fraction was also contaminated by non-desired proteins.
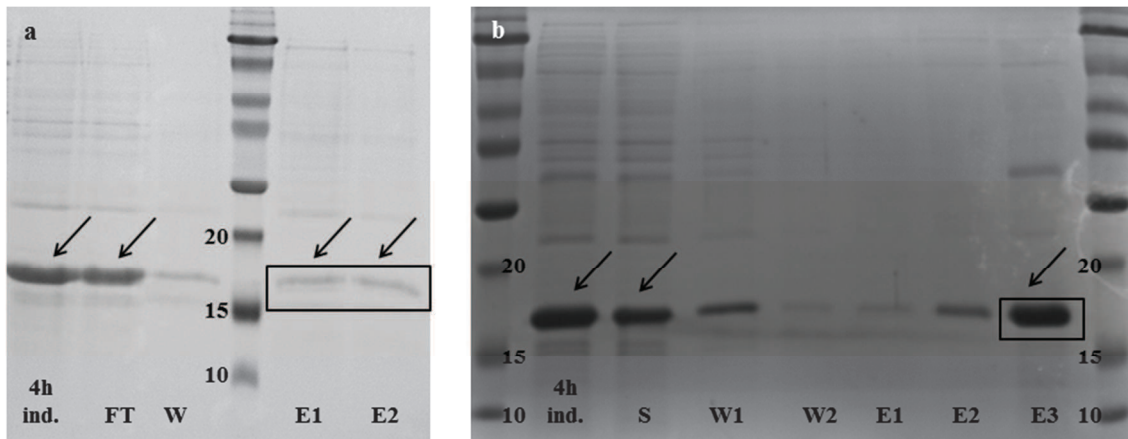
Figure 4.19 Purification of His-tagged *Hpa*-CBEL2 protein using Ni-NTA columns or Ni-NTA agarose. a: purification of the recombinant protein *Hpa*-CBEL2 using Ni-NTA spin columns. The bands were visualised on the membrane using Ponceau S stain (Section 2.2.2.12). The lanes are as follows (from the left): 4 hours induction insoluble fraction (4h ind.), flow-through collected after the sample application onto the column (FT), column wash (W), protein marker, sample elutions from the column (E1, E2). It is visible how the protein of interest is barely retained by the column and it is mainly found in the FT rather than the eluates (E1 and E2). The black arrows show the recombinant protein bands. **b**: SDS-PAGE gel (12.5%) of *Hpa*-CBEL2 purification using Ni-NTA agarose. Lanes from the left: protein marker, 4 hours induction insoluble fraction (4h ind.), supernatant collected after the sample application and spinning of the agarose (S), column washes (W1, W2), sample elutions from the agarose (E1, E2, E3). In this second case, the protein is mainly found in the last elution (highlighted by the black box and arrow).

Thus, to obtain the purified protein, a second method using Ni-NTA agarose (Figure 4.19b) was used. In this case, it was possible to successfully bind and elute the protein of interest. A significant amount of protein was however found in the supernatant (S) collected after centrifuging the agarose following the incubation with the insoluble fraction. This may be due to the saturation of the binding capacity of the agarose. However a large amount of *Hpa*-CBEL2 was recovered after the third elution (E3). In order to obtain a high elution of the protein from the agarose, it was necessary to thoroughly pipet up and down the elution buffer with the agarose and afterwards to leave the mixture in incubation at room temperature for 30 min. The first two elution steps were carried out just by mixing the buffer with the agarose and by centrifuging it

right after as suggested by the manufacturer's manual. The protein concentration in the supernatant (collected this time as it contained the eluted proteins, E) was monitored during the procedure and after the second low concentration elution, the method was changed as reported above. Using this second method the amount of contaminating bands seemed to be reduced, therefore it was adopted as the method to purify the recombinant proteins produced in bacteria. A further purification step was however required.

4.2.4.3 Last purification step and ROS assay with the purified proteins

To finally obtain the recombinant purified proteins (*Ppn*-CBEL and *Hpa*-CBEL2) the electro-elution method was used (Section 2.2.2.14).

At this point both proteins were expressed, extracted and purified using Ni-NTA agarose as described in the previous sections. Because few contaminant bands remained after the Ni-NTA agarose step (Figure 4.20a – lanes E Ni *Ppn* and E Ni *Hpa*), both fractions were further purified by electro-elution. For both proteins, the final fractions, together with the elution and supernatant after the Ni-NTA agarose were loaded onto two SDS-PAGE gels (12.5%), one of which was used in a western blot.

In Figure 4.20a it is visible how the proteins purified through electro-elution resulted much more clear of any contaminating bands, if compared to the proteins purified using the Ni-NTA agarose only. The majority of the high molecular weight bands were eliminated, as well as the lower molecular weight ones. It appeared, however, that the majority of lower molecular weight bands originated from the degradation of the two recombinant proteins (see Figure 4.20b), as visualised by the immuno-detection targeting the 6xHis tag in the western blot: in detail, many more bands resulted from the degradation of *Ppn*-CBEL (E Ni *Ppn*) protein were visible if compared with the lane showing *Hpa*-CBEL2 (E Ni *Hpa*, Figure 4.20b). The extended degradation may also have been due to an over-reaction of the chromogenic substrate (background noise) and therefore a false positive. However, it was evident how the electro-eluted proteins appeared much cleaner and less degraded that the results obtained with the Ni-NTA agarose alone.

To test if the two expressed and purified proteins were able to cause any PTI reaction, they were used in a ROS assay, both on Col-0 plants and on Col-*bak1-5 bkk1-1* mutants. Figure 4.21a shows the results of the assay.
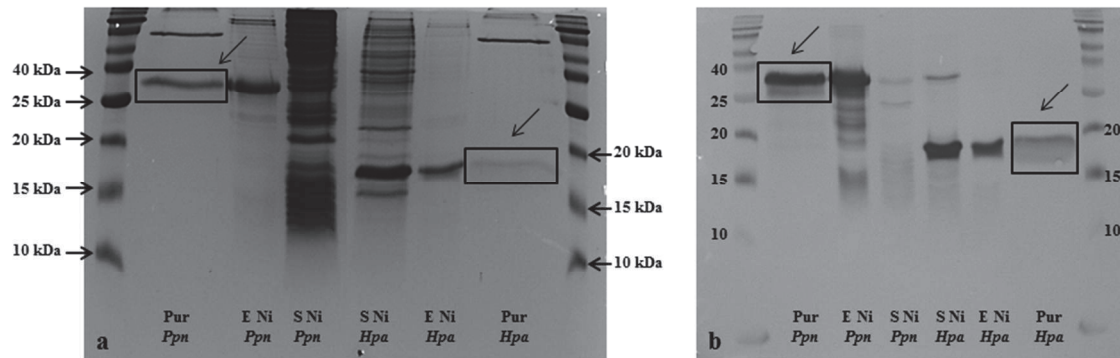
Figure 4.20 Final purification of *Ppn*-CBEL and *Hpa*-CBEL2 via electro-elution. a: SDS-PAGE gel (12.5%) stained with Coomassie Blue. The gel was loaded as follows (from the left): protein marker, electro-eluted *Ppn*-CBEL (Pur *Ppn*-CBEL, estimated molecular weight ~27.0 kDa), Ni-NTA agarose eluted *Ppn*-CBEL (E Ni *Ppn*), Ni-NTA agarose supernatant *Ppn*-CBEL (S Ni *Ppn*), Ni-NTA agarose supernatant *Hpa*-CBEL2 (S Ni *Hpa*), Ni-NTA agarose eluted *Hpa*-CBEL2 (E Ni *Hpa*), electro-eluted *Hpa*-CBEL2 (Pur *Hpa*) and finally the protein marker. **b**: western blot derived from a second gel loaded as the one in Picture **a**. It is possible to see in Picture **a**, how the majority of the contaminating bands disappear in the two purified proteins. Although a band of the same size is visible in both lanes. In picture **b**, after the immuno-detection, is visible how the electro-elution procedure made it possible to select the intact CBEL proteins rather than the degraded ones, especially in the case of *Ppn*-CBEL.

The first three histograms represent the application of flg22, *Hpa*-CBEL2 and *Ppn*-CBEL respectively on Col-0 leaf discs. It appeared clearly that, differently from the reaction obtained with flg22, both CBEL proteins did not trigger any ROS production. Similarly, no reaction was triggered on Col-*bak1-5 bkk1-1* mutants after the application of the two purified proteins, whereas, as expected (Roux et al., 2011), a reduced ROS production, in respect to the one obtained on Col-0, was found after challenging the mutant plants with flg22.

Finally, Figure 4.21b shows the leaf disks at the end of the assay (around 12 h incubation with the recombinant proteins). The leaves appeared thinner and more fragile than the others used in the assay (challenged with buffer, sdH$_2$O or flg22) and they displayed a visible yellowing around the borders. This may be due to a reaction caused by the addition of the two proteins, even though it was not in the form of ROS

production and accumulation. The colour change was found on both Col-0 and Cl-*bak1-5 bkk1-1* core leaves following the application of both *Hpa*-CBEL2 and *Ppn*-CBEL.
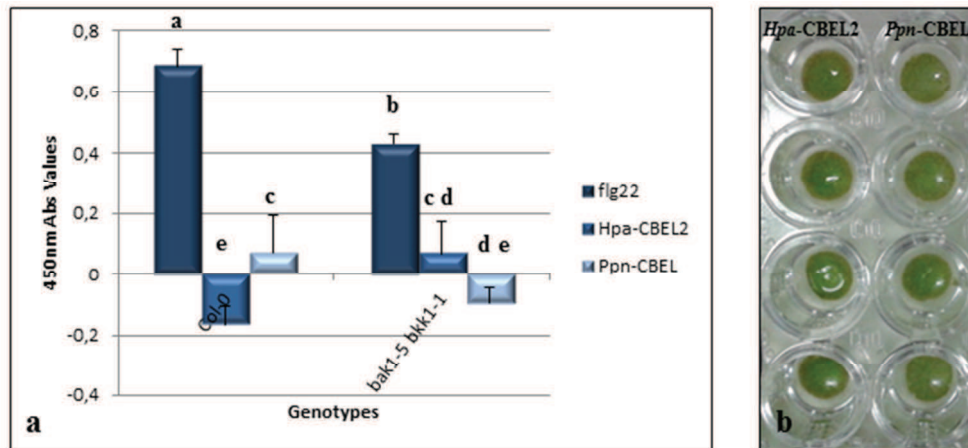
Figure 4.21 Detection of ROS accumulation in Col-0 and Col-*bak1-5 bkk1-1* plants treated with purified *Hpa*-CBEL2 and *Ppn*-CBEL. a: ROS assay to test the newly purified *Ppn*-CBEL and *Hpa*-CBEL2 proteins. 10 mM flagellin (flg22) was used as a positive control. The experiment was repeated twice. Both proteins do not seem to trigger any ROS production both in Col-0 or Col-*bak1-5 bkk1-1* plants. **b**: the leaf disks used to perform the ROS assay are shown after 12 h of incubation with the CBEL proteins. There are evident signs of yellowing around the borders of the disks.

4.3 Discussion

To understand whether the two CBEL or CBEL-like proteins found in *Hpa* may have an eliciting activity on the plant immune system as *Ppn*-CBEL, different approaches were considered.

Firstly, a bioinformatic analysis regarding the structure and conserved features was carried out. After the possibility for the two CBEL proteins of containing a PAMP molecule arose, further steps, including stable and transient plant transformation with several constructs, as well as in vitro production and activity assessment, were taken.

4.3.1 A bioinformatic study of *Hpa* CBEL proteins reveals the presence of a cellulose-binding domain

When the *Hpa* genome became available (Baxter et al., 2010), it became clear that it contained two genes encoding for CBEL or CBEL-like proteins. The importance and the interest for this discovery lies in the fact that in 2006, Gaulin and colleagues

discovered that the protein CBEL in *Ppn* contained two domains, called cellulose-binding domains (CBDs), that acted as PAMP molecules in *Arabidopsis* and *N. benthamiana*. Therefore, a bioinformatic analysis of both *Hpa* proteins was conducted in order to discover whether the two *Hpa* proteins contained or not the domain.

After aligning the three sequences (Figure 4.5) the first noticeable feature was the size of the two *Hpa* proteins. They are indeed just over half of the length of the *Ppn* protein. The reduced size of the two *Hpa* proteins, together with the reduced number of genes for CBEL or CBEL-like proteins (and other pathogenicity-related genes) found in the *Hpa* genome in respect to other oomycete species (hemibiotrophs and necrotrophs) may be accounted to the *Hpa* lifestyle (Baxter et al., 2010). Being a biotroph and relying entirely on a living organism for its development and reproduction (Coates & Beynon, 2010), *Hpa* may have evolved towards a more "low profile" behaviour by reducing the number of those genes that, because of their function, may have made the oomycete more recognizable by the plant (Baxter et al., 2010). In support to this hypothesis, in the work on *Ppn*-CBEL, it has been found that both repeated domains (each containing a CBD and a Pan/Apple-like domain) were required in order to elicit necrosis in the plants, while when challenging the plant with just one half of the protein, the expression of defence-related gene was still triggered, but necrosis was no longer registered (Gaulin et al., 2006). Thus, it seems that having just one half of the protein triggers a smaller immune reaction in the plant and therefore the microorganism is less recognizable.

A second important feature made evident by the alignment, was that the three sequences (*Hpa* and *Ppn*) share a high level of homology, especially in the part of the sequence corresponding to the end of the CBD domain and the Pan/Apple-like domain in *Ppn*-CBEL (Figure 4.5). For this reason the possibility arose that also the two *Hpa* proteins may have contained a CBD and therefore being recognized as PAMPs. After a search for the presence of the CBD with the online tool SMART, however, no CBD was recognized in neither of the *Hpa* proteins. Only when the search was extended to the outlier results, the tool found a CBD in the *Hpa*801904 sequence. This result was in accordance with what found by Larroque and colleagues (2012) in their study regarding the presence of CBM1-containing proteins in oomycetes and fungi (CBDs belong to the

family 1 of carbohydrate binding modules (CBM1s)). In their extensive study they did not discover proteins containing the CBD domain in *Hpa*. Nevertheless, Figure 4.7b shows the results of the alignment between the two *Hpa* amino acid sequences and the two CBDs of the *Ppn* protein demonstrating that the amino acids important for the backbone structure of the domain and for the binding of the substrate cellulose (Linder et al., 1995; Mattinen et al., 1998) are conserved and present in both *Hpa* proteins. In detail, four cysteines, supposed to form two disulphide bridges (see the pattern in Figure 4.7a), are conserved in both *Hpa* proteins. The pattern is highly conserved in several fungal CBDs, and it has been shown to be essential for the stabilisation of the backbone of the CBD in both cellobiohydrolases (CBD_{CBHI}) and in the CBD of the four endoglucanases (CBD_{EGI}) of the fungus *T. reesei* (Mattinen et al., 1998). In addition, in both CBEL from *Hpa* and from *Ppn*, important aromatic amino acids, represented by tyrosines (Y53 and Y54 in *Hpa* and Y51 and Y52 in *Ppn*) are conserved. The same amino acids are present also in the CBDs of several fungi and their importance for cellulose binding has been demonstrated (Linder et al., 1995; Mattinen et al., 1998). The role of these aromatic residues in *Ppn*-CBEL has been studied in detail by Gaulin and colleagues (2006) in a mutational structure-function analysis. They discovered that these residues are important for the elicitor activity of the protein. Point mutations in one of the residues reduced significantly the necrosis caused by CBEL, while it did not result in an impaired binding to cellulose. Another amino acid that resulted conserved in both *Ppn*-CBEL and *Hpa*-CBELs is glutamine (Q55 in *Hpa* and Q53 in *Ppn*, respectively), which may be involved in the binding of cellulose because surface-exposed as are the tyrosine residues (Linder et al., 1995).

Therefore, due to the presence of these important conserved features in *Hpa* proteins which are implicated both in cellulose binding and in eliciting the immune system, it became a real possibility for *Hpa*-CBELs (CBDs) to act as PAMP molecules.

4.3.2 Overexpression of *Hpa* CBEL proteins in *Arabidopsis* to shed light on their role as PAMP molecules

To study the role of the two *Hpa* CBEL proteins as PAMP, both genes have been stably introduced and expressed in *Arabidopsis* Col-0 plants via *Agrobacterium*-mediated transformation (floral dipping). Since the recognition of a PAMP molecule triggers ROS

production, callose deposition and resistance towards later infections (in between others) (Muthamilarasan & Prasad, 2013), it was thought that these events could have been all tested in the transgenic plants. Moreover, it is known that plants constantly monitor their environment and its features and, when in presence of a danger (e.g. recognition of a pathogen and its conserved PAMP molecules), they have to balance in between normal growth and defence to survive (Belkadir et al., 2014; Lozano-Durán & Zipfel, 2015). Therefore it was assumed that if the two CBEL proteins acted as PAMPs in *Arabidopsis*, when constantly expressed in the transformed plants, they would have been recognised and the recognition would have been shown as a change in developmental rate and growth of the plants.

Therefore five constructs (*Ppn*-CBEL, *Hpa*-CBEL1, *Hpa*-CBEL2, PR1-*Hpa*-CBEL1 and PR1-*Hpa*-CBEL2), with three transformed lines for each, were used in all the experiments carried out with the overexpressing plants. A ROS and a callose deposition assay were used to monitor the degree of recognition of the two *Hpa* proteins. As shown in Figure 4.9, there is actually no difference in accumulation of the peroxidase enzyme following the transformation of the plants with the proteins. Whereas, regarding the callose deposits accumulated in the plant cell walls, there is a significant difference between Col-0 (used throughout as a control) and the plants transformed with *Ppn*-CBEL. Even though there is no statistical difference in between Col-0 and the plants transformed with the four *Hpa* constructs, there is still an accumulation of callose deposits in the transformed plants which was not observed in the control ones. This fact may be linked to the previously made assumption, that due to a reduced size and more specifically, to a reduced number of CBDs in the *Hpa* proteins, the reaction triggered by the two *Hpa* proteins would be milder than the one caused by *Ppn*-CBEL (Gaulin et al., 2006). On the other hand, it is surprising that, although the transformation caused the accumulation of callose, and therefore a reaction towards the proteins, there is no actual difference in ROS production (or more specifically the accumulation of peroxidases) between the control plants and the transformants. These results may be explained with several hypotheses: firstly, it could be assumed that the accumulation of callose may be a more long-term reaction in comparison to ROS production (Luna et al., 2011; Voigt, 2014). ROS are unstable compounds, with a high turnover rate. They are toxic and produced in order to render the invasion point and the plant environment inhospitable

145

for the invading microorganisms (Torres, 2009). However, in high quantities they may become toxic also for the plant itself: it has been reported that in some cases they may be sequestered inside of callose deposits in order to lower their concentration and their toxic effect to the plant cells (Voigt, 2014). If this is the case, it could be postulated that, while the callose deposits are not only more stable compounds than ROS, but also that they exert a sort of protective action. Therefore they might have been retained by the plant, while on the other hand the plant may have adapted to the presence of the ROS in order to reduce their damaging properties. In this perspective, callose deposition may not have been triggered as a protective tool towards the non-self molecules, but mainly as a protection towards its own ROS production after the recognition of the PAMP molecules. Indeed, it has not been demonstrated yet that callose deposition is triggered because of PAMP recognition: it could be seen as a sort of consequence (Ellinger & Voigt, 2014).

A different hypothesis is based on the nature of *Ppn*-CBEL and its recognition by the plant. The mode of recognition of *Ppn*-CBEL by the plant is still not known (Gaulin et al., 2006) and a receptor has not been identified yet. It can be assumed that the protein may be recognised after its binding to cellulose on the cell wall and therefore after cell wall integrity perturbation (Gaulin et al., 2006). In this case, the sensing of the cellulose perturbation at the cell wall could have triggered the deposition of callose, whereas ROS production was not triggered because the *Ppn*-CBEL recognition by the plant is not achieved through a proper receptor.

Alternatively, it could also be considered that the pathway leading from recognition of the protein to ROS production may not pass through cell wall peroxidases (whose activity is tested in the used ROS assay) but it may trigger ROS production through the activity of NADPH oxidases (which together with mitochondria represent another ROS source) (Bolwell et al., 2001).

Finally, it could be also postulated that, although it has been demonstrated that the native signal peptide of *Ppn*-CBEL is sufficient to direct and integrate the protein in the plant cell wall (Gaulin et al., 2006), once introduced into cell wall, the proteins may not be able to properly contact the cellulose in the plant cell wall and therefore exert their eliciting activity. In the case of *Ppn*-CBEL (having two repeated domains and two

CBDs), there may still be some sort of contact and therefore callose deposition, while in the case of the *Hpa* proteins, the contact could be minimum (seen as a minor callose production and deposition).

The stably transformed plants have also been tested on their ability to resist to pathogen infections. The assumption behind the experiment was that if the expressed proteins are recognized as PAMP molecules they would have triggered defence responses such as callose deposition and ROS production and therefore they may have increased plant's basal defence and protected the plants against pathogen. The possibility of acquired resistance has been tested by infecting the plants with *Hpa* (*Hpa*-Noks1 and *Hpa*-Maks9). The results (Figure 4.10 and Figure 4.11) do not show a statistical difference in terms of resistance to the infections, in between Col-0 control plants and the transgenic plants. This may be explained with what previously said. First of all, there has not been an increase in ROS production following the stable transformation of the plants with the *Ppn* or *Hpa* proteins (or at least they were not detected with the assay used in this project). There has been, instead, callose deposition, which should have helped the plants to resist the penetration and infection of the pathogen. However, it has to be noted, that the two *Hpa* isolates used in the assay are virulent on Col-0 plants (Holub et al., 1994), forming a compatible interaction. This means that they secrete an array of effectors targeting directly the PTI machinery (Howden & Huitema, 2012). Therefore, it is possible that even if the plants were producing ROS and callose as a consequence of the expression of the CBEL proteins (recognized as PAMP molecules), this may have not been enough to protect them towards "well-armed" pathogens; it has also to be noted that for this assay the plants were infected after one week of growth while when they were checked for callose deposition they were at least four or five-week-old.

The last assessment of the function of the CBEL proteins using the stably transformed plants was done by checking whether the recognition of the proteins as PAMPs would have been mirrored in growth and developmental (phenotypical) changes in respect to untransformed Col-0 plants (Belkadir et al., 2014; Lozano-Durán & Zipfel, 2015). Even though there were no striking differences in between the transgenic plants and the controls, it was noted that plants transformed with the *Ppn* gene, showed a delay in growth rate and development. Even if not radically different from Col-0, after six week

from transplant, they showed a smaller total leaf area compared to Col-0 and even smaller if compared with the plants transformed with *Hpa*-CBEL1 and *Hpa*-CBEL2. More interestingly, when every other plant started to develop a stem, they were not even showing a bud. And afterwards, when most of the plants started to develop seeds, they were just at the bolting stage. Although it could have been expected a greater difference in between *Ppn*-CBEL transformed plants and Col-0, because of its role a PAMP (Gaulin et al., 2006), developmental differences were very clear. On the other hand, almost no difference was highlighted in between Col-0 and *Hpa*-transformed plants. Even though they may contain a PAMP molecule (CBD presence in the bioinformatic analysis and callose deposition), most probably, as previously mentioned, the reduced size and number of their predicted CBD may play a role in the level of recognition (and reaction) by the plants.

4.3.3 Transient expression of *Hpa* and *Ppn* CBEL proteins in *N. benthamiana* might reveal a PAMP role for *Hpa* CBELs

To further test the hypothesis of the presence of PAMP molecules (CBD) in the *Hpa* proteins, they have been transiently expressed in *N. benthamiana*. The experiment was repeated in two different occasions and two different vectors were used: pEarlyGate100 (pEG100) and pEarlyGate103 (pEG103). They both belong to the Gateway™ technology series and in the case of pEG103 it produces a protein fused to GFP and to a 6xHis tag at the C-terminal.

In Figure 4.15 are shown the pictures of the *N. benthamiana* leaves five days post-injection of *Agrobacteria* transformed with *Ppn* and *Hpa* CBEL proteins (in pEG100 vector). A slight discoloration of the leaf was observed in correspondence of the site of injection of the *Ppn*-CBEL protein. On the other hand no visible reaction of the plant was registered when injected with *Hpa* CBEL proteins. Surprisingly, in the repeated experiment using the pEG103 vector, visible discolouration was observed not only at the site of injection with the protein from *Ppn,* but in this case, also with the *Hpa* proteins.

These results may have been a consequence of the vector used; indeed, in the second experiment using pEG103, the CBEL proteins were produced fused to the GFP. The

protein may have acted as a molecular chaperone helping in correctly folding the expressed proteins (Betiku, 2006). On the other hand, due to the presence of two repeated domains in the *Ppn*-CBEL structure, the folding of the protein may have not been a problem even when using pEG100. In fact, the presence of the second repeated domain (not present in both *Hpa*-CBELs), which contains 12 Cys forming additional disulphide bridges, may have stabilized the protein and helped with the refolding in the plant environment. If this is the case, it could be assumed that both *Hpa* proteins are recognized as PAMPs in *N. benthamiana* and that the CBDs identified through the bioinformatic analysis may actually act as a PAMP in *Hpa*. In addition, when the *Agrobacteria* containing the two *Hpa* CBEL proteins were mixed and injected together, the site of injection showed a stronger discolouration. This may be due to additive effects of the collaboration of the two CBDs, as it happens in *Ppn*-CBEL.

4.3.4 Heterologous expression of *Ppn*-CBEL and *Hpa*-CBEL2 reveals the importance of the protein structure

The last step taken towards a deeper understanding of the role of the CBEL proteins in *Hpa* has been the heterologous expression in *E. coli*. For experimental and timing reasons, only *Ppn*-CBEL (used as a control for PAMP activity, Gaulin et al., 2006) and *Hpa*-CBEL2 were expressed. However, *Hpa*-CBEL2 showed all the relevant features (highlighted in Section 4.3.1) required for the activity. In addition, it reacted very similarly to *Hpa*CBEL1 in all the experiment performed with the CBEL proteins, therefore overall it could be considered as a good representative for both *Hpa* proteins. Finally, during the sequencing (Section 4.2.1.2) it did not show any changes in respect to the original annotated sequence.

During the steps to optimize an expression protocol for the proteins in *E.coli*, it became clear that the proteins were expressed and stored into the bacterial inclusion bodies. Similar results were obtained when Gaulin and colleagues (2006) heterologously expressed Ppn-CBEL in *E. coli*. This may be due to the early appearance of the proteins (Figure 4.17 and Figure 4.18). In fact, they seem to be expressed even in the non-induced bacteria, may be because of a "leak" in the expression system, that may cause a higher accumulation of the protein into the bacteria at levels that may result toxic for the microorganisms (Wang, 2009). In addition, it has been highlighted that at least two

disulphide bridges forms in the CBDs of the CBEL proteins (and there may be even more due to the presence of 12 Cys residues per repeated domain – see Figure 4.5). Because the *E. coli* environment differs greatly from the *Hpa* or *Ppn* environment, the different internal conditions may have led to protein misfolding and thus to the aggregation of the polypeptides in inclusion bodies (Rosano & Ceccarelli, 2014).

However, because of their composition, the inclusion bodies may even be seen as the first step towards protein purification. They are majorly composed of the recombinant proteins, and may contain also RNA, bacterial membrane phospholipids and membrane proteins (Wang, 2009). Therefore the steps that followed were simplified by the protein accumulation in inclusion bodies.

The proteins were expressed fused to a C-terminal tag composed of 6 histidine residues (His-tag) to be easily further purified using metal ion affinity chromatography. Two methods were tried: Nickel-bound columns and Nickel-bound resin (Section 4.2.4.2). As shown in Figure 4.19, the best method was the one using Nickel-bound agarose. Most probably the longer and more thorough contact of the expressed proteins (inclusion bodies mixture) with the resin, led to a better bonding between the Nickel ions and the His-tag, resulting in a better purification of the proteins of interest. After the purification step, there were still few contaminant bands (Figure 4.19). To finally clean up the proteins of interest, a final purification step was considered. The protein mixture was loaded on an SDS-PAGE gel and after a completed run the bands corresponding to the proteins of interest were excised and the proteins electro-eluted from the gel. As shown in Figure 4.20, apart from a band of around 80 kDa, found in both eluates, no other contaminant bands were present in the electro-eluted proteins. Therefore it was concluded that the residual contaminant band may have been an artefact of the methodology. Following this step the proteins were concentrated and the buffer was diluted in order to lower the SDS concentration to allow for the sample to be used in an assay.

As shown in Figure 4.21, when used in a ROS assay, the proteins did not trigger ROS production. This may be explained by the lack of protein tridimensional structure and refolding. In fact, while the expression of the proteins in the inclusion bodies may have helped with the purification steps, on the other hand the methods used to solubilise them

used harsh chemicals, such as urea, that completely destroyed the tridimensional structure. In addition, to completely purify them, two additional steps were used, in which the tridimensional structure was not conserved. In sustain to this hypothesis, as discussed in Section 4.3.1, the folding of the protein thanks to the Cys residues may have a pivotal importance on the binding to cellulose and therefore on the PAMP activity of the proteins (Gaulin et al., 2006).

However, a second hypothesis may be kept in mind. Since a recognition mechanism and a receptor for *Ppn*-CBEL are still unknown, it may also be possible that a ROS assay evaluating the accumulation of peroxidase enzymes (as ROS producer) may not be the ideal for evaluating CBEL activity. Peroxidases indeed account for around the 50% of ROS production, while the rest is produced by NADPH oxidases and mitochondria (Bolwell et al., 2001). Therefore, because of the CBEL's mode of action (Gaulin et al., 2006) a conventional ROS assay, considering ROS accumulation, rather than only one category of the producing enzymes may have been more comprehensive.

Finally, it has to be noted that, as shown in Figure 4.20, the addition of both proteins caused a discolouration of the edges of the leaf disks, which was not observed with the buffer alone. This event may still support the idea of an eliciting activity of the *Hpa* proteins and that, as previously mentioned, the ROS assay used in the project may not have been ideal for the studied proteins.

Chapter 5

The apoplastic interface in the *Arabidopsis/Hpa* interaction

Abstract

Apoplastic secreted proteins play a pivotal role during the first steps of interaction between plants and pathogens, especially filamentous fungi and oomycetes. The apoplast is the area where the plant defends itself during PAMP-triggered immunity (PTI), but at the same time is where the exchanges of nutrients and effector molecules between the pathogen and the host take place. In order to shed some light on the interactions between *Arabidopsis* and *Hpa*, selected *Arabidopsis* apoplastic proteins were studied in detail.

These proteins were selected from a previous proteomic study on the apoplastic fluid obtained from *Hpa* infected *Arabidopsis* plants. The T-DNA insertion lines were obtained from NASC and after confirming the homozygosity of the insertion they were used in sporulation assays, challenging them with three *Hpa* isolates: Cala2 (incompatible), Emoy2 (semi-compatible) and Noks1 (compatible). Finally, they were tested in a ROS assay using *Hpa*-Emoy2 spore extracts.

Among the 14 selected *Arabidopsis* genes, 7 showed an involvement in *Arabidopsis* PTI against *Hpa*: a peroxidase superfamily protein (AT4G37520), a disulphide isomerase (PDI)-like 1-1 protein (AT1G21750), a subtilase family member (AT1G32960), two serine carboxypeptidase-like proteins (AT2G27920; AT1G15000), PR5 (AT1G75040) and a calreticulin 1b (AT1G09210).

5.1 Introduction

5.1.1 Studying the apoplast to uncover the players of immunity in plant-pathogen interactions

The apoplast, or the area outside the plasma membrane, including the plant cell walls and the spaces in between the cells (Hammerschmidt, 2010; Delaunois et a., 2014), is the first plant environment colonized by pathogens and the place where the first interaction between the host and the pathogen takes place (Delaunois et al., 2014; Gupta et al., 2015). This is especially true for filamentous pathogens and more in particular for biotrophs (e.g. *Hpa*), which utilize the apoplast as the space to live and proliferate and most importantly, a place where to find nutrients and exchange molecules with the host (Doehlemann & Hemetsberger, 2013). The apoplast is a complex environment, where proteins, ions and metabolites are secreted by the plant cells to communicate with their surroundings and the rest of the plant. It is, indeed, an important area for cell-to-cell communication and signalling both in normal and pathogenic conditions (Agrawal et al., 2010).

The proteins secreted into the apoplast usually carry a signal peptide at their *N*-terminal and follow the endoplasmic reticulum (ER)-Golgi pathway. However, it has been proposed that in the apoplast it is also possible to find proteins deriving from an alternative route, called leaderless secretion pathway (LSP). These proteins do not show a "classical" signal for the export outside of the plant cell, but are however found in the apoplastic space (accounting for almost 50% of the total secreted proteins), therefore an alternative mode of export has been proposed (Agrawal et al., 2010; Delaunois et al., 2014; Gupta et al., 2015). When speaking of secreted apoplastic proteins, a distinction has to be made: on one side there are the soluble proteins dispersed in the apoplastic fluid (apoplastic fluid proteome), while on the other side there are the proteins linked to the plant cell wall through ionic bonds (cell wall proteome) (Delaunois et al., 2014).

When studying host-pathogen interactions, considering the apoplastic space and the apoplastic proteins involved in crosstalk between the organisms, is of great importance. Essential events take place in the apoplast, such as pathogen recognition, host counterattack, effectors release, making this space a very important area where the fate

of the interaction is decided (Hammerschmidt, R., 2010; Doehlemann & Hemetsberger, 2013).

5.1.2 Technical approaches to the study of apoplastic proteins

As mentioned above, the apoplast is where the entering pathogens are perceived. As a consequence, profound changes in the apoplastic proteome are initiated. For these reasons, studying the proteins that play a role in the interaction with a pathogen and their modulation, may help to shed light on the complicated matter of plant-microbe interactions (Delaunois et al., 2014; Gupta et al., 2015).

5.1.2.1 Methods to isolate the apoplastic proteins during plant-pathogen interactions

To do so, a proteomic approach is often preferred. As a first step in a comprehensive proteomic study, the sample collection is of fundamental importance. Two main methods exist to "produce" an apoplastic secretome: an *in vitro* and an *in planta* method (Delaunois et al., 2014; Agrawal et al., 2015). The first, is used to produce a so-called cell culture filtrate (CFF): in brief, a plant cell suspension is challenged with a molecule of interest (a PAMP or SA for instance) and afterwards all the secreted proteins (secretome) are collected following filtration (to eliminate plant cells), centrifugation and protein precipitation. This method has been preferred in the past, because simple, reproducible and because it was possible to recover a high protein yield (Agrawal et al., 2010). However, there is no doubt that this method does not take into consideration the whole range of physiological responses that the plant, as a whole organism, creates when interacting with the pathogen. Therefore, the *in planta* method, which makes use of the whole plant challenged with a molecule or a pathogen, generates a more representative proteome than the *in vitro* method (Delaunois et al., 2014; Agrawal et al., 2015). In this case, though, the protein collection may be more complicated, leading even to a lower protein yield, and in addition the risk of contaminating the apoplastic sample with some cytoplasmic components may be increased. There are mainly two techniques to recover apoplastic proteins from plants or plant organs (*in planta* method): the vacuum-infiltration-centrifugation (VIC) method and the newer gravity extraction method (GEM). In the first one, the plant or the infected parts (e.g. leaves) are thoroughly washed in water or buffer and afterwards they are vacuum infiltrated, either

with water or with an infiltration buffer. Subsequently, they are centrifuged at low speed in order to collect the apoplastic proteins, while minimising the cytoplasmic contamination due to cellular rupture. The GEM method, on the other hand, is simpler and more reproducible and it does not use the vacuum infiltration step. In addition, after the centrifugation step, a CTAB extraction is performed in order to remove the contaminants that may interfere with the following proteomic steps (Agrawal et al., 2010).

5.1.2.2 How to investigate the apoplastic proteome

Once the protein samples (infected or PAMP-treated and control) have been collected, they have to be assessed for cytoplasmic proteins contamination. There are mainly two methods that use cytoplasmic enzymatic markers. In one case, the activity of the cytoplasmic enzymes is evaluated. Enzymes such as glucose-6-phosphate dehydrogenase (G6PDH), glyceraldehyde-3-phosphate dehydrogenase (GAPDH) or malate dehydrogenase (MDH) are used for such assays. In the other case, the presence of the same enzymes can be also detected by Western Blotting. In addition, the presence of actin or ribulose-1,5-bisphosphate carboxylase/oxygenase (RuBisCO – for chloroplast contamination assessment) can be used (Agrawal et al., 2010; Gupta et al., 2015). Alternatively, the enrichment of apoplastic proteins can be measured by the use of apoplastic markers such as β-1,3-glucanase or in the case of *Arabidopsis* plants, the Pathogenesis-related protein 1 (PR1) (Gupta et al., 2015).

Once the quality of the isolated apoplastic samples has been proved, before proceeding with the protein identification, the samples have to be normalised in order to be able to appreciate the differences in protein abundance due the interaction with the pathogen. This could be done in two ways: by normalising using the total protein amount or using the fresh tissue amount. In the first case, the same amount of starting proteins is used in the following identification steps. This method, though, could suffer the influence of the infection by the pathogen. In fact, upon pathogen recognition some proteins are produced more abundantly, while some others are inhibited by the effectors delivered by the pathogen. Therefore, starting with the same protein amount may mask some of the differences caused by the infection, especially in the case of low abundance proteins. For this reason, the second method, which employs the same amount of

starting material (e.g. leaves) may turn out to be more sensitive in highlighting the pathogen modulation even of less represented proteins (Gupta et al., 2015).
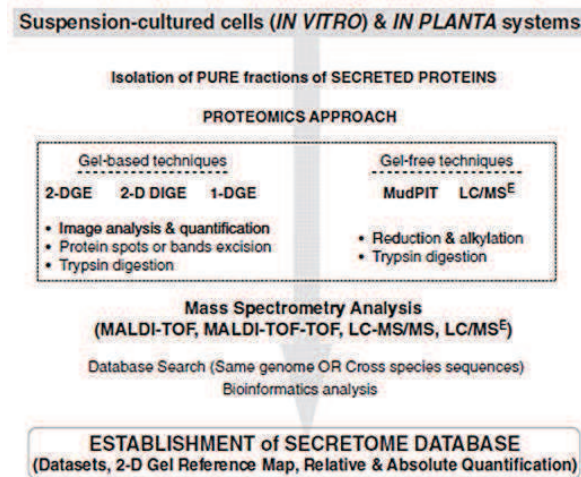
Figure 5.1 Proteomic techniques used to study the apoplastic secretome. Schematic representation of several proteomic approaches to identify secreted apoplastic proteins collected both from *in vitro* and *in planta* methods. Collected proteins are fractionated through in gel-based or gel-free techniques. Subsequently they are analysed through mass spectrometry analysis and finally identified using bioinformatics. The obtained data can then be used to establish secretome databases or to make protein quantification, to understand their modulation and abundance following a pathogen infection (Agrawal et al., 2010).

After quality control and normalisation, the proteins have to be separated in order to be finally analysed and identified by mass spectrometry. Two main groups of techniques are used to fractionate the proteins: gel-based techniques and gel-free techniques (Figure 5.1). The main gel-based technique used is bi-dimensional electrophoresis (2-DGE), resolving proteins on the base of their isoelectric point (pI) and their molecular weight (MW). However, in the case of low concentrated protein samples a different method, that labels the proteins with fluorophores, can be used. This technique, called DIGE (difference gel electrophoresis), allows to differentially label different protein samples (e.g. control and treated) and to load them onto the same gel. In this way a lower amount of starting proteins is required and it is often found in association with 2-DGE (2-D DIGE). Other labelling techniques have been introduced in order to increase the precision of the quantification (fundamental when analysing the protein modulation due to pathogen infection). These techniques are known as isotope-assisted quantification techniques as they use isotope labelling of the proteins; the labelling can

be done either *in vitro* (chemical: isotope coding affinity tag or ICAT and isobaric tags for relative and absolute quantitation or iTRAQ) or *in vivo* (metabolic: stable isotope labelling by amino acid in cell culture or SILAC) (Agrawal et al., 2010; Delaunois et al., 2014). Monodimensional gels (1-DGE) are also often use to separate proteins, thanks to their reproducibility and feasibility as a technique (Agrawal et al., 2010). However, it has to be kept in mind that gel-based techniques may fail to properly separate all the proteins contained in a sample (for instance, protein spots overlapping on a bidimensional gel), therefore leading to an incomplete protein identification. To overcome these problems, gel-free techniques that make use of liquid chromatography (LC) to separate the proteins have been developed. For instance, the MudPIT technique is composed of two chromatographic steps: strong cation exchange followed by a reversed-phase chromatography (Delaunois et al., 2014). Nevertheless, to achieve a complete proteome representation, gel-based and gel-free techniques are often coupled (Agrawal et al., 2010; Delaunois et al., 2014).

Protein identification is achieved via mass spectrometry (MS). The main protein ionization techniques used in apoplastic proteomics are matrix-assisted laser desorption ionisation (MALDI) or the electrospray ionization (ESI). To separate and detect the ions, instead, the main adopted techniques use time of flight (TOF) or quadrupole mass analyser, while to improve sensitivity and accuracy tandem mass spectrometry (MS/MS) is often applied (Delaunois et al., 2014).

5.1.3 Proteins modulated in the apoplastic proteome during plant-pathogen interactions

During plant-pathogen interactions, plants react by producing an arsenal of molecules to contrast the spreading of the infection. Many molecules with antimicrobial properties are produced such as phytoalexins and cyclotides (small proteins), reactive oxygen species, callose and many others. There is also an increased production of extracellular adenosine triphosphate (eATP) (Mott et al., 2014).

However, the main players of plant immunity are proteins. There are many that are expressed or modulated when a pathogen is recognized. For instance, there is an increased production in proteins carrying leucine-rich repeats (LRRs), most probably

with a role in perception and signalling (putative receptors) of the invading microorganisms; other induced proteins are the receptor-like kinases (RLKs) composed of a DUF26 domain, known to be secreted (Delaunois et al., 2014). Well-known proteins, produced after the recognition of pathogen elicitors by pattern recognition receptors (PRRs) are the so-called pathogenesis-related proteins (PRs). They have been classified in 17 groups (Table 5.1), depending on their sequence homology, pI or their migration into a native protein gel (there are indeed many criteria considered for their classification). These proteins are mainly localized into the apoplast and vacuoles, and in some cases healthy plants are almost devoid of them. They are induced upon pathogen recognition, but their expression is faster during an incompatible interaction. In many cases, these proteins will cause the production and release of endogenous host elicitors (damage-associated molecular patterns - DAMPs) to amplify the immune response towards the invading microorganisms (Doehlemann & Hemetsberger, 2013; Sudisha et al., 2012). PR proteins represent 10-15% of the modulated apoplastic proteins during plant-pathogen interactions (Delaunois et al., 2014).

As shown in Table 5.1, there are proteins responsible for ROS metabolism, such as peroxidases (PR 9) or oxalate oxidases (PR 15/16); they either produce ROS in order to attack the pathogen or they try to detoxify the apoplastic environment, to balance in between the attack and the damaging effect of ROS on cells. Among these enzymes, superoxide dismutases are also produced. Because of the great importance in cell protection, the cell wall is constantly modified and reinforced. During pathogen infection, enzymes (such as glucanases - PR 2) able to remodel the cell wall are expressed. These enzymes, such as xylanases, xyloglucanases and β-1,3-endoglucanases also contribute to a reinforcement of the elicitation of the immune system because they may cause the release of oligogalacturonides, recognised as DAMPs. These cell wall remodelling enzymes are often co-induced with chitinases (PR 3/4/8/11). They may altogether contribute to the degradation of the fungal pathogen's cell wall (glucans and chitin respectively), both killing the pathogen and releasing molecules recognised as PAMPs by the plant and once again reinforcing the danger signal. In addition, in between the PR proteins modulated during plant-pathogen interactions there are also proteolytic enzymes (PR 17) in particular subtilisin-like proteinases (PR 7) or aspartate proteinases and peptidases (Sudisha et al., 2012; Delaunois et al., 2014).

There are also proteins directly involved in protection against pathogens, such as proteinase inhibitors (PR 6), which are exclusively induced upon contact with a pathogen and are able to stop the proteinases secreted by the microorganisms. They are divided into 3 groups, depending on their proteinase specificity: serine proteinase inhibitors, cysteine proteinase inhibitors or aspartate/metallo proteinase inhibitors (Sudisha et al., 2012). Other plant defensive proteins are plant defensin or defensin-like proteins (PR 12), characterized by an antimicrobial activity through protein synthesis inhibition (Carvalho Ade & Gomes, 2011); thionins (PR 13), displaying antifungal or antibacterial activity (Pelegrini & Franco, 2005); and finally thaumatin-like proteins (TLPs – PR 5), so called because of the high sequence homology with thaumatin (sweet-tasting protein from *Thaumatococcus daniellii*) and characterized by antifungal properties (Petre et al., 2011) (Sudisha et al., 2012).

Table 5.1 Classification and main features and functions of the pathogenesis-related proteins.

PR groups	Features/Activity
PR 1	Most abundant PR group. Often used as a marker for plant immunity
PR 2	They have β-1,3-glucanase activity; often associated with callose formation
PR 3/4/8/11	They show chitinase-like activity
PR 5	They share homology with thaumatin (thaumatin-like proteins or TLPs)
PR 6	Proteinase inhibitors, induced ONLY in response to insect or pathogen attack
PR 7	Endoproteinase activity. They share homology with subtilisin-like proteinases
PR 9	Glycoproteins with peroxidase-like activity
PR 10	Intracellular defence proteins with ribonuclease activity and structure
PR 12	Defensin-like proteins. Divided in 4 groups.
PR 13	Thionins. They are found in cell walls and vacuoles
PR 14	Lipid transfer proteins (LTPs). Involved in lipid transfer among organelles. Found in cell walls
PR 15/16	Oxalate oxidases or oxalate oxidase-like proteins (OLPs). They generate ROS
PR 17	They show a proteolytic-like activity

The table shows the 17 groups in which the PR proteins are classified. The main features/activity for each group are also described (the grouping and relevant information have been adapted from Sudisha et al., 2012).

5.1.4 Aim of the study on *Arabidopsis* apoplastic proteins

As mentioned above, apoplastic proteins play a very important role in plant-pathogen interactions. In order to obtain a more complete view on the players involved in the *Arabidopsis*/*Hyaloperonospora* interaction, apoplastic *Arabidopsis* proteins were selected from a study carried out by a previous PhD student (Gülin Boztaş) in collaboration with The Sainsbury Laboratory (Norwich, UK), where she focused on the secreted *Hpa* proteins.

The main objectives of this project were as follows:

➢ Select secreted pathogen-modulated *Arabidopsis* apoplastic proteins
➢ Identify homozygous T-DNA lines for each gene
➢ Determine their role in the *Arabidopsis* immune reaction against *Hpa*

5.2 Results

5.2.1 Bioinformatic identification of *Arabidopsis* apoplastic proteins

To understand more about the *Arabidopsis* response during the interaction with *Hpa*, a proteomic study on *Hpa*-infected *Arabidopsis* apoplastic fluid was previously carried out in our laboratory in collaboration with the Sainsbury Laboratory (Norwich, UK).

The proteins were identified via mass spectrometry and the results were as follows: 106 *Hpa* proteins, 159 *Arabidopsis* up-regulated proteins and 84 *Arabidopsis* down-regulated proteins. Further investigations showed that 61 of the 159 *Arabidopsis* up-regulated proteins carried a signal peptide, while among the 84 down-regulated ones, only 20 were found to contain the signal peptide. The proteins found through SignalP carry a N-terminal signal peptide and are usually accepted to be secreted via the conventional ER-Golgi route. However, as mentioned in Section 5.1.1, apoplastic secreted proteins can also follow an alternative pathway, called leaderless secretion pathway (LSP) and they usually account for the 50% of all apoplastic secreted proteins (Agrawal et al., 2010; Delaunois et al., 2014; Gupta et al., 2015). Therefore, it has to be considered that among all the identified apoplastic proteins not highlighted as secreted

by SignalP, there may be several that are secreted through the alternative pathway. The remaining proteins are most probably a consequence of ruptured cells due to the apoplastic fluid extraction method. For this project, only the proteins identified through SignalP were considered.
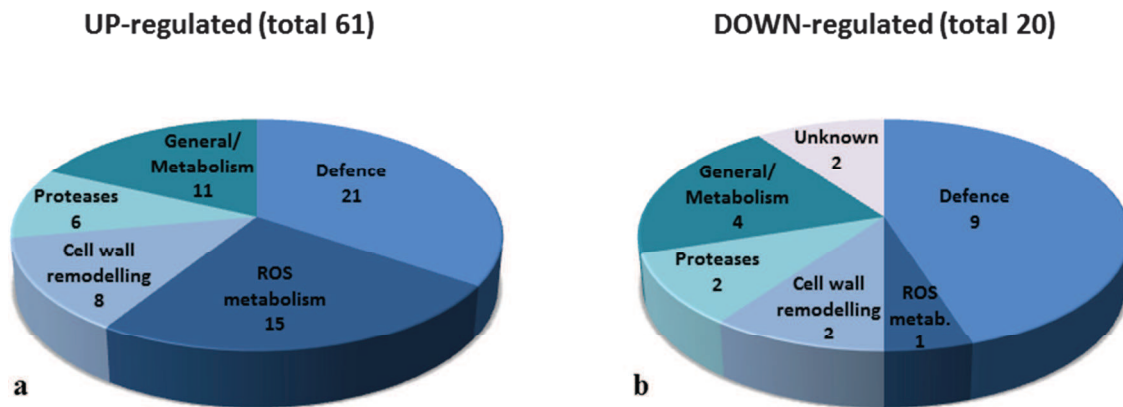
Figure 5.2 Schematic representation of the main categories represented by the up- and down-regulated secreted apoplastic proteins. The graphs show the categories represented by the *Arabidopsis* up- and down-regulated (after *Hpa* infection) secreted apoplastic proteins, found via SignalP. There are proteins directly involved in defence, ROS metabolism, cell wall metabolism and also proteins having proteases function or having general functions or metabolic functions. Among the down-regulated ones there are also 2 proteins of unknown function.

Figure 5.2 shows a grouping of the *Arabidopsis* up- and down-regulated proteins after *Hpa* infection. Considering the up-regulated proteins (Figure 5.2a), the main category is represented by proteins directly involved in defence (21 proteins) such as chitinases, glycosil hydrolases or PR1 proteins. The second category is the one containing proteins involved in ROS metabolism (15 proteins): including peroxidases, FAD-binding berberine-like proteins or germin-like proteins. Following, the group of proteins involved in general plant growth and development/metabolism (11) such as purple acid phosphatases, fasciclin-like proteins or β-glucosidases. The last two categories of up-regulated secreted apoplastic proteins are represented by proteins involved in cell wall remodelling (8, including pectin lyases, pectin methylesterases or glyceril phosphodiesterases) and in proteins/peptides degradation (6, such as serine carboxypeptidases, aleurain-like proteases or aspartyl proteases). On the other hand, among the down-regulated group of proteins (Figure 5.2b), those involved in defence are still the most represented ones, with 9 secreted proteins. With 4 secreted apoplastic

proteins is the category of proteins involved in general plant development/metabolism, while two proteins have been found to be secreted in the groups containing proteins involved in proteolysis and cell wall remodelling. Only one protein involved in ROS metabolism was down-regulated following *Hpa* infection and found to be secreted through the conventional pathway. Two proteins with unknown function were also found.

5.2.2 Elucidating the role of some of the apoplastic proteins using T-DNA mutants

Among the 61 up-regulated (due to *Hpa* infection) and secreted apoplastic proteins, a total of 11 genes were initially selected from the five different categories, to be further studied in order to understand their implication and importance in *Arabidopsis* immune reaction; while among the 20 secreted down-regulated proteins, a total of three genes, representing the categories of defence genes and genes involved in proteolysis and general/metabolism were selected.

Table 5.2 shows the AGI code, the function/activity for each gene selected and the category to which they belong to. In regard to the up-regulated genes, all five categories were represented with at least one gene selected. In detail, 5 genes directly involved with defence were chosen, including two PR genes (PR4 with chitinase activity and PR5), a curculin-like protein, a chitinase and a plant basic secretory (PBS) protein. Among the ROS metabolism group, two genes were selected, corresponding to a FAD-binding berberine protein and a peroxidase. One gene, a pectin lyase, was chosen in the group of proteins involved with cell wall metabolism, while two genes, corresponding to a subtilase and to a serine carboxypeptidase, were selected in the group of proteins acting as proteases or peptidases. Finally, the gene encoding for a protein disulphide isomerase was picked in the group of general development/metabolism. On the other hand, only three categories were represented for the down-regulated genes: defence, proteases and general development/metabolism. Briefly, the selected genes were as follows: a leucine-rich repeat (LRR) protein (defence group), probably with a receptor activity, a serine carboxypeptidase (proteases) and a calreticulin 1b protein (general/metabolism).

Table 5.2 Up- and down-regulated genes encoding for secreted apoplastic proteins selected for further analysis.

	Category	AGI code	NASC ID	Role/Function
Up-regulated	**Defence**	AT5G18470	N960018 N502990	Curculin-like lectin family protein
		AT2G43590	N859959 N673299	Chitinase family protein
		AT3G04720	N666544	PR 4
		AT1G75040	N668298 N533489	PR 5 – thaumatin-like protein
		AT2G15220	N628725	Plant basic secretory protein(BSP)
	ROS metabolism	AT1G26390	N666563	FAD-binding berberine
		AT4G37520	N660456 N677370 N631947	Peroxidase superfamily protein
	Cell wall remodelling	AT5G41870	N660148	Pectin lyase-like protein
	Proteases	AT1G32960	N663184 N680109	Subtilase family protein
		AT1G15000	N674359 N571144 N639700	Serine carboxypeptidase-like
	General/Metabolism	AT1G21750	N653755 N654518	Protein disulphide isomerase (PDI)-like 1-1
Down-reg	**Defence**	AT3G12145	N593764	Leucine-rich repeat (LRR) protein
	Proteases	AT2G27920	N653018 N650477	Serine carboxypeptidase-like
	General/Metabolism	AT1G09210	N680289 N681945	Calreticulin 1b

15 genes involved in defence, ROS metabolism, cell wall remodelling, general developmental/metabolic processes or with a role as proteases were selected because they resulted up- or down-regulated in the secreted (following SignalP prediction) *Arabidopsis* apoplastic proteome after *Hpa* infection. The AGI code of the gene, the role or function of the genes and the NASC number of the selected T-DNA lines for each gene are given. For some genes, only one T-DNA line was found.

The up-regulated proteins are more likely a representation of the *Arabidopsis* induced immune response triggered by the *Hpa* infection; whereas the down-regulated proteins are most probably a result of the *Hpa* effectors targeting the *Arabidopsis* defence machinery. For these reasons, in order to understand more about the plant response, efforts were focused more on the up-regulated proteins; therefore more genes were

selected from this group of proteins. For each selected gene, the corresponding T-DNA mutant seeds were obtained from the Nottingham *Arabidopsis* Stock Centre (NASC) and where possible, at least two if not three different insertion lines were obtained (a total of 25 T-DNA mutant lines; see Table 5.2). This was done to ensure that the observed phenotype derived from a real gene interruption.

5.2.2.1 Identification of homozygous T-DNA insertion lines

Every T-DNA line obtained was screened to check whether the line was homozygous for the T-DNA insertion. Briefly, few seeds for each line were sown and when the plants were at the rosette stage, a piece of leaf was collected for DNA extraction and PCR. The DNA was extracted using a fast method (see Section 2.2.1.4). Because all lines belonged to the SALK collection, the primers used for the PCR were designed using the T-DNA Primer Design Tool on the Salk Institute Genomic Analysis Laboratory (SIGnAL) iSect Toolbox page (http://signal.salk.edu/isects.html). For the full primer list see the Appendix. In brief, the PCR reaction was set up by combining the extracted DNA and three primers for each line (Figure 5.3a). Two of the three primers were the genomic left and right primer (LP and RP), which were generated for each gene of interested by the online tool (see above). The third primer corresponded to the left border (BP, border primer) of the inserted T-DNA, and therefore the same T-DNA primer was used to screen every gene. Since all the T-DNA lines were Columbia background, wt Col-0 DNA was extracted as well and used in the PCR as a control. Three different outcomes were possible: wild type (WT), heterozygous (HT) or homozygous (HM) insertion (Figure 5.3b). In the case of a plant with no T-DNA insertion (WT) the band size should have been between 900 and 1100 bps (product obtained with the LP and RP). In the case of a homozygous plant line (T-DNA inserted in both chromosomes), the obtained band size should have been 410+N (0-300 bps) bps. This represents the product of the amplification of the DNA between the BP and the RP: in detail, the region between the BP and the end of the T-DNA is 110 bps, while the amplification product from the RP to the flanking region is 300 bps. The variable N depends on the actual insertion point of the T-DNA. Finally, in the case of a heterozygous plant (one insertion in one chromosome), the result is a combination of the two previous results (WT band + HM band) (Figure 5.3 and Figure 5.4).
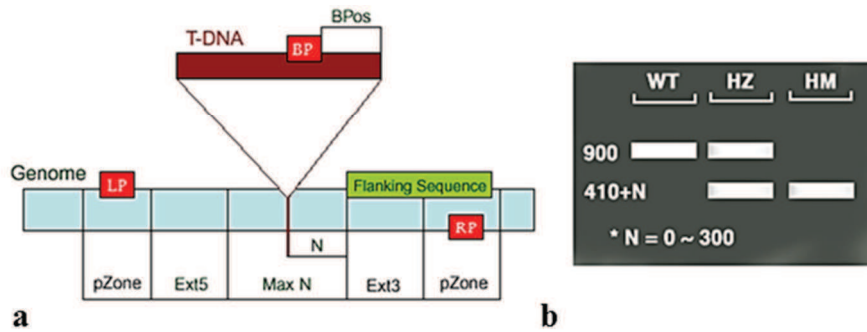
Figure 5.3 Salk line T-DNA insertion confirmation protocol. a: schematic representation of the T-DNA insertion point. The primers used in the insertion confirmation PCR are as follows: **LP** (left genomic primer), positioned on the left border of the gene of interest; **RP** (right genomic primer), located on the right border of the gene of interest; **BP** (T-DNA border primer), T-DNA left border primer, located on the inserted T-DNA. The p-zone represents the left and right areas on the gene, usually used by the software to pick the primers, while Ext5 and Ext3 are the areas not used to pick the primers. N represents the difference between the actual insertion point and the flanking region (0-300 bps), while BPos is the distance from the border to the insertion. **b**: possible outcomes of the PCR reaction using the extracted DNA and the LP, RP and BP primers altogether. If the plant is wild type (**WT**, no T-DNA insertion), the obtained product is 900-110 bps long. If the plant is homozygous (**HM**, insertion in both chromosomes), the product is 410 bps + N, where N, as mention above, could be 0-300 bps. 410 bps is the result of the aplification of the T-DNA left border (BP+BPos) of 110 bps and the of the amplification of le genomic right border (RP+flanking sequence to N) of 300 bps. If the plant if heterozygous (**HZ**, T-DNA insertion in one chromosome) the resulting bands are a combination of the WT and HM results (adapted from Salk Institute Genomic Analysis Laboratory (SIGnAL) website: http://signal.salk.edu/tdnaprimers.2.html).
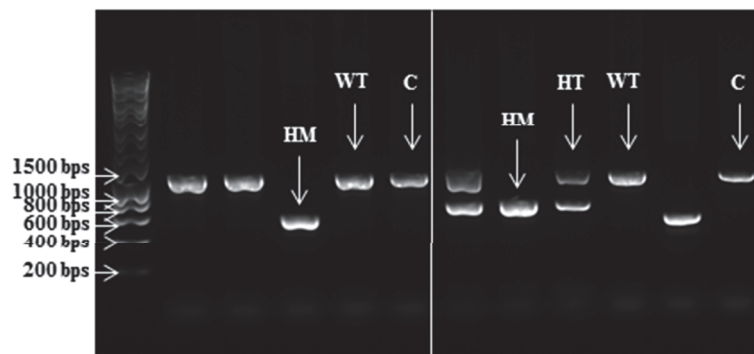
Figure 5.4 Confirmation of T-DNA insertions by PCR amplification. The picture shows an example of two different PCR reactions to confirm the presence of the insert into the gene of interest. For both genes (separated by the white line), several plants were screened: 4 in the first case and 5 in the second case. Each lane represents a different plant (different DNA sample collected) analysed. In both cases a reaction was set up using wt Col-0 DNA (**c**) to be used as a reference on the gel. Both PCR reactions were set up using a genomic LP and RP (different for each gene screened) and the middle primer (BP) pairing with the T-DNA. At least one homozygous (HM) plant for each gene was found; it is noticeable the expected difference in size in between the two genes (see above for the explanation). In the second sample there are also two heterozygous plants (HT) characterised by two bands, one corresponding to the wt gene amplification (higher band) while the other corresponding to the amplification result due to the presence of the T-DNA (lower band). Finally, in both samples, a band is present from un-transformed plant (WT). DNA ladder: HyperLadder 1kb (Bioline, UK).

After the screening of the 25 T-DNA insertion lines obtained (Table 5.2), it was possible to find at least 1 homozygous plant for 22 lines. Unfortunately, for 3 genes (two up-regulated: pectin lyase and PR4 and one down-regulated: LRR family protein) no HM plant was found. Therefore, the category of cell wall remodelling enzyme in the up-regulated proteins and the defence category among the down-regulated ones were no longer represented in this study.

The HM plants were brought to the seed stage and afterwards the seeds were collected and stored for further studies.

5.2.3 Screening mutant lines

To determine the role that the secreted apoplastic proteins have in defence against *Hpa*, the selected homozygous T-DNA lines were challenged with 3 *Hpa* isolates: *Hpa*-Cala2, *Hpa*-Emoy2, and *Hpa*-Noks1. Considering that the T-DNA mutant lines are Columbia background, one isolate was incompatible (Cala2), one was semi-incompatible (Emoy2) and one was compatible (Noks1). The use of isolates with different ability to grow and develop on Col-0 accession highlights the importance and the role of each selected gene in *Arabidopsis* immune response against this pathogen.

In every experiment, around 25 seeds were sown in each pot and 3 pots were usually sown for each T-DNA line. Col-0 and Ws-*eds1* were sown in each tray as controls.

5.2.3.1 Sporulation assay using an incompatible *Hpa* isolate: Cala2

The first approach adopted to study the function and role of the selected apoplastic proteins considered the use of an incompatible *Hpa* isolate: Cala2. This isolate does not grow on Columbia plants, because of the recognition of the *Hpa* avirulence gene *ATR2* by *Arabidopsis* resistance genes *RPP2A* and *RPP2B* (Sinapidou et al., 2004). Being all Col-0 background, the T-DNA lines used should not support the growth and development (in terms of completion of the life cycle), unless the deleted gene studied plays a pivotal role in defence and recognition. Therefore, one-week-old seedlings were spray inoculated with 5×10^4 spores ml^{-1} of *Hpa*-Cala2 spores. After one week of incubation at 16 °C and 12h light/12h dark regime the potential sporangiophores were counted as explained in Section 2.2.3.3.

As expected, no sporangiophores were observed on Col-0 wt seedlings. Similarly almost no sporangiophores were found on the studied T-DNA lines and definitely no difference was registered in between Col-0 wt plants and the T-DNA lines.

5.2.3.2 Sporulation assay using a semi-compatible *Hpa* isolate: Emoy2

In a second attempt to study the importance of the selected genes in *Arabidopsis* resistance towards *Hpa*, the semi-compatible isolate Emoy2 was used. In the wt accession Col-0, the resistance gene *RPP4* confers resistance to *Hpa*-Emoy2 (van der Biezen et al., 2002).

As previously described, one-week-old seedlings (Col-0 and T-DNA lines) were spray inoculated with 5×10^4 spores ml^{-1} of *Hpa*-Emoy2 spores. After one week incubation at 16 °C with a 12h light/12h dark regime, the visible sporangiophores were counted under a stereoscope (Section 2.2.3.3).

No statistical difference was recovered in between Col-0 and the T-DNA lines. This may be a consequence of the semi-incompatibility in the Col-0/Emoy2 interaction, due to the recognition of *ATR4* (*Avr* gene in Emoy2) by the Col-0 resistance (*R*) gene *RPP4*.

5.2.3.3 Sporulation assay using a compatible *Hpa* isolate: Noks1

Since no enhanced pathogen growth, hence no *Arabidopsis* enhanced susceptibility was recorded in the previous experiments, probably due to the incompatibility (given by *R*-genes mediated resistance) between the isolates (Cala2 and Emoy2) and the *Arabidopsis* accession used (Columbia, both as a reference and as the background for the mutant lines) (Holub et al., 1994), a third approach was attempted. In this case, the compatible isolate Noks1 was used. Similarly, one-week-old seedlings were spray-inoculated with *Hpa*-Noks1 spores (5×10^4 spores ml^{-1}), incubated for one week at 16 °C with a light regime of 12h light/12h dark. After one week the spores were counted as explained in Section 2.2.3.4.

Figure 5.5 shows the results of the spore counting for each T-DNA mutant line. Several lines showed an increased spore number in respect to Col-0. Because of the number of

the T-DNA lines studied they were divided in four trays (represented by the four graphs in Figure 5.7), however in every tray Col-0 wt was included as well as a reference in order to normalise the obtained results: there are indeed variation in the infection intensity among the four trays as indicated by the different spore number on Col-0 plants. The statistical difference between the T-DNA and Col-0 spore number was calculated separately for each tray.
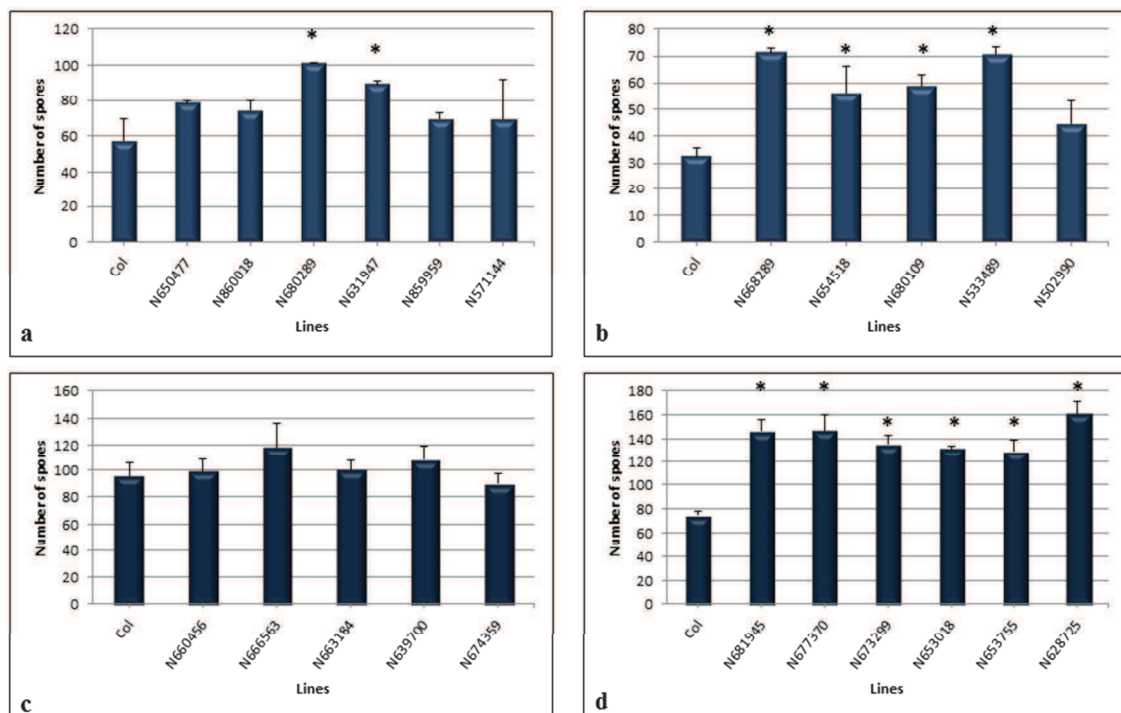
Figure 5.5 Sporulation on T-DNA lines infected with *Hpa*-Noks1. The four graphs (**a**, **b**, **c**, **d**) show the number of spores obtained by inoculating each T-DNA line (the NASC ID number is shown; see Table 5.2 for details) with *Hpa*-Noks1 spores. Each graph represents a different tray: in each tray Col-0 wt plants have been sown as well as a reference. It is noticeable that 12 T-DNA lines allow an increase in sporulation of *Hpa* (see Table 5.3 for a more detailed representation): the black asterisks represent statistical different results in comparison to Col-0 plants (statistical analysis performed using One-Way ANOVA, Dunnet post-test).

The lines that allowed an increased sporulation are schematised in Table 5.3: each line is assigned to its gene. In addition the function of the gene and its regulation during *Arabidopsis*/*Hpa* interaction are also indicated. Finally, the T-DNA insertion point into the gene sequence is showed as well.

Table 5.3 T-DNA mutant lines showing enhanced susceptibility towards *Hpa*-Noks1.

NASC ID	Function	AGI code	Regulation	T-DNA ins.
N668289 N533489	Pathogenesis-related 5 (PR5) thaumatin-like protein	AT1G75040	UP	exon 3' UTR
N631947 N677370	Peroxidase superfamily protein	AT4G37520	UP	5' UTR exon
N628725	Plant basic secretory protein (BSP)	AT2G15220	UP	exon
N654518 N653755	Protein disulphide isomerase (PDI)-like 1-1	AT1G21750	UP	exon exon
N673299	Chitinase family protein	AT2G43590	UP	3'UTR
N680109	Subtilase family protein	AT1G32960	UP	exon
N680289 N681945	Calreticulin 1b	AT1G09210	DOWN	exon exon
N653018	Serine carboxypeptidase-like	AT2G27920	DOWN	exon

Schematic summary of the previously (Figure 5.7) identified T-DNA lines that showed an increased in Noks1 sporulation in comparison to Col-0 wt. The T-DNA lines are identified by their NASC number and grouped together when representing different insertions in the same gene (indicated with an AGI code). It is also possible to find the function of the genes of interest and their regulation (up- or down-regulated) during the interaction between *Arabidopsis* and *Hpa* (see Section 5.2.1 and Table 5.2) and the T-DNA insertion position (T-DNA ins.) in the last column.

Six up-regulated and 2 down-regulated genes were found to be important during *Arabidopsis*/*Hpa* interaction. Among the up-regulated, PR5, a peroxidase, a basic secretory protein, a PDI-like protein, a chitinase and a subtilase seem to play an important role in defence, while among the down-regulated, calreticulin 1b and a serine carboxypeptidase-like were found. In detail, in few cases, the same phenotype was confirmed for all the T-DNA lines obtained for a specific gene (see Table 5.2 and Table 5.3). Briefly, PR 5 (up-regulated), together with PDI (up-regulated), BSP (up-regulated) and calreticulin 1b (down-regulated) showed enhanced susceptibility to the infection in all the obtained T-DNA lines for the gene. While the peroxidase gene (up-regulated) showed this phenotype for two out of three T-DNA lines. As for the chitinase (up-regulated) and for the serine carboxypeptidase (down-regulated), only one T-DNA line out of two obtained for each gene showed enhanced susceptibility.

5.2.3.4 Challenging the T-DNA mutant plants with *Hpa*-Emoy2 spore extracts in a ROS assay

To add more information on the role of the *Arabidopsis* apoplastic secreted proteins, the T-DNA lines selected and used in the previous sporulation assays were challenged in a ROS assay using the *Hpa*-Emoy2 crude extracts (see Chapter 3).

Figure 5.6 shows the results of the ROS assay: among the T-DNA lines studied, five (black asterisks) were found to produce a significantly lower amount of ROS in comparison to that produced by Col-0 plants (used as control and reference for the reaction). In addition, three more lines (indicated by the red asterisks) were included among the ones accumulating significantly less ROS in respect to Col-0. This result was achieved when the statistical analysis was deepened using a 2-paired T-student test ($p < 0.05$), where the T-DNA lines and Col-0 were directly compared.
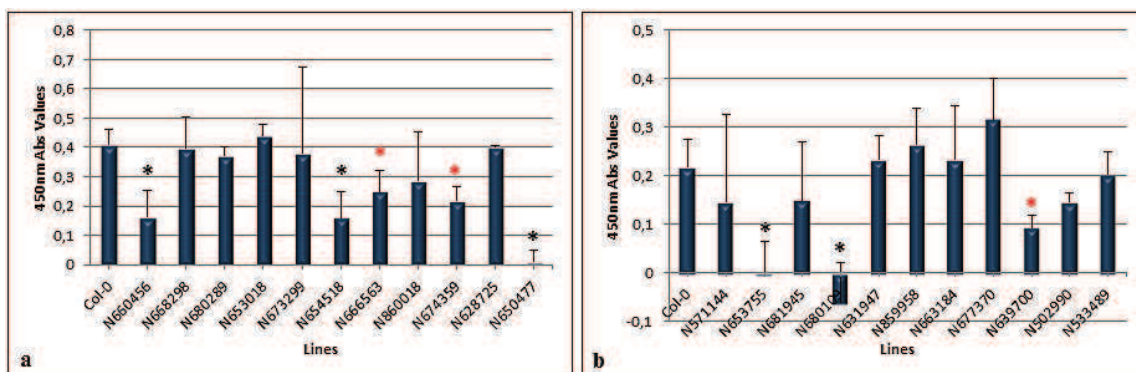
Figure 5.6 ROS assay on selected T-DNA lines using *Hpa*-Emoy2 spore extracts. The selected homozygous T-DNA lines were further screened in a ROS assay using the *Hpa*-Emoy2 spore extracts (previously seen in Chapter 3); Col-0 wt was included as a reference and a control. Among them, 5 produced significantly less ROS following the application of the spore extract, according to the Dunnet post-hoc test (ANOVA One-way). However on a more thorough statistical analysis using a 2-pair T-student test, 3 more lines were found to produce significantly less ROS in comparison to Col-0 wt. Statistical analysis: ANOVA One-way (Dunnet post-hoc test), 2-pair T-student test ($p < 0.05$). The black asterisks indicate results statistically different from Col-0 wt according to Dunnet test, while the red ones were obtained using the T-student test ($p < 0.05$).

The results have been schematized in Table 5.4: the T-DNA lines producing a significant lower amount of ROS have been indicated by their NASC ID number, the function of their represented gene, the gene's AGI code, its regulation during *Arabidopsis*/*Hpa* interactions and finally the T-DNA insertion point.

Table 5.4 T-DNA lines producing statistically lower amount of ROS when challenged with *Hpa*-Emoy2 spore extracts.

NASC ID	Function	AGI code	Regulation	T-DNA ins.
N660456	Peroxidase superfamily protein	AT4G37520	UP	exon
N654518 N653755	Protein disulphide isomerase (PDI)-like 1-1	AT1G21750	UP	exon exon
N674359 N639700	Serine carboxypeptidase-like	AT1G15000	UP	exon 5'UTR
N666563	FAD-binding berberine family protein	AT1G26390	UP	exon
N680109	Subtilase family protein	AT1G32960	UP	exon
N650477	Serine carboxypeptidase-like	AT2G27920	DOWN	exon

T-DNA lines that showed a statistically lowered amount of ROS after being challenged in a ROS assay with *Hpa*-Emoy2 spore extracts. The table also reports the corresponding gene's AGI code, gene's function and the gene's regulation during *Arabidopsis* interaction with *Hpa*. The last column shows the T-DNA insertion (T-DNA ins.) position in the sequence of the gene of interest.

In detail, one line (N660456), out of three studied, representing a peroxidase protein, showed a lower accumulation of ROS when challenged with Emoy2 spore extracts. Similarly, two lines (N674359 and N639700) out of three representing a serine carboxypeptidase showed a reduced ROS accumulation in comparison to Col-0. In the case of the subtilase (N680109) and the down-regulated serine carboxypeptidase (N650477) only one line out of two obtained showed a lower accumulation of ROS in respect to the control. As for the PDI-like protein, both the obtained T-DNA lines showed a similar behaviour in producing a significant lower amount of ROS than Col-0. Finally, in the case of the FAD-binding berberine protein the only line obtained showed a reduced ROS production.

5.2.3.5 Summary of the obtained results

Among the lines that showed enhanced susceptibility towards *Hpa*-Noks1 infection and the ones that showed a reduction in ROS accumulation, it is possible to find some common T-DNA insertion lines (Table 5.5). In addition, the peroxidase superfamily protein (AT4G37520) and the serine carboxypeptidase-like (AT2G27920) displayed T-

DNA lines with lowered ROS accumulation (indicated by *) and T-DNA lines with *Hpa*-Noks1 enhanced susceptibility (indicated by **). Finally two genes (PR5, AT1G75040 and calreticulin 1b, AT1G09210) showed enhanced susceptibility towards Noks1 infection, while one gene (up-regulated serine carboxypeptidase, AT1G15000) showed lowered ROS accumulation. The seven identified genes (Table 5.5, Table 5.6 and Table 5.7) may play an important role during *Arabidopsis*/*Hpa* interaction.

Table 5.5 Genes that showed both enhanced susceptibility towards *Hpa*-Noks1 and lowered ROS accumulation.

NASC ID	Function	AGI code	Regulation	T-DNA ins.
N654518	Protein disulphide	AT1G21750	UP	exon
N653755	isomerase (PDI)-like 1-1			exon
N680109	Subtilase family protein	AT1G32960	UP	exon

The NASC ID number, the gene function, the AGI code and the regulation are indicated. The T-DNA insertion position in the sequence of the gene of interest is shown in the last column.

Table 5.6 Genes involved in both ROS production and resistance towards *Hpa*-Noks1.

NASC ID	Function	AGI code	Regulation	T-DNA ins.
*N660456	Peroxidase superfamily	AT4G37520	UP	exon
**N631947	protein			5' UTR
**N677370				exon
*N650477	Serine	AT2G27920	DOWN	exon
**N653018	carboxypeptidase-like			exon

The table shows the genes (peroxidase and serine carboxypeptidase) having T-DNA lines showing either * lowered ROS accumulation or **enhanced susceptibility towards *Hpa*-Noks1. The gene's function, the AGI code, the regulation during the interaction with *Hpa* are also reported, together with the T-DNA insertion (T-DNA ins.) position into the gene sequence.

Table 5.7 Genes showing either *Hpa*-Noks1 enhanced susceptibility or lowered ROS accumulation.

NASC ID		Function	AGI code	Regulation	T-DNA ins.
N668289 N533489	▪	PR 5 – thaumatin-like protein	AT1G75040	UP	exon 3' UTR
N680289 N681945	▪	Calreticulin 1b	AT1G09210	DOWN	exon exon
N674359 N639700	➢	Serine carboxypeptidase-like	AT1G1500	UP	exon 5' UTR

The table shows the genes whose insertion lines showed an enhanced susceptibility towards Noks1 (indicated by the black square) or lowered ROS accumulation (indicated by the black and white arrow). The gene's function, the AGI code, the regulation during the interaction with *Hpa* are also reported, together with the T-DNA insertion (T-DNA ins.) position into the gene sequence.

5.3 Discussion

To conclude the study on *Arabidopsis*/*Hpa* interaction, genes encoding for apoplastic secreted proteins were selected (from a previous proteomic study on the apoplastic proteome) and studied in a functional investigation using reverse genetics.

T-DNA insertion lines for the selected genes were obtained from the Nottingham *Arabidopsis* Stock Centre (NASC) and screened for their homozygosity. The confirmed homozygous plants were then used in experiments to determine the importance of the genes in the interaction between the plant and the pathogen. The mutant plants were therefore challenged with three different *Hpa* isolates (Cala2, Emoy2 and Noks1), in order to identify which gene deletion would lead to an enhanced susceptibility or resistance (in terms of increased or decreased number of sporangiophores or spores) to *Hpa*, and consequently its importance during the interaction. Finally, the plants were also screened in a ROS assay using *Hpa*-Emoy2 spore extracts (see Chapter 3).

5.3.1 Gene selection and identification of homozygous T-DNA insertion lines

During the interaction between *Arabidopsis* (Ws-*eds1*) and *Hpa* (Emoy2), 159 *Arabidopsis* proteins resulted up-regulated due to the infection, while 84 resulted down-regulated (see Section 5.2.1). The identified proteins were analysed with the online tool

SignalP, to look for proteins secreted through the "traditional" pathway ER-Golgi. As a result, a total of 61 proteins were found to be secreted according to SignalP among the up-regulated proteins, whereas 20 proteins were found to be secreted among the down-regulated. As shown in Figure 5.2, they were further divided into 5 categories including defence, ROS metabolism, cell wall remodelling, general/metabolism and proteins with protease activity. To study their involvement in the *Arabidopsis*/*Hpa* interaction, seeds impaired in selected genes (see Table 5.2 for the complete list of selected genes and the corresponding T-DNA lines) were obtained from NASC. At least one gene per category was chosen among the up-regulated proteins, while a total of three categories were represented by T-DNA lines among the down-regulated ones (Table 5.2).

As mentioned, all the categories in the up-regulated proteins were considered. The criteria used for selection included proteins that are used by the plant as a defence against the invading pathogen (during PAMPs recognition and PAMP-triggered immunity; Ingle et al., 2006), but they also represent proteins regulated by the pathogen itself (Asai & Shirasu, 2015). In fact, during a compatible interaction, pathogen-secreted effectors are able not only to target the PTI machinery in order to lower the host defences (as may happen in the case of some of the down-regulated proteins; Howden & Huitema, 2012) but also to target plant's proteins that are related to host metabolism, to take advantage of host-produced nutrients (Asai & Shirasu, 2015).

In addition, it has to be noted that, where possible, for each gene at least two independent T-DNA lines (representing different insertion points in the gene sequence) were obtained. It is indeed elucidated by the SIGnAL website (http://signal.salk.edu/tdna_FAQs.html) that during the creation of the SALK line (Alonso et al., 2003) using *Agrobacterium* mediated transformation, the random integration of the transferred T-DNA may have happened in more than one locus into the *Arabidopsis* genomic DNA: as a result around 50% of the produced lines contains only one T-DNA insertion, while the other 50% contains two or more. For each T-DNA insertion line, the gene of interest was sequenced and only the genes containing one T-DNA insertion per gene of interest were selected. However, the absence of a T-DNA insertion anywhere else in the genome cannot be ensured. For this reason it is recommended to obtain at least two different insertion lines per gene studied, to make

sure that the resulting phenotype derives from the knock out of the gene of interest rather than the knock out of a random gene in the *Arabidopsis* genome.

As seen in Section 5.2.2.1, the obtained seeds were germinated and the plants were screened for homozygosity, and only the confirmed homozygous lines were used for the following experiments. This was done to ensure the actual knock out of the studied gene for both alleles, in order to make sure that the observed phenotype in the subsequent experiments was a result of the disappearance of the function of the gene.

5.3.2 Functional study of the T-DNA lines

To determine the involvement of the selected *Arabidopsis* apoplastic secreted proteins during *Arabidopsis* interaction with *Hpa*, the T-DNA lines were challenged with different *Hpa* isolates. Three different isolates, with different levels of compatibility with *Arabidopsis* Col-0 (background ecotypes for all the T-DNA lines), were chosen: *Hpa*-Cala2 (incompatible, due to *Hpa ATR2* recognition by *Arabidopsis RPP2a* and *RPP2b*), *Hpa*-Emoy2 (semi-compatible, due to recognition of *ATR4* by *RPP4*) and *Hpa*-Noks1 (compatible interaction) (Holub et al., 1994).

5.3.2.1 The T-DNA lines did not show enhanced susceptibility towards incompatible and semi-compatible *Hpa* isolates

When challenged with *Hpa*-Cala2 and *Hpa*-Emoy2, the selected T-DNA lines did not show signals of enhanced susceptibility in respect to Col-0 wt (used as a control in all the experiments), visible in the form of pathogen development, growth or sporulation.

This outcome may indicate that the studied genes are not implicated in the resistance mechanisms involving plant resistance (*R*) genes, and therefore ETI. In fact, in the case of the isolates Cala2 and Emoy2, the source of incompatibility is the recognition of effectors (*ATR2* and *ATR4*, respectively) by Col-0 *RPP2a/RPP2b* and *RPP4* resistance genes (Sinapidou et al., 2004; Holub et al., 1994). The immune reaction caused by the recognition of effectors (effector-triggered immunity; ETI) is greater in amplitude in respect to the one caused by PAMPs recognition (PAMP-triggered immunity; PTI) culminating with extensive host cell death at the interaction sites and hypersensitive response (HR) (Tsuda & Katagiri, 2010). For instance, as in the case of the interaction

175

between the two *Hpa* isolates Cala2 and Emoy2 and Col-0, the established ETI completely or almost completely stops the growth and the development of the pathogen. Therefore, it can be assumed that the studied genes are not involved in steps downstream the recognition between R genes and avirulence factors. Consequently, it can be speculated that these genes might play a role during PTI rather than ETI. Indeed, in the light of what mentioned above, their impairment does not allow enhanced pathogen growth; leading to the conclusion that their role in defence is at a previous stage that is not relevant when compared to the important immune reaction established during ETI.

This conclusion may be supported by the fact that, on the other hand, using a compatible host-pathogen combination (where no ETI is established, but the only source of resistance is given by PTI), a difference, in terms of enhanced sporulation, was noticeable.

5.3.2.2 Several T-DNA lines showed enhanced susceptibility towards the compatible isolate *Hpa*-Noks1

As mentioned above, the observable differences in growth, development and pathogen sporulation were observed during the compatible interaction between Col-0 plants and *Hpa*-Noks1.

In this case, most probably, the lack of a single gene due to the T-DNA insertion is visible as a change in the interaction phenotype (in terms of *Arabidopsis* enhanced susceptibility or *Hpa* enhanced spore production). This may have happened because not masked by the strong immune reaction (ETI) triggered by the recognition of an *Hpa* effector by an *Arabidopsis* resistance (*R*) gene. In fact, when the gene was inactivated due to the T-DNA insertion, the pathogen was able to proliferate on the transgenic plants, complete its life cycle and produce more spores than on Col-0 wt plants.

It has to be noted though, that not in all cases, every T-DNA line for the same gene showed the same phenotype. When comparing Table 5.2 and Table 5.3, only four genes showed enhanced susceptibility in all the obtained T-DNA: pathogenesis-related 5 (PR 5; up-regulated), protein disulphide isomerase-like 1-1 (PDI-like 1-1; up-regulated), plant basic secretory protein (BSP; up-regulated, even though in this case only one T-

DNA line was available for this study) and calreticulin 1b (down-regulated). Other genes showed enhanced susceptibility towards the infection, but only in one T-DNA line out of two available: the chitinase (up-regulated), the subtilase (up-regulated) and the serine carboxylase (down-regulated). As for the peroxidase, for which three T-DNA lines were obtained from NASC, two out of three showed the altered phenotype, while one line did not show any difference from Col-0. This behaviour may be referred to the suggestion given by the SIGnAL website in obtaining more than one T-DNA line per gene (see Section 5.3.1), due to the possible presence of a T-DNA insertion in other points of the *Arabidopsis* genome other than the gene of interest (Alonso et al., 2003). Therefore, if this was the case, the enhanced susceptibility visible in a T-DNA line rather than the second one, could be due to the knockout of a maybe more important gene in the defence pathway than the one studied. On the other hand, the difference in phenotype in between different lines for the same gene may be also due to the insertion point of the T-DNA in the studied gene. As shown in Table 5.3, different T-DNA lines corresponding to different insertion points were obtained: these were both exons and 3' UTR or 5' UTR. It has to be noted that not in all insertion events the gene will be completely knocked out and therefore, a reasonable amount of protein could still be produced (Krysan et al., 1999).

Having said that, most probably, only in the case of PR 5, PDI-like 1-1, calreticulin 1b and the peroxidase (since two lines out of three showed the phenotype) it could be speculated that they play an important role in the *Arabidopsis* Col-0 immune defense reaction against *Hpa*-Noks1 during PTI.

5.3.2.3 A further test on the T-DNA lines reveals new proteins that might play a role in *Arabidopsis* PTI

To gain further understanding on the role of the selected genes in *Arabidopsis* immune reaction, the T-DNA lines were also challenged in a ROS assay using *Hpa*-Emoy2 spore extracts seen in Chapter 3.

On this occasion, only three genes showed a lower ROS accumulation for all the T-DNA lines obtained: the up-regulated serine carboxypeptidase, the PDI-like 1-1 protein and the FAD-binding berberine-like (although in this case only one line was available

for the study). On the other hand only one peroxidase T-DNA line out of three and one T-DNA out of two for the subtilase and the down-regulated serine carboxypeptidase was recorded. As mentioned in the previous section, this latter outcome may be the consequence of a different T-DNA insertion and gene knock out in the *Arabidopsis* genome or a different level of inactivation in the studied gene due to the T-DNA insertion position inside of the gene sequence (exon, 3' UTR or 5' UTR).

Therefore, it is safe to include in the relevant protein for ROS accumulation due to the interaction of Col-0 with the *Hpa*-Emoy2 spore extracts only the upregulated serine carboxypeptidase and the PDI-like 1-1 protein. Indeed as previously said not enough lines were obtained for the FAD-binding berberine-like, although involved with ROS production.

5.3.3 Seven *Arabidopsis* genes appear to be involved in the interaction with *Hpa*

In summary, it can be noted that several T-DNA lines (and therefore their related genes) resulted involved in the interaction between *Arabidopsis* and *Hpa*, showed either in the form of enhanced susceptibility of the T-DNA lines towards the isolate Noks1 (see Table 5.3) or in a lowered accumulation of ROS when challenged with Emoy2 spore extracts (see Table 5.4).

5.3.3.1 Protein disulphide isomerase-like and subtilase family proteins

When considering all the obtained T-DNA lines per studied gene, the same resulting phenotype in both the sporulation and ROS assay was achieved only in the case of the gene encoding for the protein disulphide isomerase (PDI)-like 1-1 (AT1G21750, see Table 5.5). This protein resulted up-regulated due to the *Hpa* infection during the previous proteomic study (see Section 5.1.4). In this case, both the T-DNA lines carried a T-DNA insertion in the exon moiety. As described by Krysan and colleagues (1999), a T-DNA integration in an exon results in a gene knock out with subsequent loss of function. Therefore it can be assumed that the resulting phenotype, obtained with both the T-DNA lines and in both assays, may be a real consequence of the gene function knock out and therefore revealing the importance of the gene during the interaction.

The protein is also known as *At*PDIL1-1 or *, At*PDI5 and is present at the membrane, at the plant cell wall, but it can also be found in the endoplasmic reticulum (ER), where it exerts the role of disulphide isomerase; it is indeed a protein with foldase and chaperone function, helping in protein folding by creating or rearranging disulphide bridges in nascent proteins in the ER (The Arabidopsis Information Resource, TAIR; Yuen et al., 2013). PDI5 has a classical domain composition (similar to the ones found in animals and yeasts), containing one catalytic thioredoxin-like domain, two non-catalytic domains and one catalytic thioredoxin-like domain at the end (Yuen et al., 2013). Although the results obtained with the two T-DNA lines demonstrated a role in immunity against *Hpa* (see Table 5.5), it is not completely clear from the current literature the cellular localisation of this protein. There are indeed proofs that localise the protein as a ER resident (containing both a signal peptide, used to screen and initially select the proteins for our study and the ER resident peptide KDEL) (Yuen et al., 2013); therefore it seems not to be found in the apoplast as previously assumed. However, the *Arabidopsis* PDI2 (belonging to the same family of proteins of PDI5) has been localised in the secretory pathway (ER-Golgi-vacuoles and cell wall) (Cho et al., 2011). It could therefore been assumed that also PDI5, in specific occasions, might be found on the outside of the cell. In a similar way, a study by Ondzighi and colleagues (2008) demonstrated the role of PDI5 in programmed cell death (PCD) during seed development. They also showed that plants impaired in PDI5 produced a majority of non-viable seeds. In conclusion, it has to be noted, that PDI5 has been associated to functions not directly related to plant immunity and most probably it is most of the times present in the ER of the cell. However, in the light of the obtained results, it could be hypothesized that, under certain conditions, PDI5 could be translocated in the apoplastic space where it might exert roles linked to plant immunity.

A special mention has to done for the T-DNA line N680109, corresponding to the up-regulated subtilase family protein (AT1G32960). In fact, as shown in Table 5.5, this line showed both enhanced susceptibility towards *Hpa*-Noks1 and a lowered ROS accumulation when challenged with *Hpa*-Emoy2 spore extracts. In this case, differently from the protein disulphide isomerase, that showed this results for both of the obtained T-DNA lines, only one line (but the same line in both assays) showed the phenotype. This could be due to the T-DNA insertion point in the second obtained line. The protein,

also known as *At*SBT3.3, is an extracellular serine-type endopeptidase, involved in proteolysis and in induced systemic resistance (TAIR). In their review, Figueiredo and colleagues (2014) reported the importance of extracellular subtilisin-like proteases (subtilases) in plant innate immune responses. In particular, in a recent study by Ramírez and colleagues (2013) an additional role for the *At*SBT3.3 has been revealed: it appears to be involved in innate immune priming. Indeed, not only its overexpression induced pathogen resistance, but in addition its deletion enhanced pathogen susceptibility; it was also demonstrated that the expression of *At*SBT3.3 induced durable chromatin remodeling and salicylic acid-dependent priming of defense genes (Ramírez et al., 2013). The results obtained with the T-DNA line (enhanced *Hpa*-Noks1 susceptibility and lowered ROS accumulation) for *At*SBT3.3 are therefore in accordance with its important role in plant innate immunity established in the aforementioned studies.

5.3.3.2 Peroxidase superfamily protein and serine carboxypeptidase protein

In addition to the previously seen genes, also the up-regulated peroxidase protein (AT4G37520) and the down-regulated serine carboxypeptidase protein (AT2G27920) may be considered relevant genes during the interaction between *Arabidopsis* and *Hpa* (see Table 5.6). In this case, although not all the T-DNA lines gave the same outcome during the sporulation assay and the ROS assay as did the ones obtained for the PDI-like 1-1 gene, they can still be included in the analysis of results. As showed in Table 5.6, indeed, one line for the peroxidase gene accumulated a lowered amount of ROS, while the remaining two lines for the gene allowed enhanced Noks1 sporulation. A similar outcome was obtained for the serine carboxypeptidase-like gene where one line showed enhanced susceptibility while the other a lowered ROS accumulation. In this light, all the obtained lines for those two genes showed an impaired defense during the interaction with *Hpa* (either in ROS accumulation or enhanced pathogen sporulation).

The studied peroxidase gene corresponds to peroxidase 50 or PER50 (TAIR) and belongs to class III peroxidases (Cosio and Dunand, 2009). These enzymes are secreted and reside into the cell wall. They have been attributed different roles in plants such as wound repair, detoxification from H_2O_2, but they are also well-known for their role in

plant immunity, facilitating the lignification process due to pathogen recognition and participating in the production of the ROS burst during PTI and during the hypersensitive response (HR) (Cosio and Dunand, 2009). Therefore, it is not surprising that plants impaired in this gene (T-DNA lines) showed a compromised immunity towards *Hpa*.

Similarly, the serine carboxypeptidase-like protein or SCLP51 (TAIR) T-DNA lines showed enhanced susceptibility towards the *Hpa* infection and elicitation. Once again, a role in plant immunity has been demonstrated for this proteases. Indeed, in their study Liu and colleagues (2008) suggested that a rice serine carboxypeptidase (*Os*BISCPL1) might be involved in the regulation of genes implicated in defense against pathogens and in oxidative stress regulation. By transforming *Arabidopsis* plants with *Os*BISCPL1 they showed that it conferred resistance towards *Pseudomonas syringae* pv. *tomato* and *Alternaria brassicicola* and that the expression of defense genes such as PR1, PR2, PR5 and PDF1.2 was constitutively enhanced. In the light of these results, of its extracellular localization and of the results obtained using the corresponding T-DNA lines, it is not difficult to believe that analogously the *Arabidopsis* SCLP51 may have a role in defense against *Hpa*.

5.3.3.3 Pathogenesis-related 5 protein, calreticulin 1b and up-regulated serine carboxypeptidase

Finally, three more genes showed an important involvement in the interaction between *Arabidopsis* and *Hpa* (see Table 5.7). Although they did not show significant results in both the used assays (ROS accumulation and pathogenicity assay), they resulted important in one or the other assay. In detail, the pathogenesis-related 5 gene (PR5, AT1G75040) and the calreticulin 1b gene (AT1G09210) showed enhanced susceptibility during the interaction with *Hpa*-Noks1 for both obtained lines per gene. The importance of the pathogenesis-related genes in plant immunity has been thoroughly explained in Section 5.1.3. They are indeed known for their induction upon pathogen recognition and PR5 proteins, in particular, are known for antifungal activities (Sudisha et al., 2012; Hu & Reddy, 1997). Therefore the increased susceptibility of the two T-DNA lines corresponding to the PR5 gene is in accordance with the overall role of the PR proteins in plants' immunity.

Calreticulin 1b, or AtCRT1B, is one of the three *Arabidopsis* calreticulins. They are known to be involved in protein folding and response to oxidative and salt stress (TAIR). The two T-DNA lines studied showed enhanced susceptibility towards *Hpa*-Noks1 infection. This result could be explained with a role in immunity for this protein. Although it has not been demonstrated yet for this protein, it has been shown for the remaining two *Arabidopsis* calreticulins (AtCRT2 and AtCRT3). Initially only AtCRT3 was thought to be involved in plant immunity. In fact it is important for the responses to the bacterial PAMP elf18, being most probably involved in the correct folding of the elf18 receptor EFR (Christensen et al., 2010). In addition, recently, Qiu and colleagues (2012) demonstrated a role also for AtCRT2 in immunity other than in the regulation of the cellular levels of Ca^{2+}. Therefore, after the obtained results with the T-DNA lines and in the light of this study, it could be speculated that also AtCRT1B might play a role in *Arabidopsis* immunity and more specifically, towards *Hpa* infection. This could be achieved either directly or indirectly by regulating the intracellular Ca^{2+} levels, important for the triggering of PTI. A Ca^{2+} influx is indeed one of the first event following PAMP recognition (Boller and Felix, 2009).

In a similar way, two out of three lines (a significant number as previously explained in Section 5.3.1) of the up-regulated serine carboxypeptidase gene (AT1G15000) exhibited a lowered ROS accumulation in comparison to Col-0. This protein is also known as AtSCPL50 and it is found in the extracellular region or in the vacuole (TAIR). Similarly to what mentioned in Section 5.3.3.2, this protein acts as a protease and it might have a role in plant immunity as demonstrated for the rice OsBISCPL1 (Liu et al., 2008). Once again, its loss (due to the T-DNA gene interruption), may have had consequences in the signalling process during the recognition of PAMPs contained in the *Hpa*-Emoy2 spore extracts leading to a lowered accumulation of ROS.

Therefore, it can be concluded that in an overall view, seven genes among the ones considered at the beginning of the study showed a strong and confirmed involvement in PTI during *Arabidopsis*/*Hpa* interaction.

Chapter 6

General discussion and concluding remarks

This PhD research project investigated the interaction between the model plant *Arabidopsis* and the oomycete biotroph *H. arabidopsidis* with the main aim of discovering new PAMP molecules deriving from the pathogen, identifying genes involved in PTI and possible putative related receptors that may be involved in the recognition of these PAMPs in *Arabidopsis*. In addition, other aspects of the interaction, such as PAMP recognition specificity (among *Arabidopsis* accessions and among several plant families) and the players involved in the responses to the pathogen, have been investigated. Indeed, many studies have been carried out in the past on the effectors and *R*-genes side of the interaction (Rehmany et al., 2005; Sohn et al., 2007; Rentel et al., 2008; Fabro et al., 2011; Bailey et al., 2011; Goritschnig et al., 2012), while less has been investigated about PAMPs. To date, only one PAMP molecule originating from *Hpa* has been found, known as nlp24, deriving from the Nep1-like protein *Ha*NLP3 (Oome et al., 2014; Bohm et al., 2014) and this has been reported while carrying out this work.

6.1 To recapitulate

A three-way approach has been followed in order to thoroughly cover the aforementioned points. In detail, extracts were obtained from the pathogen asexual spores and studied with a "work in progress" attitude (Chapter 3). Secondly, two *Hpa* genes encoding for cellulose-binding elicitor lectin (CBEL) proteins (Baxter et al., 2010) were investigated (Chapter 4). They were chosen because orthologues of the *P.*

parasitica var. *nicotianae* CBEL protein which was discovered to contain two domains (CBDs) acting as PAMP molecules (Gaulin et al., 2006). Finally, to address the matter of *Arabidopsis* responses during *Hpa* infection, genes involved in the interaction with the pathogen were studied with a reverse-genetics approach (Chapter 5).
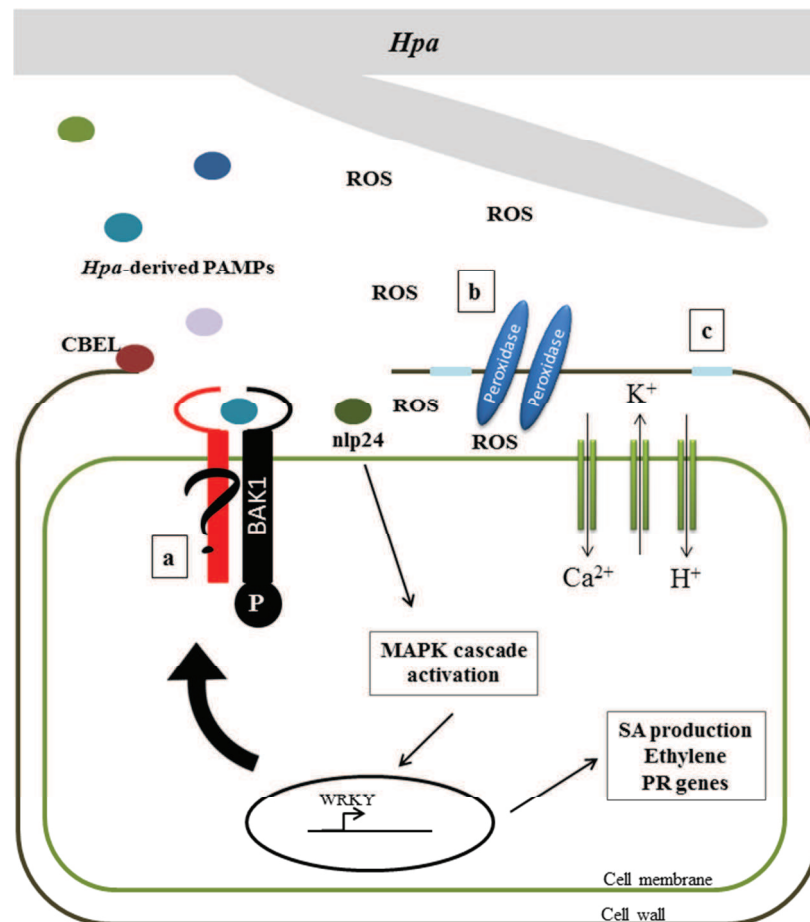
Figure 6.1 Model of PTI in *Arabidopsis*/*Hpa* interaction. The picture shows a schematized model of the interaction between *Arabidopsis* and *Hpa*, created by combining the finding of this project and the existing literature. *Hpa* contains PAMP molecules (some of which may be of proteinaceous nature), that are recognised by an unknown (see the question mark on the red coloured receptor), which relies on BAK1 to transmit the signal internally (**a**). Following the recognition, ion channels might be activated (this normally happens during PAMP recognition, Boller & Felix, 2009; Zipfel & Robatzek, 2010), causing alkalinisation of the extracellular space. Cell wall peroxidases are activated and start to produce ROS molecules (**b**; O'Brien et al., 2012; Daudi et al., 2012), together with the deposition of callose (**c**; Ellinger & Voigt, 2014). We also speculated that the two *Hpa* CBEL proteins might act as PAMPs molecules. They might be recognised because of their binding to the plant cell wall (as it happens for CBEL from *Ppn*, Gaulin et al., 2006). A mechanism of recognition is not yet known, but it could be hypothesised that their binding to the cell wall might cause a destruction of the cell wall integrity, which is recognised by the surveillance mechanisms of the plant cell (Nühse, 2012). Finally, it is known that the *Hpa* molecule nlp24 is recognised as a PAMP in *Arabidopsis* (Oome et al., 2014). It activates a MAPK cascade, which leads to the transcription and production of defence genes (e.g. PR1) and the production of ethylene and salicylic acid (SA). In addition, PRRs might be over-expressed after PAMP recognition in a positive-feedback mechanism (Boller & Felix, 2009).

Figure 6.1 shows a model of PTI during *Arabidopsis*/*Hpa* interaction. The knowledge derived from recent literature about PAMPs in *Hpa*, together with the accepted processes activated during PTI (please see Section 1.4.1.2), have been integrated with the main findings of this project.

In regard to *Hpa*-derived PAMPs, it can be shown that the pathogen spores contain molecules of proteinaceous nature able to trigger signs of PTI, such as ROS production and callose deposition (see Figure 6.1b and c; Torres et al., 2006; O'Brien et al., 2012; Luna et al., 2011). Unfortunately, due to the nature of the pathogen (obligate biotroph; Coates & Beynon, 2010), it was impossible to obtain an extract of the developed organism devoid of plant contaminants (see Section 3.2.4). It would have been interesting and more inclusive to also consider in the analysis the molecules deriving from the whole organism (including hyphae, haustoria, etc.). It is in fact possible that certain PAMP molecules may be produced and expressed later in the development, because maybe not required at the spore stage. Regarding this point, it has to be noted, that *Hpa* CBEL proteins once expressed in *N. benthamiana* were able to cause an immune reaction (see Section 4.2.3), while the spore extracts failed at triggering ROS production when tested on *Nicotiana* (see Section 3.2.5.4). This might be explained considering that, due to the role of CBEL in the oomycete (adhesion of the mycelium to cellulosic substrates, as seen in *Ppn*; Gaulin et al., 2002), they might be expressed at a later stage, during the attachment of the spore to the leaf at the beginning of the infection process. Therefore, there is the possibility that CBEL proteins act as PAMPs also in *Hpa* but they were not present into the spore extracts simply because they represent a stage where the two proteins are not expressed yet.

Regarding the *Arabidopsis* receptors involved in PAMP recognition, it has emerged during the project that the co-receptor BAK1 is involved in the recognition of the active molecules contained into the spore extracts (Figure 6.1a). On the other hand, the SOBIR1 adaptor, often associated with RLPs, does not play an active role in the recognition and the signalling of the molecules. This might lead to the conclusion that RLKs rather than RLPs are involved in *Hpa*-derived PAMPs, therefore narrowing the future studies on receptors may be a way further. However, it has to be kept in mind

that, as aforementioned, the molecules extracted from the *Hpa* asexual spores might not be completely representative of all the PAMPs produced by the oomycete.

As for the genes involved in the *Arabidopsis* response to the pathogen, seven genes have emerged to be involved in the reaction towards *Hpa* (they are not represented in Figure 6.1 for the sake of clarity in the representation). As seen in Chapter 5, three of them exploit proteolytic functions. This is in line with current research (Figueiredo et al., 2014; Liu et al., 2008) on plant defensive tools. In fact, proteases are both used to target and kill the microorganism and to reinforce the signals triggered by PAMP molecules. By targeting and degrading pathogen's proteins or enzymes, proteases might release peptides or protein sections, which may be recognized as PAMPs by the plant, enhancing the response against the invading microbe. For instance, a role of plant proteases in promoting PAMP detection was hypothesized for the newly discovered *Hpa* PAMP nlp24 (Oome et al., 2014). Because the PAMP molecule nlp24 is embedded inside of the protein *Ha*NLP3, plant proteases might play a role in partially degrading the *Hpa* protein, participating in its recognition by the plant (Oome et al., 2014). The remaining highlighted genes instead were directly involved in defence, such as the PR5 protein or the peroxidase. More studies are needed in order to shed light on the role of the PDI-like 1-1 protein, since its subcellular localization and role it is still not completely clarified.

In conclusion, although more still can be done, the obtained results contribute to the picture on the molecules, the signalling and the responses involved in PAMP-triggered immunity in the interaction between *Arabidopsis* and *Hpa*.

6.2 Conclusions and future research directions

This work aimed at laying the bases for studies on PAMP molecules from *Hpa* and their receptors and defence pathways in *Arabidopsis*, in order to help filling the gap that currently exists in the research on *Hpa*/*Arabidopsis* pathosystem.

Following on what has been done in this project, future works might focus on: simplifying the complex mixture of molecules represented by the *Hpa* spore extracts; screening the libraries of mutants for RLKs and RLPs to identify the receptor/s involved

in the recognition of the active molecules present in the extracts and finally digging deeper into the plant responses to those molecules.

In order to achieve these goals, it would be necessary to standardise the conditions for the fractionation procedure, since it still represents the way to reduce the complexity of the extracts. Once identified the fraction containing the most of the active molecules, this could be characterized by mass spectrometry (since it has been shown in this study that at least one of the active molecules is of proteinaceous nature). With the help of bioinformatics, the identified proteins contained in the active fraction, might be screened for PAMP characteristics, including patterns/domains presence and conservation in the oomycete order and role in the fitness of the oomycete. This will allow to hypothesize which protein might act as PAMP molecule and their role might be confirmed by heterologous expression and purification to study their activity. Once identified, the new PAMP molecule could be also used to screen mutant libraries for PRRs, with a focus on RLKs, since it has been demonstrated in this study that the co-receptor BAK1 (often associated with RLKs) is involved in the recognition of the active molecules contained in the spore extracts. On the other hand, the screening of the *Arabidopsis* collection of mutants for the RLKs with the spore extracts might help elucidating which ones are involved in the binding and signalling of the *Hpa* active molecules. Once identified, they could also be used to finally pull-down the related PAMP molecule that they bind. The identified *Arabidopsis* receptors could ultimately be transferred into crop plants, threatened by oomycetes, to confer them resistance to devastating diseases.

In addition, since during the project a role for the two *Hpa* CBEL proteins as PAMPs has been hypothesized, it would be interesting to finally understand their role. First of all, they could be heterologously expressed and purified as seen in this study. Afterwards, refolding them into their tridimensional conformation might help in the study of their role as PAMP molecules, testing them in a ROS assay or callose deposition assay or testing the phosphorylation of MAPKs and following the expression of defence-related genes, such as PR1, after their infiltration into *Arabidopsis*. Both in the case of the PAMP identified in the extracts or in the case of CBEL, it would also be necessary to further study their ability of causing a reaction in other plant families and

certainly on other Brassicas, other than *Arabidopsis*. Finally, if *Hpa* gene knock-out will become a possibility, it might also be possible to suppress the expression of the identified PAMP genes (e.g. nlp24, or CBELs if they are confirmed as PAMPs or any other PAMP molecule derived from *Hpa*) and further the understanding of their biological role in *Hpa*, by observing the derived phenotype. This has been done before for CBEL in *Ppn* showing that the protein is involved in perception and adhesion to cellulose and deposition of the oomycete cell wall (Gaulin et al., 2002).

Finally, regarding the defence reactions triggered by the plants toward the oomycete, a more in depth study on the *Arabidopsis* genes, highlighted in this study (Chapter 5) as important during PTI, would be interesting. In fact, these genes have roles in immunity against pathogens, therefore they could all be exploited in the future as target for effectors from *Hpa*.

Appendix

Hpa-801903

ATGGTCGAGCTCGCGTCCATTGCTGTGTTGTCCGTATTATCTCTATCAATCGCTGCGGGCGATACGTGCAACAATG
CTAACGGCAACAGTTGCGGAGACGCTACCGCTGCGTACTGCTGTCAGGAGAACCTCTACTGTATGCCTTGGAGCTC
GGATTACTACCAGTGCCTTCCACTGCCTGGTCAGTGCGGACGGCAATTCACCAACTACGACTTTAACGGAGGCGAC
ATCAAGACAATCTACGGTCTCCAACCGGGTGATTGCTGTGCGGCGTGCCTGGCGACGGCTGGTTGTCTCGCCTATA
CTTTCATGAACAGCTACCCCGGGACGACCGCCTGCTATTTAAAGGCGGGCATGGGAACCCCGCAAGAGGCCTCTG
GATTCGTTTCAGCCGTCGTCGATAGCTACACCAGCGATCAGGACAGGACTCCAAAGCTGCTCCGATTTCTCGCTGA
GATCAAGAATACCAGCAACGTGCCAATGGTC**TAA**

Hpa-801904

ATGTTGCGCACGTTTACCGTTCTAGCTGCAAGTATCGTCGTTCTCGATGGCACTTCCGCCACGGCATGCCCAAACT
CTTACTTTGGTCGCTGTGGCACTGCTTCGAAACCCGAGTGCTGCCCAAGTGGAAACTACTGCATGCCATGGACATC
CGGCTATTACCAGTGTCTTCCTGTGCCATCGCAGTGTGCCCGACAGTTCACTGGCTACGACTTCTACGGCGGTGAC
ATCAAGACGGTGTATGGGTTACAGCCCGGTGACTGCTGCGCGACGTGCTTAGCTACCAGGGGGTGTTTGGCGTAC
ACTTTTGTCAACGAGCACTCAGGAACTACGGCGTGCTTTTTAAAGGCAGGCATGGGCAAACCGAGAAAGGTTGCG
GGGTCGATCTCTGCCGTCATTGACCGCTACAACAGTGGCCAGGACCATACTCCGAAGCGACGACTTCAAGGCACT
GACGTATTAGGAGGTTCAGGACTTCCCATAACGCTCGACGTGCTT**TAA**

X97205 Cellulose-Binding Elicitor Lectin - CBEL (*P. parasitica var. nicotianae*)

ATGATTGCTCGCATTACCGTAGTCTTCGCTGGTCTCGTAGCTGTCGTCTCTGGTGCCTGCTCGACTCCCTCATTCGG
CAACTGTGGCTCTGATGCTGCCGGCGTGAGCTGCTGCCAGAGCACGCAGTACTGCCAACCTTGGAACGCCAACTA
CTACCAGTGCCTCGATCTCCCTGCTAAATGCGCTCAGCAGTTCCCGAACGTCGACTTCAATGGAGACGACATCCAG
ACCATCTACGGCATTCAGCCCGGAGAATGCTGCACGCGCTGCAGCGAGACTGCTGGTTGCAAGGCCTACACCTTC
GTGAACAGCAATCCGGGCCAACCGGCGTGCTACCTGAAGAGCGGCACTGGTACAAGGACGCCCTCGGTTGGAGC
AGTCTCGGGCATCTTGACGGGAACGTCAACAACCCCGACGCCGACCCCAACAATGACGCCAACGCCAACGCCGAC
GACATCATCGCCAACCTGCACCACGGCACCGTATGGCTCCTGTGGCTCCAGTAACGGAGCTACGTGCTGCCCGAG
CGGCTACTACTGCCAACCATGGAACGACAGTTTTTACCAGTGCATCCAGCCGCCAGCGAAATGCTCGAAACAACTC
ACCGACAAGGACTACTACGGCAACGACATTAAGACCGTCTACGTGAGCCTCCCGTCGCTTTGCTGTGATGCCTGTG
CTAGCACGGCAGGATGCAAGGCGTACACGTACATCAACAACAACCCCGGTCAGCCTGTGTGCTACTTGAAGAGCG
CTGCGGGAACTGCCACCACCAAGATCGGTGCTGTGTCGGGGACTCTCAAC**TAA**

NM_127025.2 *Arabidopsis thaliana* - Pathogenesis-related (PR1) - Signal peptide

ATGAATTTTACTGGCTATTCTCGATTTTTAATCGTCTTTGTAGCTCTTGTAGGTGCTCTTGTTCTTCCCTCGAAAGCT

	Signal peptide		Stop codon

Table 1 Primer list for the amplification of *Hpa*-801903 and *Hpa*-801904 genes, *Ppn-CBEL* gene PR1 signal peptide.

Gene ID	Forward primer	Reverse primer
Hpa-801903	**ACAAGTTTGTACAAAAAAGCAGCTTA**ATGGTCGAGCTCGCGTCCATTGC	**ACCACTTTGTACAAGAAAGCTGGGTA**TTAGACCATTGGCACGTTGCTGGT
Hpa-801904	**ACAAGTTTGTACAAAAAAGCAGCTTA**ATGTTGCGCACGTTTACCGTTCT	**ACCACTTTGTACAAGAAAGCTGGGTA**TTAAAGCACGTCGAGCGTTATGGG
X97205 CBEL *Ppn*	**ACAAGTTTGTACAAAAAAGCAGGCTTA**ATGATTGCTCGCATTACC	**ACCACTTTGTACAAGAAAGCTGGGTA**TTAGTTGAGAGTCCCCGA

The primers used contain the AttB1 (highlighted in red) and the AttB2 (highlighted in blue) sequences for the following Gateway® cloning into pEG100, pEG103 and pDest17 vectors. In addition, it has to be noted that the reverse primers used to amplify the *Hpa* sequences to be cloned in pDest17 (bacterial protein expression vector) do not contain the stop codon. The sequences are given in 5' → 3' direction.

Table 2 Primers used to exchange the signal peptide in *Hpa*-801903 and *Hpa*-801904 with the signal peptide of the *A. thaliana* PR1 protein.

Gene ID	Forward primer	Reverse primer
PR1 SP with *Hpa*-801903	**ACAAGTTTGTACAAAAAAGCAGGCTTA**ATGAATTTTACTGGCTATTCT	TGCACGTATC**AGCTTTCGAGGGAAGAAC**
PR1 SP with *Hpa*-801904	**ACAAGTTTGTACAAAAAAGCAGGCTTA**ATGAATTTTACTGGCTATTCT	GGCATGCCGT**AGCTTTCGAGGGAAGAAC**
Hpa-801903 with PR1 SP	**TTCCCTCGAAAGCT**GATACGTGCAACAA	**ACCACTTTGTACAAGAAAGCTGGGTA**TTAGACCATTGGCACGTTGCTGGT
Hpa-801904 with PR1 SP	**TTCCCTCGAAAGCT**ACGGCATGCCCAAA	**ACCACTTTGTACAAGAAAGCTGGGTA**TTAAAGCACGTCGAGCGTTATGGG

The red highlighted sequences correspond to the AttB1 sequence, while the blue ones refer to the AttB2 sequence. Because the primers are designed to link the signal peptide of the *At* Pr1 protein to the sequences of *Hpa*-801903 and *Hpa*-801904, the two forward primers for the *Hpa* sequences (Hpa-801903/04 with PR1 SP) and the two reverse primers for the PR1 signal peptide sequence (PR1 SP with Hpa-801903/04) consist of half sequence from the *Hpa* genes and half the sequence from the PR1 signal peptide (in bold). The sequences are given in 5' → 3' direction.

Table 3 Right (RP) and left primer (LP) sequences for each T-DNA lines used in the project.

NASC ID	T-DNA line	Right Primer (RP)	Left Primer (LP)
N666563	SALK_083228	CCCAAAGAAGGATTGGAGAAG	TGTGACTTAATATAAACCGTCCC
N660456	SALK_063662	CTATCATCAACAGCGGCTAGC	TAGGAGCATCCAGCATTCTTG
N677370	SALK_147859	TAGGAGCATCCAGCATTCTTG	AAATTCAATATAGGCGGGTGG
N631947	SALK_131947	TGACGCTATCATCACTGATGC	ACCATGTCAACTGTTTCGGAC
N860018	SALK_034283	TTTCCATTTTCCACACCAGTC	TCCATTGTTCGTCAAGATTCC
N502990	SALK_002990	AAATTTCTTCCGAAGGGTTTTAC	AAAAGAGGGGGTCGAAATATG
N663184	SALK_086092	AAAACGCATGCGAACATTTAC	TCACACACACCTTGTCTTTGC
N680109	SALK_107460	GAGGACCTAACTCGATGTCCC	CTTGGGGAGGAAGAAAAGATG
N660148	SALK_122988	TGAAATCGTTTTCGATTTTGG	ATAACAACGTCGTTGAGTCCG
N674359	SALK_033176	TCTGTTCTGTATGGAATCGCC	CTCTTTTCGGCCCAATAAAAC
N571144	SALK_071144	GTAAAGATGCTCAGCGACCTG	GCAGTGAAGCAGTAGAATCCG
N639700	SALK_139700	TTGAAATCATCTGCGAATTCC	GTAAAGATGCTCAGCGACCTG
N859959	SALK_043790	TTTTGTTTGTTCAATCATTGGG	TATTGTGTGTTGCTGCTCTGG
N673299	SALK_118982	CAGCAACACACAATACCCATG	CGTATAGCGGACTGAAATCATC
N666544	SALK_082089	AAAACTTCAGCACTCCAATTCTG	AACAATGAGATGGCCTTGTTG
N668298	SALK_055063	ATTGCTGTTATGGCCACAGAC	CATTTCATTAATGGCTCGCTC

Table 3 Continued.

N533489	SALK_033489	CATTTCATTAATGGCTCGCTC	AAGGAACAATTGCCCTACCAC
N628725	SALK_128725	AAAGAAAGACCGGTCGTAGTTTC	CGGCCACGATTACGAATAAAC
N653755	SALK_136642	ATCTTCAGGTGTGGACACTGC	CAGCTCCTTCCATAGCCATAAC
N654518	SALK_015253	TTGCTACATCCAACAAGGGAC	GAGGCAGCCATTATTGTTCTG
N680289	SALK_132644	TGTACACATTTATCCTCCGCC	TGTCAAACTGGTGTGACCATG
N681945	SALK_005910	CGGGCTTCACTGAACATATTC	AAAACTTTGCTTCAATGGGTG
N593764	SALK_093764	CCTGATTACATCAGCGAGCTC	CACCCATCTATTTAGGCGGAC
N653018	SALK_009683	GGGCTTTGGTTTAAAGTCTG	AAGGTTGAACCAATAGCATTGAC
N650477	SALK_150477	TGCGTGTAAGGGTTTTTAACAG	TGAAACCCGTAATTGAAGACG

In the Table are reported the NASD ID numbers, together with the SALK numbers, of all the T-DNA lines obtained from NASC and used in the project. The right primer (RP) and left primer (LP) sequences for each line are given (5' → 3'). The T-DNA primer (LBb1.3) sequence used was ATTTTGCCGATTTCGGAAC.

References

Agrawal, G. K., Jwa, N.-S., Lebrun, M.-H., Job, D. & Rakwal, R. (2010) Plant secretome: Unlocking secrets of the secreted proteins. *Proteomics*, 10, 1-29.

Allen, T. W., Martinez, A. & Burpee, L. L. (2004) *Pythium* blight of turfgrass. *The Plant Health Instructor*, DOI;10.1094/PHI-I-2004-0929-01.

Alonso, J. M., Stepanova, A. N., Leisse, T. J., Kim, C. J., Chen, H., Shinn, P., Stevenson, D. K., Zimmerman, J., Barajas, P., Cheuk, R., Gadrinab, C., Heller, C., Jeske, A., Koesema, E., Meyers, C. C., Parker, H., Prednis, L., Ansari, Y., Choy, N., Deen, H., Geralt, M., Hazari, N., Hom, E., Karnes, M., Mulholland, C., Ndubaku, R., Schimdt, I., Guzman, P., Aguilar-Henonin, L., Schmid, M., Weigel, D., Carter, D. E., Marchand, T., Risseeuw, E., Brodgen, D., Zeko, A., Crosby, W. L., Berry, C. C. & Ecker, J. R. (2003) Genome-wide insertional mutagenesis of *Arabidopsis thaliana*. *Science*, 301, 653-657.

Asai, S. & Shirasu, K. (2015) Plant cells under siege: plant immune system versus pathogen effectors. *Current Opinion in Plant Biology*, 28, 1-8.

Bailey, K., Çevik, V., Holton, N., Byrne-Richardson, J., Sohn, K. H., Coates, M., Woods-Tör, A., Aksoy, H. M., Hughes, L., Baxter, L., Jones, J. D. G., Beynon, J., Holub, E. B. & Tör, M. (2011) Molecular cloning of ATR5[Emoy2] from *Hyaloperonospora arabidopsidis*, an avirulence determinant that triggers RPP5-mediated defense in *Arabidopsis*. *Molecular Plant-Microbe Interactions*, 24 (7), 827-838.

Bajorath, J., Saenger, W. & Pal, G. P. (1988) Autolysis and inhibition of proteinase k, a subtilisin-related serine proteinase isolated from the fungus *Tritirachium album* Limber. *Biochimica et Biophysica Acta*, 954 (2), 176-182.

Bauer, Z., Gómez-Gómez, L., Boller, T. & Felix, G. (2001) Sensitivity of different ecotypes and mutants of *Arabidopsis thaliana* toward the bacterial elicitor flagellin correlates with the presence of receptor-binding sites. *The Journal of Biological Chemistry*, 276 (49), 45669-45676.

Baxter, L., Tripathy, S., Ishaque, N., Boot, N., Cabral, A., Kemen, E., Thines, M., Ah-Fong, A., Anderson, R., Badejoko, W., Bittner-Eddy, P., Boore, J. L., Chibucos, M. C., Coates, M., Dehal, P., Delehaunty, K., Dong, S., Downton, P., Dumas, B., Fabro, G., Fronick, C., Fuestenberg, S. I., Fulton, L., Gaulin, E., Govers, F., Hughes, L., Humphray, S., Jiang, R. H. Y., Judelson, H., Kamoun, S., Kyung, K., Meijer, H., Minx, P., Morris, P., Nelson, J., Phuntumart, V., Qutob, D., Rehmany, A., Rougon-Cardoso, A., Ryden, P., Torto-Alalibo, T., Studholme, D., Wang, Y., Win, J., Wood, J., Clifton, S. W., Rogers, J., Van den Ackerveken, G., Jones, J. D. G., McDowell, J. M., Beynon, J. & Tyler, B. (2010) Signatures of adaptation to obligate biotrophy in the *Hyaloperonospora arabidopsidis* genome. *Science*, 330, 1549-1551.

Beddington, J. (2010) Food security: contributions from science to a new and greener revolution. *Philosophical Transactions of the royal Society B*, 365, 61-71.

Belkhadir, Y., Yang, L., Hetzel, J., Dangl, J. L. & Chory, J. (2014) The growth-defense pivot: crisis management in plants mediated by LRR-RK surface receptors. *Trends in Biochemical Sciences*, 39 (10), 447-456.

Betiku, E. (2006) Molecular chaperones involved in heterologous protein folding in *Escherichia coli*. *Biotechnology and Molecular Biology Review*, 1 (2), 66-75.

Bohm, H., Albert, I., Oome, S., Raaymakers, T. M., Van den Ackerveken, G. & Nürnberger, T. (2014) A conserved peptide pattern from a widespread microbial virulence factor triggers pattern-induced immunity in *Arabidopsis*. *PLOS Pathogens*, 10 (11), 1-11.

Boller, T. & Felix, G. (2009) A renaissance of elicitors: perception of microbe-associated molecular patterns and danger signals by pattern-recognition receptors. *Annual Review of Plant Biology*, 60, 379-406.

Bolwell, G. P., Bindschedler, L. V., Blee, K. A., Butt, V. S., Davies, D. R., Gardner, S. L., Gerrish, C. & Minibayeva, F. (2001) The apoplastic burst in response to biotic stress in plants: a three-component system. *Journal of Experimental Botany*, 53 (372), 1367-1376.

Boraston, A. B., Bolam, D. N., Gilbert, H. J. & Davies, G. J. (2004) Carbohydrate-binding modules: fine-tuning polysaccharide recognition. *Biochemical Journal*, 382, 769-781.

Botella, M. A., Parker, J. E., Frost, L. N., Bittner-Eddy, P. D., Beynon, J. L., Daniels, M. J., Holub, E. B. & Jones, J. D. G. (1998) Three genes of the *Arabidopsis RPP*1 complex resistance locus recognize distinct *Peronospora parasitica* avirulence determinants. *The Plant Cell*, 10, 1847-1860.

Bouché, N. & Bouchez, D. (2001) *Arabidopsis* gene knockout: phenotypes wanted. *Current Opinion in Plant Biology*, 4, 111-117.

Boyd, L. A., Ridout, C., O'Sullivan, D. M., Leach, J. E. & Leung, H. (2013) Plant-pathogen interactions: disease resistance in modern agriculture. *Trends in Genetics*, 29 (4), 233-240.

Bruce, T. J. A. (2012) GM as a route for delivery of sustainable crop protection. *Journal of Experimental Botany*, 63 (2), 537-541.

Brunner, F., Rosahl, S., Lee, J., Rudd, J. J., Geiler, C., Kauppinen, S., Rasmussen, G., Scheel, D. & Nürnberger, T. (2002) Pep-13, a plant defense-inducing pathogen-associated pattern from *Phytophthora* transglutaminases. *The EMBO Journal*, 21 (24), 6681-6688.

Cabral, A., Oome, S., Sander, N., Küfner, I., Nürnberger, T. & Van den Ackerveken, G. (2012) Nontoxic Nep1-like proteins of the downy mildew pathogen *Hyaloperonospora arabidopsidis*: repression of necrosis-inducing activity by a surface-exposed region. *Molecular Plant-Microbe Interactions*, 25 (5), 697-708.

Carbohydrate-Active Enzyme Database (CAZY): http://www.cazy.org/.

Carris, L. M., Little, C. R. & Stiles, C. M. (2012) Introduction to fungi. *The Plant Health Instructor*, DOI: 10.1094/PHI-I-2012-0426-01.

Carvalho Ade, O. & Gomes, V. M. (2011) Plant defensins and defensin-like peptides – biological activities and biotechnological applications. *Current Pharmaceutical Design*, 17 (38), 4270-4293.

Chakraborty, S. & Newton, A.C. (2011) Climate change, plant diseases and food security: an overview. *Plant Pathology*, 60, 2-14.

Cheong, J. J. & Hahn, M. G. (1991) A specific, high-affinity binding-site for the hepta-beta-glucoside elicitor exists in soybean membranes. *Plant Cell*, 3, 137-147.

Chinchilla, D., Zipfel, C., Robatzek, S., Kemmerling, B., Nürnberger, T., Jones, J. D., Felix, G. & Boller, T. (2007) A flagellin-induced complex of the receptor FLS2 and BAK1 initiates plant defence. *Nature*, 448, 497-500.

Chinchilla, D., Shan, L., He, P., de Vries, S. & Kemmerling, B. (2009) One for all: the receptor-associated kinase *BAK1*. *Trends in Plant Science*, 14 (10), 535-541.

Cho, E. J., Yuen, C. Y. L., Kang, B.-H., Ondzighi, C. A., Staehelin, L. A. & Christopher, D. A. (2011) Protein disulphide isomerase-2 of *Arabidopsis* mediates protein folding and localizes to both the secretory pathway and nucleus, where it interacts with maternal effect embryo arrest factor. *Molecules and Cells*, 32, 459-475.

Christensen, A., Svensson, K., Thelin, L., Zhang, W., Tintor, N., Prins, D., Funke, N., Michalak, M., Schulze-Lefert, P., Saijo, Y., Sommarin, M., Widell, S. & Persson, S. (2010) Higher plants calreticulins have acquired specialized functions in *Arabidopsis*. *PLOS One*, 5 (6), 1-18.

Coates, M. E. & Beynon, J. L. (2010) *Hyaloperonospora arabidopsidis* as a pathogen model. *Annual Review of Phytopathology*, 48, 329-345.

Cosio, C. & Dunand, C. (2009) Specific functions of individual class III peroxidase genes. *Journal of Experimental Botany*, 60 (2), 391-408.

Costantinescu, O. & Fatehi, J. (2002) *Peronospora*-like fingi (Chromista, Peronosporales) parasitic on Brassicaceae and related hosts. *Nova Hedwigia*, 74, 291-338.

Daudi, A., Cheng, Z., O'Brien, J. A., Mammarella, N., Khan, S., Ausubel, F. M. & Bolwell, G. P. (2012) The apoplastic oxidative burst peroxidase in *Arabidopsis* is a major component of pattern-triggered immunity. *The Plant Cell*, 24, 275-287.

Dawson, W. O., Garnsey, S. M., Tatineni, S., Folimonova, S. Y., Harper, S. J. & Gowda, S. (2013) Citrus tristeza virus-host interactions. *Frontiers in Microbiology*, 4 (88), 1-10.

Dean, R., Van Kan, J. A. L., Pretorius, Z. A., Hammond-Kosack, K. E., Di Pietro, A., Spanu, P. D., Rudd, J. J., Dickman, M., Kahmann, R., Ellis, J. & Foster, G. D. (2012) The top 10 fungal pathogens in molecular plant pathology. *Molecular Plant Pathology*, 13 (4), 414-430.

Decraemer, W. & Hunt, D. J. (2006) Structure and classification. In: Perry, R. N. & Moens, M., (eds.) *Plant Nematology*. Wallingford, Oxfordshire: CAB International, pp. 3-32.

Delaunois, B., Jeandet, P., Clément, C., Baillieul, F., Dorey, S. & Cordelier, S. (2014) Uncovering plant-pathogen crosstalk through apoplastic proteomic studies. *Frontiers in Plant Science*, 5 (249), 1-18.

Dodds, P.N. & Rathjen, J. P. (2010) Plant immunity: towards an integrated view of plant-pathogen interactions. *Nature Reviews Genetics*, 11, 539-548.

Doehlemann, G. & Hemetsberger, C. (2013) Apoplastic immunity and its suppression by filamentous plant pathogens. *New Phytologist*, 1-16.

Earley, K. W., Haag, J. R., Pontes, O., Opper, K., Juehne, T., Song, K. & Pikaard, C. S. (2006) Gateway-compatible vectors for plant functional genomics and proteomics. *The Plant Journal*, 45 (4), 616-629.

Ebeling, W., Hennrich, N., Klockow, M., Metz, H., Orth, H. D. & Lang, H. (1974) Proteinase K from *Tritirachium album* Limber. *European Journal of Biochemistry*, 47, 91-97.

Ellinger, D. & Voigt, C. A. (2014) Callose biosynthesis in *Arabidopsis* with a focus on pathogen response: what we have learned within the last decade. *Annals of Botany*, 1-10.

Erwin, D. C. & Ribeiro, O. K. (1996) *Phytophthora* diseases worldwide. St Paul, MN: *American Phytopathological Society*.

Fabro, G., Steinbrenner, J., Coates, M., Ishaque, N., Baxter, L., Studholme, D. J., Körner, E., Allen, R. L., Piquerez, S. J. M., Rougon-Cardoso, A., Greenshield, D., Lei, R., Badel, J. L., Caillaud, M. C., Sohn, K. H., Van der Ackerveken, G., Parker, J. E., Beynon, J. & Jones, J. D. G. (2011) Multiple candidate effectors from the oomycete pathogen *Hyaloperonospora arabidopsidis* suppress plant immunity. *PLoS Pathogens*, 7 (11), e1002348.

Felix, G., Duran, J. D., Volko, S. & Boller, T. (1999) Plants have a sensitive perception system for the most conserved domain of bacterial flagellin. *The Plant Journal*, 18 (3), 265-276.

Fey, S. J. & Larsen, P. M. (2001) 2D or not 2D. *Current Opinion in Chemical Biology*, 5, 26-33.

Figueiredo, A., Monteiro, F. & Sebastiana, M. (2014) Subtilisin-like proteases in plant-pathogen recognition and immune priming: a perspective. *Frontiers in Plant Science*, 5 (739), 1-5.

Flood, J. (2010) The importance of plant health to food security. *Food Security*, 2, 215-231.

Food and Agriculture Organization of the United Nations (FAO). (2003) Trade reforms and food security. conceptualizing the linkages. Rome (Italy).

Food and Agriculture Organization of the United Nations (FAO). (2011) Climate change, water and food security. Rome (Italy).

Forestry Images: http://www.forestryimages.org; http://www.bugwood.org

Gabor, B. K., O'Gara, E. T., Philip, B. A., Horan, D. P. & Hardham, A. R. (1993) Specificities of monoclonal antibodies to *Phytophthora cinnamoni* in two rapid diagnostic assays. *Plant Disease,* 77 (12), 1189-1197.

Gaulin, E., Jauneau, A., Villalba, F., Rickauer, M., Esquerré-Tugayé, M.-T. & Bottin, A. (2002) The CBEL glycoprotein of *Phytophthora parasitica* var. *nicotianae* is involved in cell wall deposition and adhesion to cellulosic substrates. *Journal of Cell Science*, 115, 4565-4575.

Gaulin, E., Dramé, N., Lafitte, C., Torto-Alalibo, T., Martinez, Y., Ameline-Torregrosa, C., Khatib, M., Mazarguil, H., Villalba-Mateos, F., Kamoun, S., Mazars, C., Dumas, B., Bottin, A., Esquerré-Tugayé, M.-T. & Rickauer, M. (2006) Cellulose binding domains of a Phytophthora cell wall protein are novel pathogen-associated molecular patterns. *The Plant Cell*, 18, 1766-1777.

Gómez-Gómez, L., Felix, G. & Boller, T. (1999) A single locus determines sensitivity to bacterial flagellin in *Arabidopsis thaliana. The Plant Journal*, 18, 277-284.

Gómez-Gómez, L. & Boller, T. (2000) FLS2: an LRR receptor-like kinase involved in the perception of the bacterial elicitor flagellin in *Arabidopsis. Molecular Cell*, 5, 1003-1011.

Gonzáles-Fernández, R., Prats, E. & Jorrín-Novo, J. V. (2010) Proteomics of plant pathogenic fungi. *Journal of Biomedicine and Biotechnology*, 2010 (932527), 1-37.

Goritschnig, S., Krasileva, K. V., Dhalbeck, D. & Staskawicz, B. J. (2012) Computational prediction and molecular characterization of an oomycete effector and the cognate *Arabidopsis* resistance gene. *PLOS Genetics*, 8 (2), 1-12.

Greeff, C., Roux, M., Mundy, J. & Petersen, M. (2012) Receptor-like kinase complexes in plant innate immunity. *Frontiers in Plant Science*, 3, 1-7.

Gregory, P.J., Johnson, S. N., Newton, A. C. & Ingram, S. I. (2009) Integrating pests and pathogens into the climate change/food security debate. *Journal of Experimental Botany*, 60 (10), 2827-2838.

Guest, D. & Brown, J. (1997) Infection processes. In: Brown, J. F. & Ogle, H. J. (eds.) *Plant Pathogens and Plant Diseases*, Rockvale Publications, 245-262.

Gupta, R., Eui Lee, S., Agrawal, G. K., Rakwal, R., Park, S., Wang, Y. & Kim, S. T. (2015) Understanding the plant-pathogen interactions in the context of proteomic-generated apoplastic proteins inventory. *Frontiers in Plant Science*, 6 (352), 1-7.

Gust, A. A. & Felix, G. (2014) Receptor like proteins associate with *SOBIR1*-type of adaptors to form bimolecular receptor kinases. *Current Opinion in Plant Biology*, 21, 104-111.

Hammerschmidt, R. (2010) The dynamic apoplast. *Physiological and Molecular Plant Pathology*, 74, 199-200.

Hardham, A. R. (2007) Cell biology of plant-oomycete interactions. *Cellular Microbiology*, 9 (1), 31-39.

Hee, K. & Li, J. (2002) BRI1/BAK1, a receptor kinase pair mediating brassinosteroid signaling. *Cell*, 110, 203-212.

Henry, G., Thonart, P. & Ongena, M. (2012) PAMPs, MAMPs, DAMPs and others: an update on the diversity of plant immunity elicitors. *Biotechnology, Agronomy, Society and Environment*, 16 (2), 257-268.

Herman, M. & Williams, M. (2012) Fighting for their lives: plants and pathogens. *The Plant Cell*, 24, 1-15.

Holub, E. B (2008) Natural history of *Arabidopsis thaliana* and oomycete symbioses. *European Journal of Plant Pathology*, 122, 91-109.

Holub, E. B., Beynon, J. L. & Crute, I. R. (1994) Phenotypic and genotypic characterization of interactions between isolates of *Peronospora parasitica* and accessions of *Arabidopsis thaliana*. *Molecular Plant-Microbe Interactions,* 7, 223-239.

Hoorn, R. A. L. & Kamoun, S. (2008) From guard to decoy: a new model for perception of plant pathogen effectors. *Plant Cell*, 20, 2009-2017.

Howden, A. J. M. & Huitema, E. (2012) Effector-triggered post-translational modifications and their role in suppression of plant immunity. *Frontiers in Plant Science*, 3 (160), 1-6.

Hu, X. & Reddy, A. S. N. (1997) Cloning and expression of a PR5-like protein from *Arabidopsis*: inhibition of fungal growth by bacterially expressed protein. *Plant Molecular Biology*, 34, 949-959.

Huang, H.-J., Evans, N., Li, Z.-Q., Eckert, M., Chevre, A.-M., Renard, M. & Fitt, B. D. (2006) Temperature and leaf wetness duration affect phenotypic expression of Rlm6-mediated resistance to *Leptosphaeria maculans* in *Brassica napus*. *New Phytologist*, 170, 129-141.

Hulvey, J. P., Padgett, D. E. & Bailey, J. C. (2007) Species boundaries within *Saprolegnia* (Saprolegniales, Oomycota) based on morphological and DNA sequence data. *Mycologia*, 99 (3), 421-429.

Ingle, R. A., Carstens, M. & Denby, K. J. (2006) PAMP recognition and the plant-pathogen arms race. *BioEssays*, 28, 880-889.

Jones, D. G. & Dangl, J. L. (2006) The Plant immune system. *Nature*, 444, 323-329.

Jones, J. T., Haegeman, A., Danchin, E. G. J., Gaur, H. S., Helder, J., Jones, M. G. K., Kikuchi, T., Manzanilla-López, R., Palomares-Rius, J. E., Wesemael, W. M. L. & Perry, R. N. (2013) Top 10 plant-parasitic nematodes in molecular plant pathology. *Molecular Plant Pathology*, 14 (9), 946-961.

Kamoun, S., van West, P., de Jong, A. J., de Groot, K. E., Vleeshouwers, V. G. A. A. & Govers, F. (1997) A gene encoding a protein elicitor of *Phytophthora infestans* is down-regulated during infection of potato. *Molecular Plant-Microbe Interactions*, 10 (1), 13-20.

Kamoun, S. (2003) Molecular genetics of pathogenic oomycetes. *Eukaryotic Cell*, 2 (2), 191-199.

Kamoun, S., Furzer, O., Jones, J. D. G., Judelson, H. S., Ali, G. S., Dalio, R. J. D., Roy, S. G., Schena, L., Zambounis, A., Panabières, F., Cahill, D., Ruocco, M., Figueiredo, A., Chen, X.-R., Hulvey, J., Stam, R., Lamour, K., Gijzen, M., Tyler, B. M., Grünwald, N. J., Mukhtar, M. S., Tomé, D. F. A., Tör, M., Van der Ackerveken, G., McDowell, J., Daayf, F., Fry, W. E., Lindqvist-Kreuze, H., Meijer, H. J. G., Petre, B., Ristaino, J., Yoshida, K., Birch, P. R. J. & Govers, F.

(2015) The Top 10 oomycete pathogens in molecular plant pathology. *Molecular Plant Pathology*, 16 (4), 413-434.

Kawamura, Y., Hase, S., Takenaka, S., Kanayama, Y., Yoshioka, H., Kamoun, S. & Takahashi, H. (2008) INF1 elicitin activates jasmonic acid- and ethylene-mediated signalling pathways and induces resistance to bacterial wilt disease in tomato. *Journal of Phytopathology*, 157 (5), 287-297.

Khatib, M., Lafitte, C., Esquerré-Tugayé, M.-T., Bottin, A. & Rickauer, M. (2004) The CBEL elicitor of *Phytophthora parasitica* var. *nicotianae* activates defence in *Arabidopsis thaliana* via three different signaling pathways. *New Phytologist*, 162, 501-510.

Koch, E. & Slusarenko, A. (1990) *Arabidopsis* is susceptible to infection by a downy mildew fungus. *The Plant Cell*, 2, 437-445.

Koornneef, M. & Meinke, D. (2010) The development of *Arabidopsis* as a model plant. *The Plant Journal*, 61, 909-921.

Koressaar, T. & Remm, M. (2007) Enhancements and modifications of primer design program Primer3. *Bioinformatics*, 23 (10), 1289-91.

Krasileva, K. V., Zheng, C., Leonelli, L., Gorischnig, S., Dahlbeck, D. & Staskavicz, B. J. (2011) Global analysis of *Arabidopsis*/downy mildew interactions reveals prevalence of incomplete resistance and rapid evolution of pathogen recognition. *PLOS One*, 6 (12), 1-11.

Krysan, P. J., Young, J. C. & Sussman, M. R. (1999) T-DNA as an insertional mutagen in *Arabidopsis*. *The Plant Cell*, 11, 2283-2290.

Kunze, G., Zipfel, C., Robatzek, S., Niehaus, K., Boller, T. & Felix, G. (2004) The N terminus of bacterial elongation factor Tu elicits innate immunity in *Arabidopsis* plants. *Plant Cell*, 16, -3496-3507.

Laemmli, U. K. (1970) Cleavage of structural proteins during the assembly of the head of bacteriophage T4. *Nature*, 227, 680-685.

Larroque, M., Barriot, R., Bottin, A., Barre, A., Rougé, P., Dumas, B. & Gaulin, E. (2012) The unique architecture and function of cellulose-interacting proteins in oomycetes revealed by genomic and structural analyses. *BMC Genomics*, 13 (605), 1-15.

Letunic, I., Doerks, T. & Bork, P. (2012) SMART7: recent updates to the protein domain annotation resource. *Nucleic Acids Research*, doi:10.1093/nar/gkr931.

Li, J., Wen, J., Lease, K. A., Doke, J. T., Tax, F. E. & Walker, J. C. (2002) BAK1, an *Arabidopsis* LRR receptor-like protein kinase, interacts with BRI1 and modulates brassinosteroid signaling. *Cell*, 110, 213-222.

Liebrand, T. W. H., van de Burg, H. A. & Joosten, M. H. A. J. (2013) Two for all: receptor-associated kinases *SOBIR1* and *BAK1*. *Trends in Plant Science*, 20, 1-10.

Linder, M., Mattinen, M.-L., Kontteli, M., Lindeberg, G., Ståhlberg, J., Brakenberg, T., Reinikainen, T., Pettersson, G. & Annila, A. (1995) Identification of functionally important amino acids in the cellulose-binding domain of *Trichoderma reesei* cellobiohydrolase I. *Protein Science*, 4, 1056-1064.

Liu, H., Wang, X., Zhang, H., Yang, Y., Ge, X. & Song, F. (2008) A rice serine carboxypeptidase-like gene OsBISCPL1 is involved in regulation of defence responses against biotic and oxidative stress. *Gene*, 420 (1), 57-65.

Lloyd, S. R., Schoonbeek, H., Trick, M., Zipfel, C. & Ridout, J. (2014) Methods to study PAMP-triggered immunity in *Brassica* species. *Molecular Plant-Microbe Interactions*, 27 (3), 286-295.

Lombard, V., Golaconda Ramulu, H., Drula, E., Coutinho, P. M. & Henrissat, B. (2014) The Carbohydrate-active enzymes database (CAZy) in 2013. *Nucleic Acids Research*, 42, 490-495.

Lozano-Durán, R. & Zipfel, C. (2015) Trade-off between growth and immunity: role of brassinosteroids. *Trends in Plant Science*, 20 (1), 12-19.

Lucas, J., Hayter, J. & Crute, I. (1995) the downy mildews: host specificity and pathogenesis. In: Singh, U. & Singh, R. (eds.) *Pathogenesis and host specificity in plant diseases*, Oxford, UK, 217-234.

Luna, E., Pastor, V., Robert, J., Flors, V., Mauch-Mani, B. & Ton, J. (2011) Callose deposition: a multifaceted plant defense response. *Molecular Plant-Microbe Interactions*, 24 (2), 183-193.

Ma, Z., Song, T., Zhu, L., Ye, W., Wang, Y., Shao, Y., Dong, S., Zhang, Z., Dou, D., Zheng, X., Tyler, B. M. & Wang, Y. (2015) A *Phytophthora sojae* glycoside hydrolase 12 protein is a major virulence factor during soybean infection and is recognized as a PAMP. *The Plant Cell*, 27, 2057-2072.

Mansfield, J., Genin, S., Magori, S., Citovsky, V., Sriariyanum, M., Ronald, P., Dow, M., Verdier, V., Beer, S. V., Machado, M. A., Toth, I., Salmond, G. & Foster, G. D. (2012) Top 10 plant pathogenic bacteria in molecular plant pathology. *Molecular Plant Pathology*, 13 (6), 614-629.

Martínez-Maqueda, D., Hernández-Ledesma, B., Amigo, L., Miralles, B. & Gómez-Ruiz, J. Á. (2013) Extraction/fractionation techniques for proteins and peptides and protein digestion. In: Toldrá, F. & Nollet, L. M. L. (eds) *Proteomics in foods: principles and applications*. Springer, New York, 21-50.

Mattinen, M.-L., Linder, M., Drakenberg, T. & Annila, A. (1998) Solution structure of the cellulose-binding domain of endoglucanase I from *Trichoderma reesei* and its interaction with cello-oligosaccharides. *European Journal of Biochemistry*, 256, 279-286.

Mazzotta, S. & Kemmerling, B. (2011) Pattern recognition in plant innate immunity. *Journal of Plant Pathology*, 93 (1), 7-17.

Mélida, H., Sandoval-Sierra, J. V., Diéguez-Uribeondo, J. & Bulone, V. (2012) Analyses of extracellular carbohydrates in oomycetes unveil the existence of three different cell wall types. *Eukaryotic Cell*, 12 (2), 194-203.

Melotto, M., Underwood, W., Koczan, J., Nomura, K., He, S. Y. (2006) Plant stomata function in innate immunity against bacterial invasion. *Cell*, 126, 969-980.

Monaghan, J. & Zipfel, C. (2012) Plant pattern recognition receptor complexes at the plasma membrane. *Current Opinion in Plant Biology*, 15, 349-357.

Moreno, P., Ambrós, S., Albiach-Martí, M. R., Guerri, J. & Peña, L. (2008) *Citrus tristeza virus*: a pathogen that changed the course of the citrus industry. *Molecular Plant Pathology*, 9 (2), 251-268.

Mott, G. A., Middleton, M. A., Desveaux, D. & Guttman, D. S. (2014) Peptides and small molecules of the plant-pathogen apoplastic arena. *Frontiers in Plant Science*, 5 (677), 1-12.

Muthamilarasan, M. & Prasad, M. (2013) Plant innate immunity: an updated insight into defense mechanism. *Journal of Biosciences*, 38 (2), 1-17.

Nemri, A., Atwell, S., Tarone, A. M., Huang, Y. S., Zhao, K., Studholme, D. J., Nordborg, M. & Jones, J. D. (2010) Genome-wide survey of *Arabidopsis* natural

variation in downy mildew resistance using combined association and linkage mapping. *Proceeding of the Nation Academy of Science*, 107 (22), 10302-10307.

Nguyen, H. P., Chakravarthy, S., Velásquez, A. C., McLane, H. L., Zeng, L., Nakayashiki, H., Park, D., Collmer, A. & Martin, G. B. (2010) Methods to study PAMP-triggered immunity using tomato and *Nicotiana benthamiana*. *Molecular Plant-Microbe Interactions,* 23 (8), 991-999.

Nühse, T. S. (2012) Cell wall integrity signaling and innate immunity in plants. *Frontiers in Plant Science*, 3 (280), 1-5.

Nürnberger, T., Nennstiel, D., Jabs, T., Sacks, W. R., Hahlbrock, K. & Scheel, D. (1994) High affinity binding of a fungal oligopeptide elicitor to parley plasma membranes triggers multiple defense responses. *Cell*, 78, 449-460.

Nürnberger, T., Brunner, F., Kemmerling, B. & Piater, L. (2004) Innate immunity in plants and animals: striking similarities and obvious differences. *Immunological Reviews*, 198, 249-266.

O'Brien, J. A., Daudi, A., Finch, P., Butt, V. S., Whitelegge, J. P., Souda, P., Ausubel, F. M. & Bolwell, G. P. (2012) A peroxidase-dependent apoplastic burst in cultured *Arabidopsis* cells functions in MAMP-elicited defence. *Plant Physiology*, 158, 2013-2027.

Ondzighi, C. A., Christopher, D. A., Cho, E. J., Chang, S.-C. & Staehelin, L. A. (2008) *Arabidopsis* protein disulphide isomerase-5 inhibits cysteine proteases during trafficking to vacuoles before programmed cell death of the endothelium in developing seeds. *The Plant Cell*, 20, 2205-2220.

Oome, S., Raaymakers, T. M., Cabral, A., Samwel, S., Böhm, H., Albert, I., Nürnberger, T. & Van den Ackerveken, G. (2014) Nep1-like proteins from three kingdoms of life act as a microbe-associated molecular pattern in *Arabidopsis*. *Proceedings of the National Academy of Sciences*, 111 (47), 16955-16960.

Parker, J. E., Holub, E. B., Frost, L. N., Falk, A., Gunn, N. D. & Daniels, M. S. (1996) Characterization of *eds1*, a mutation in *Arabidopsis* suppressing resistance to *Peronospora parasitica* specified by several different *RPP* genes. *Plant Cell,* 8, 2033-2046.

Pautasso, M., Döring, T. F., Garbelotto, M., Pellis, L. & Jeger, M. J. (2012) Impacts of climate change on plant diseases-opinions and trends. *European Journal of Plant Pathology*, DOI 10.1007/s10658-012-993-1.

Pelegrini, P. B. & Franco, O. L. (2005) Plant γ-thionins: novel insights on the mechanism of action of a multi-functional class of defense proteins. *The International Journal of Biochemistry & Cell Biology*, 37, 2239-2253.

Penn, C. W. & Luke, C. J. (1992) Bacterial flagellar diversity and significance in pathogenesis. *FEMS Microbiology Letters*, 79, 331-336.

Petre, B., Major, I., Rouhier, N. & Duplessis, S. (2011) Genome-wide analysis of eukaryote thaumatin-like proteins (TLPs) with an enphasis on poplar. *BMC Plant Biology*, 11 (33), 1-16.

Prigneau, O., Achbarou, A., Bouladoux, N, Mazier, D. & Desportes-Livage, I. (2000) Identification of proteins in *Encephalitozoon intestinalis*, a microsporidian pathogen of immunocompromised humans: an immunoblotting and immunocytochemical study. *Journal of Eukaryotic Microbiology,* 47, 48-56.

Qi, A. & Fitt, B. (2014) Can crop disease control cope with climate change? *Outlooks on Pest Management*, DOI:10.1564/v25_dec_05. www.pestoutlook.com

Qiu, Y., Xi, J., Du, L., Roje, S. & Poovaiah, B. W. (2012) A dual regulatory role of *Arabidopsis* calreticulin-2 in plant innate immunity. *The Plant Journal*, 69, 489-500.

Ramírez, V., López, A., Mauch-Mani, B., Gil, M. J. & Vera, P. (2013) An extracellular subtilase switch for immune priming in *Arabidopsis*. *PLOS Pathogens*, 9 (6), 1-15.

Rehmany, A. P., Gordon, A., Rose, L. E., Allen, R. L., Armstrong, M. R., Whisson, S. C., Kamoun, S., Tyler, B. M., Birch, P. R. J. & Beynon, J. L. (2005) Differential recognition of highly divergent downy mildew avirulence gene alleles by *RPP1* resistance genes from two *Arabidopsis* lines. *The Plant Cell*, 17, 1839-1850.

Rentel, M. C., Leonelli, L., Dahlbeck, D., Zhao, B. & Staskawicz, B. J. (2008) Recognition of the *Hyaloperonospora parasitica* effector ATR13 triggers resistance against oomycete, bacterial, and viral pathogens. *Proceedings of the National Academy of Science*, 105 (3), 1-6.

Riethmüller, A., Voglmayr, H., Göker, M. Weiβ, M. & Oberwinkler, F. (2002) Phylogenetic relationships of the downy mildews (Peronosporales) and related groups based on nuclear large subunit ribosomal DNA sequences. *Mycologia*, 94 (5), 834-849.

Robinson, S. M. & Bostock, R. M. (2015) β-glucans and eicosapolyenoic acids as MAMPs in plant-oomycete interactions: past and present. *Frontiers in Plant Science*, 5 (797), 1-10.

Rosano, G. L. & Ceccarelli E. A. (2014) Recombinant protein expression in *Escherichia coli*: advances and challenges. *Frontiers in Microbiology*, 5 (174), 1-17.

Roux, M., Schwessinger, B., Albrecht, C., Chinchilla, D., Jones, A., Holton, N., Malinovsky, F., G., Tör, M., de Vries, S. & Zipfel, C. (2011) The *Arabidopsis* leucine-rich repeat receptor-like kinases BAK1/SERK3 and BKK1/SERK4 are required for innate immunity to hemibiotrophic and biotrophic pathogens. *The Plant Cell*, 23, 2440-2455.

Saharan, G. S., Verma, P. R., Meena, P. D. & Kumar, A. (2014) White rust of Crucifers: ecology and management. Springer India, 1-6.

Schneider, C. A., Rasband, W. S. & Eliceiri, K. W. (2012) NIH Image to ImageJ: 25 years of image analysis. *Nature Methods*, 9, 671-675.

Scholthof, K.-B. G., Adkins, S., Czosnek, H., Palukaitis, P., Jacquot, E., Hohn, T., Hohn, B., Saunders, K., Candresse, T., Ahlquist, P., Hemenway, C. & Foster, G. D. (2011) Top 10 plant viruses in molecular plant pathology. *Molecular Plant Pathology*, 12 (9), 938-954.

Schornack, S., Huitema, E., Cano, L. M., Bozkurt, T. O., Oliva, R., Van Damme, M., Schwizer, S., Raffaele, S., Chaparro-Garcia, A., Farrer, R., Segretin, M. E., Bos, J., Haas, B. J., Zody, M. C., Nusbaum, C., Win, J., Thines, M. & Kamoun, S. (2009) Ten things to know about oomycete effectors. *Molecular Plant Pathology*, 10 (6), 795-803.

Schultz, J., Milpetz, F., Bork, P. & Ponting, C. P. (1998) SMART, a simple modular architecture research tool: identification of signaling domains. *Proceedings of the National Academy of Sciences*, 95, 5857-5864.

Schwessinger, B., Roux, M., Kadota, Y., Ntoukakis, V., Sklenar, J., Jones, A. M. & Zipfel, C. (2011) Phosphorylation-dependent differential regulation of plant growth, cell death, and innate immunity by the regulatory receptor-like kinase BAK1. *PLoS Genetics*, 7 (4), e1002046.

Séjalon, N., Villalba, F., Bottin, A., Rickauer, M., Dargent, R., & Esquerré-Tugayé, M. T. (1995) Characterization of a cell-surface antigen isolated from the plant pathogen *Phytophthora parasitica* var. *nicotianae*. *Canadian Journal of Botany*, 73 (1), 1104-1108.

Séjalon-Delmas, N., Villalba Mateos, F., Bottin, A., Rickauer, M., Dargent, R. & Esquerré-Tugayé, M. T. (1997) Purification, elicitor activity, and cell wall localization of a glycoprotein from *Phytophthora parasitica* var. *nicotianae*, a fungal pathogen of tobacco. *Phytopathology*, 87, 9, 899-909.

Sigrist, C. J. A., de Castro, E., Cerutti, L., Cuche, B. A., Hulo, N., Bridge, A., Bougueleret, L. & Xenarios, I. (2012) New and continuing development at PROSITE. *Nucleic Acids Research*, doi:10.1093/nar/gks1067, 1-4.

Sinapidou, E., Williams, K., Bahkt, S., Tör, M., Crute, I., Bittner-Eddy, P. & Beynon, J. (2004) Two TIR:NB:LRR genes are required to specify resistance to *Peronospora parasitica* isolate Cala2 in *Arabidopsis*. *The Plant Journal*, 38 (6), 898-909.

Slusarenko, A. J. & Schlaich, N. L. (2003) Downy mildew of *Arabidopsis thaliana* caused by *Hyaloperonospora parasitica* (formerly *Peronospora parasitica*). *Molecular Plant Pathology*, 4 (3), 159-170.

Simple Modular Architecture Research Tool (SMART): http://smart.embl-heidelberg.de/.

Sohn, K. H., Lei, R., Nemri, A. & Jones, J. D. G. (2007) The downy mildew effector proteins ATR1 and ATR13 promote disease susceptibility in *Arabidopsis thaliana*. *The Plant Cell*, 19, 4077-4090.

Solovyeva, I., Schmuker, A., Cano, L. M., van Damme, M., Ploch, S., Kamoun, S. & Thines, M. (2015) Evolution of *Hyaloperonospora* effectors: ATR1 effector homologs from sister species of the downy mildew pathogen *H. arabidopsidis* are not recognised by RPP1 [WsB]. *Mycological Progress*, 14 (53), 1-9.

Soylu, E. M. & Soylu, S. (2003) Light and electron microscopy of the compatible interaction between *Arabidopsis* and the downy mildew pathogen *Peronospora parasitica*. *Journal of Phytopathology*, 151, 300-306.

Stassen, J. H. M. & Van den Ackerveken, G. (2011) How do oomycete effectors interfere with plant life? *Current Opinion in Plant Biology*, 14, 407-414.

Strange, R. N. & Scott, P. R. (2005) Plant disease: a threat to global food security. *Annual Review of Phytopathology*, 43, 83-116.

Strullu-Derrien, C., Kernick, P., Rioult, J. P. & Strullu, D. G. (2011) Evidence of parasitic Oomycetes (Peronosporomycetes) infecting the stem cortex of the Carboniferous seed fern *Lyginopteris oldhamia*. *Proceedings of the Royal Society*, 278, 675-680.

Sudisha, J., Sharathchandra, R. G., Amruthesh, K. N., Kumar, A. & Shekar Shetty, H. (2012) Pathogenesis related proteins in plant defense response. In: Mérillon, J. M. & Ramawat, K. G. (eds.) *Plant defence: biological control*. © Springer Science+Business Media B.V., pp. 379-403.

Talbot, N. J. (2010) Lining the sweet life: how does a plant pathogenic fungus acquire sugar from plants? *PLOS Biology*, 8 (2), e1000308.

The Arabidopsis Information Resource (TAIR): www.arabidopsis.org

Thines, M. & Choi, Y.-J. (2016) Evolution, diversity, and taxonomy of the Peronosporaceae, with focus on the genus *Peronospora*. *Phytopathology*, 106 (1), 6-18.

Thines, M. & Kamoun, S. (2010) Oomycete-plant coevolution: recent advances and future prospects. *Current Opinion in Plant Biology*, 13, 427-433.

Thuerig, B., Felix, G., Binder, A., Boller, T. & Tamm, L. (2006) An extract of *Penicillium chrysogenum* elicits early defense-related responses and induces resistance in *Arabidopsis thaliana* independently of known signalling pathways. *Physiological and Molecular Plant Pathology,* 67, 180-193.

Tör, M., Lotze, M. T. & Holton, N. (2009) Receptor-mediated signalling in plants: molecular patterns and programmes. *Journal of Experimental Botany*, 60 (13), 3645-3654.

Torres, M. A., Jones, J. D. G. & Dangl, J. L. (2006) Reactive oxygen species signaling in response to pathogens. *Plant Physiology*, 141, 373-378.

Torres, M. A. (2009) ROS in biotic interactions. *Physiologia Plantarum*, 138, 414-429.

Tsuda, K. & Katagiri, F. (2010) Comparing signaling mechanisms engaged in pattern-triggered and effector-triggered immunity. *Current Opinion in Plant Biology*, 13, 459-465.

Underwood, W. (2012) The plant cell wall: a dynamic barrier against pathogen invasion. *Frontiers in Plant Science*, 3 (85), 1-6.

Untergrasser, A., Cutcutache, I., Koressaar, T., Ye, J., Faircloth, B. C., Remm, M. & Rozen, S. G. (2012) Primer3 - new capabilities and interfaces. *Nucleic Acids Research*, 40 (15), e115.

Van Buyten, E. & Höfte, M. (2013) *Pythium* species from rice roots differ in virulence, host colonization and nutritional profile. *BMC Plant Biology*, 13 (203), 1-17.

van der Biezen, E. A., Freddie, C. T., Kahn, K., Parker, J. E. & Jones, J. D. (2002) *Arabidopsis RPP4* is a member of the *RPP5* multigene family of TIR-NB-RR genes and confers downy mildew resistance through multiple signalling components. *The Plant Journal*, 29 (4), 439-451.

Vert, G. (2008) Plant signaling: brassinosteroids, immunity and effectors are BAK! *Current Biology*, 18, 936-965.

Vetter, M. M., Kronholm, I., He, F., Häweker, H., Reymond, M., Bergelson, J., Robatzek, S. & de Meaux, J. (2012) Flagellin perception varies quantitatively in *Arabidopsis thaliana* and its relatives. *Molecular Biology and Evolution*, 29 (6), 1655-1667.

Vidaver, A. K. & Lambrecht, P. A. (2004) Bacteria as plant pathogens. *The Plant Health Instructor*, DOI: 10.1094/PHI-I-2004-0809-01.

Vidhyasekaran, P. (2013) PAMP signaling in plant innate immunity. In: Vidhyasekaran (ed.) *PAMP signals in plant innate immunity: signal perception and trasduction*. Signaling and Communication in plants, 21, Sringer, Dordrecht, 17-115.

Villalba Mateos, F., Rickauer, M. & Esquerré-Tugayé, M.-T. (1997) Cloning and characterization of a cDNA encoding an elicitor of *Phytophthora parasitica* var. *nicotianae* that shows cellulose-binding and lectin-like activities. *Molecular Plant-Microbe Interactions*, 10 (9), 1045-1053.

Voigt, C. A. (2014) Callose-mediated resistance to pathogenic intruders in plant-defense related papillae. *Frontiers in Plant Science*, 5 (168), 1-6.

Wang, G., Ellendorff, U., Kemp, B., Mansfield, J. W., Forsyth, A., Mitchell, K., Bastas, K., Liu, C.-M., Woods-Tör, A., Zipfel, C., de Wit, P. J. G. M., Jones, J. D. G., Tör, M. & Thomma, B. P. H. J. (2008) A genome-wide functional investigation into the roles of receptor-like proteins in *Arabidopsis*. *Plant Physiology*, 147, 503-517.

Wang, L. (2009) Towards revealing the structure of bacterial inclusion bodies. *Prion*, 3 (3), 139-145.

Wawra, S., Belmonte, R., Löbach, L., Saraiva, M., Willems, A. & van West, P. (2012) Secretion, delivery and function of oomycete effector proteins. *Current Opinion in Microbiology*, 15, 685-691.

Wei, L., Xue, A. G., Cober, E. R., Babcock, C., Zhang, J., Zhang, S., Li, W., Wu, J. & Liu, L. (2011) Pathogenicity of *Pythium* species causing seed rot and damping-off in soybean under controlled conditions. *Phytoprotection*, 91, 3-10.

Whisson, S. C., Boevink, P. C., Moleleki, L., Avrova, A. O., Morales, J. G., Gilroy, E. M., Armstrong, M. R., Grouffaud, S., van West, P., Chapman, S., Hein, I., Toth, I. K., Pritchard, L. & Birch, P. R. J. (2007) A translocation signal for delivery of oomycete effector proteins into host plant cells. *Nature*, 450, 115-118.

Wilson, R. A. & Talbot, N. J. (2009) Under pressure: investigating the biology of plant infection by *Magnaporthe oryza*. *Nature Reviews: Microbiology*, 7, 185-195.

Yuen, C. Y. L., Matsumoto, K. O. & Christopher, D. A. (2013) Variation in the subcellular localization and protein folding activity among *Arabidopsis thaliana* homologs of protein disulphide isomerase. *Biomolecules*, 3, 848-869.

Zipfel, C. (2009) Early molecular events in PAMP-triggered immunity. *Current Opinion in Plant Biology*, 12, 414-420.

Zipfel, C. & Robatzek, S. (2010) Pathogen-associated molecular pattern-triggered immunity: veni, vidi…? *Plant Physiology*, 154, 551-554.

Role of the penetration-resistance genes *PEN1*, *PEN2* and *PEN3* in the hypersensitive response and race-specific resistance in *Arabidopsis thaliana*

Oskar N. Johansson[1], Elena Fantozzi[2], Per Fahlberg[1], Anders K. Nilsson[1], Nathalie Buhot[1], Mahmut Tör[2] and Mats X. Andersson[1,*]

[1]*Department of Biological and Environmental Sciences, University of Gothenburg, Box 461, Göteborg, SE-405 30 Sweden, and*

[2]*National Pollen and Aerobiology Research Unit, Institute of Science and the Environment, University of Worcester, Worcester WR2 6AJ, UK*

SUMMARY

Plants are highly capable of recognizing and defending themselves against invading microbes. Adapted plant pathogens secrete effector molecules to suppress the host's immune system. These molecules may be recognized by host-encoded resistance proteins, which then trigger defense in the form of the hypersensitive response (HR) leading to programmed cell death of the host tissue at the infection site. The three proteins PEN1, PEN2 and PEN3 have been found to act as central components in cell wall-based defense against the non-adapted powdery mildew *Blumeria graminis* fsp. *hordei* (*Bgh*). We found that loss of function mutations in any of the three *PEN* genes cause decreased hypersensitive cell death triggered by recognition of effectors from oomycete and bacterial pathogens in Arabidopsis. There were considerable additive effects of the mutations. The HR induced by recognition of AvrRpm1 was almost completely abolished in the *pen2 pen3* and *pen1 pen3* double mutants and the loss of cell death could be linked to indole glucosinolate breakdown products. However, the loss of the HR in *pen* double mutants did not affect the plants' ability to restrict bacterial growth, whereas resistance to avirulent isolates of the oomycete *Hyaloperonospora arabidopsidis* was strongly compromised. In contrast, the double and triple mutants demonstrated varying degrees of run-away cell death in response to *Bgh*. Taken together, our results indicate that the three genes *PEN1*, *PEN2* and *PEN3* extend in functionality beyond their previously recognized functions in cell wall-based defense against non-host pathogens.

Keywords: hypersensitive response, programmed cell death, penetration resistance genes, defense no death, indole glucosinolates, *Arabidopsis thaliana*, *Pseudomonas syringae*, *Hyaloperonospora arabidopsidis*.

INTRODUCTION

In the absence of mobile and specialized immune cells, such as are present in mammals, plants rely on the innate immunity of all living cells. Recognition of pathogens takes place at two conceptually different levels (Dodds and Rathjen, 2010). The first is the detection of conserved microbial molecular cues, microbe-associated molecular patterns (MAMPs). Recognition of these is mediated by plasma membrane localized receptors and triggers intracellular signaling comprising ion fluxes across the plasma membrane, mitogen-activated protein kinase signaling cascades, an oxidative burst and induction of phospholipases. This results in defense responses such as a strengthened cell wall, synthesis of phytoalexins and preparation of the

plant cell for attack (Pitzschke *et al.*, 2009; Ronald and Beutler, 2010). This so-called MAMP-triggered immunity (MTI) is sufficient to stop many non-adapted pathogens from successfully colonizing the plant and causing disease.

Pathogens circumvent and repress MTI by the production of effector proteins which interfere with plant defense signaling (Bent and Mackey, 2007; Deslandes and Rivas, 2012). In turn, plants have evolved cognate resistance (R) proteins which sense the activity of the effectors and induce a strong defense response, referred to as effector-triggered immunity (ETI). The latter is characterized by a hypersensitive response (HR), often culminating in programmed cell death of the host tissue. Successful ETI is

also linked to the establishment of heightened resistance in distal parts of the plant, termed systemic acquired resistance. While the HR as a whole efficiently stops the pathogen, the actual function of cell death in restricting pathogen growth has been questioned (Mur *et al.*, 2008). Several studies point to somewhat varying roles of cell death in the HR (Clough *et al.*, 2000; Jurkowski *et al.*, 2004; Hofius *et al.*, 2009; Coll *et al.*, 2010; Hackenberg *et al.*, 2013). The known plant R-proteins are divided into two classes, TIR-NB-LRR and CC-NB-LRR. These appear to differ in their requirements for downstream signaling components (Bent and Mackey, 2007). Cell death following effector recognition has been linked to activation of metacaspases (Coll *et al.*, 2010), components of the autophagic system (Hofius *et al.*, 2009) and fusion events between the vacuole and plasma membrane (Hatsugai *et al.*, 2009) and catalase activity (Hackenberg *et al.*, 2013).

Many obligate biotrophic fungi, such as the powdery mildews, produce specialized structures that penetrate the plant cell wall to form a feeding structure (haustorium) in close association with the plant plasma membrane. The non-adapted mildews are often resisted at the level of cell wall penetration as the epidermal cell reinforces the cell wall and secretes antifungal compounds to stop the penetration attempt (Huckelhoven and Panstruga, 2011). In the model system of *Arabidopsis thaliana* (hereafter Arabidopsis) and the non-adapted mildew *Blumeria graminis* sp. *hordei* (*Bgh*), pathogen growth is restricted at the cell wall level and 80–90% of fungal penetration attempts fail. In the few instances when penetration is successful the epidermal cells undergo programmed cell death and the infection is stopped. Two major pathways for the cell wall-based defense against mildews are recognized (Huckelhoven and Panstruga, 2011). Both pathways are most likely triggered by recognition of MAMPs. The PEN1 pathway is linked to secretory membrane traffic. The PEN1 syntaxin interacts with VAMP721/722 and SNAP33, together with an ADP ribosylation factor (ARF) GTPase and the corresponding GTP exchange factor GNOM, to mediate secretion of exosomes to form the papilla (Nielsen and Thordal-Christensen, 2013). Loss of PEN1 function leads to almost 90% penetration success of *Bgh* spores (Collins *et al.*, 2003). The PEN2/PEN3 pathway is linked to metabolism and transport of tryptophan-derived secondary metabolites. *PEN2* encodes a peroxisome-localized myrosinase involved in hydrolyzing indole glucosinolates (Lipka *et al.*, 2005) and *PEN3* encodes a plasma membrane-localized ABC transporter (Stein *et al.*, 2006). The current model predicts that PEN2 produces an active compound which is excreted into the apoplast by PEN3 to stop fungal ingress (Bednarek *et al.*, 2009).

All three PEN proteins have been ascribed additional roles other than that of cell wall-based defense. For instance, PEN1 was shown to be involved in recycling of K^+ channels during stomatal closure (Eisenach *et al.*, 2012),

PEN2 in oomycete defense (Schlaeppi and Mauch, 2010) and PEN3 in heavy metal transport (Kim *et al.*, 2007). The PEN2 and PEN3 proteins are also involved in MAMP-triggered deposition of callose in response to the bacterial MAMP flagellin (Clay *et al.*, 2009). In addition, loss of PEN1 and PEN3 is linked to an induction of salicylic acid (SA)-dependent resistance to adapted pathogens (Kobae *et al.*, 2006; Stein *et al.*, 2006; Zhang *et al.*, 2007, 2008). Furthermore, the cell wall-based defenses as such are suppressed by bacterial effectors (Hauck *et al.*, 2003).

In this study, we show that loss of PEN1, PEN2 and PEN3 causes a weakened HR response following activation of both CC-NB-LRR and TIR-NB-LRR R-proteins as well as unregulated cell death in response to a non-adapted powdery mildew.

RESULTS

Loss of *PEN1*, *PEN2* or *PEN3* results in attenuated hypersensitive cell death after recognition of the *Pseudomonas syringae* effectors AvrRpm1 and AvrRps4

As several previous studies point to possible functions of the PEN proteins other than in cell wall-based defense against fungi, we investigated in closer detail the transcriptional behavior of *PEN1*, *PEN2* and *PEN3* in the context of pathogen response. Expression data for *PEN1*, *PEN2* and *PEN3* were retrieved from all 504 available arrays annotated as 'biotic stress' using Genevestigator (Hruz *et al.*, 2008). Experiments were filtered for statistically significant ($P < 0.05$) up- or downregulation of *PEN1*, *PEN2* or *PEN3* and grouped with regard to experimental setup (Figure S1 in Supporting Information). As expected, all three *PEN* genes were upregulated in response to non-adapted powdery mildews. In addition, recognition of *Pseudomonas syringae* pv. *tomato* (*Pst*) effectors also caused transcriptional activation of all three *PEN* genes. Induction following AvrRps4 recognition was dependent on EDS1, as expected for a TIR-NB-LRR class R-protein (Bartsch *et al.*, 2006). Taken together, this suggests that the *PEN* genes might play a role in ETI in addition to cell wall-based defenses. Thus, we infiltrated leaves from the *pen* single mutants with *Pst* DC3000 expressing the effectors AvrRpm1 or AvrRps4 and measured the HR-related cell death as release of cellular electrolytes (Mackey *et al.*, 2002). The non responsive mutants *eds1* (Falk *et al.*, 1999) and *rpm1* (Grant *et al.*, 1995) were used as controls for AvrRps4 and AvrRpm1, respectively. All three mutant lines demonstrated significantly decreased electrolyte leakage compared with the wild type in response to AvrRpm1 and AvrRps4 ($P < 0.05$, Figure 1). The *pen2* and *pen3* mutants exhibited the largest difference compared with the wild type in response to both AvrRpm1 and AvrRps4. In *pen2* and *pen3*, the maximum release of electrolytes was reduced by about 50% compared with the wild type (Figure 1, Table 1).
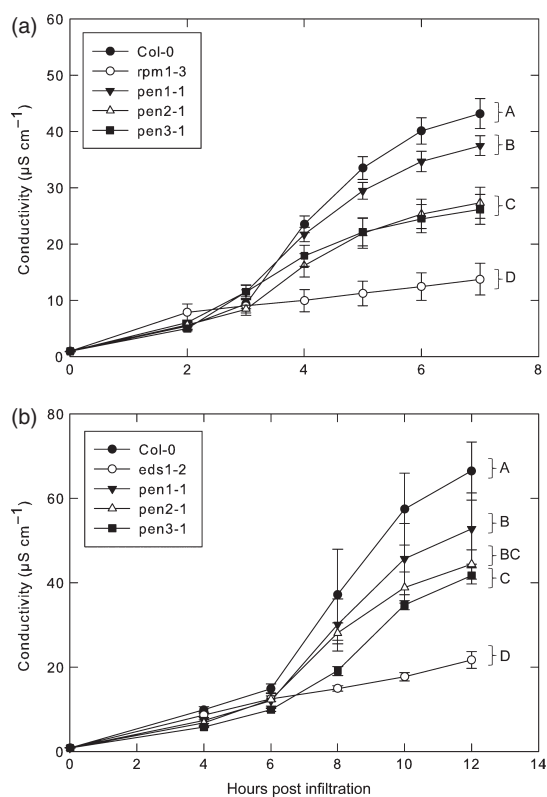
(a)

(b)

Figure 1. Loss of function mutations in PEN1, PEN2 and PEN3 result in decreased cell death induced by recognition of AvrRpm1 and AvrRps4. Leaf disks were prepared from the indicated Arabidopsis lines and infiltrated with *Pseudomonas syringae* pv. *tomato* expressing AvrRpm1 (a) or AvrRps4 (b). The disks were incubated in water and the conductivity of the bathing solution was measured at the time points indicated. The mean and standard deviation of six replicates are shown. Letters A–D on the right indicate experimental groups with significant differences ($P < 0.05$, ANOVA with Tukey's *post-hoc* test). The experiments were repeated three times with similar results.

Independent T-DNA insertion lines in *PEN1*, *PEN2* and *PEN3* exhibited very similar phenotypes to those of the point mutants (Figure S2). Thus, loss of any of the three PEN proteins appears to lead to attenuated HR-induced cell death mediated through the CC-NB-LRR protein RPM1 and the TIR-NB-LRR protein RPS4.

As the next step, all three *pen* mutant lines were crossed together to generate the three possible double mutant combinations and the triple mutant. Often, the triple and double *pen1 pen3* mutants developed chlorosis in their leaves and showed growth retardation compared with the wild type at later developmental stages (Figure S3a). The phenotype was not always consistent as it seemed to vary between growth cabinets, but generally presented itself at an older age. In general, the triple mutant of older plants (7–8 weeks' cultivation under short-day conditions)

displayed a stunted growth phenotype and chlorosis, starting at the tips of older leaves. As both the *pen1* and *pen3* mutations have been linked to accumulation of SA (Stein *et al.*, 2006; Zhang *et al.*, 2007), resulting in induction of basal resistance and PR gene expression, we quantified the level of free SA in all the mutant lines used for HR analysis (Figure S3b). Compared with the wild type, only the double *pen1pen2* mutant displayed a significant ($P < 0.05$) increase at 5 weeks in free SA level. None of the single mutants displayed a significantly increased SA level compared with the wild type.

Cell death triggered by recognition of AvrRpm1 and AvrRps4 in the double and triple mutant lines was also tested by quantification of electrolyte leakage (Figure 2). The phenotype of both *pen1* and *pen2* in response to AvrRpm1 (Figure 2a) and AvrRps4 (Figure 2b) was enhanced by addition of the *pen3* mutation. Ion leakage measured from the triple mutant and the two double mutants *pen1 pen3* and *pen2 pen3* was reduced by about 80% compared with the wild type in response to AvrRpm1. The same mutant lines were as unresponsive to AvrRps4 as the *eds1* mutant. The ion leakage phenotypes were supported by scoring the visible collapse of leaves attached to the plant after infiltration with *Pst* (Table 1).

Next, the single, double and triple *pen* mutants were assayed for their ability to restrict bacterial growth. Leaves were infiltrated with *Pst* expressing AvrRpm1 or AvrRps4 and the bacterial growth was quantified after 3 days (Figure 3a,b). There was no detectable loss of resistance in any of the tested mutants against the two different *Pst* strains. In fact, it appeared that, if anything, some of the double mutations conferred a little more resistance to avirulent *Pst* than the Col-0 wild type. The growth of virulent *Pst* (DC3000) was also assayed on the series of mutant lines (Figure 3c). None of the mutants displayed increased susceptibility against virulent *Pst*. On the contrary, mutant combinations including *pen3* conferred slightly increased resistance to the bacterium.

Indole glucosinolate breakdown products contribute to the hypersensitive cell death triggered by *Pst* effectors

PEN2 encodes a β-thioglucoside hydrolase which cleaves precursor glucosinolates into unstable aglycones (Bednarek *et al.*, 2009). Glucosinolates are linked mainly to defense against insects in cruciferous plants (Hopkins *et al.*, 2009). In addition, many recent reports indicate that this class of compounds plays a role in defense against microbial pathogens (Tierens *et al.*, 2001; Fan *et al.*, 2011; Bednarek, 2012; Hiruma *et al.*, 2013). The enzymes CYP79B2 and CYP79B3 convert tryptophan into indol-3-yl-acetaldoxime (I3A). The latter is a precursor to auxin, camalexin and indolic glucosinolates such as indole-3-methyl-glucosinolate (I3G) and 4-methoxyindol-3-ylmethylglucosinolate (4MI3G) via CYP81F2-dependent methoxylation of

Table 1 Summarized phenotypes for ion leakage and collapse assays. Ion leakages are shown as mean percentage of Col-0 (WT) and standard deviation of six replicates for the 7 and 12 h post-inoculation (hpi) time point shown in Figures 1 and 2. Fifteen leaves from three separate plants were analyzed for tissue collapse at at 7 hpi for AvrRpm1 and 12 hpi for AvrRps4

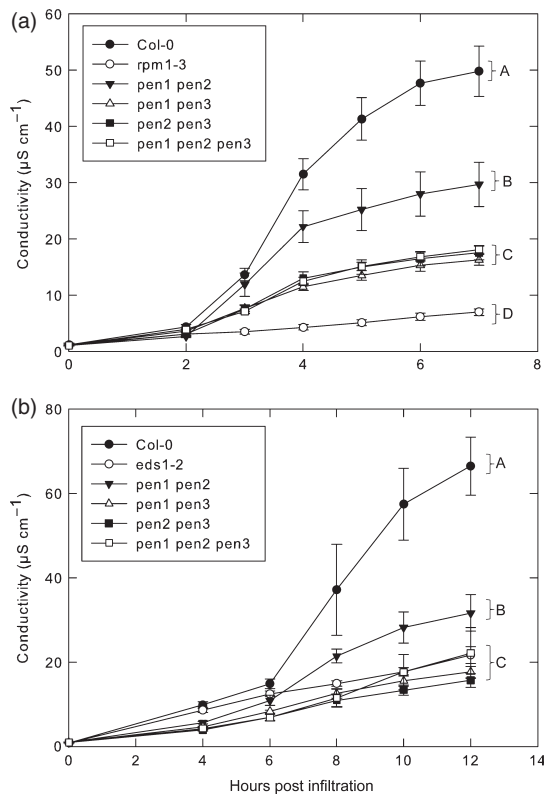| Line	Ion leakage (% of WT)		Collapse (collapsed/total infiltrated leaves)	
	AvrRpm1 (7 hpi)	AvrRps4 (12 hpi)	AvrRpm1 (7 hpi)	AvrRps4 (12 hpi)
Col-0 WT	100	100	14/15	9/15
rpm1-3	17 ± 6	n.d.	0/15	n.d.
eds1	n.d.	33 ± 3	n.d.	0/15
pen1	80 ± 4	79 ± 13	10/15	7/15
pen2	59 ± 6	67 ± 5	8/15	3/15
pen3	57 ± 6	62 ± 3	4/15	6/15
pen1 pen2	56 ± 8	48 ± 7	6/15	3/15
pen1 pen3	31 ± 2	27 ± 2	1/15	0/15
pen2 pen3	33 ± 2	23 ± 2	2/15	0/15
pen1 pen2 pen3	34 ± 2	33 ± 9	2/15	0/15

n.d., not determined.

Figure 2. Additive effects on loss of hypersensitive response-related cell death of the *pen* mutations.
Leaf disks were prepared from the indicated Arabidopsis lines and infiltrated with *Pseudomonas syringae* pv. *tomato* expressing AvrRpm1 (a) or AvrRps4 (b). The disks were incubated in water and the conductivity of the bathing solution was measured at the time points indicated. The mean and standard deviation of six replicates are shown. Letters A–D on the right indicate experimental groups with significant differences ($P < 0.05$, ANOVA with Tukey's *post-hoc* test). The experiments were repeated twice with similar results.

indole-3-methyl-glucosinolate (I3G). Several mutants in the indole glucosinolate biosynthetic network (Bones and Rossiter, 1996) (Figure S4) have been assayed for loss of cell death following recognition of AvrRpm1 (Figure 4a). The *cyp79b2 cyp79b3* double mutant (Zhao *et al.*, 2002) as well as the *ugt74B1* single mutant (Grubb *et al.*, 2004) displayed significantly reduced HR following inoculation with *Pst* expressing AvrRpm1 ($P < 0.05$). The reduction in ion leakage of the double *cyp79B2 cyp79B3* mutant compared with the wild type was very similar to that of the *pen2* mutant (Figure S5). The *CYP71B15* (PAD3) loss of function mutant *pad3-1* (Glazebrook and Ausubel, 1994) and the T-DNA insertion mutant of the *CYP81F2* (Clay *et al.*, 2009) gene demonstrated no significant difference in cell death compared with the wild type after infiltration with *Pst* expressing AvrRpm1.

To test if the breakdown product of indole-3-glucosinolate, indole-3-acetonitrile, could induce cell death, leaf disks were infiltrated with indole-3-acetonitrile or butyronitrile suspended in water at 100–400 μM and ion leakage measured over a period of 72 h (Figure 4b). Both concentrations of indole-3-acetonitrile induced significant ion leakage over a period of 24–72 h, whereas the aliphatic nitrile butyronitrile did not induce any ion leakage exceeding mock treatment.

Combination of the *pen1* mutation with *pen2* or *pen3* causes spread of cell death following inoculation with the non-host powdery mildew *Bgh*

The *pen* mutants were originally isolated in forward genetic screens for mutants displaying loss of pre-penetration defense against *Bgh* (Collins *et al.*, 2003; Lipka *et al.*, 2005; Stein *et al.*, 2006) and successfully penetrating *Bgh* spores are generally resisted by HR-like cell death of the epidermal cell. To assess the impact of the different *pen*-mutant combinations on *Bgh* development at the plant epi-
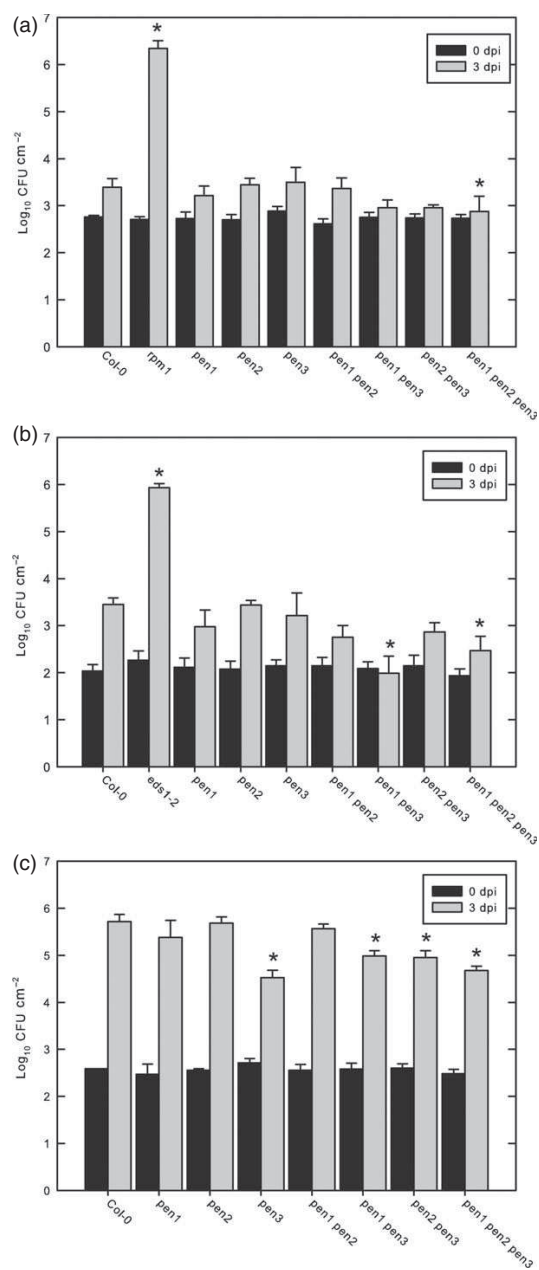
Figure 3. Loss of hypersensitive response-related cell death in the *pen* mutants does not compromise defense against avirulent *Pseudomonas syringae* pv. *tomato* (*Pst*).

Leaves of the indicated line were infiltrated with *Pst* expressing AvrRpm1 (a), AvrRps4 (b) or the virulent DC3000 strain (c). At the indicated time points leaf disks were punched out and the number of colony forming units (CFU) per leaf area determined after serial dilution and cultivation on selective media. The mean and standard deviation of three replicates for day 0 and four replicates for day 3 are shown. The asterisk (*) indicates significant difference from Col-0 ($P < 0.05$, ANOVA with Tukey's *post-hoc* test). The experiments were repeated twice with similar results. dpi, days post-inoculation.
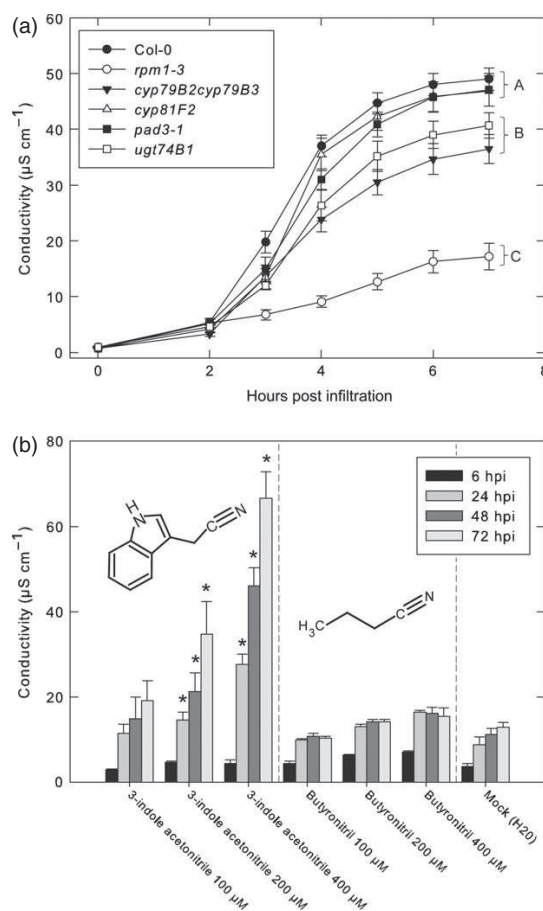

Figure 4. Indolic glucosinolates and their breakdown products are involved in cell death response to the bacterial effector AvrRpm1.

(a) Leaf disks from the indicated mutant lines were infiltrated with *Pseudomonas syringae* pv. *tomato* DC3000 expressing AvrRpm1, the disks were incubated in water and the amount of electrolytes lost from the leaf tissue was quantified by measurement of the conductivity of the bathing solution at the indicated time points. The average and standard deviation of six replicates are shown. The letters A–C on the right indicate experimental groups with significant differences ($P < 0.05$, ANOVA with Tukey's *post-hoc* test).

(b) Leaf disks were infiltrated with various concentrations of indole-3-acetonitrile (I3A) or butyronitrile and the conductivity of the bathing solution was measured at indicated times. The average and standard deviation of three replicates are shown. The asterisk (*) indicates significant difference from mock infiltration at the corresponding time point ($P < 0.05$, ANOVA with Tukey's *post-hoc* test). Both experiments were repeated twice with similar results. hpi, hours post-infiltration.

dermis, all the *pen* mutants were inoculated with *Bgh* and the pre- and post-penetration (Figure 5c) defense was scored at 72 h post-inoculation. The penetration and subsequent epidermal cell death rate was, as expected, very high for the combination mutants containing *pen1* and moderate for combinations containing *pen2* or *pen3* (Lipka *et al.*, 2005). The double mutants and the triple mutant displayed a striking cell death phenotype upon inoculation
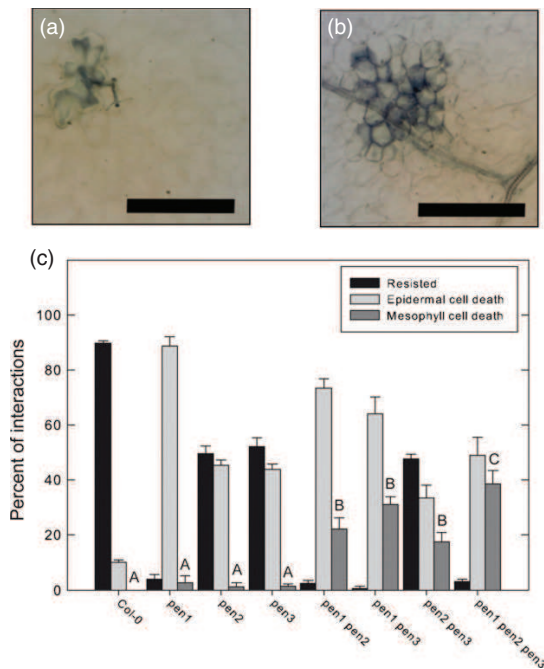
Figure 5. Combination of *pen* mutations causes runaway cell death during defense against the non-host powdery mildew *Blumeria graminis* fsp. *hordei* (*Bgh*).
The indicated lines were inoculated with *Bgh* spores and stained with trypan blue at 3 days post-inoculation. Resistance, epidermal cell death (a) and large mesophyll cell death lesions (b) were counted (c). Average and standard deviations of a total of 50 interactions in three leaves counted from three separate plants of each genotype is shown. Scale bars indicate 0.1 mm. The letters A–C indicate experimental groups with significant differences ($P < 0.05$, ANOVA with Tukey's *post-hoc* test). The experiment was repeated twice with similar results.

with *Bgh* (Figure 5a,b): about 30% of the interaction events resulted in cell death spreading into the mesophyll. There was a significant shift towards more of the spreading cell death events in the double and the triple mutants than were observed in the single mutants. It should be noted that virtually no growth of secondary hyphae of *Bgh* could be observed on any of the tested mutant lines. Thus, all the tested lines displayed complete resistance against *Bgh*.

Loss of function mutations in *PEN1, PEN2* and *PEN3* cause decreased effector triggered resistance to *Hyaloperonospora arabidopsidis*

To evaluate if the PEN proteins are involved in other R-protein-mediated defense responses besides those triggered by RPM1 and RPS4, we used the oomycete *Hyaloperonospora arabidopsidis* (*Hpa*) which causes downy mildew. The Arabidopsis wild type Col-0 is resistant against several isolates of *Hpa* through avirulence (Avr)-R gene interactions (Holub, 2007). Inoculation with *Hpa* is also one of the treatments that causes transcriptional activation of the *PEN*

genes (Figure S1). The Cala2 isolate of *Hpa* produces the effector ATR2, which is recognized by the two TIR-NB-LRR R-proteins RPP2A and RPP2B in Arabidopsis and triggers an EDS1-dependent defense response (Sinapidou *et al.*, 2004). We categorized the interactions at the microscopic level as rapid localized cell death, spreading cell death, trailing necrosis and no cell death with free hyphal growth (Figure 6a–d). Inoculation of the Col-0 wild type with *Hpa*-Cala2 resulted in rapid host cell death at almost all interaction sites and no further spread of the pathogen. In contrast, the *pen3* mutant displayed a significantly higher proportion of interaction sites with extensive trailing necrosis and about 30% of the sites displayed hyphae outgrowing the cell death. The *pen1* and *pen2* single mutants displayed no phenotypic alterations compared with the wild type. The *pen1 pen2* double mutant, on the other hand, displayed clearly increased trailing necrosis compared with the wild type. Surprisingly, the *pen1 pen3* double mutant had a less severe phenotype than the *pen3* single mutant. The *pen2 pen3* double mutant and the triple mutant had similar phenotypes to *pen3* (Fig. 6e).

Since the *pen* mutations clearly affected the HR induced by recognition of Cala2, we also investigated the sporulation of a *Hpa*-Cala2 isolate on these different mutants. The Cala2 isolate is in general unable to sporulate on wild-type Col-0 plants (Sinapidou *et al.*, 2004). We obtained similar results with the Col-0 wild type throughout our experiments (Figure 6f). Some *pen3* mutant plants displayed an increase in sporulation compared with the wild type, but this was too variable between individual plants to be statistically significant. However, the *pen1 pen2* and triple mutants supported substantially more sporulation than the wild type, whereas the *pen2 pen3* and *pen1 pen3* mutants were similar in this respect to the *pen3* single mutant. Finally, the triple mutant also displayed a chlorotic phenotype after inoculation with *Hpa*-Cala2 (Figure 6g).

DISCUSSION

Cell wall-based defense to non-adapted powdery mildews is most likely dependent on MAMP-triggered immunity and two major pathways are implicated in this defense, one defined by PEN1 and the other by PEN2 and PEN3 (Huckelhoven and Panstruga, 2011). The latter pathway entails the production and likely secretion of reactive indole compounds into the apoplast (Bednarek, 2012). The PEN1 pathway is dependent on membrane fusion and transcytosis events, but it is not well understood how these actually contribute to stopping the fungus in the apoplast (Nielsen and Thordal-Christensen, 2013). While the three *PEN* genes are major players in cell wall-based defense against non-adapted fungi, their functionality clearly extends beyond this. Data from multiple array experiments demonstrate transcriptional activation of all three *PEN* genes in response to various biotic stresses,
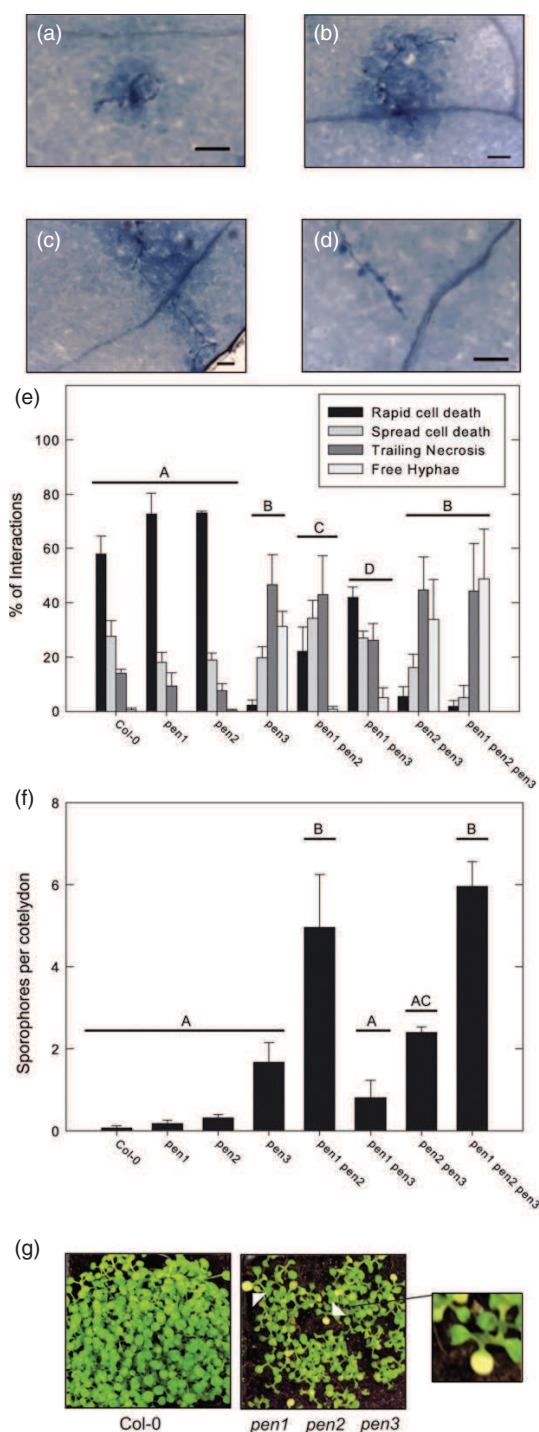
Figure 6. The *pen* mutations confer reduced cell death and reduced resistance against the avirulent *Hyaloperonospora arabidopsidis* (*Hpa*) isolate Cala2.

Seedlings of the indicated lines were inoculated with *Hpa* isolate Cala2 and stained with trypan blue after 3 days and the interaction sites were scored as rapid cell death (a), more diffusely spread cell death (b), trailing necrosis (c) or free hyphae outgrowing the cell death (d). Scale bars indicate 0.1 mm. The percentage of each category is presented as the average and standard deviation of three biological replicates (e). The number of sporophores were counted at 7 days post-inoculation (f). The average and standard deviation of three replicates are shown. The letters A–D indicate experimental groups with significant differences ($P < 0.05$, ANOVA with Tukey's *post-hoc* test). (g) Chlorosis (white arrows) of infected *pen* triple mutant plants upon infection by *Hpa*, including a close-up picture of chlorosis. The experiment was repeated twice with similar results.

lapse, was strongly affected in *pen1 pen3* and *pen2 pen3* double mutants. In fact, the phenotype of these mutants was reminiscent of the non-responding *rpm1* and *eds1* mutants for AvrRpm1 and AvrRps4, respectively. This result is in contrast with a previous study which reports increased HR in the *pen3* mutant towards *P. syringae* expressing AvrRpt2 (Kobae *et al.*, 2006). However, the cell death triggered by recognition of AvrRpt2 differs significantly from that triggered by AvrRps4 or AvrRpm1 with regard to downstream components (Hofius *et al.*, 2009). Thus requirement for or involvement of the *PEN* genes appears to vary between different effector R-protein pairs.

The actual ability to restrict the bacteria from proliferating in the tissue was not measurably decreased in any of the tested mutant lines. Thus, the *pen* double mutants confer something akin to a 'defense no death' phenotype as has also been reported by other studies (Clough *et al.*, 2000; Jurkowski *et al.*, 2004; Hofius *et al.*, 2009; Coll *et al.*, 2010; Hackenberg *et al.*, 2013). There are two previous contrasting reports on the resistance phenotype of the *pen3* mutant toward virulent *Pst* DC3000 (Kobae *et al.*, 2006; Xin *et al.*, 2013). One of these show a loss of resistance (Xin *et al.*, 2013) and the other, like this study, shows increased resistance in *pen3* (Kobae *et al.*, 2006). However, the different methods of inoculation used might explain the difference. In this study and in the study by Kobae *et al.* (2006) syringe infiltration was used, whereas Xin *et al.* (2013) used dipping inoculation. There might thus be quite a large difference in outcome depending on whether or not large amounts of inoculum directly reach the intercellular space in the mesophyll. Additionally, a PEN3–GUS fusion construct was shown to be highly expressed in the guard cells of Arabidopsis leaves, suggesting that PEN3 could play a role in resistance prior to bacterial entry into the mesophyll (Kobae *et al.*, 2006).

The connection between the swift cell death conferred by recognition of bacterial effectors and an actual ability to restrict the growth of the bacteria thus appears rather weak. It is well established that the HR triggered by bacterial effectors is characterized by a high degree of redundancy (Tsuda *et al.*, 2009) and cannot be considered a

including both *Pst* and *Hpa*. Cell death in response to recognition of AvrRpm1 and AvrRps4 secreted by *Pst*, as measured by ion leakage or macroscopic signs of leaf col-

straight pathway from recognition towards cell death. Thus, it may not be surprising that pathways, other than those culminating in cell death, might be sufficient to restrict the bacterial growth. We would also argue that this could be partly explained by the hemibiotrophic lifestyle of *Pst*, which multiplies in the apoplast, and thus may not be as severely affected by plant cell death. In accordance with this line of reasoning, an obligate biotroph such as *Hpa* might be more affected by host cell death. This seems to hold true for the *Hpa* isolate Cala2. In this case, the *pen* mutants, evidently affected in induction of cell death, also supported a large increase in sporulation and growth of the oomycete compared with the wild type. Clearly, loss of the *PEN* genes affects not only penetration resistance against non-adapted powdery mildew but also HR induced after recognition of pathogenic effectors.

How might these very strong effects on the HR caused by the loss of the different *PEN* genes be explained mechanistically? In theory, the attenuated HR might be explained by two non-mutually exclusive scenarios. Firstly, the PEN proteins might be directly involved in the signal transduction pathway or the execution of the cell death triggered by recognition of pathogenic effectors. Secondly, the PEN proteins may not be directly involved in the defense pathway, but their loss causes secondary effects that attenuate defense triggered by recognition of pathogenic effectors. We cannot completely distinguish between these scenarios from the genetic data presented here alone. We would, however, argue that the available data point to a direct involvement of the PEN2 and PEN3 proteins in the HR, whereas the role of PEN1 is more difficult to explain. The most straightforward secondary effect would be the previously reported induction of SA-dependent signaling in the *pen1* and *pen3* mutants (Stein *et al.*, 2006; Zhang *et al.*, 2007). However, we could not detect any substantial increase of free SA in the mutants cultivated under our conditions. Thus, induction of SA signaling does not seem to be a great contributor to the HR phenotype observed.

The actual mechanisms leading from activation of R-proteins to the execution of HR-related cell death in plants is still quite poorly understood, although several different second messengers and pathways are implied (Mur *et al.*, 2008). Therefore it is not easy to envision exactly how the PEN proteins would fit in mechanistically. The results from the experiments with both avirulent *Pst* and *Hpa* suggest that if PEN2 and PEN3 are directly involved in the HR they are not linked to each other in the same way as in cell wall-based resistance against non-adapted powdery mildew. PEN2 is a myrosinase which cleaves precursor glucosinolates into reactive compounds. It is thought that these are then exported to the apoplast through PEN3. We found that mutants lacking indole-3-methyl-glucosinolates also had an attenuated cell death response. In addition, infiltration with pure indole-3-acetonitrile caused cell death. These factors

taken together suggest a direct link from indole-glucosinolates through cleavage by PEN2 to cell death. Since *pad3-1* and *cyp81F2* mutants lacked a discernible HR phenotype, we can conclude that camalexin and 4MI3G are probably not involved in triggering HR-related cell death, although 4MI3G has been implicated in other defense responses triggered by MAMP recognition (Clay *et al.*, 2009).

The loss of HR is counterintuitive to the previous reports on phenotypes with increased resistance against virulent pathogens in the *pen1* (Zhang *et al.*, 2008) and *pen3* (Kobae *et al.*, 2006; Stein *et al.*, 2006) mutants. On the other hand, we could also measure an increased resistance caused by the *pen3* mutation to virulent *Pst* and the double and triple *pen* mutants displayed runaway cell death in response to *Bgh*. The latter appears similar to that observed in the *pen1 syp122* double mutant (Zhang *et al.*, 2007). Importantly, none of the tested lines supported any secondary post-invasive growth of *Bgh*. The cell death triggered upon successful fungal penetration of the epidermal cell wall by *Bgh* is much less well studied than the HR induced by recognition of the Avr proteins that was studied using *Hpa* and *Pst*. It is known that the post-penetration cell death induced in defense against *Bgh* depends strongly on EDS1 and its interaction partners SAG101 and PAD4 (Lipka *et al.*, 2005), but the exact mechanism for the triggering of post-penetration cell death by *Bgh* is not well understood.

Thus, clearly, the loss of *PEN* genes results in strikingly different effects on responses to different pathogens and different effectors in Arabidopsis. There were several interesting genetic interactions between the *pen* mutations in the two different pathosystems. The *pen3* mutation conferred the greatest single mutant phenotype to avirulent *Hpa* Cala2 and also a similar loss of HR upon recognition of avirulent *Pst* as the *pen2* mutation did. In contrast, the HR phenotype against *Hpa* Cala2 caused by the *pen3* mutation was suppressed by the *pen1* mutation. Again, surprisingly, the *pen1* and the *pen2* mutations together increased susceptibility to the Cala2 isolate of *Hpa*. Thus, whereas loss of PEN2 and PEN3 always seems to decrease HR and increase susceptibility, the loss of PEN1 has somewhat different effects on the outcome of the HR triggered by different effectors.

PEN3 was recently shown to accumulate in the plasma membrane upon infection with *Pst* and flg22 recognition (Underwood and Somerville, 2013; Xin *et al.*, 2013). PEN3 is also phosphorylated in response to flg22 (Benschop *et al.*, 2007). Taken together, this adds to our notion that PEN3 is involved in the HR. The additive effect of the *pen2* mutation in the *pen3* background on HR cell death would be consistent with a broader role for PEN3 than just transporting the tryptophan-derived indole compounds produced by PEN2 from glucosinolate precursors. It was recently shown that coronatine, a jasmonic acid–isoleucine mimic produced by *Pst*, reduces the transcription of *MYB51*

and thereby suppresses accumulation of 4MI3G and 1MI3G (Millet *et al.*, 2010; Geng *et al.*, 2012). Thus, a virulent pathogen apparently targets the very same system we found to be implicated in the HR and previously linked to MTI. Furthermore, given that the *pen3* mutation also has an additive effect in both *pen1* and *pen2* mutant backgrounds with regards to ion leakage, we reason that at least two parallel pathways could contribute to cell death during the HR response to the *Pst* effectors AvrRpm1 and AvrRps4. It is also possible that the effect of the *pen3* mutation in *Hpa* resistance is not only linked to cell death but possibly also to a reduction in the release of antimicrobial compounds into the apoplast and thus accumulation within the cells.

The contribution of PEN1 to the HR is more difficult to explain mechanistically and it is well known that loss of PEN1 has indirect effects in terms of increased SA content and thereby increased resistance to adapted powdery mildew (Zhang *et al.*, 2007). Membrane trafficking and fusion events have been linked to HR induced by effector recognition, for example fusion of the vacuolar membrane with the plasma membrane (Hatsugai *et al.*, 2009; Teh and Hofius, 2014). In addition, PEN1 is phosphorylated in response to recognition of flg22 (Benschop *et al.*, 2007) and the ortholog of PEN1 in tobacco has been shown to be targeted by bacterial effectors (Heese *et al.*, 2005). PEN1 is also involved in K^+ channel transport (Eisenach *et al.*, 2012). A partial explanation for the reduced electrolyte leakage following AvrRpm1 recognition in *pen1* mutants could simply be that fewer membrane-bound ion channels are present at the plasma membrane and one of the major ions leaked from plant cells undergoing HR is K^+ (Atkinson *et al.*, 1985; Demidchik *et al.*, 2014). This would, however, not explain the combinatory effect of losing PEN1 and PEN3 on *Hpa* sporulation.

To conclude, we suggest an extension of the role of *PEN1, PEN2* and *PEN3* in Arabidopsis defenses against adapted and non-adapted pathogens. We provide evidence for the involvement of the PEN proteins in both CC-NB-LRR- and TIR-NB-LRR-mediated ETI for *Pst* and TIR-NB-LRR-mediated ETI for *Hpa*. Our results indicate that breakdown products of indole glucosinolates are directly involved in the pathogen-induced cell death. This broadens the role of these compounds from previously known roles in insect resistance and MTI to ETI as well. Further studies are required for a better understanding of the molecular details of the involvement of the three PEN proteins and the indole compounds in the HR. Finally, the effector-triggered resistance of Arabidopsis to *Pst* is clearly not dependent on swift host cell death associated with the HR.

EXPERIMENTAL PROCEDURES

Growth conditions and plant material

Arabidopsis plants were cultivated in 8-h light (22°C, 90–115 µE)/16-h dark cycles (18°C) in 5 cm × 5 cm pots on perlite mixed soil (S-jord, Hasselfors Garden, http://www.hasselforsgarden.se/) supplemented with plant nutrient ('Blomstra', Cederoth International, http://www.cederroth.com/en/). Unless stated otherwise, green leaf tissue from 6 to 7-week-old plants was used for pathogen inoculation. The Arabidopsis mutant lines used in this study are listed in Table S1. Double and triple *pen* mutants were constructed by crossing the single mutants and screening the subsequent F_2 and in some cases F_3 generations using the PCR markers in Table S2. The DNA was extracted as described by Edwards *et al.* (1991). In short, leaf material was heated (96°C) in DNA extraction buffer [0.2 M 2-amino-2-(hydroxymethyl)-1,3-propanediol (TRIS)-HCl pH 7.5, 0.25 M NaCl, 25 mM EDTA and SDS 0.5%], precipitated in 2-propanol, washed in 70% ethanol and dissolved in TE-buffer (pH 7.5). The PCR reactions were performed in a thermal cycler; 3 min initial denaturation at 96°C followed by 40 cycles of 96°C for 15 sec, 55°C for 30 sec and 68°C for 1 min and a final extension at 68°C for 10 min using Platinum Taq polymerase (Clontech Laboratories, http://www.clontech.com/) according to the manufacturer's instructions. The PCR products were digested overnight and separated on 3–4% agarose gels. The T-DNA-insertion mutants for *PEN* genes were obtained from the Nottingham Arabidopsis Stock Centre and genotyped by PCR using the primers listed in Table S2.

Pathogen inoculation and other assays

Conductivity measurements were performed on vacuum-infiltrated leaf disks as described in (Mackey *et al.*, 2002). In short, leaf disks (7 mm diameter) were punched out and vacuum infiltrated with bacterial suspension prepared from overnight culture of bacteria on Kings Broth (KB)–Agar F (BioLife, Milano, Italy, www.biolifeit.com) supplemented with 50 µg ml^{-1} rifampicin and kanamycin, OD_{600} 0.01 or 0.1 for DC3000:AvrRpm1 and DC3000:AvrRps4. The disks were rinsed with water and placed in 10 ml of deionized water. The conductivity of the bathing solution was measured at the indicated time points. All ion leakage experiments were performed at least three times for AvrRpm1 and twice for AvrRps4 with similar results. Ion leakage following infiltration with nitriles was measured similarly. Nitrile stock solutions in methanol (6.4 mM) were diluted in deionized water. Water solutions were infiltrated into the abaxial side of leaves using a syringe, disks were punched out (five per replicate in three replicates), rinsed (30 min), placed in deionized water and the conductivity of the bathing solution was measured at indicated time points. *Hpa* isolates were prepared for inoculum and assessment of cell death and sporulation as described in Tor *et al.* (2002) and *Bgh* inoculations were as described Pinosa *et al.* (2013). Cell death, oomycete and fungal hyphae were visualized by trypan blue staining as described in Koch and Slusarenko (1990). Bacterial viability assays using *Pst* were performed as in Morel and Dangl (1999). In short, the abaxial sides of plant leaves were infiltrated with bacterial suspension from overnight plating of bacteria OD_{600} 0.00002 for DC3000 and DC3000:AvrRpm1 and OD_{600} 0.0001 for DC3000:AvrRps4. Three replicates with four leaf disks, each from separate leaves, were used for day 0 and four replicates for day 3. Leaf disks were homogenized for 4 sec in 100 µl $MgCl_2$ using an electric drill with an Eppendorf pestle as the drill bit. Samples were quick spun to pellet cell debris and the supernatant was serially diluted in 1/10 increments, once for day zero and five times for day three. All dilutions were plated on KB-media supplemented with 50 µg ml^{-1} rifampicin and kanamycin in two technical replicates. Samples were counted 2 days after plating. All presented experiments were repeated at least twice with similar results.

Salicylic acid quantification

Leaf disks were punched out from leaves in three independent biological replicates and were submerged in hot 2-propanol for 5 min and a known amount of deuterated SA was added. After drying under nitrogen, the disks were extracted in methanol and the SA quantified by LC-MS/MS as described in Pan *et al.* (2010) using an Agilent 1260 HPLC system coupled to an Agilent 6410 triple quadrupole mass spectrometer (http://www.agilent.com/).

Statistical analysis

Quantitative data were subjected to one-way ANOVA analysis with a subsequent Tukey's *post-hoc* test using GRAPHPAD PRISM 6 (Graph-Pad Software, Inc., http://www.graphpad.com/) with significance accepted at $P < 0.05$. Data presented are either denoted with an asterisk for significant difference compared with the wild type or mock treatment or alternatively assigned a group letter A–D where there are significant differences between groups but not within groups.

SUPPORTING INFORMATION

Additional Supporting Information may be found in the online version of this article.
Figure S1. Public microarray data supports induction of the *PEN1*, *PEN2* and *PEN3* genes during biotic stress.
Figure S2. Independent T-DNA insertion lines display similar conductivity to that of point mutations in the *PEN* genes.
Figure S3. *pen* double and triple mutant combinations display chlorotic leaf tips and stunted growth during aging.
Figure S4. Indole glucosinolate biosynthetic network.
Figure S5. The *pen2* and *cyp79B2/B3* mutants displays similar loss of cell death induced by recognition of AvrRpm1 secreted by *Pseudomonas syringae* pv. *tomato* DC3000.
Table S1. Mutant lines used in this study.
Table S2. The PCR-based markers used for genotyping of *pen* mutant lines.

REFERENCES

Atkinson, M.M., Huang, J.S. and Knopp, J.A. (1985) The hypersensitive reaction of tobacco to pseudomonas syringae pv. pisi: activation of a plasmalemma K/H exchange mechanism. *Plant Physiol.* **79**, 843–847.

Bartsch, M., Gobbato, E., Bednarek, P., Debey, S., Schultze, J.L., Bautor, J. and Parker, J.E. (2006) Salicylic acid-independent ENHANCED DISEASE SUSCEPTIBILITY1 signaling in Arabidopsis immunity and cell death is regulated by the monooxygenase FMO1 and the Nudix hydrolase NUDT7. *Plant Cell*, **18**, 1038–1051.

Bednarek, P. (2012) Chemical warfare or modulators of defence responses – the function of secondary metabolites in plant immunity. *Curr. Opin. Plant Biol.* **15**, 407–414.

Bednarek, P., Pislewska-Bednarek, M., Svatos, A. *et al.* (2009) A glucosinolate metabolism pathway in living plant cells mediates broad-spectrum antifungal defense. *Science*, **323**, 101–106.

Benschop, J.J., Mohammed, S., O'Flaherty, M., Heck, A.J., Slijper, M. and Menke, F.L. (2007) Quantitative phosphoproteomics of early elicitor signaling in Arabidopsis. *Mol. Cell. Proteomics*, **6**, 1198–1214.

Bent, A.F. and Mackey, D. (2007) Elicitors, effectors, and R genes: the new paradigm and a lifetime supply of questions. *Annu. Rev. Phytopathol.* **45**, 399–436.

Bones, A.M. and Rossiter, J.T. (1996) The myrosinase-glucosinolate system, its organisation and biochemistry. *Physiol. Plant.* **97**, 194–208.

Clay, N.K., Adio, A.M., Denoux, C., Jander, G. and Ausubel, F.M. (2009) Glucosinolate metabolites required for an Arabidopsis innate immune response. *Science*, **323**, 95–101.

Clough, S.J., Fengler, K.A., Yu, I.C., Lippok, B., Smith, R.K. and Bent, A.F. (2000) The Arabidopsis dnd1 "defense, no death" gene encodes a mutated cyclic nucleotide-gated ion channel. *Proc. Natl Acad. Sci. USA*, **97**, 9323–9328.

Coll, N.S., Vercammen, D., Smidler, A., Clover, C., Van Breusegem, F., Dangl, J.L. and Epple, P. (2010) Arabidopsis type I metacaspases control cell death. *Science*, **330**, 1393–1397.

Collins, N.C., Thordal-Christensen, H., Lipka, V. *et al.* (2003) SNARE-protein-mediated disease resistance at the plant cell wall. *Nature*, **425**, 973–977.

Demidchik, V., Straltsova, D., Medvedev, S.S., Pozhvanov, G.A., Sokolik, A. and Yurin, V. (2014) Stress-induced electrolyte leakage: the role of K + -permeable channels and involvement in programmed cell death and metabolic adjustment. *J. Exp. Bot.* **65**, 1259–1270.

Deslandes, L. and Rivas, S. (2012) Catch me if you can: bacterial effectors and plant targets. *Trends Plant Sci.* **17**, 644–655.

Dodds, P.N. and Rathjen, J.P. (2010) Plant immunity: towards an integrated view of plant-pathogen interactions. *Nat. Rev. Genet.* **11**, 539–548.

Edwards, K., Johnstone, C. and Thompson, C. (1991) A simple and rapid method for the preparation of plant genomic DNA for PCR analysis. *Nucleic Acids Res.* **19**, 1349.

Eisenach, C., Chen, Z.H., Grefen, C. and Blatt, M.R. (2012) The trafficking protein SYP121 of Arabidopsis connects programmed stomatal closure and K(+) channel activity with vegetative growth. *Plant J.* **69**, 241–251.

Falk, A., Feys, B.J., Frost, L.N., Jones, J.D., Daniels, M.J. and Parker, J.E. (1999) EDS1, an essential component of R gene-mediated disease resistance in Arabidopsis has homology to eukaryotic lipases. *Proc. Natl Acad. Sci. USA*, **96**, 3292–3297.

Fan, J., Crooks, C., Creissen, G., Hill, L., Fairhurst, S., Doerner, P. and Lamb, C. (2011) Pseudomonas sax genes overcome aliphatic isothiocyanate-mediated non-host resistance in Arabidopsis. *Science*, **331**, 1185–1188.

Geng, X.Q., Cheng, J.Y., Gangadharan, A. and Mackey, D. (2012) The coronatine toxin of pseudomonas syringae is a multifunctional suppressor of Arabidopsis defense. *Plant Cell*, **24**, 4763–4774.

Glazebrook, J. and Ausubel, F.M. (1994) Isolation of phytoalexin-deficient mutants of Arabidopsis thaliana and characterization of their interactions with bacterial pathogens. *Proc. Natl Acad. Sci. USA*, **91**, 8955–8959.

Grant, M.R., Godiard, L., Straube, E., Ashfield, T., Lewald, J., Sattler, A., Innes, R.W. and Dangl, J.L. (1995) Structure of the Arabidopsis RPM1 gene enabling dual specificity disease resistance. *Science*, **269**, 843–846.

Grubb, C.D., Zipp, B.J., Ludwig-Muller, J., Masuno, M.N., Molinski, T.F. and Abel, S. (2004) Arabidopsis glucosyltransferase UGT74B1 functions in glucosinolate biosynthesis and auxin homeostasis. *Plant J.* **40**, 893–908.

Hackenberg, T., Juul, T., Auzina, A. *et al.* (2013) Catalase and NO CATALASE ACTIVITY1 promote autophagy-dependent cell death in Arabidopsis. *Plant Cell*, **25**, 4616–4626.

Hatsugai, N., Iwasaki, S., Tamura, K., Kondo, M., Fuji, K., Ogasawara, K., Nishimura, M. and Hara-Nishimura, I. (2009) A novel membrane fusion-mediated plant immunity against bacterial pathogens. *Genes Dev.* **23**, 2496–2506.

Hauck, P., Thilmony, R. and He, S.Y. (2003) A Pseudomonas syringae type III effector suppresses cell wall-based extracellular defense in susceptible Arabidopsis plants. *Proc. Natl Acad. Sci. USA*, **100**, 8577–8582.

Heese, A., Ludwig, A.A. and Jones, J.D. (2005) Rapid phosphorylation of a syntaxin during the Avr9/Cf-9-race-specific signaling pathway. *Plant Physiol.* **138**, 2406–2416.

Hiruma, K., Fukunaga, S., Bednarek, P., Pislewska-Bednarek, M., Watanabe, S., Narusaka, Y., Shirasu, K. and Takano, Y. (2013) Glutathione and tryptophan metabolism are required for Arabidopsis immunity during the

hypersensitive response to hemibiotrophs. *Proc. Natl Acad. Sci. USA*, **110**, 9589–9594.

Hofius, D., Schultz-Larsen, T., Joensen, J., Tsitsigiannis, D.I., Petersen, N.H., Mattsson, O., Jorgensen, L.B., Jones, J.D., Mundy, J. and Petersen, M. (2009) Autophagic components contribute to hypersensitive cell death in Arabidopsis. *Cell*, **137**, 773–783.

Holub, E.B. (2007) Natural variation in innate immunity of a pioneer species. *Curr. Opin. Plant Biol.* **10**, 415–424.

Hopkins, R.J., van Dam, N.M. and van Loon, J.J.A. (2009) Role of glucosinolates in insect-plant relationships and multitrophic interactions. *Annu. Rev. Entomol.* **54**, 57–83.

Hruz, T., Laule, O., Szabo, G., Wessendorp, F., Bleuler, S., Oertle, L., Widmayer, P., Gruissem, W. and Zimmermann, P. (2008) Genevestigator v3: a reference expression database for the meta-analysis of transcriptomes. *Adv. Bioinformatics*, **2008**, 420747.

Huckelhoven, R. and Panstruga, R. (2011) Cell biology of the plant-powdery mildew interaction. *Curr. Opin. Plant Biol.* **14**, 738–746.

Jurkowski, G.I., Smith, R.K. Jr, Yu, I.C., Ham, J.H., Sharma, S.B., Klessig, D.F., Fengler, K.A. and Bent, A.F. (2004) Arabidopsis DND2, a second cyclic nucleotide-gated ion channel gene for which mutation causes the "defense, no death" phenotype. *Mol. Plant Microbe Interact.* **17**, 511–520.

Kim, D.Y., Bovet, L., Maeshima, M., Martinoia, E. and Lee, Y. (2007) The ABC transporter AtPDR8 is a cadmium extrusion pump conferring heavy metal resistance. *Plant J.* **50**, 207–218.

Kobae, Y., Sekino, T., Yoshioka, H., Nakagawa, T., Martinoia, E. and Maeshima, M. (2006) Loss of AtPDR8, a plasma membrane ABC transporter of Arabidopsis thaliana, causes hypersensitive cell death upon pathogen infection. *Plant Cell Physiol.* **47**, 309–318.

Koch, E. and Slusarenko, A. (1990) Arabidopsis is susceptible to infection by a downy mildew fungus. *Plant Cell*, **2**, 437–445.

Lipka, V., Dittgen, J., Bednarek, P. *et al.* (2005) Pre- and postinvasion defenses both contribute to nonhost resistance in arabidopsis. *Science*, **310**, 1180–1183.

Mackey, D., Holt, B.F. 3rd, Wiig, A. and Dangl, J.L. (2002) RIN4 interacts with Pseudomonas syringae type III effector molecules and is required for RPM1-mediated resistance in Arabidopsis. *Cell*, **108**, 743–754.

Millet, Y.A., Danna, C.H., Clay, N.K., Songnuan, W., Simon, M.D., Werck-Reichhart, D. and Ausubel, F.M. (2010) Innate immune responses activated in Arabidopsis roots by microbe-associated molecular patterns. *Plant Cell*, **22**, 973–990.

Morel, J.-B. and Dangl, J.L. (1999) Suppressors of the Arabidopsis lsd5 Cell death mutation identify genes involved in regulating disease resistance responses. *Genetics*, **151**, 305–319.

Mur, L.A.J., Kenton, P., Lloyd, A.J., Ougham, H. and Prats, E. (2008) The hypersensitive response; the centenary is upon us but how much do we know? *J. Exp. Bot.* **59**, 501–520.

Nielsen, M.E. and Thordal-Christensen, H. (2013) Transcytosis shuts the door for an unwanted guest. *Trends Plant Sci.* **18**, 611–616.

Pan, X.Q., Welti, R. and Wang, X.M. (2010) Quantitative analysis of major plant hormones in crude plant extracts by high-performance liquid chromatography-mass spectrometry. *Nat. Protoc.* **5**, 986–992.

Pinosa, F., Buhot, N., Kwaaitaal, M., Fahlberg, P., Thordal-Christensen, H., Ellerstrom, M. and Andersson, M.X. (2013) Arabidopsis phospholipase Ddelta is involved in basal defense and non-host resistance to powdery mildew fungi. *Plant Physiol.* **163**, 896–906.

Pitzschke, A., Schikora, A. and Hirt, H. (2009) MAPK cascade signalling networks in plant defence. *Curr. Opin. Plant Biol.* **12**, 421–426.

Ronald, P.C. and Beutler, B. (2010) Plant and animal sensors of conserved microbial signatures. *Science*, **330**, 1061–1064.

Schlaeppi, K. and Mauch, F. (2010) Indolic secondary metabolites protect Arabidopsis from the oomycete pathogen Phytophthora brassicae. *Plant Signal. Behav.* **5**, 1099–1101.

Sinapidou, E., Williams, K., Nott, L., Bahkt, S., Tor, M., Crute, I., Bittner-Eddy, P. and Beynon, J. (2004) Two TIR:NB:LRR genes are required to specify resistance to Peronospora parasitica isolate Cala2 in Arabidopsis. *Plant J.* **38**, 898–909.

Stein, M., Dittgen, J., Sánchez-Rodríguez, C., Hou, B.-H., Molina, A., Schulze-Lefert, P., Lipka, V. and Somerville, S. (2006) Arabidopsis PEN3/PDR8, an ATP biznding cassette transporter, contributes to nonhost resistance to inappropriate pathogens that enter by direct penetration. *Plant Cell*, **18**, 731–746.

Teh, O.K. and Hofius, D. (2014) Membrane trafficking and autophagy in pathogen-triggered cell death and immunity. *J. Exp. Bot.* **65**, 1297–1312.

Tierens, K., Thomma, B.P.H., Brouwer, M., Schmidt, J., Kistner, K., Porzel, A., Mauch-Mani, B., Cammue, B.P.A. and Broekaert, W.F. (2001) Study of the role of antimicrobial glucosinolate-derived isothiocyanates in resistance of Arabidopsis to microbial pathogens. *Plant Physiol.* **125**, 1688–1699.

Tor, M., Gordon, P., Cuzick, A., Eulgem, T., Sinapidou, E., Mert-Turk, F., Can, C., Dangl, J.L. and Holub, E.B. (2002) Arabidopsis SGT1b is required for defense signaling conferred by several downy mildew resistance genes. *Plant Cell*, **14**, 993–1003.

Tsuda, K., Sato, M., Stoddard, T., Glazebrook, J. and Katagiri, F. (2009) Network properties of robust immunity in plants. *PLoS Genet.* **5**, e1000772.

Underwood, W. and Somerville, S.C. (2013) Perception of conserved pathogen elicitors at the plasma membrane leads to relocalization of the Arabidopsis PEN3 transporter. *Proc. Natl Acad. Sci. USA*, **110**, 12492–12497.

Xin, X.F., Nomura, K., Underwood, W. and He, S.Y. (2013) Induction and suppression of PEN3 focal accumulation during Pseudomonas syringae pv. tomato DC3000 infection of Arabidopsis. *Mol. Plant Microbe Interact.* **26**, 861–867.

Zhang, Z., Feechan, A., Pedersen, C., Newman, M.A., Qiu, J.L., Olesen, K.L. and Thordal-Christensen, H. (2007) A SNARE-protein has opposing functions in penetration resistance and defence signalling pathways. *Plant J.* **49**, 302–312.

Zhang, Z., Lenk, A., Andersson, M.X., Gjetting, T., Pedersen, C., Nielsen, M.E., Newman, M.A., Hou, B.H., Somerville, S.C. and Thordal-Christensen, H. (2008) A lesion-mimic syntaxin double mutant in Arabidopsis reveals novel complexity of pathogen defense signaling. *Mol. Plant*, **1**, 510–527.

Zhao, Y.D., Hull, A.K., Gupta, N.R., Goss, K.A., Alonso, J., Ecker, J.R., Normanly, J., Chory, J. and Celenza, J.L. (2002) Trp-dependent auxin biosynthesis in Arabidopsis: involvement of cytochrome P450s CYP79B2 and CYP79B3. *Genes Dev.* **16**, 3100–3112.